January 2010

Proteomics Assisted Discovery Of Novel Proteins In Assembly And Regulation Of Photosystem II

Kimberly Wegener
Washington University in St. Louis

WASHINGTON UNIVERSITY IN ST. LOUIS

Division of Biology and Biomedical Sciences

Plant Biology

Dissertation Examination Committee:

Himadri Pakrasi, Chair

Robert Blankenship

Tuan-Hua David Ho

Joseph Jez

Robert Kranz

Thomas Smith

PROTEOMICS ASSISTED DISCOVERY OF NOVEL PROTEINS IN ASSEMBLY AND REGULATION OF PHOTOSYSTEM II

by

Kimberly Marie Wegener

A dissertation to the Graduate School of Arts and Sciences of Washington University in partial fulfillment of the requirements for the degree of Doctor of Philosophy

December 2010

Saint Louis, Missouri

ABSTRACT OF THE DISSERTATION

PROTEOMICS ASSISTED DISCOVERY OF NOVEL PROTEINS IN ASSEMBLY AND REGULATION OF PHOTOSYSTEM II

by

Kimberly M. Wegener

Doctor of Philosophy in Biology and Biomedical Sciences

(Plant Biology)

Washington University in St. Louis, 2010

Professor Himadri B. Pakrasi, Chairperson

Cyanobacteria, the only prokaryotes capable of oxygenic photosynthesis, are present in diverse ecological niches and play crucial roles in global carbon and nitrogen cycles. To proliferate in nature, cyanobacteria utilize a host of stress responses to maintain photosynthesis under periodic changes in environmental conditions. Recent advances in proteomic study have enabled a systems-level analysis of cellular functions in many systems. Because proteins are directly responsible for cellular functions, measurements of protein abundances provide significant clues to the modulation of cellular functions during different environmental perturbations. A detailed knowledge of the composition of, as well as the dynamic changes in, the proteome is necessary to gain fundamental insights into such stress responses. Toward this goal, we have performed a large-scale proteomic analysis of the widely studied model cyanobacterium *Synechocystis* sp. PCC 6803 under 33 different environmental conditions. Photosystem II (PSII) is a large membrane protein complex that performs the water oxidation reactions of the photosynthetic electron transport chain in cyanobacteria, algae, and plants. Subsequently, we also performed an

accurate mass tag (AMT) high-sensitivity proteomic analysis of PSII complexes purified from the cyanobacterium *Synechocystis* sp. PCC 6803.

Taken together, these proteomics studies revealed novel information into the function and assembly of Photosystem II. We identified six PSII associated proteins that are encoded by a single operon containing nine genes, *slr0144* to *slr0152*. This operon encodes proteins that are not essential components of the PSII holocomplex but accumulate to high levels in precomplexes lacking any of the lumenal proteins PsbP, PsbQ, or PsbV. Genetic deletion of this operon shows that removal of these protein products does not alter photoautotrophic growth or PSII fluorescence properties. Nonetheless these proteins confer fitness under competition in high light intensities. However, the deletion mutation does result in decreased PSII-mediated oxygen evolution and an altered distribution of the S states of the catalytic Mn cluster. PSII complexes isolated from *Δslr0144 – slr0152* also show decreased photosynthetic capacity and altered polypeptide composition. These data demonstrate that the proteins encoded by the genes in this operon are necessary for optimal function of PSII and function as accessory proteins during assembly of the PSII complex. Based on these results, we have named the products of the *slr0144 – slr0152* operon Pap (photosystem II assembly proteins). Additionally, through this proteomics study, we identified the protein sll1390, which we have named Psb32. To investigate its function, we analyzed subcellular localization of Psb32 and the impact of genetic deletion of the *psb32* gene on PSII. Psb32 is an integral membrane protein, primarily located in the thylakoid membranes. Although not required for cell viability, Psb32 protects cells from oxidative stress and additionally confers a selective fitness advantage in mixed culture experiments. Specifically, Psb32 protects PSII from photodamage and accelerates its repair. Thus, we propose that Psb32 plays an important role in minimizing the effect of photoinhibition on PSII. Together, the proteins of the pap operon and Psb32 represent new components in PSII assembly and function.

ACKNOWLEDGMENTS

Many thanks to my thesis advisor Himadri Pakrasi and past and present members of his lab group for seven years of advice, discussions, and support. In particular, thanks to the graduate students of the lab (Johnna Roose, Michelle Liberton, Jeff Cameron, Stefan Bennewitz, and Larry Page) for years of conversations about dogs, cooking, mushroom hunting, gems, the Cardinals, and many other brain breaks from the photosynthesis. Thank you to Nir Keren and Leeann Thornton for laying the foundations for this work and their continued intellectual contributions.

This work would not have been possible without the technical expertise of the Richard Smith's group at Pacific Northwest National Laboratory, particularly Jon Jacobs. I would also like to thank the National Science Foundation for funding this work. Special thanks to Ningning Ma, a very talented undergraduate who worked on this project. Additional thanks go to my thesis committee members (Bob Blankenship, Tuan-Hua David Ho, Bob Kranz, Joe Jez, and Tom Smith) for their fresh ideas on my research.

Finally, thank you to my family and friends for their unwavering support. Thanks, Billy and Juliet for keeping me smiling and a special thanks to my mom, for copyediting this dissertation.

TABLE OF CONTENTS

Chapter 4: The Psb32 Protein Aids in Repairing Photodamaged Photosystem II

Chapter 5: Psb32 is Associated with Inactive PSII Complexes

Chapter 6: Conclusion

Appendix I: The Extrinsic Proteins of Photosystem II

LIST OF TABLES

Chapter 6: Conclusions

Appendix I: The Extrinsic Proteins of Photosystem II

LIST OF FIGURES

Chapter 1: Introduction

Chapter 2: Global Proteomics Reveal an Atypical Strategy for Carbon/Nitrogen Assimilation by a Cyanobacterium under Diverse Environmental Perturbations

Chapter 3: High Sensitivity Proteomics Assisted Discovery of a Novel Operon Involved in the Assembly of Photosystem II, a Membrane Protein Complex

Chapter 4: The Psb32 Protein Aids in Repairing Photodamaged Photosystem II

Chapter 5: Psb32 is Associated with Inactive PSII Complexes

Chapter 6: Conclusions

Appendix I: The Extrinsic Proteins of Photosystem II

ABBREVIATIONS

AMT	accurate mass and time tag
CAB	chlorophyll a/b binding
CHAPS	3-[(3-cholamidopropyl)dimethylammonio]-1-propanesulfonic acid
Chl	chlorophyll
Cm	chloramphenicol
d	day
DCBQ	2,6-dichloro-p-benzoquinone
DCMU	3-(3,4-dichlorophenyl)-1,1-dimethylurea
DTT	Dithiothreitol
Fe	Iron
FTICR	Fourier transform ion cyclotron resonance
GL	growth light
H	hours
HL	high light
HPLC	high performance liquid chromatography
LC	liquid chromatography
LED	light-emitting diode
LL	low light

MALDI	matrix-assisted laser desorption/ionization
Min	minute
ML	medium light
Mn	manganese
MS	mass spectroscopy
N	nitrogen
NET	normalized elution time
NH_4	ammonia
Nm	nanometer
NO_3	nitrate
OEC	oxygen evolving complex
ORF	open reading frame
P	phosphate
PAGE	polyacrylamide gel electrophoresis
Pap	Photosystem II assembly protein
pD1	D1 precursor protein
PEG	polyethylene glycol
PM	plasma membrane
PMT	putative mass tag

PNNL	Pacific Northwest National Laboratory
PSI	Photosystem I
PSII	Photosystem II
ROS	reactive oxygen species
RT PCR	reverse transcriptase polymerase chain reaction
S	sulfate
SCPs	Small CAB-like Proteins
SCX	strong cation exchange chromatography
SDS	sodium dodecyl sulfate
SMBD	small molecule binding domain
TES	2-{[2-hydroxy-1,1-bis(hydroxymethyl)ethyl]amino}ethanesulfonic acid
TFA	trifluroacetic acid
TM	thylakoid membrane
TMH	transmembrane helix
TPR	tetratricopeptide repeats
UMC	unique mass class
V4R	4-vinyl reductase
WT	wild type

Chapter 1

INTRODUCTION

Oxygenic Photosynthesis

Oxygenic photosynthesis is a series of enzymatic reactions in which photons are converted to chemical energy in the thylakoid membranes of cyanobacteria and chloroplasts. This crucial series of reactions is catalyzed by four large enzyme complexes, utilizing photons to oxidize water into molecular oxygen, generating protons that are used for ATP generation, and electrons that move down the electron transport chain to ultimately reduce NADP (Fig. 1). Photosystem II (PSII) is the first enzyme complex of the pathway and with the excitation of light can transfer electrons to plastoquinone (PQ), concomittaly producing molecular oxygen and releasing protons into the lumenal space. The mobile carrier PQ then transfers the electrons to cytochrome b_6f (cyt b_6f), releasing additional protons into the lumen. From there the electrons move to the soluble copper protein plastocyanin (PC). PSI utilized light energy to transfer the electrons from PC to ferredoxin (Frd) to reduce NADP. The proton gradient in the internal lumenal space then produces ATP via ATP synthase.

Structure and Function of Photosystem II

PSII is a multi-subunit membrane protein complex containing 20 protein subunits and 56 cofactors (Fig. 2A). Light energy is captured by chlorophylls and initiates electron transfer from water through a series of redox active cofactors to plastoquinones in the membrane. The catalytic center of the oxygen evolving machinery is an inorganic Mn_4-Ca_1-Cl_x cluster coordinated by several ligands of the core integral membrane proteins of PSII and protected by the extrinsic proteins associated with the lumenal side of the complex. Recent crystal structures of cyanobacterial PSII complexes have increased our understanding of the structure and mechanism of this enzyme (Zouni et al., 2001; Kamiya and Shen, 2003; Ferreira et al., 2004; Loll et al., 2005), but this static picture is incomplete. PSII is a dynamic enzyme with a complex

biogenesis pathway and an intricate cycle of damage and repair under physiological conditions (Baena-Gonzalez and Aro, 2002).

Despite the large number of components, PSII can be divided into two functional domains (1) the electron transfer domain, comprised of the integral membrane helices and cofactors and (2) the oxygen evolving complex (OEC), located on the lumenal face of the complex including the loop regions of several membrane proteins and the extrinsic proteins. The catalytic center of the OEC is a tetranuclear manganese cluster that together with calcium and chloride ions sequentially removes four electrons from two water molecules to form molecular oxygen. All of the crystal structures of cyanobacterial PSII show that the ligands to this catalytic center are provided by the intrinsic protein components (Kamiya and Shen, 2003; Ferreira et al., 2004; Loll et al., 2005). This is in agreement with previous biochemical and genetic studies in a number of different organisms that have shown the extrinsic proteins are not necessary for oxygen evolution activity. However, the extrinsic proteins are required to enhance oxygen evolution activity and serve important roles *in vivo* including forming a protective barrier around the manganese cluster and concentrating the essential Ca^{2+} and Cl^{-} ions within the OEC (Seidler, 1996).

While the core membrane protein components of PSII are generally conserved in sequence and spatial arrangement among different organisms, there is considerable heterogeneity regarding the extrinsic proteins of the OEC. In most organisms, three to four extrinsic proteins are associated with the lumenal side of PSII, but only one protein, PsbO, is present in all oxygenic photosynthetic organisms. The other extrinsic proteins are PsbP, PsbQ, PsbR, PsbU, PsbV, and Psb27, which associate with PSII in various combinations depending on the organism.

PSII Biogenesis and Repair Cycle

The PSII biogenesis pathway involves an ordered accumulation of PSII subunits and integration of cofactors (Fig. 3). Based on labeling studies in higher plants and studies of complexes in cyanobacteria, the following order of assembly has been proposed for PSII (Aro et al., 2005; Rokka et al., 2005; Keren et al., 2005). At the periplasmic membrane, the D2 and cytochrome b_{559} subunits associate to form a pre-complex into which the precursor form of the D1 protein (pD1) is inserted. The pD1 protein contains a C-terminal extension, which is processed by the CtpA protease to yield the mature form of the D1 protein. The CP47 protein associates with the D1-D2-b_{559} subcomplex, followed by the CP43 protein. This precomplex is then translocated to the thylakoid membrane. A number of other low molecular weight membrane proteins are also integrated into the complex. Next, the Mn cluster and extrinsic proteins bind to the lumenal side of the complex. Finally, these PSII monomers associate to form dimers (>700 kDa) (Kern et al., 2005). In addition to the protein subunits visualized in the structural models of PSII, we have shown that a number of other proteins associate with cyanobacterial PSII complexes purified using a histidine-tagged version of the membrane protein CP47 (Kashino et al., 2002). While some of these novel PSII-associated proteins are stoichiometric components of the fully assembled PSII complex such as PsbQ (Thornton et al., 2004; Roose et al., 2007), others, such as the Psb27 protein, are predicted to transiently associate with PSII complexes during biogenesis or repair (Roose and Pakrasi, 2004; Nowaczyk et al., 2006; Mamedov et al., 2007).

The association of cofactors with the functional complex is less defined. The mechanism of integration for some of these cofactors has been well documented, as is the case for the Mn_4-Ca_1-Cl_x cluster. It is known that after the incorporation of the CP43 protein, all of the ligands for the $Mn_4Ca_1Cl_x$ cluster are present within the complex and presumably integration of this catalytic center occurs. However, the integration of other cofactors, including the insertion of chlorophyll into the chlorophyll containing proteins D1, D2, CP47, and CP43, remains a mystery. However, because free chlorophyll is highly damaging in the presence of light, it has been theorized that

there must be chlorophyll chaperone proteins that safely sequester chlorophyll until it is inserted into the chlorophyll containing proteins D1, D2, cyt_{b559}, CP43, and CP47. These chlorophyll chaperones must be present in both the plasma membrane and thylakoid membrane systems, as some of the chlorophyll containing proteins of PSII are translated and inserted at each cellular location (Keren et al., 2005).

Photodamage and Damage by Reactive Oxygen Species to PSII

Although light is required for photosynthetic reactions, it is also damaging to the photosynthetic reaction centers. In particular PSII is highly susceptible to light damage, termed photodamage (Powles, 1984; Prásil et al., 1992; Aro et al., 1993; Andersson and Aro, 2001). Photodamage is repaired by *de novo* protein synthesis, allowing PSII function to return to normal (Prásil et al., 1992; Aro et al., 1993; Andersson and Aro, 2001). This damage and repair cycle allows photosynthesis to function at certain light intensities. While photodamage occurs constantly, it increases proportionally with light intensity (Park et al., 1995; Tyystjärvi and Aro, 1996; Anderson and Chow, 2002; Nishiyama et al., 2004). When the rates of damage exceed the rates of repair, PSII is no longer functional, a process termed photoinhibition.

In addition to light, reactive oxygen species (ROS) can also cause damage to PSII. ROS can be produced as a byproduct of the light reactions of photosynthesis. Reduction of oxygen by photosystem I, the acceptor side of photosynthesis, can lead to the generation of superoxide radicals (O_2^-), which can convert to hydrogen peroxide (H_2O_2) and hydroxyl radicals ($^{\cdot}OH$) (Asada, 2003). On the donor side, transfer of excitation energy from chlorophyll to oxygen can result in the production of singlet oxygen ($^1O_2$) (Knox and Dodge, 1985; Asada, 2003). Cells have many strategies for dealing with ROS, including antioxidants, like α-tocopherol and β-carotene, and ROS scavenging enzymes, such as superoxide dismutase (Asada, 2003; Havaux et al., 2005).

However, like photodamage and repair, this cycle of ROS damage and repair can also be stressed by increased light intensity so that damage accumulates (Asada, 2003).

Photosystem II Turnover

As a result of its normal function, the PSII enzyme undergoes frequent turnover, due mainly to irreversible damage to the D1 protein (Andersson and Aro, 2001; Aro et al., 2005). The damaged D1 protein must be detected, proteolytically removed and replaced with a newly synthesized copy, a process that requires at least partial disassembly of the complex (Fig. 3). The removal of the D1 protein is suspected to require partial disassembly of the complex by requiring the dissociation of the lumenal proteins and the catalytic Mn cluster. Specifically, the Mn atoms of the oxygen evolving center and the extrinsic proteins must be released from the damaged complex, and then re-bound to newly assembled PSII centers to restore oxygen evolving activity. Because many of these cofactors would be toxic in large quantities if left free in the cell, it is likely there are chaperone proteins to sequester these cofactors before complex assembly and during complex repair and degradation. Such a group of proteins, SCPs (Small CAB-like Proteins) have recently been reported as a mechanism to sequester chlorophylls from damaged PSII complexes until they are recycled into new complexes (Vavilin and Vermaas, 2007). Because the half life of chlorophyll is much greater than that of the proteins into which it is inserted, the chlorophyll is then recycled into new proteins (Vavilin and Vermaas, 2007). Thus in addition to the major components, many proteins associate with PSII throughout its lifecycle.

Study of partially assembled complexes has revealed that PSII biogenesis and repair requires a host of accessory proteins. One well studied example of these assembly proteins include CtpA, a protease which must process the D1 protein before PSII can be assembled (Roose and Pakrasi, 2004). Another accessory protein, PratA, has recently been identified as required for preD1 processing, at the plasma membrane (Klinkert et al., 2004). Other accessory

proteins identified through proteomic study of PSII (Kashino et al., 2002; Wegener et al., 2008) include Psb27, which was subsequently shown to aid in assembly of the catalytic manganese cluster (Nowaczyk et al., 2006; Roose and Pakrasi, 2008) and Psb29, which provides PSII tolerance to high light intensities (Wang, 2004; Keren et al., 2005).

PSII complexes are in a constant state of flux within the cell. While cells maintain a large pool of fully assembled and functional PSII complexes via an efficient repair mechanism, sub-populations of partially assembled PSII complexes also exist. Thus at any one time, photosynthetic organisms contain a mixed population of PSII complexes, including: subassembled complexes, missing stoichiometric protein components and containing extraneous assembly proteins; fully assembled, functioning complexes; and damaged complexes, missing stoichiometric protein components and containing extraneous repair proteins. These categories of complexes have different levels of activity and thus the activity of an organism's at any given time is an average of all PSII complexes present. Thus complexes isolated using histidine tagging on CP47, which is inserted into PSII precomplexes early in assembly, represent an average of all the populations of PSII *in vivo*. Reciprocal purifications utilizing histidine tags on other PSII proteins can be used to isolated specific populations of PSII complexes. For instance, complexes isolated utilizing a histidine tag on PsbQ identified a subpopulation of PSII that is more highly active and contains more of the stoichiometric proteins and cofactors that complexes isolated utilizing histidine tag on CP47, indicating that complexes containing PsbQ are the final form of assembled functional PSII (Roose et al., 2007). In contrast, complexes isolated utilizing a histidine tag on Psb27 contain a fully assembled core but are lacking the manganese cluster and the lumenal proteins and have no PSII mediated oxygen evolution activity, suggesting that these complexes are an assembly intermediate (Roose 2008). Complexes isolated utilizing a histidine tag on PsbP contain the D2, CP47, and PsbO proteins, representing another assembly intermediate (Roose, Wegener, and Pakrasi, unpublished data). These diverse PSII complexes are diagrammed in Figure 4.

Advances in Proteomics

While transcriptomics has traditionally been used to capture a static picture of a system's state as a whole, recent advances in proteomics have allowed researchers a second mode to assay organisms at the global levels. Recent advances in high throughput proteomic technology and informatics tools have allowed high-confidence quantitative and qualitative proteome determination of several model organisms such as *E. coli*, *Saccharomyces cerevisiae*, *Drosophila melanogaster*, and *Caenorhabditis elegans* (Tonella et al., 2001; Mawuenyega et al., 2002; Brunner et al., 2007; Schmidt et al., 2007). These results have enabled a systems-level analysis of cellular functions, which can then be analyzed by traditional genetic and biochemical methodology. Like all techniques, though proteomics does have inherent biases (particularly due to the abundance and sequence properties of individual proteins), it allows for a discovery-based approach revealing broad protein abundance observations for any organism with a sequenced genome.

This Work

While the stoichiometric components of PSII have been well characterized, much about the assembly and repair cycles remain unknown. Without precise and controlled assembly and repair, damaged complexes would accumulate in photosynthetic organisms, preventing photosynthesis. The goal of this work was to discover novel PSII proteins and elucidate their roles on cellular physiology and photosynthesis. Taking advantage of modern proteomics technology, this work focuses on 1) global proteomic changes under sub-optimal photosynthetic conditions, 2) the polypeptide composition of functional and subassembled PSII complexes, and 3) the role of several PSII assembly/repair proteins on cellular physiology and photosynthesis.

Cyanobacteria are considered to be the progenitor of the modern chloroplast and indeed PSII is remarkably conserved throughout photosynthetic organisms. The unicellular

cyanobacteria *Synechocystis* sp. PCC 6803 (hereafter *Synechocystis*) has long been a model organism for photosynthetic research. It's fully sequenced genome (Kaneko et al., 1996), small gene families, natural DNA competence, and efficient double homologous recombination make it an attractive genetic system. Additionally, *Synechocystis* can be grown photoheterotrophically with glucose, allowing for study of otherwise lethal photosynthetic mutations (Pakrasi, 1995). Highly active PSII complexes can be easily isolated utilizing a histidine tag on the large integral membrane protein CP47 (Kashino et al., 2002). Lastly, biochemical assays to probe PSII activity and assembly have been previously established. Taken together, the combination of genetic and biochemical tools for Synechocystis make it an ideal system for this study.

Chapter 2 describes experiments designed to better understand the protein composition of Synechocystis as a whole under conditions that are not optimal for photosynthesis. High throughput analysis of total cellular extracts allowed us to make qualitative determinations of protein expression from 33 environmental conditions and quantitative determinations of protein levels from 12 of those conditions. Notably, our analysis revealed that a common stress response under various environmental perturbations, irrespective of amplitude and duration, is the activation of atypical pathways for the acquisition of carbon and nitrogen from urea and arginine. In particular, arginine is catabolized via putrescine to produce succinate and glutamate, sources of carbon and nitrogen, respectively. This study provides the most comprehensive functional and quantitative analysis of the *Synechocystis* proteome to date, and shows that a significant stress response of cyanobacteria involves an uncommon mode of acquisition of carbon and nitrogen.

The protein library established by the experiments detailed in Chapter 2 allowed for an in depth analysis of the protein components of isolated PSII. In Chapter 3, we again utilized high throughput proteomics to analyze and quantify protein levels in highly active, fully assembled complexes to those missing the lumenal PSII proteins *psbV*, *psbP*, or *ΔpsbQ*. We identified over 200 proteins associated with isolated PSII complexes, a substantial number more than the highest previous determination of 32 (Kashino et al., 2002). This analysis identified six PSII

associated proteins that increased in abundance in the mutant complexes and that are encoded by a single operon containing nine genes, *slr0144* to *slr0152*. This operon encodes proteins that are not essential components of the PSII holocomplex but accumulate to high levels in precomplexes lacking any of the lumenal proteins PsbP, PsbQ, or PsbV. Genetic deletion of this operon shows that removal of these protein products does not alter photoautotrophic growth or PSII fluorescence properties. However, the deletion mutation does result in decreased PSII-mediated oxygen evolution and an altered distribution of the S states of the catalytic Mn cluster. PSII complexes isolated from *Δsllr0144 – slr0152* also show decreased photosynthetic capacity and altered polypeptide composition. These data demonstrate that the proteins encoded by the genes in this operon are necessary for optimal function of PSII and function as accessory proteins during assembly of the PSII complex. Based on these results, we have named the products of the *slr0144 – slr0152* operon Pap (photosystem II assembly proteins).

Also identified in the isolated PSII complexes, as well as found in a previous proteomic study of PSII (Kashino et al., 2002), was Sll1390 (hereafter referred to as Psb32). To date, only one homolog of Psb32, TLP18.3 (At1g54780) in *Arabidopsis thaliana* has been investigated (Sirpio et al., 2007). While plants lacking TLP18.3 showed no significant phenotypes under normal growth conditions, these mutants did display increased susceptibility to photoinhibition and altered growth under fluctuating light. The authors found that this was due to decreased efficiency of repair of PSII due to decreased D1 turnover and decreased complex dimerization (Sirpio et al., 2007). In Chapter 4, we analyzed subcellular localization of Psb32 and the impact of genetic deletion of the *psb32* gene on PSII. Here we show that Psb32 is an integral membrane protein, primarily located in the thylakoid membranes. Although not required for cell viability, Psb32 protects cells from oxidative stress and additionally confers a selective fitness advantage in mixed culture experiments. Specifically, Psb32 protects PSII from photodamage and

accelerates its repair. Thus, we propose that Psb32 plays an important role in minimizing the effect of photoinhibition on PSII.

Psb32 function is further analyzed in Chapter 5, utilizing strains that contain a histidine-tagged version of the Psb32 protein (HisPsb32) or Psb32 overexpressed to high levels. We found that both these strains behave physiologically like WT. However, isolation of chlorophyll containing complexes from HisPsb32 revealed that these complexes have remarkably reduced levels of oxygen evolution activity and manganese. Conversely, the overexpression of Psb32 also results in decreased oxygen evolution in PSII parameters of complexes isolated using a histidine tag on CP47.

Chapter 6 summarizes the key findings of this research and the latest model of PSII assembly and repair in cyanobacteria. The implications of my findings with respect to our current view of the structure of PSII and the functions of other potential PSII assembly factors are discussed. Additionally, the effect of environmental stress on PSII structure and function will be discussed.

REFERENCES

Anderson JM, Chow WS (2002) Structural and functional dynamics of plant photosystem II. Philos Trans R Soc Lond, B **357:** 1421-1430

Andersson B, Aro EM (2001) Photodamage and D1 Protein Turnover. *In* EM Aro, B Andersson, eds, Regulation of Photosynthesis, Vol 11. Kluwer, Dordrecht, pp 377-394

Aro EM, Suorsa M, Rokka A, Allahverdiyeva Y, Paakkarinen V, Saleem A, Battchikova N, Rintamaki E (2005) Dynamics of photosystem II: a proteomic approach to thylakoid protein complexes. J Exp Bot **56:** 347-356

Aro EM, Virgin I, Andersson B (1993) Photoinhibition of Photosystem II. Inactivation, protein damage and turnover. Biochim Biophys Acta **1143:** 113-134

Asada K (2003) The water-water cycle in chloroplasts: Scavenging of active oxygens and dissipation of excess photons. Annu Rev Plant Phys **50:** 601-639

Baena-Gonzalez E, Aro EM (2002) Biogenesis, assembly and turnover of photosystem II units. Philos Trans R Soc Lond B Biol Sci **357:** 1451-1459; discussion 1459-1460

Brunner E, Ahrens CH, Mohanty S, Baetschmann H, Loevenich S, Potthast F, Deutsch EW, Panse C, de Lichtenberg U, Rinner O, Lee H, Pedrioli PGA, Malmstrom J, Koehler K, Schrimpf S, Krijgsveld J, Kregenow F, Heck AJR, Hafen E, Schlapbach R, Aebersold R (2007) A high-quality catalog of the *Drosophila melanogaster* proteome. Nat Biotech **25:** 576-583

Ferreira KN, Iverson TM, Maghlaoui K, Barber J, Iwata S (2004) Architecture of the photosynthetic oxygen-evolving center. Science **303:** 1831-1838

Havaux M, Eymery F, Porfirova S, Rey P, Dormann P (2005) Vitamin E protects against photoinhibition and photooxidative stress in *Arabidopsis thaliana*. Plant Cell **17:** 3451-3469

Kamiya N, Shen JR (2003) Crystal structure of oxygen-evolving photosystem II from *Thermosynechococcus vulcanus* at 3.7-A resolution. Proc Natl Acad Sci U S A **100:** 98-103

Kaneko T, Sato S, Kotani H, Tanaka A, Asamizu E, Nakamura Y, Miyajima N, Hirosawa M, Sugiura M, Sasamoto S, Kimura T, Hosouchi T, Matsuno A, Muraki A, Nakazaki N, Naruo K, Okumura S, Shimpo S, Takeuchi C, Wada T, Watanabe A, Yamada M, Yasuda M, Tabata S (1996) Sequence analysis of the genome of the unicellular cyanobacterium *Synechocystis* sp. strain PCC 6803. Sequence determination of the entire genome and assignment of potential protein-coding regions. DNA Res **3:** 109-136

Kashino Y, Lauber WM, Carroll JA, Wang Q, Whitmarsh J, Satoh K, Pakrasi HB (2002) Proteomic analysis of a highly active photosystem II preparation from the cyanobacterium *Synechocystis* sp. PCC 6803 reveals the presence of novel polypeptides. Biochemistry **41:** 8004-8012

Keren N, Liberton M, Pakrasi HB (2005) Photochemical competence of assembled photosystem II core complex in cyanobacterial plasma membrane. J Biol Chem **280:** 6548-6553

Keren N, Ohkawa H, Welsh EA, Liberton M, Pakrasi HB (2005) Psb29, a conserved 22-kD protein, functions in the biogenesis of photosystem II complexes in *Synechocystis* and *Arabidopsis*. Plant Cell **17:** 2768-2781

Kern J, Loll B, Luneberg C, DiFiore D, Biesiadka J, Irrgang KD, Zouni A (2005) Purification, characterisation and crystallisation of photosystem II from *Thermosynechococcus elongatus* cultivated in a new type of photobioreactor. Biochim Biophys Acta **1706:** 147-157

Klinkert B, Ossenbuhl F, Sikorski M, Berry S, Eichacker L, Nickelsen J. (2004) PratA, a periplasmic tetratricopeptide repeat protein involved in biogenesis of photosystem II in *Synechocystis* sp. PCC 6803. J Biol Chem **279**: 44639-44644

Knox JP, Dodge AD (1985) Singlet oxygen and plants. Phytochemistry **24:** 889-896

Loll B, Kern J, Saenger W, Zouni A, Biesiadka J (2005) Towards complete cofactor arrangement in the 3.0 A resolution structure of photosystem II. Nature **438:** 1040-1044

Mamedov F, Nowaczyk MM, Thapper A, Rogner M, Styring S (2007) Functional characterization of monomeric photosystem II core preparations from *Thermosynechococcus elongatus* with or without the Psb27 protein. Biochemistry **46:** 5542-5551

Mawuenyega KG, Kaji H, Yamauchi Y, Shinkawa T, Saito H, Taoka M, Takahashi N, Isobe T (2002) Large-scale identification of *Caenorhabditis elegans* proteins by multidimensional liquid chromatography tandem mass spectrometry. J Proteome Res **2:** 23-35

Nishiyama Y, Allakhverdiev SI, Yamamoto H, Hayashi H, Murata N (2004) Singlet oxygen inhibits the repair of Photosystem II by suppressing the translation elongation of the D1 protein in *Synechocystis* sp. PCC 6803. Biochemistry **43:** 11321-11330

Nowaczyk MM, Hebeler R, Schlodder E, Meyer HE, Warscheid B, Rogner M (2006) Psb27, a cyanobacterial lipoprotein, is involved in the repair cycle of photosystem II. Plant Cell **18:** 3121-3131

Pakrasi HB (1995) Genetic analysis of the form and function of Photosystem I and Photosystem II. Annu Rev Genet **29:** 755-776

Park YI, Chow WS, Anderson JM (1995) Light inactivation of functional photosystem II in leaves of peas grown in moderate light depends on photon exposure. Planta **196:** 401-411

Powles SB (1984) Photoinhibition of photosynthesis induced by visible light. Annu Rev Plant Phys **35:** 15-44

Prásil O, Adir N, Ohad I (1992) Dynamics of photosystem II: mechanism of photoinhibition and recovery processes. *In* J Barber, ed, Topics in Photosynthesis: The Photosystems: Structure, Function and Molecular Biology, Vol 11. Elsevier Science Publishers, Amsterdam, pp 295-348

Rokka A, Suorsa M, Saleem A, Battchikova N, Aro EM (2005) Synthesis and assembly of thylakoid protein complexes: multiple assembly steps of photosystem II. Biochem J **388:** 159-168

Roose JL (2008) Assembly and function of cyanobacterial photosystem II. Washington University in St. Louis, St. Louis

Roose JL, Kashino Y, Pakrasi HB (2007) The PsbQ protein defines cyanobacterial Photosystem II complexes with highest activity and stability. Proc Natl Acad Sci U S A

Roose JL, Pakrasi HB (2004) Evidence that D1 processing is required for manganese binding and extrinsic protein assembly into photosystem II. J Biol Chem **279:** 45417-45422

Roose JL, Pakrasi HB (2008) The Psb27 protein facilitates manganese cluster assembly in photosystem II. J Biol Chem **283:** 4044-4050

Schmidt MW, Houseman A, Ivanov AR, Wolf DA (2007) Comparative proteomic and transcriptomic profiling of the fission yeast *Schizosaccharomyces pombe.* Mol Syst Biol **3**

Seidler A (1996) The extrinsic polypeptides of Photosystem II. Biochim Biophys Acta **1277:** 35-60

Sirpio S, Allahverdiyeva Y, Suorsa M, Paakkarinen V, Vainonen J, Battchikova N, Aro EM (2007) TLP18.3, a novel thylakoid lumen protein regulating photosystem II repair cycle. Biochem J **406:** 415-425

Thornton LE, Ohkawa H, Roose JL, Kashino Y, Keren N, Pakrasi HB (2004) Homologs of plant PsbP and PsbQ proteins are necessary for regulation of photosystem ii activity in the cyanobacterium *Synechocystis* 6803. Plant Cell **16:** 2164-2175

Tonella L, Hoogland C, Binz P-A, Appel RD, Hochstrasser DF, Sanchez J-C (2001) New perspectives in the *Escherichia coli* proteome investigation. Proteomics **1:** 409-423

Tyystjärvi E, Aro EM (1996) The rate constant of photoinhibition, measured in lincomycin-treated leaves, is directly proportional to light intensity. Proc Natl Acad Sci U S A **93:** 2213-2218

Vavilin D, Vermaas W (2007) Continuous chlorophyll degradation accompanied by chlorophyllide and phytol reutilization for chlorophyll synthesis in *Synechocystis* sp. PCC 6803. Biochim Biophys Acta **1767:** 920-929

Wang HL, Postier BL, Burnap, RL (2004) Alterations in global patterns of gene expression in *Synechocystis* sp. PCC 6803 in response to inorganic carbon limitation and the inactivation of ndhR, a LysR family regulator. J Biol Chem **279:** 5739-5751

Wegener KM, Welsh EA, Thornton LE, Keren N, Jacobs JM, Hixson KK, Monroe ME, Camp DG, 2nd, Smith RD, Pakrasi HB (2008) High sensitivity proteomics assisted discovery of a novel operon involved in the assembly of photosystem II, a membrane protein complex. J Biol Chem **283:** 27829-27837

Zouni A, Witt HT, Kern J, Fromme P, Krauss N, Saenger W, Orth P (2001) Crystal structure of photosystem II from *Synechococcus elongatus* at 3.8 A resolution. Nature **409:** 739-743

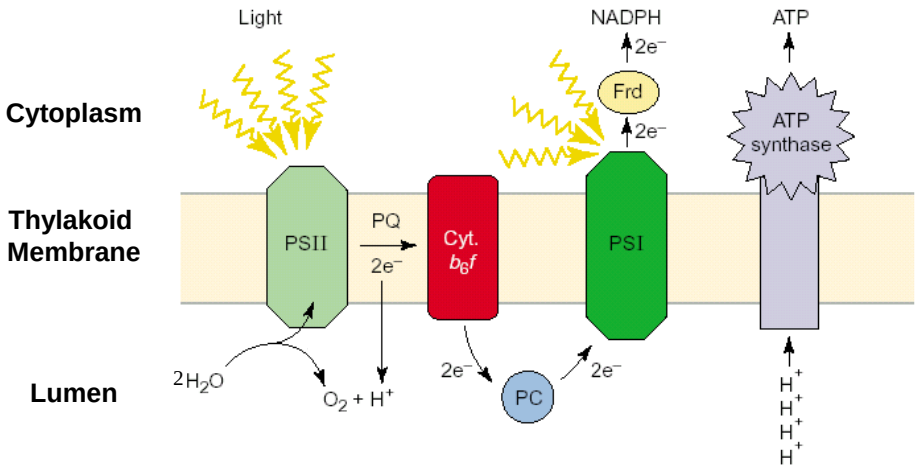

Figure 1. The Reactions of Oxygenic Photosynthesis. The membrane protein complexes and associated enzymes of the electron transfer chain; Photosystem II (PSII), Cytochrome b_6f complex (Cyt b_6f), Photosystem I (PSI), ATP synthase, plastocyanin (PC), and ferredoxin (Fd). Details of the electron transfer reaction is described in the text.

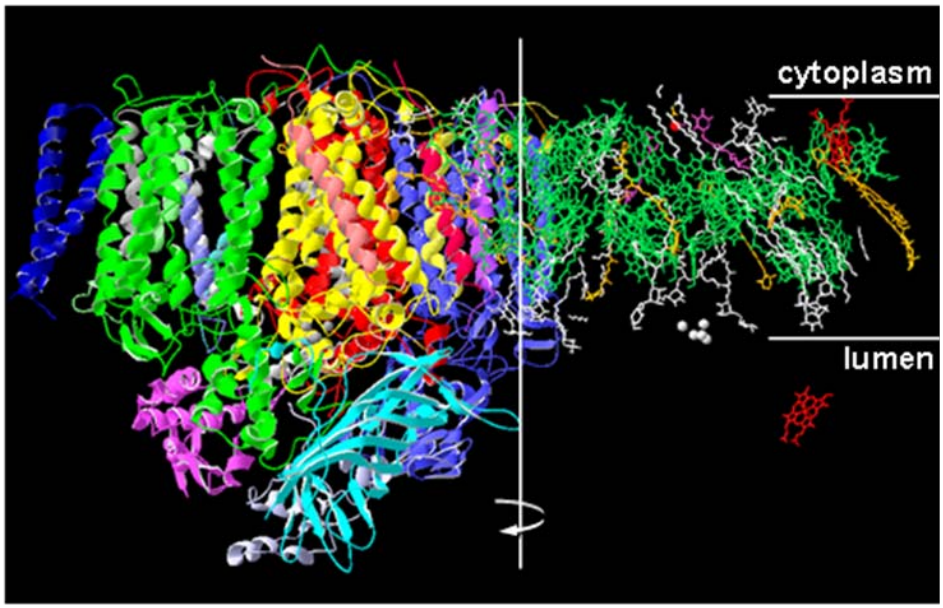

Figure 2. PSII Structure. Current structural model of cyanobacterial PSII at 3.0Å-resolution showing a dimer viewed along the membrane plane with one monomer displaying the protein subunits in ribbon form and the other monomer displaying the associated cofactors (PDB ID 2AXT)

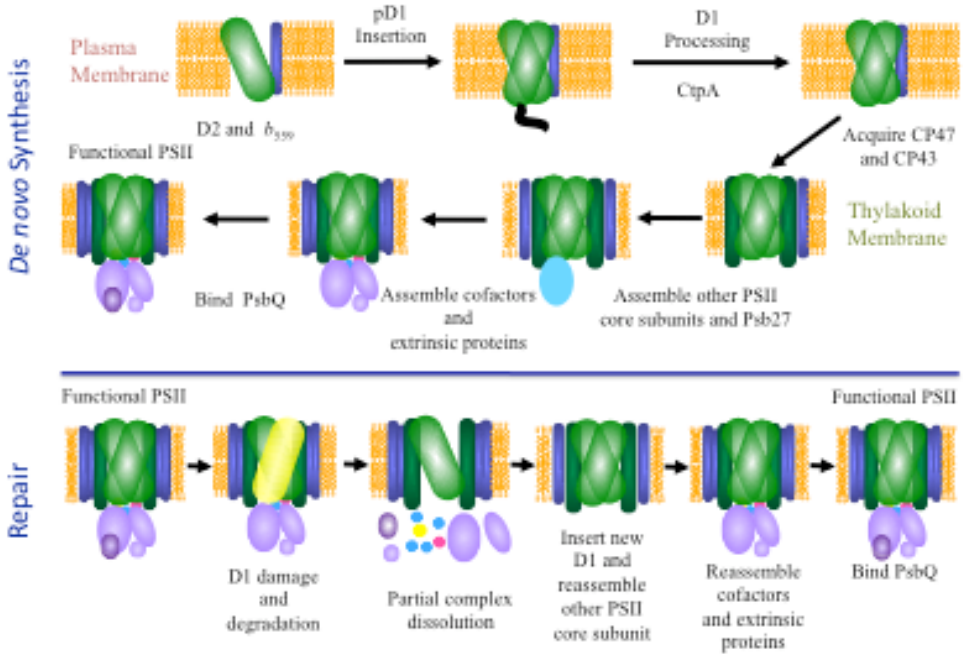

Figure 3. Schematic model of PSII biogenesis and repair in cyanobacteria. The top half of the cycle represents steps in the synthesis half of the pathway resulting in fully assembled complexes on the far left, and the bottom half of the cycle shows the disassembly of the complex and removal of the damaged D1 protein.

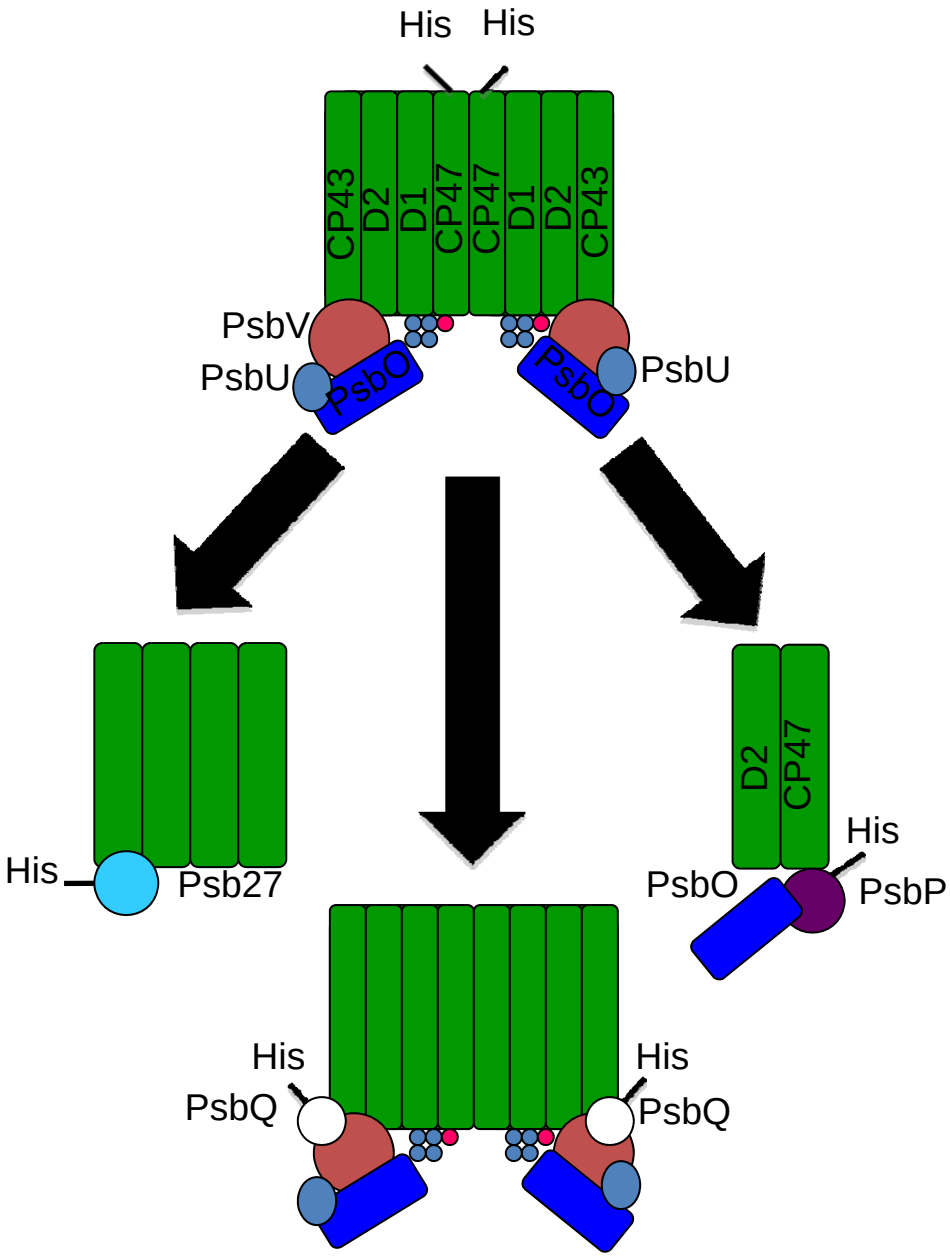

Figure 4. Populations of PSII *in vivo*. Complexes isolated utilizing a histidine tag on CP47 represent an average of all complexes existing at any given time. Reciprocal purification with tags on Psb27, PsbQ, and PsbP reveal additional details of complexes containing those proteins.

Chapter 2

GLOBAL PROTEOMICS REVEAL AN ATYPICAL STRATEGY FOR CARBON/NITROGEN ASSIMILATION BY A CYANOBACTERIUM UNDER DIVERSE ENVIRONMENTAL PERTURBATIONS

This chapter was adapted from:

Wegener KM*, Singh AK*, Jacobs JM, Elvitigala T, Welsh EA, Keren N, Gritsenko MA, Ghosh BK, Camp II DG, Smith RD, and Pakrasi HB Global proteomics reveal an atypical strategy for carbon/nitrogen assimilation by a cyanobacterium under diverse perturbations. *Mol Cell Proteom***.** **Under Review**

*- Equal Contribution

SUMMARY

Cyanobacteria, the only prokaryotes capable of oxygenic photosynthesis, are present in diverse ecological niches and play crucial roles in global carbon and nitrogen cycles. To proliferate in nature, cyanobacteria utilize a host of stress responses to accommodate periodic changes in environmental conditions. A detailed knowledge of the composition of, as well as the dynamic changes in, the proteome is necessary to gain fundamental insights into such stress responses. Toward this goal, we have performed a large-scale proteomic analysis of the widely studied model cyanobacterium *Synechocystis* sp. PCC 6803 under 33 different environmental conditions. The resulting high-quality dataset consists of 22,318 unique peptides corresponding to 2,369 proteins, a coverage of 65% of the predicted proteome. Quantitative determination of protein abundances has led to the identification of 1,221 differentially regulated proteins. Notably, our analysis revealed that a common stress response under various environmental perturbations, irrespective of amplitude and duration, is the activation of atypical pathways for the acquisition of carbon and nitrogen from urea and arginine. In particular, arginine is catabolized via putrescine to produce succinate and glutamate, sources of carbon and nitrogen, respectively. This study provides the most comprehensive functional and quantitative analysis of the *Synechocystis* proteome to date, and shows that a significant stress response of cyanobacteria involves an uncommon mode of acquisition of carbon and nitrogen.

INTRODUCTION

Most organisms experience daily changes in environmental conditions in their natural habitats. Typically, they tightly coordinate growth with cellular energy levels to survive unfavorable conditions. Photosynthetic organisms, whose energy requirements for cellular metabolism are derived from sunlight, offer attractive model systems to understand the impact of environmental perturbations on organismal physiology. This is particularly true for cyanobacteria, oxygenic photosynthetic prokaryotes of ancient lineage. During their evolution, cyanobacteria have survived large changes in environmental conditions (Kasting, 2004). Additionally, they can readily adapt their cellular metabolism to daily changes in light quality and quantity. Integration of nutrient specific pathways with photosynthetic processes is a key survival mechanism employed by cyanobacteria under changing environmental conditions (Tsinoremas et al., 1991; Lindahl and Florencio, 2003; Singh et al., 2008). Such adaptation strategies allow cyanobacteria to balance the supply of electrons from photosynthetic processes with the demands of cellular metabolism, and prevent the generation of damaging reactive oxygen species by excess reducing power.

Assimilation of carbon and nitrogen in photosynthetic organisms is one of the main sinks for the reducing power produced by the light reactions of photosynthesis. Accordingly, cyanobacteria have developed intricate mechanisms to control and coordinate several pathways involved in the acquisition of carbon and nitrogen. For example, PII, a regulatory protein, has been suggested to balance the acquisition of the two nutrients by sensing the carbon/nitrogen ratio (Forchhammer, 2004). Thioredoxins have also been shown to link the activity of the photosynthetic electron transport chain with carbon and nitrogen assimilation (Lindahl and Florencio, 2003). Despite the active participation of these proteins, cyanobacteria can assimilate carbon and nitrogen at disparate levels exceeding cellular demands. Excess carbon and nitrogen are stored in the forms of glycogen and cyanophycin granules, respectively, and are subsequently utilized under limiting conditions. *Synechocystis* sp. PCC 6803 (hereafter

Synechocystis), a model cyanobacterium, utilizes the oxidative pentose phosphate and glycolytic pathways to obtain carbon from glycogen granules (Yang et al., 2002). However, the pathway for utilization of cyanophycin is not well understood. Cyanophycin is a polymer of aspartic acid and arginine, which must be further catabolized to meet the nitrogen requirement for cellular metabolism. There are at least five known pathways for the catabolism of arginine in prokaryotes. Among them, a pathway utilizing arginase and the urea cycle has been shown to be active in *Synechocystis* (Quintero et al., 2000).

Our understanding of gene regulation linked to the assimilation of carbon and nitrogen, as well as broader cellular adaptation mechanisms under different environmental conditions, have significantly benefited from global transcriptional analysis of *Synechocystis* (Singh et al., 2010). Generally, it has been observed that such perturbations lead to downregulation of genes involved in light absorption and photosystems, as well as in carbon fixation and nitrogen assimilation. However, many of the studies have reported a complex regulation of genes involved in carbon and nitrogen assimilation. For example, upon preferential illumination of photosystem II, genes involved in nitrogen assimilation using nitrate (NO_3^-) as a substrate respond negatively, whereas those involved in utilization of either ammonia (NH_3), urea or arginine as substrate respond positively (Singh et al., 2009). Despite these transcriptomic studies, the impact of transcript regulation on protein levels remains poorly understood, in part due to several previous studies showing poor correlation between transcriptomic and proteomic datasets (Ideker et al., 2001; Corbin et al., 2003). Because proteins are directly responsible for cellular functions, measurements of protein abundances are expected to provide significant clues to the modulation of cellular functions during different environmental perturbations. Several proteomic studies under diverse environmental conditions have been undertaken in *Synechocystis* (Sazuka and Ohara, 1997; Sazuka et al., 1999; Fulda et al., 2000; Sergeyenko and Los, 2000; Wang et al., 2000; Huang et al., 2002; Simon et al., 2002; Herranen et al., 2004; Huang et al., 2004; Gan et al., 2005; Srivastava et al., 2005; Fulda et al., 2006; Huang et al., 2006; Kurian et al., 2006; Kurian et

al., 2006; Perez-Perez et al., 2006; Gan et al., 2007; Mata-Cabana et al., 2007; Pisareva et al., 2007). However, such studies have not yielded a comprehensive understanding of cellular adaptations, either due to low proteome coverage or due to the limited information on the changes in protein abundance.

Recent advances in high throughput proteomic technology and informatics tools have allowed high-confidence quantitative and qualitative proteome determination of several model organisms such as *E. coli*, yeast, *Drosophila*, and *C. elegans* (Tonella et al., 2001; Mawuenyega et al., 2002; Brunner et al., 2007; Schmidt et al., 2007). These results have enabled a systems-level analysis of cellular functions. Recently, we have used such improved proteomic tools to examine the proteome of a cyanobacterium *Cyanothece* sp. ATCC 51142, resulting in a coverage of ~68% (Stöckel *et al*., submitted to Molecular and Cellular Proteomics, Manuscript number MO:00173-MCP). In the current study, we have used LC-MS/MS to analyze the proteome of *Synechocystis* across 33 different environmental conditions. Our efforts have led to a 65% proteome coverage, resulting in the most complete functional and quantitative description of the proteome of *Synechocystis*, to date. Our analyses of differentially regulated proteins show that *Synechocystis* activates alternate pathways for the acquisition of carbon and nitrogen under diverse environmental conditions.

MATERIALS AND METHODS

Culture conditions

Synechocystis cultures were grown to a density of $2x10^8$ cells/mL as described (Wegener et al., 2008). Cells were harvested by centrifugation at 6000 x g for 5 min at 22^{o}C and washed twice with 100 mM TES, pH 8.0. The washed cells were inoculated into complete BG11 medium and sampled after 0, 4, 6, 8, and 16 days. For growth under nutrient deplete conditions, washed cells were grown in BG11 depleted of either NO_3^- (nitrogen depletion), sulfate (sulfur depletion) or phosphate (phosphorus depletion), and sampled after 6 days. For iron depletion, cells were incubated twice in 20 mM MES, 10 mM EDTA, pH 5.0 for 10 min, then inoculated in BG11 depleted of iron, and sampled after 6 days. Also, after 6 days, starved cultures were supplemented with 17.65 mM NO_3^-, 32 μM NH_4^+, 301 μM sulfate, 175 μM phosphate, or 30 μM iron as appropriate, and sampled after 4 and 24 h. For salt stress, 0.5 M NaCl was added to cells grown in complete BG11 and sampled after 0.5, 6, and 24 h. Cells were also collected after 3 and 6 days growth in the presence of 5 mM glucose and 10 μM 3-(3', 4'-dichlorophenyl)-1,1-dimethylurea (DCMU). For high CO_2 treatment, cells grown in 3% CO_2 were sampled after 1 and 25 h, transferred back to air level (0.3%) CO_2, and sampled after 2 h. Lastly, cells were subjected to heat (38°C) or cold (22°C) shock and sampled after 1, 4, and 24 h.

Sample preparation

Cells were harvested by centrifugation at 6000 x g for 5 min at 4^{o}C. Membrane and soluble fractions from total cell extracts were prepared as described (35) with minor modifications. The lysis buffer lacked any detergent and cells were broken by using 6 cycles of 1 min break, 1 min rest on ice. The cell lysates were fractionated by centrifugation at 150,000 x g at 4°C for 20 min. The supernatant comprising soluble fractions were transferred to separate tubes. The pellet comprising membrane fractions was washed with 100 mM ammonium bicarbonate buffer (pH 8.0)

and centrifuged again at 150,000 x g at 4°C for 20 min. The protein concentrations of soluble and membrane fractions were determined by BCA assay (Pierce, Rockford, IL). Soluble fractions were denatured and reduced using 8 M Urea and 5 mM DTT (Sigma-Aldrich, St. Louis, MO) at 37˚C for 60 min. Membrane fractions were treated identically, except for the addition of 1% CHAPS for 45 min prior to digestion. All samples were then diluted with 5 volumes of 25 mM ammonium bicarbonate prior to tryptic digestion using sequencing-grade modified porcine trypsin (Promega, Madison, WI) at a 1:50 (w/w) trypsin-to-protein ratio for 5 h at 37˚C. The digestions were stopped by boiling for 5 minutes followed by cooling on ice. Samples were separated using strong cation exchange chromatography (SCX) with a PolySulfoethyl A, 200 mm x 2.1 mm, 5 µM, 300-Å column and a 10 mm x 2.1 mm guard column (PolyLC, Inc., Columbia, MD) at a flow rate of 0.2 mL/min. The SCX peptide fractionation was carried out as previously described (Wegener et al., 2008). The peptides were resuspended in 900 µL of mobile phase A, and separated on an Agilent 1100 HPLC system (Agilent, Palo Alto, CA) equipped with a quaternary pump, degasser, diode array detector, Peltier-cooled autosampler and fraction collector (both set at 4 ºC). A total of 25 fractions were collected for each sample.

Reversed phase LC separation and MS/MS analysis of peptides.

The LC separation and MS/MS analysis have been extensively reported (Shen Y and Veenstra TD, 2001) with the coupling of a constant pressure (5,000 psi) reversed phase capillary liquid chromatography system (150 µm i.d. × 360 µm o.d. × 65 cm capillary; Polymicro Technologies Inc., Phoenix, AZ). Analyses performed utilized both Finnigan LCQ and LTQ ion trap mass spectrometers (ThermoFinnigan, San Jose, CA) using an electrospray ionization source manufactured in-house. Each unfractionated and SCX fraction was analyzed via capillary LC-MS/MS.

LC-MS/MS data analysis

ExtractMSn (version 4.0) and SEQUEST (Version v.27, Rev 12, Thermo Fisher Scientific, Waltham MA) (Eng, et al., 1994) analysis software was used to match the MS/MS fragmentation spectra to sequences from the 2004 Cyanobase (http://genome.kazusa.or.jp/cyanobase) annotation of *Synechocystis* (3,663 total entries, no enzyme search, ±3 Da tolerance for parent MS peak). Search was performed using default parameters with no-enzyme rules within a +/- 1.5 Da parent mass window, +/- 0.5 fragment mass window, average parent mass, and monoisotopic fragment mass. The criteria selected for filtering for both LCQ and LTQ data followed methods based upon a reverse database false positive model, which provides a target of 95% confidence in peptide identifications (Qian et al., 2005). Specific filter criteria for this study to achieve this level of confidence includes DelCN ≥0.1 coupled with Xcorr of ≥1.6 for full tryptic charge state +1, ≥2.4 for charge state +2, and ≥3.2 for charge state +3. For partial tryptic, Xcorr ≥4.3 for charge state +2 and ≥4.7 for charge state +3. An additional 8 proteins and 180 peptides were included from wild type spectra MSMS_01 - MSMS_06 (NCBI GEO accession GSE9577) (Wegener et al., 2008).

Data Processing and Analysis

Peptides matching multiple proteins were assigned to each of the matching proteins. Protein spectral counts were calculated by summing numbers of observed peptides for each protein in all fractions. For sample replicates, all combinations of soluble and membrane replicate pairings were summed, and the average and standard deviation of these combinations were used for the final values. Differentially expressed proteins were identified using three criteria: [(i) $mean1/mean2 \geq 1.5$, (ii) $mean1 - mean2 > 1$, and (iii) $(mean1 - 2stddev1) - (mean2 + 2stddev2) > 0$] where mean1 and stddev1 are the values of largest mean of the treatment or control. Proteins were categorized as up- or down-regulated, based on whether peptide abundances were higher or lower in the treated sample compared to the control sample. Transmembrane helices

were predicted with TMHMM (Krogh et al., 2001). SignalP (Emanuelsson et al., 2007) was used to predict cleavage sites for signal peptides using the Gram-negative bacteria setting. TMHMM predicted helices shorter than 15 amino acids and those overlapping with signal peptides were discarded. Proteins were considered to be membrane proteins if at least one transmembrane helix was predicted. Peptide hydrophobicities were calculated by summing the hydrophobicities of the amino acid sequences using the Kyte and Doolittle scale. Peptide hydrophobicity, length, and mass histograms were generated for the subset of observed fully tryptic peptides of ≥ 5 amino acids in length and ≥ 500 Da and compared to ideal tryptic digests of the observed proteins, using the same constraints.

RESULTS

Determination of the composition of Synechocystis proteome

To obtain a comprehensive proteomic description of *Synechocystis*, we collected samples from cells grown under 33 different environmental conditions. These included time series studies of *Synechocystis* growth under nutrient-limiting conditions followed by recovery under nutrient-sufficient conditions. The kinetics of pigment loss, a typical observable phenotype associated with nutrient starvation in cyanobacteria, were quite variable between nutritional conditions (Fig. 1), possibly due to the ability of cyanobacteria to store some, but not all, nutrients in the form of inclusion bodies that can be utilized during starvation. Therefore, we used a strategy that involved prolonged starvation for nitrate, phosphate, sulfate, or iron for 6 days followed by recovery with the addition of the limiting nutrient. This "starve and recovery strategy" resulted in a uniform recovery response. We also exposed cells to excess sodium chloride (2 M), CO_2 (3%) with a recovery under ambient air, glucose (5 mM), as well as low (20^{o}C) and high (38^{o}C) temperatures.

We utilized a sensitive LC-MS/MS peptide-based "bottom-up" approach to maximize the proteome coverage of *Synechocystis* (Page et al., 2004). Figure 2 describes various steps involved in the identification of proteins under multiple environmental conditions. Total cell extracts were prepared from *Synechocystis* cells grown under the 33 environmental conditions. To increase the coverage of membrane proteins, total cellular extracts were separated into membrane and soluble fractions by centrifugation prior to tryptic digestion. The resulting peptide mixtures were then subjected to LC-MS/MS to generate datasets for each sample, which were analyzed using SEQUEST (37). These spectra identifications were then used to determine spectral counts for each peptide. The counts from the membrane and soluble datasets were then combined for each condition and the technical replicates were averaged. Lastly, the peptides

were mapped back to their corresponding proteins and the final compiled dataset was then analyzed statistically.

We identified a total of 22,318 unique tryptic peptides with a confidence criterion of 95% (supplemental Tables 1 and 2). A small subset, 441, was identified by single peptide observation (supplemental Table 3). These observed peptides correspond to 2,369 proteins of the predicted 3,663 for the *Synechocystis* genome, a coverage of 65% (supplemental Table 4). *Synechocystis* contains seven endogenous plasmids in addition to 1 circular chromosome (Kaneko et al., 2003). Most of the proteins encoded by the predicted genes in plasmids are of unknown function. For example, the combined hypothetical and unknown genes comprise ~45% of the predicted chromosomal genes. In contrast, the endogenous plasmids pSYSA, pSYSX, pSYSM, and pSYSG contain ~87, 79, 73, and 62% unknown and hypothetical genes. Analysis of the proteome obtained in the present study shows that the coverage was highest for the circular chromosome (69%) (Fig. 3A). This is expected because a large number of predicted genes in the chromosome are known to code for functional proteins. However, we could also identify 24 to 44% proteins encoded by genes on the plasmids (Fig. 3A). This result suggests that these plasmid proteins are active in the physiology of *Synechocystis*.

Of the 69% protein coverage for the chromosome, the majority of detected proteins belonged to 14 known functional categories (Fig. 3B). Importantly, the observed proteins were uniformly distributed among different functional categories (Fig. 3B). We have identified more than 90% proteins involved in amino acid biosynthesis; energy metabolism; purines, pyrimidines, nucleosides, and nucleotides; and translation processes. Similarly, more than 75% proteins involved in cell envelope; cellular processes; central intermediary metabolism; photosynthesis; transcription; and transport have been identified. As expected, the lowest proteins coverage was obtained for unknown (48%), hypothetical (59%), and other (56%) categories.

Several proteomic studies have been previously undertaken in *Synechocystis* (Sazuka and Ohara, 1997; Sazuka et al., 1999; Fulda et al., 2000; Sergeyenko and Los, 2000; Wang et

al., 2000; Huang et al., 2002; Simon et al., 2002; Herranen et al., 2004; Huang et al., 2004; Gan et al., 2005; Srivastava et al., 2005; Fulda et al., 2006; Huang et al., 2006; Kurian et al., 2006; Kurian et al., 2006; Perez-Perez et al., 2006; Gan et al., 2007; Mata-Cabana et al., 2007; Pisareva et al., 2007). These studies have resulted in a combined observation of 1,099 proteins (supplemental Table 5). A comparative analysis of these previously identified proteins with those identified in the present study shows that 1,010 proteins were commonly identified (Fig. 3C). Eighty-nine previously identified proteins were not observed in our study whereas 1,359 proteins were uniquely observed in the present study. A large number of these proteins (758) are currently annotated as either hypothetical or unknown in Cyanobase (Nakamura et al., 1998). Thus, our results have provided direct proof of the functional role of over one half of hypothetical and unknown proteins in *Synechocystis*.

Cyanobacteria contain a greater number of membrane proteins compared to heterotrophic bacteria. This is due to the presence of an internal thylakoid membrane system, where the light reactions of photosynthesis occur. Therefore, a special emphasis in the current study was given towards identification of the *Synechocystis* proteome that is not biased towards any of the known factors. Analysis of the proteome data observed in this study shows that it consisted of 67% and 55% of predicted soluble and membrane proteins, respectively (inset, Fig. 4A). Importantly, increasing numbers of trans-membrane helices had little impact on the identification of membrane proteins (Fig. 4A). Identification of a large number of membrane proteins in our study is due to the initial separation of membrane fractions from soluble fractions as well as the use of an optimized solubilization buffers. An examination of the hydrophobicity of the observed peptides showed a similar distribution to that of the predicted tryptic peptides from the genome (Fig. 4B). However, analysis of a subgroup of membrane proteins showed that most of the identified peptides were from the cytosolic loop regions of the proteins. A study of the peptides identified showed that the masses of peptides observed also followed a similar distribution to that predicted, except in the case of the peptides less than 2000 Da, which were

underidentified (Fig. 4C). Other bias analysis determined that detection of the observed peptides was somewhat decreased for the shortest category (5-10 amino acids) (Fig. 4D). However, the observation of peptides was independent of pI, as shown by the similarity of the distribution of identified and predicted peptides (Fig. 4E). Taken together, theses bias analyses show that overall, there was very little technical bias in peptide observation.

Quantitative analysis of protein response to various perturbations

We re-examined 12 environmental conditions for quantitative determination of protein abundance (Table 1). A total of 1,221 differentially regulated proteins were identified (supplemental Tables 6 and 7). The number of differentially regulated proteins in each condition varied from a low of 267 (cold shock) to a high of 553 (nitrogen depletion) proteins (Table 1). A majority of differentially regulated proteins (56 - 76%) in most conditions, with the exception of cold shock and nitrogen depletion, were upregulated. Under cold stress and nitrogen depletion, approximately 62% and 86% of the differentially regulated proteins, respectively, were downregulated. However, addition of either nitrate or ammonia to the nitrogen-depleted cells had significant effects on the expression patterns of proteins. Under these conditions, the number of upregulated proteins increased from 77 to 231 (with nitrate repletion) and 257 (with ammonia repletion). At the same time, the number of downregulated proteins decreased from 476 to 150 (with nitrate repletion) and 141 (with ammonia repletion). The number of up- and down-regulated proteins during recovery in the presence of either nitrate or ammonia was similar to those of other nutrients. A small number of proteins were differentially expressed in a stress-specific manner (Table 1). Most of these proteins have no known functions.

Examination of cellular processes based on differential regulation of their associated proteins showed that the responses varied widely between conditions and, surprisingly, were not correlated with observed physiological responses (Fig. 5). For example, depletion of iron, phosphate, sulfate and nitrogen was accompanied by significant chlorosis and slow growth.

However, we observed that most processes were downregulated significantly only under nitrogen depletion and, to some extent, under iron depletion. In fact, in most other conditions, we noticed that majority of proteins in cellular processes were upregulated. This is even true for ribosomal proteins, whose expression has been typically linked with the growth of an organism. Though the number of differentially regulated ribosomal proteins varied depending on conditions, we found that ribosomal proteins were downregulated under nitrogen, phosphate, and iron depletion, and upregulated under sulfate depletion and heat shock. As expected, the majority of ribosomal proteins were upregulated during all recovery stages. A large number of proteins with unknown functions (~ 40%) showed significant differential regulation. Several of these proteins showed stress specific regulation, providing evidence of their crucial roles in cellular adaptation (Fig. 5).

Proteins involved in amino acid biosynthesis, glucose metabolism, TCA cycle, and cytochrome b_6f complex showed strong upregulation in majority of environmental conditions. In general, enzymes known to catalyze key reactions in any given pathway were differentially regulated. For example, glycogen phosphorylase, which catalyzes the release of glucose from glycogen, was strongly upregulated in all studied conditions. We also found that fructose-bisphosphate aldolase, which catalyzes the formation of glyceraldehyde 3-phosphate and dihydroxyacetone phosphate from fructose 1,6-bisphosphate, and pyruvate dehydrogenase, which converts pyruvate into acetyl-CoA, were strongly upregulated in all conditions. Similarly, key proteins involved in the biosynthesis of amino acids belonging to aromatic, aspartic acid, branched chain, serine and glutamate families were strongly differentially regulated. For example, chorismate synthase was strongly upregulated in most environmental conditions. Chorismate is a key intermediate involved in the biosynthesis of phenylalanine, tyrosine and tryptophan. Similarly, diaminopimelate decarboxylase that catalyzes the synthesis of lysine, and acetolactate synthase that catalyzes the first step in the biosynthesis of leucine, isoleucine and valine were strongly upregulated under most environmental conditions. In contrast, most photosynthesis related proteins, including phycobiliproteins, did not show significant changes in their abundance.

Similarly, very few proteins involved in pigment biosynthesis showed differential regulation. However, proteins with other critical functions were differentially regulated. For example, heme oxygenase, involved in the multi-step monooxygenase reaction to produce biliverdin IXα and CO from protoheme, was downregulated during nutrient depletion conditions.

Analysis of Photosystem II proteins

Of the cannonical PSII proteins (Kashino et al., 2002), we identified 23 proteins in our study, which were distributed between the 33 environmental conditions (supplemental Table 4). As a whole, all detected PSII proteins were differentially less abundant under nitrate and sulfur depletion conditions (supplemental Tables 6 and 7). This agrees with previous data showing that these two conditions have detrimental effects on photosynthetic capacity. However, in all conditions where it was possible to determine differential ratios, the manganese stabilizing protein, PsbO (Sll0427), was increased in abundance as compared to levels found in BG11 (supplemental Tables 6 and 7).

Concordance between transcriptomic and proteomic datasets

The global scale of proteome coverage and protein expression profiles obtained in this study enabled the first large-scale comparison of gene expression at the RNA and protein levels in *Synechocystis*. The differentially regulated proteins identified under cold shock, phosphate, sulfate, nitrogen, and iron depletions were compared with the differentially regulated transcripts identified during the respective DNA microarray studies (Suzuki et al., 2001; Singh et al., 2003; Suzuki et al., 2004; Osanai et al., 2006; Zhang et al., 2008). To allow for a uniform comparison, all five transcriptomic datasets were reanalyzed. We used a fold change of 1.5 to identify differentially regulated genes from these datasets. Concordance analysis showed that the expression changes between these two studies were quite low. However, we note that while the

comparisons were done between datasets generated under similar conditions, there are differences in some of the growth and sampling regimes between our proteomic experiments and the previously published microarray studies. Agreement between the two studies was lowest for sulfate depletion and highest for nitrogen depletion (Table 2). However, analysis of correlated and anti-correlated genes revealed some interesting results. Stress-specific genes showed similar expression patterns in both transcriptomic and proteomic studies. For example, expression of nutrient specific transporters showed strong concordance. The relatively higher concordance seen under nitrogen depletion was due to similar expression patterns of ribosomal and photosynthesis genes. On the other hand, expression patterns of photosynthetic genes were anti-correlated under iron depletion with downregulation of transcript levels and upregulation of protein levels.

Alternate pathway for assimilation of nitrogen and carbon under various perturbations

Several proteins involved in nitrogen assimilation showed significant differential regulation. Generally, proteins involved in the transport of nitrate were downregulated in cells grown under nutrient depletion, cold and heat shock. Repletion of nutrients to starved cells led to the upregulation of these transporter proteins. Interestingly, recovery of nitrogen-depleted cells in the presence of ammonia did not lead to the upregulation of nitrate transport proteins. To compensate for reduced nitrate uptake, cells upregulate proteins involved in transport and utilization of urea and arginine. UrtE (Sll0374) and UrtD (Sll0764), which are involved in transport of urea, were strongly upregulated under most environmental conditions. Our data also showed that urease which converts urea into CO_2 and ammonia was upregulated by 4-fold under most conditions. Similarly, BgtB (Sll1270), and to some extent BgtA (Slr1735), the periplasmic and ATP-binding components of an arginine transporter, were upregulated under most conditions. We also determined that cyanophycinase, involved in the breakdown of cyanophycin into arginine and aspartic acid, was somewhat upregulated under a number of conditions. These results suggest that a common response in *Synechocystis* under different perturbations is to reduce the

uptake of nitrate and increase the uptake of alternate nitrogen sources.

Arginine and aspartic acid must be further catabolized to acquire nitrogen for cellular metabolism. In *Synechocystis*, an arginine catabolic pathway has been described which combines the arginase pathway and urea cycle (Quintero et al., 2000). All proteins in this pathway were detected in our study. However, none of them showed significant differential levels, suggesting that this pathway is not the preferred route for arginine catabolism under these perturbations. Further analysis suggested that arginine is preferentially broken down into agmantine via arginine decarboxylase. In particular, arginine decarboxylase (Slr1312 and Slr0662), the first committed enzymes in this pathway, were upregulated 1.5 to 3 fold as compared to control conditions (Fig. 6, supplemental Table 8). Agmantine can subsequently be catabolized into putrescine via the putative agmantinase (Sll1077) or arginase (Sll0228). These two proteins were not observed in the control cells; however, peptides corresponding to these proteins were detected under various environmental conditions, providing support for the involvement of this alternative pathway during various perturbations (supplemental Table 4). Putrescine is known to play a critical role in DNA, RNA and protein synthesis, as well as in cell proliferation and differentiation. Furthermore, putrescine serves as a source for carbon and nitrogen in *E. coli* and *Pseudomonas* (Kurihara et al., 2005; Chou et al., 2008), where it is converted to succinate. Examination of proteins involved in putrescine degradation suggested that this pathway is also active in *Synechocystis* (Fig. 6, supplemental Table 8). Slr1022 shows strong similarity to the proteins (YgjG and SpuC) involved in degradation of putrescine into aminobutyrate in *E. coli* and *Pseudomonas* (Kurihara et al., 2005; Chou et al., 2008). Further evidence that succinate is produced from arginine came from the strong upregulation of succinate dehydrogenase and malate dehydrogenase (Fig. 6, supplemental Table 8). Thus conversion of arginine into succinate not only allows generation of TCA cycle intermediates but in the process releases glutamate, ammonia and CO_2. Ammonia is assimilated into glutamate, whereas CO_2 is fixed by ribulose 1,5-bisphosphate carboxylase oxygenase. Indeed, we found that transporters of

free inorganic carbon were not differentially regulated. However, several carbon concentrating mechanism proteins, required for concentrating intracellular carbon, showed significant upregulation.

DISCUSSION

Here, we report the most comprehensive functional and quantitative analysis of the *Synechocystis* proteome to date. The resulting proteome consists of 2,369 unique proteins (65% of the predicted proteins), 1,221 of which have been identified as differentially regulated under 12 different environmental conditions. Several bias analyses show that proteins identified in this study are representative of the entire proteome. Importantly, functional category based analysis shows that the observed proteins were uniformly distributed. Identification of 758 proteins of unknown function, of which 326 were differentially regulated, provides direct evidence of their roles in *Synechocystis* physiology. Taken together, this study has revealed the global proteomic makeup of *Synechocystis* and has facilitated a systems-level analysis of cellular response under different environmental conditions.

Analysis of 1,221 differentially regulated proteins shows that *Synechocystis* utilizes few stress-specific proteins to optimize cellular functions under perturbations (Table 1). Many of these proteins have no known function. In contrast, a large number of proteins associated with housekeeping functions were commonly differentially regulated. For example, key proteins involved in the biosynthesis of all amino acid families were strongly upregulated. These results suggest that despite the prolonged starvation for essential nutrients, cells continue to maintain a metabolically active state by seeking either the limiting nutrients, or alternate nutrients for growth. Typically, transporters involved in the acquisition of iron, sulfate and phosphate were upregulated. While sulfate transporters were specifically upregulated under sulfate depletion, expression of iron transporters was also upregulated under phosphate depletion and vice versa. In contrast, nitrate transporters were downregulated under nitrogen depletion. In fact, they were also downregulated under other environmental conditions. Previous studies using DNA microarrays have also shown strong downregulation of nitrate transporters under various environmental conditions (Singh et al., 2008; Singh et al., 2009). It has been suggested that changes in environmental conditions lead to reduced transport of nitrate while simultaneously activating the

pathway involved in the transport of alternate nitrogen substrates including ammonia, urea and arginine. A similar mechanism under changing nutrient conditions is apparent from the analysis of proteomic datasets. Our data shows that the preferred substrates for nitrogen acquisition are urea and arginine.

The most striking cellular strategy revealed from the analysis of differentially regulated proteins is the way in which the cells acquire carbon and nitrogen under different perturbations. Our results suggest that any change in conditions, irrespective of their amplitudes or durations, immediately leads to the activation of alternate pathways towards the acquisition of carbon and nitrogen. Although the majority of perturbations had little impact on levels of proteins involved in photosynthesis, they affected the efficiency of photosynthetic light reactions, resulting in a lower production of energy. It should be mentioned that most photosynthetic proteins were identified as strongly downregulated under nitrogen depletion and therefore, the lack of differential regulation was not because of our inability to detect peptides. The assimilation of carbon and nitrogen is an energy intensive process, requiring significant amounts of ATP, NADPH and reduced ferredoxin. Therefore, decreased energy production leads to the activation of alternate carbon and nitrogen assimilation pathways. Our data strongly suggest that under the different environmental perturbations, urea and arginine are the preferred substrates for both carbon and nitrogen. Cells also actively seek internal/external carbon sources, as is apparent from the upregulation of proteins involved in glycolysis and glucose transport. Arginine is preferentially catabolized via putrescine using the pathway recently characterized in *E. coli* and *Pseudomonas* (Kurihara et al., 2005; Chou et al., 2008). Activation of this pathway allows cells to obtain both carbon in the form of succinate, and CO_2 and nitrogen in the form of glutamate and ammonia. Aspartic acid, which can be generated from cyanophycin, can serve two purposes. It can be utilized for the synthesis of methionine, lysine and threonine. Additionally, it can be combined with 2-oxoglutarate to produce glutamine, which can then be combined with ammonia to produce glutamate. This result also indirectly suggests that arginine is not directly converted to glutamate using the previously

identified pathway (Quintero et al., 2000). The utility of this arrangement is that 2-oxoglutarate generated by glycolysis is channeled towards the production of glutamate.

In conclusion, the proteome analysis presented in this study has provided a unique and comprehensive catalogue of the proteomic makeup of *Synechocystis* under various environmental conditions. We believe that the knowledge of the functional information of when and how proteins with known as well as unknown functions are expressed is going to be a strong basis for future experimental studies. Analysis of dynamic changes in the proteome has provided insights into cellular adaptations under various environmental perturbations. Our results showed that a key cellular adaptation leads to the activation of alternate pathways for the acquisition of carbon and nitrogen, which are the two major sinks for reducing powers generated by the photosynthetic light reactions in cyanobacteria.

REFERENCES

Brunner E, Ahrens CH, Mohanty S, Baetschmann H, Loevenich S, Potthast F, Deutsch EW, Panse C, de Lichtenberg U, Rinner O, Lee H, Pedrioli PGA, Malmstrom J, Koehler K, Schrimpf S, Krijgsveld J, Kregenow F, Heck AJR, Hafen E, Schlapbach R, Aebersold R (2007) A high-quality catalog of the *Drosophila melanogaster* proteome. Nat Biotech **25:** 576-583

Chou HT, Kwon DH, Hegazy M, Lu CD (2008) Transcriptome analysis of agmatine and putrescine catabolism in *Pseudomonas aeruginosa* PAO1. J Bacteriol **190:** 1966-1975

Corbin RW, Paliy O, Yang F, Shabanowitz J, Platt M, Lyons CE, Root K, McAuliffe J, Jordan MI, Kustu S, Soupene E, Hunt DF (2003) Toward a protein profile of *Escherichia coli*: comparison to its transcription profile. Proc Natl Acad Sci U S A **100:** 9232-9237

Emanuelsson O, Brunak S, von Heijne G, Nielsen H (2007) Locating proteins in the cell using TargetP, SignalP and related tools. Nat Protoc **2:** 953-971

Eng JK, McCormack AL, Yates JR (1994) An approach to correlate tandem mass spectral data of peptides with amino acid sequences in a protein database. J Am Soc Mass Spectrom **5:** 976-989

Forchhammer K (2004) Global carbon/nitrogen control by PII signal transduction in cyanobacteria: from signals to targets. FEMS Microbiol Rev **28:** 319-333

Fulda S, Huang F, Nilsson F, Hagemann M, Norling B (2000) Proteomics of *Synechocystis* sp. strain PCC 6803: Identification of periplasmic proteins in cells grown at low and high salt concentrations. Eur J Biochem **267:** 5900-5907

Fulda S, Mikkat S, Huang F, Huckauf J, Marin K, Norling B, Hagemann M (2006) Proteome analysis of salt stress response in the cyanobacterium *Synechocystis* sp. strain PCC 6803. Proteomics **6:** 2733-2745

Gan CS, Chong PK, Pham TK, Wright PC (2007) Technical, experimental, and biological variations in isobaric tags for relative and absolute quantitation (iTRAQ). J Proteome Res **6:** 821-827

Gan CS, Reardon KF, Wright PC (2005) Comparison of protein and peptide prefractionation methods for the shotgun proteomic analysis of *Synechocystis* sp. PCC 6803. Proteomics **5:** 2468-2478

Herranen M, Battchikova N, Zhang P, Graf A, Sirpio S, Paakkarinen V, Aro EM (2004) Towards functional proteomics of membrane protein complexes in *Synechocystis* sp. PCC 6803. Plant Physiol **134:** 470-481

Huang F, Fulda S, Hagemann M, Norling B (2006) Proteomic screening of salt-stress-induced changes in plasma membranes of *Synechocystis* sp. strain PCC 6803. Proteomics **6:** 910-920

Huang F, Hedman E, Funk C, Kieselbach T, Schroder WP, Norling B (2004) Isolation of outer membrane of *Synechocystis* sp. PCC 6803 and its proteomic characterization. Mol Cell Proteomics **3:** 586-595

Huang F, Parmryd I, Nilsson F, Persson AL, Pakrasi HB, Andersson B, Norling B (2002) Proteomics of *Synechocystis* sp. strain PCC 6803: Identification of plasma membrane proteins. Mol Cell Proteomics **1:** 956-966

Ideker T, Thorsson V, Ranish JA, Christmas R, Buhler J, Eng JK, Bumgarner R, Goodlett DR, Aebersold R, Hood L (2001) Integrated genomic and proteomic analyses of a systematically perturbed metabolic network. Science **292:** 929-934

Kaneko T, Nakamura Y, Sasamoto S, Watanabe A, Kohara M, Matsumoto M, Shimpo S, Yamada M, Tabata S (2003) Structural analysis of four large plasmids harboring in a unicellular cyanobacterium, *Synechocystis* sp. PCC 6803. DNA Res **10:** 221-228

Kashino Y, Lauber WM, Carroll JA, Wang Q, Whitmarsh J, Satoh K, Pakrasi HB (2002) Proteomic analysis of a highly active photosystem II preparation from the cyanobacterium

Synechocystis sp. PCC 6803 reveals the presence of novel polypeptides. Biochemistry **41:** 8004-8012

Kasting JF (2004) When methane made climate. Sci Am **291:** 78-85

Krogh A, Larsson B, von Heijne G, Sonnhammer EL (2001) Predicting transmembrane protein topology with a hidden Markov model: application to complete genomes. J Mol Biol **305:** 567-580

Kurian D, Jansen T, Maenpaa P (2006) Proteomic analysis of heterotrophy in *Synechocystis* sp. PCC 6803. Proteomics **6:** 1483-1494

Kurian D, Phadwal K, Maenpaa P (2006) Proteomic characterization of acid stress response in *Synechocystis* sp. PCC 6803. Proteomics **6:** 3614-3624

Kurihara S, Oda S, Kato K, Kim HG, Koyanagi T, Kumagai H, Suzuki H (2005) A novel putrescine utilization pathway involves gamma-glutamylated intermediates of *Escherichia coli* K-12. J Biol Chem **280:** 4602-4608

Lindahl M, Florencio FJ (2003) Thioredoxin-linked processes in cyanobacteria are as numerous as in chloroplasts, but targets are different. Proc Natl Acad Sci U S A **100:** 16107-16112

Mata-Cabana A, Florencio FJ, Lindahl M (2007) Membrane proteins from the cyanobacterium *Synechocystis* sp. PCC 6803 interacting with thioredoxin. Proteomics **7:** 3953-3963

Mawuenyega KG, Kaji H, Yamauchi Y, Shinkawa T, Saito H, Taoka M, Takahashi N, Isobe T (2002) Large-scale identification of *Caenorhabditis elegans* proteins by multidimensional liquid chromatography tandem mass spectrometry. J Proteome Res **2:** 23-35

Nakamura Y, Kaneko T, Hirosawa M, Miyajima N, Tabata S (1998) CyanoBase, a www database containing the complete nucleotide sequence of the genome of *Synechocystis* sp. strain PCC6803. Nucleic Acids Res **26:** 63-67

Osanai T, Imamura S, Asayama M, Shirai M, Suzuki I, Murata N, Tanaka K (2006) Nitrogen induction of sugar catabolic gene expression in *Synechocystis* sp. PCC 6803. DNA Res **13:** 185-195

Page JS, Masselon CD, Smith RD (2004) FTICR mass spectrometry for qualitative and quantitative bioanalyses. Curr Opin Biotechnol **15:** 3-11

Perez-Perez ME, Florencio FJ, Lindahl M (2006) Selecting thioredoxins for disulphide proteomics: target proteomes of three thioredoxins from the cyanobacterium *Synechocystis* sp. PCC 6803. Proteomics **6 Suppl 1:** S186-195

Pisareva T, Shumskaya M, Maddalo G, Ilag L, Norling B (2007) Proteomics of *Synechocystis* sp. PCC 6803. Identification of novel integral plasma membrane proteins. FEBS J **274:** 791-804

Qian WJ, Liu T, Monroe ME, Strittmatter EF, Jacobs JM, Kangas LJ, Petritis K, Camp DG, 2nd, Smith RD (2005) Probability-based evaluation of peptide and protein identifications from tandem mass spectrometry and SEQUEST analysis: the human proteome. J Proteome Res **4:** 53-62

Quintero MJ, Muro-Pastor AM, Herrero A, Flores E (2000) Arginine catabolism in the cyanobacterium *Synechocystis* sp. strain PCC 6803 involves the urea cycle and arginase pathway. J Bacteriol **182:** 1008-1015

Sazuka T, Ohara O (1997) Towards a proteome project of cyanobacterium *Synechocystis* sp. strain PCC 6803: linking 130 protein spots with their respective genes. Electrophoresis **18:** 1252-1258

Sazuka T, Yamaguchi M, Ohara O (1999) Cyano2Dbase updated: linkage of 234 protein spots to corresponding genes through N-terminal microsequencing. Electrophoresis **20:** 2160-2171

Schmidt MW, Houseman A, Ivanov AR, Wolf DA (2007) Comparative proteomic and transcriptomic profiling of the fission yeast *Schizosaccharomyces pombe*. Mol Syst Biol **3**

Sergeyenko TV, Los DA (2000) Identification of secreted proteins of the cyanobacterium *Synechocystis* sp. strain PCC 6803. FEMS Microbiol Lett **193:** 213-216

Shen Y ZR, Belov ME, Conrads TP, Anderson GA, Tang K, Pasa-Tolic L,, Veenstra TD LM, Smith RD. (2001) Packed capillary reversed-phase liquid chromotaography with high-

performance electrospray ionization Fourier transform ion cyclotron resonance mass spectrometry for proteomics. Anal Chem **73:** 1766-1775

Simon WJ, Hall JJ, Suzuki I, Murata N, Slabas AR (2002) Proteomic study of the soluble proteins from the unicellular cyanobacterium *Synechocystis* sp. PCC6803 using automated matrix-assisted laser desorption/ionization-time of flight peptide mass fingerprinting. Proteomics **2:** 1735-1742

Singh AK, Bhattacharyya-Pakrasi M, Elvitigala T, Ghosh B, Aurora R, Pakrasi HB (2009) A systems-level analysis of the effects of light quality on the metabolism of a cyanobacterium. Plant Physiol **151:** 1596-1608

Singh AK, Elvitigala T, Bhattacharyya-Pakrasi M, Aurora R, Ghosh B, Pakrasi HB (2008) Integration of carbon and nitrogen metabolism with energy production is crucial to light acclimation in the cyanobacterium *Synechocystis*. Plant Physiol **148:** 467-478

Singh AK, Elvitigala T, Cameron JC, Ghosh B, Bhattacharyya-Pakrasi M, Pakrasi HB (2010) Integrative analysis of large scale expression profiles reveals core transcriptional response and coordination between multiple cellular processes in a cyanobacterium. BMC Systems Biology **4**: 105

Singh AK, McIntyre LM, Sherman LA (2003) Microarray analysis of the genome-wide response to iron deficiency and iron reconstitution in the cyanobacterium *Synechocystis* sp. PCC 6803. Plant Physiol **132:** 1825-1839

Srivastava R, Pisareva T, Norling B (2005) Proteomic studies of the thylakoid membrane of *Synechocystis* sp. PCC 6803. Proteomics **5:** 4905-4916

Suzuki I, Kanesaki Y, Mikami K, Kanehisa M, Murata N (2001) Cold-regulated genes under control of the cold sensor Hik33 in *Synechocystis*. Mol Microbiol **40:** 235-244

Suzuki S, Ferjani A, Suzuki I, Murata N (2004) The SphS-SphR two component system is the exclusive sensor for the induction of gene expression in response to phosphate limitation in *Synechocystis*. J Biol Chem **279:** 13234-13240

Tonella L, Hoogland C, Binz PA, Appel RD, Hochstrasser DF, Sanchez JC (2001) New perspectives in the *Escherichia coli* proteome investigation. Proteomics **1:** 409-423

Tsinoremas NF, Castets AM, Harrison MA, Allen JF, Tandeau de Marsac N (1991) Photosynthetic electron transport controls nitrogen assimilation in cyanobacteria by means of posttranslational modification of the glnB gene product. Proc Natl Acad Sci U S A **88:** 4565-4569

Wang Y, Sun J, Chitnis PR (2000) Proteomic study of the peripheral proteins from thylakoid membranes of the cyanobacterium *Synechocystis* sp. PCC 6803. Electrophoresis **21:** 1746-1754

Wegener KM, Welsh EA, Thornton LE, Keren N, Jacobs JM, Hixson KK, Monroe ME, Camp DG, 2nd, Smith RD, Pakrasi HB (2008) High sensitivity proteomics assisted discovery of a novel operon involved in the assembly of photosystem II, a membrane protein complex. J Biol Chem **283:** 27829-27837

Yang C, Hua Q, Shimizu K (2002) Quantitative analysis of intracellular metabolic fluxes using GC-MS and two-dimensional NMR spectroscopy. J Biosci Bioeng **93:** 78-87

Zhang Z, Pendse ND, Phillips KN, Cotner JB, Khodursky A (2008) Gene expression patterns of sulfur starvation in *Synechocystis* sp. PCC 6803. BMC Genomics **9:** 344

Table 1. Numbers of differentially regulated proteins under 12 environmental conditions.

Treatment	Number of Proteins			
	Differentially Abundant	Upregulated	Downregulated	Stress Specific
CO_2	312	192 (62%)	120 (38%)	16
Cold Shock	267	102 (38%)	165 (62%)	12
Heat Shock	382	214 (56%)	168 (44%)	12
Fe Depletion	401	235 (59%)	166 (41%)	12
Fe Repletion	375	244 (65%)	131 (35%)	21
N Depletion	553	77 (14%)	476 (86%)	26
N Repletion	381	231 (61%)	150 (39%)	29
NH_4 Repletion	398	257 (65%)	141 (35%)	18
P Depletion	356	268 (75%)	88 (25%)	4
P Repletion	415	316 (76%)	99 (24%)	5
S Depletion	395	247 (63%)	148 (37%)	18
S Repletion	376	275 (73%)	101 (27%)	19

Table 2. Concordance between transcriptomic and proteomic studies in *Synechocystis*.

	Cold Stress	Fe Depletion	P Depletion	S Depletion	N Depletion
Number of Genes Correlated	8	56	57	14	110
Number of Genes Anti-Correlated	13	53	16	5	26
Total genes differentially expressed in proteomic and transcriptomic datasets	21	109	73	19	136

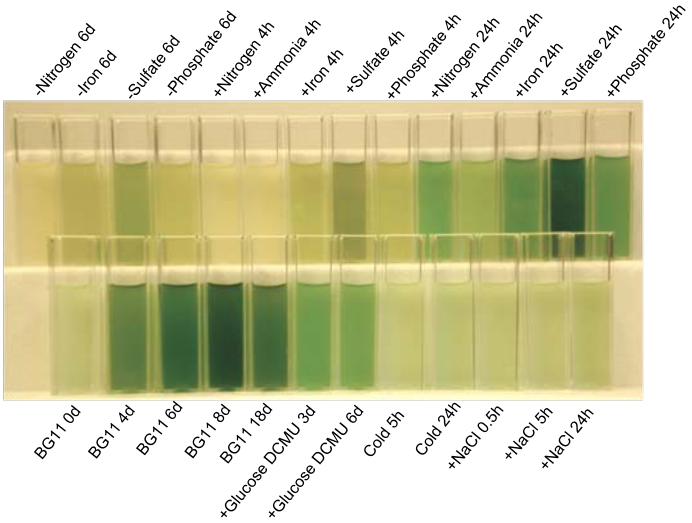

Fig. 1. Physiological characteristics of *Synechocystis* cultures used for proteomic analysis. *Synechocystis* cells were grown under various environmental conditions as described in the Experimental Procedures. At specific time points, 3 ml cultures were transferred to cuvettes and photographed.

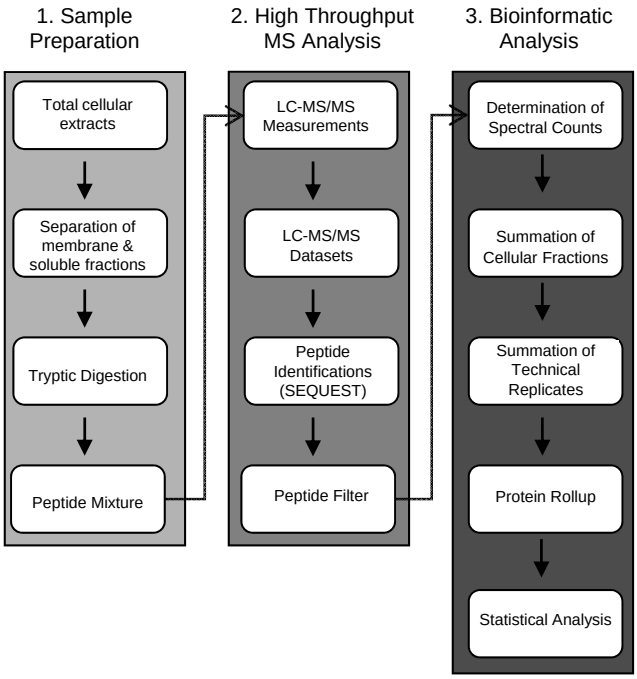

Fig. 2. Experimental Design. A flow chart describing various steps involved in the identification of *Synechocystis* proteome. Each step has been described in detail in the Experimental Procedures.

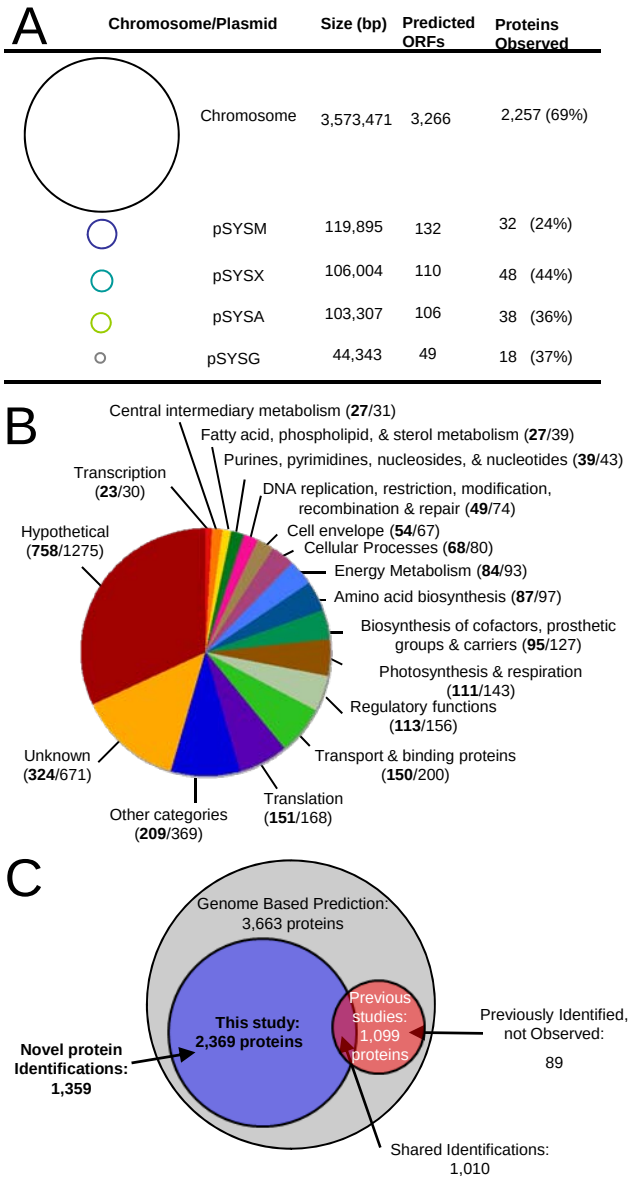

Fig. 3. Proteome Coverage. (A) Distribution of observed proteins among the different DNA elements. The numbers in parentheses indicate the observed proteins out of the total predicted proteins. (B) Distribution of the observed proteins in various functional categories. The numbers in parentheses indicate the observed proteins (bold font) out of the total predicted proteins. (C) Comparative analysis of proteins identified in this study (blue circle) with previously published proteomic studies (red circle) as a fraction of the predicted proteome (grey circle).

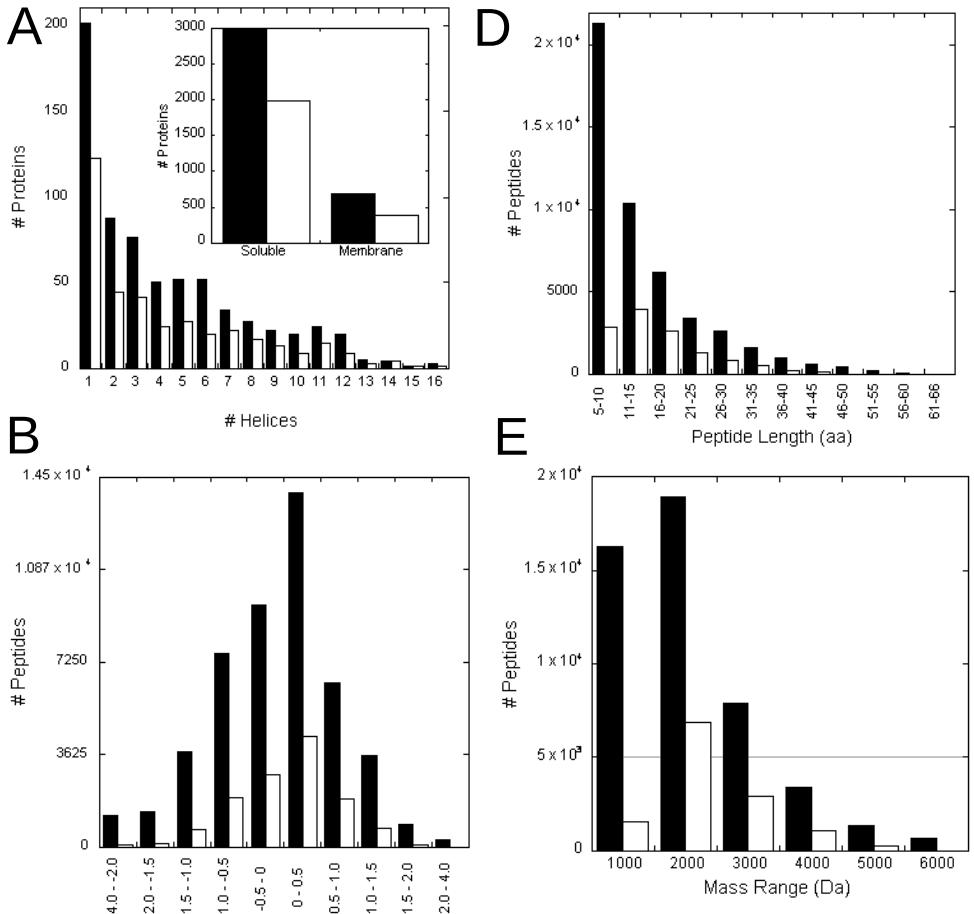

Fig. 4. Proteome Bias Analysis. Black and white bars indicate the numbers of predicted and observed proteins, respectively. (A) Detection of membrane proteins as a function of transmembrane helices. Inset shows the number of soluble and membrane proteins detected in the present study. (B) Detection of peptides of varying hydrophobicities versus the predicted peptides. (C) Detection of peptides of varying masses versus the predicted peptides. (D) Detection of peptides of varying lengths versus the predicted peptides. (E) Detection of peptides of varying pIs versus the predicted peptides.

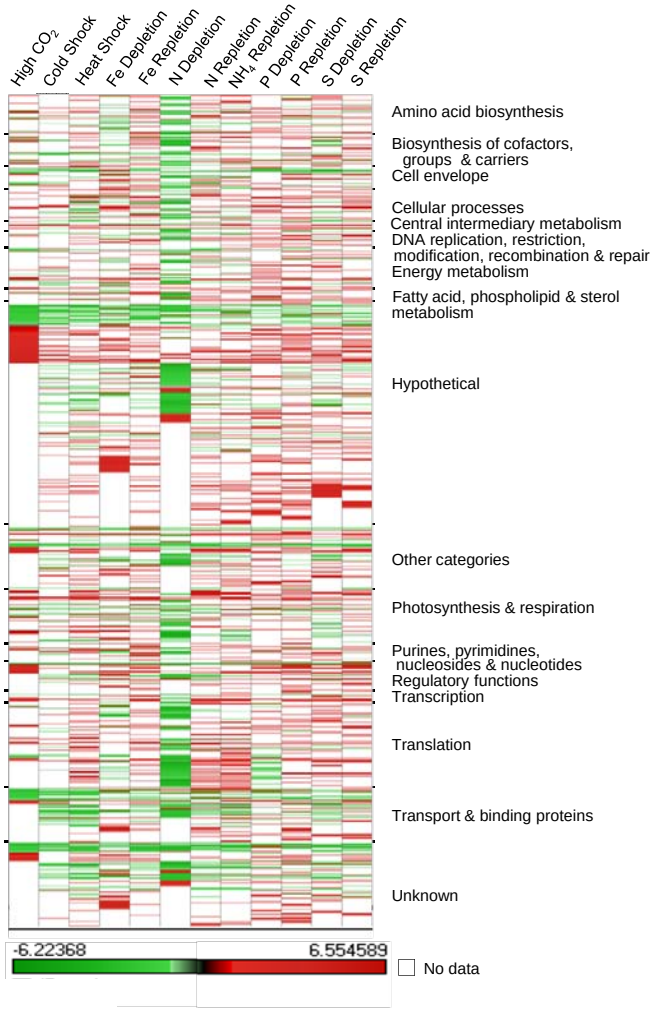

Fig. 5. Differential Regulation of Proteins under Different Perturbations. 1,221 differentially regulated proteins were grouped in functional categories and a heat map was generated using Spotfire 7.0. Color bar indicates protein fold change in experimental conditions as compared to levels in complete BG11.

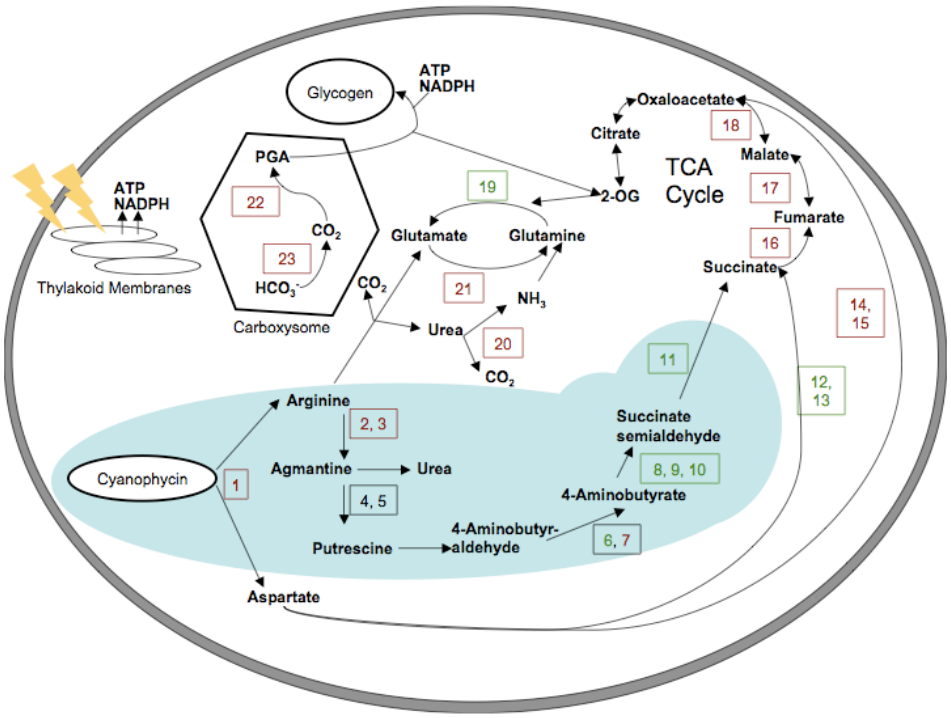

Fig. 6. Global Stress Response under Different Perturbations. Numbers denote the enzymes required for various reactions, colors indicate either increased (red) or decreased (green) protein abundances under stress conditions compared to those in the BG11 control sample. Black color indicates that proteins are not observed in BG11 control sample. Numbers correspond to the following enzymes: 1=cyanophycinase, 2 & 3=arginine decarboxylase, 4=agatinase, 5=arginase, 6 & 7=4-Aminobutryaldehyde dehydrogenase, 8-10=4-Aminobutyrate transaminase, 11=aldehyde dehydrogenase, 12=adenylosuccinate lyase, 13=L-argininosuccinate lyase, 14=L-aspartic acid oxidase, 15=aspartic acid aminotransferase, 16=succinyl-CoA synthetase, 17=succinate dehydrogenase, 18=malate dehydrogenase, 19=Glu synthase, 20=urease, 21=Glu-NH_3 ligase, 22= ribulose 1,5-bisphosphate carboxylase oxygenase, 23=carbon concentrating mechanism proteins. Abundance values for these proteins are provided in Dataset S6.

Chapter 3

HIGH SENSITIVITY PROTEOMICS ASSISTED DISCOVERY OF A NOVEL OPERON INVOLVED IN THE ASSEMBLY OF PHOTOSYSTEM II, A MEMBRANE PROTEIN COMPLEX

This chapter was adapted from:

Wegener KM, Welsh EA, Thornton LE, Keren N, Jacobs JM, Hixson KK, Monroe ME, Camp II DG, Smith RD, Pakrasi HB (2008) High sensitivity proteomics assisted discovery of a novel operon involved in the assembly of photosystem II, a membrane protein complex. *J Biol Chem* 283: 27829-27837.

SUMMARY

Photosystem II (PSII) is a large membrane protein complex that performs the water oxidation reactions of the photosynthetic electron transport chain in cyanobacteria, algae, and plants. The unusual redox reactions in PSII often lead to damage, degradation and reassembly of this molecular machine. To identify novel assembly factors for PSII, an accurate mass tag (AMT) high-sensitivity proteomic analysis of PSII complexes purified from the cyanobacterium *Synechocystis* sp. PCC 6803 was performed. This analysis identified six PSII associated proteins that are encoded by a single operon containing nine genes, *slr0144* to *slr0152*. This operon encodes proteins that are not essential components of the PSII holocomplex but accumulate to high levels in precomplexes lacking any of the lumenal proteins PsbP, PsbQ, or PsbV. The operon contains genes with putative binding domains for Chl and bilin, suggesting these proteins may function as a reservoir for cofactors needed during the PSII lifecycle. Genetic deletion of this operon shows that removal of these protein products does not alter photoautotrophic growth or PSII fluorescence properties. Nonetheless these proteins confer fitness under competition in high light intensities. However, the deletion mutation does result in decreased PSII-mediated oxygen evolution and an altered distribution of the S states of the catalytic Mn cluster. PSII complexes isolated from *Δsllr0144 – slr0152* also show decreased photosynthetic capacity and altered polypeptide composition. These data demonstrate that the proteins encoded by the genes in this operon are necessary for optimal function of PSII and function as accessory proteins during assembly of the PSII complex. Based on these results, we have named the products of the *slr0144 – slr0152* operon Pap (photosystem II assembly proteins).

INTRODUCTION

Photosystem II (PSII) is the multi-component enzyme complex in cyanobacteria, algae and plants that catalyzes the light-driven oxidation of water to molecular oxygen. The active complex is a dimer consisting of 2 identical monomers with more than 20 proteins, identified through genetic, biochemical, and structural studies. In addition to its protein components, PSII also has a large number of cofactors including chlorophylls (Chls), pheophytins, plastoquinones, Mn atoms, calcium, chloride, non-heme iron, and heme groups (Ferreira et al., 2004; Loll et al., 2005). Removal of these subunits or cofactors can slow or even completely halt water oxidation.

The assembly of this crucial complex is an intricate process. The steps of protein assembly into the complex are ordered and well regulated (Rokka et al., 2005). D2, cytochrome b_{559} and PsbI bind to form a receptor complex into which the D1 precursor protein (pD1) is inserted (Muller and Eichacker, 1999; Zhang and Aro, 2002). The CP47 protein then joins the precomplex, followed by the low molecular weight proteins PsbH, PsbM and PsbT. The C-terminal extension of pD1 is then processed by the lumenal protease CtpA into the mature D1 protein (Zhang and Aro, 2002). Next, the CP43 and PsbK proteins associate. At this point, the soluble lumenal extrinsic proteins (PsbO, PsbP, PsbQ, PsbU and PsbV) can also bind to the complex. These lumenal proteins are not essential for photosynthesis but are located in close proximity to the site of water oxidation, enhance oxygen evolution, and have roles in protecting the catalytic Mn cluster from damage (Seidler, 1996; Thornton et al., 2004). The presence of some of these proteins can be viewed as an indicator of the functional state of the complex, as PsbQ is solely associated with dimerized complexes that are fully assembled and highly active (Roose et al., 2007). Finally, the monomeric complex dimerizes. Figure 1 shows a simplified schematic of PSII assembly in cyanobacteria.

The steps involved in the association of cofactors with the functional complex are less defined. The mechanism of integration of some of these cofactors has been well documented, as is the case for the Mn cluster. It is known that after the incorporation of the CP43 protein, all of

the ligands for the $Mn_4Ca_1Cl_x$ cluster are present within the complex and presumably integration of this catalytic center occurs. However the integration of other cofactors, including the insertion of Chl into the Chl containing proteins D1, D2, CP47, and CP43, remains undefined.

In addition to the initial assembly of the subunit proteins and cofactors into this large membrane complex, PSII is frequently damaged in the course of its natural function (Keren et al., 2005). The D1 protein becomes irreversibly damaged and the lumenal proteins and the catalytic Mn cluster must be dissociated so that the damaged D1 protein can be removed and a new copy inserted into the complex (Andersson and Aro, 2001). Because many of the PSII cofactors would be highly detrimental in large quantities if free in the cell, it is likely there are chaperone proteins, which sequester these cofactors before assembly and during the repair and degradation of the PSII complex. As an example, Small CAB-like Proteins (SCPs) have recently been proposed to sequester Chls from damaged PSII complexes until they are recycled into new complexes (Vavilin and Vermaas, 2007). It is likely that intermediaries may also hold other cofactors of the complex during complex repair. Thus, in addition to the complexity of its composition, PSII also has an intricate lifecycle of repair and degradation. Therefore beside the stoichiometric components of the holocomplex necessary for enzyme activity, other accessory proteins must associate with PSII throughout its lifecycle to repair the protein components and recycle cofactors.

Although high-resolution crystal structures are available for cyanobacterial PSII (Ferreira et al., 2004; Loll et al., 2005), not all of the biochemically identified proteins and cofactors have been visualized in the current structures. Indeed the most comprehensive of these structures only displays 20 proteins and 77 cofactors per monomer (Loll et al., 2005). Previous analysis in *Synechocystis* sp. PCC 6803 utilizing the strain HT3, which contains a hexahistidine tag on the core membrane protein CP47 (Bricker et al., 1998), has identified 31 polypeptides associated with active PSII complexes using denaturing electrophoretic separation followed by MALDI mass spectrometry (MS) and N-terminal amino acid sequencing (Kashino et al., 2002). This analysis revealed that there were non-characterized PSII associated proteins that represent non-

stoichiometric proteins that transiently associate with the complex as well as stoichiometric complex members not part of the crystallized complex.

In this study, we undertook a global proteomics analysis of isolated PSII complexes, comparing protein profiles of HT3 to those of *ΔpsbV* HT3, *ΔpsbP* HT3, and *ΔpsbQ* HT3 in *Synechocystis* 6803. These mutants contain PSII complexes that have been arrested at the currently understood end point of assembly (see Fig. 1). The sensitivity of these techniques allowed for identification of not only the stoichiometric components of active PSII complexes, but also for the identification of proteins transiently associated with PSII throughout its lifecycle, such as assembly, repair, or degradation partners. From the results, we identified an operon of unknown function that contains binding domains for photosynthetic cofactors. This operon is syntenically conserved among cyanobacteria. Deletion of the operon shows that although it is not required for photoautotrophy, it does stabilize photosynthetic capacity, in whole cells and in isolated complexes, indicating a function in PSII-mediated activity. We have named the products of this operon Photosystem II assembly proteins (pap).

MATERIALS AND METHODS

Growth Conditions

All chemicals used for media and other experiments are from Sigma (St. Louis, MO) unless otherwise noted. *Synechocystis* cultures were grown at 30°C under 20 μmol photons m^{-2} s^{-1} white fluorescent light in TES buffered BG11 medium (Allen, 1968). Stock cultures were maintained on solid medium (BG11 supplemented with 1.5% (w/v) agar), and used to inoculate liquid cultures for each experiment. When needed for mutants, growth medium was supplemented with 10 μg/mL spectinomycin, 2 μg/mL gentamycin, and 10 μg/mL chloramphenicol (Cm). To create a putative mass tag (PMT) library, cultures were grown in complete BG11 as well as in media deplete of nitrogen, phosphorous, sulfur, or iron; media containing sodium chloride, 3-(3,4-dichlorophenyl)-1,1-dimethylurea (DCMU), or carbon dioxide; or cultures were subjected to heat or cold shock. Experiments utilizing low and high light were conducted at 10 and 100 μmol photons m^{-2} s^{-1}, respectively.

PSII Preparation

PSII was isolated from HT3, Δ*psbV* HT3, Δ*psbQ* HT3, and Δ*psbP* HT3 strains as described previously (Kashino et al., 2002). HT3 indicates the 6-His tagged CP47 used to affinity purify the complex (Bricker et al., 1998). The final eluate from a Ni-NTA Agarose (Qiagen, Inc., Valencia, CA) column was suspended in 50 mM MES-NaOH pH 6.0, 10 mM $CaCl_2$, 25% glycerol with 0.04% dodecyl maltoside. PSII was isolated from HT47GM (Roose, 2008) and Δ*slr0144–slr0152* HT47GM strains as described (Roose et al., 2007).

Spectrophotometric Assays

Cell growth was monitored by measuring light scattering at 730nm on a μQuant microplate spectrophotometer (Bio-Tek Instruments, Inc., Toronto, Canada). Chl concentrations were

determined by methanol extraction and absorbance at 652 and 665 nm in a DW2000 spectrophotometer (SLM-Aminco, Urbana, IL) (Porra et al., 1989).

AMT Peptide Identification

To create the AMT library, cellular samples were digested with sequencing grade modified trypsin (Promega, Madison, WI), using a ratio of 1:100 (wt/wt) protease to protein sample for 4 h at 37 °C. Digests were desalted using Supelco Superclean SCX tubes (St. Louis, MO) and the pH of each digestion was adjusted to 3.5 using formic acid. The SCX resin was conditioned with acetonitrile followed by 1M sodium formate. The column was washed with 25% acetonitrile in 500 mM ammonium acetate, pH 8.5 and re-equilibrated with 5% acetonitrile in 10 mM ammonium formate, pH 3.5. Peptide mixtures were loaded onto the resin and washed with 5% acetonitrile in 10 mM ammonium formate, pH 3.5. Peptides were eluted with 25% acetonitrile in 500 mM ammonium acetate, pH 8.5, followed by 100% acetonitrile. Eluted peptides were concentrated via Speedvac (ThermoSavant, San Jose, CA) to protein concentrations of 1.0 mg/mL, as determined by BCA assay (Pierce, Rockford, IL).

Peptides were putatively identified using a capillary liquid chromatography (LC) system, a pair of model 100mL 100DM syringe pumps (Teledyne-Isco, Lincoln, NE), a series D controller (Teledyne-Isco, Lincoln, NE) and an in-house manufactured mixer, capillary column selector, and sample loop. Separations were achieved with a 5000 psi reversed-phase in-house packed capillary (150 μm i.d., 360 μm o.d., 60 cm long; Polymicro Technologies, Phoenix, AZ) by using an exponential gradient of 2 mobile-phase solvents consisting of 0.2% acetic acid and 0.05% trifluroacetic acid (TFA) in water and 0.1% TFA in 90% acetonitrile. Flow through the capillary HPLC column was ≈1.8 μL/min when equilibrated to 100% mobile-phase 0.2% acetic acid and 0.05% TFA.

For each sample, 10 μg was infused into a LCQ conventional ion trap MS (ThermoFinnigan, San Jose, CA) operating in a data dependent MS/MS mode over a 400 to 2000

m/Z range. For each cycle, the 3 most abundant ions from MC analysis were selected for MS/MS analysis by using a collision energy setting of 45%. Dynamic exclusion was used to discriminate against previously analyzed ions. The collision induced dissociation spectra from the conventional ion trap mass spectrophotometer were analyzed using SEQUEST (Eng, 1994) and the genome sequence of *Synechocystis* 6803 (Nakamura et al., 1998). PMT identifications were made based on a SEQUEST cross correlation (Xcorr) score ≥ 2.0, regardless of charge or mass.

Using the same LC conditions, 5 μg of sample analyzed in the ion trap was then analyzed in duplicate or triplicate by FTICR-MS. The FTICR mass spectrometers use ESI interfaced with an electrodynamic ion funnel assembly coupled to a radio frequency quadropole for collisional ion focusing and highly efficient ion accumulation and transport to a cylindrical FTICR for cell analysis (Harkewicz et al., 2002).

The resultant FTICR data was processed using the PRISM Data Analysis system, software tools developed in-house. First the MS data was de-isotoped, giving the monoisotopic mass, charge, and intensity of the major peaks in each mass spectrum. Then the data was examined in a 2D fashion to find groups of mass spectral peaks that were observed in sequential spectra. Each group, known as a unique mass class (UMC), has a median mass, central normalized elution time (NET), and abundance estimate, computed by summing the intensities of the MS peaks that compromise the UMC. The identity of each UMC was determined by comparing the mass and NET of each UMC with the mass and NET's of the 4423 PMT's in the *Synechocystis* 6803 AMT database (generated using the peptides observed from 23 LC/MS/MS). Search tolerances were ± 6 ppm for the mass and ±5% of the total run time for the elution time.

PSII Proteomics

PSII preparations of approximately 1 mg protein were analyzed at Pacific Northwest National Laboratory (PNNL) for protein identification. The PSII samples were denatured by addition of equal volumes of 7 M urea, 2 M thiourea, and 1% CHAPS in 50 mM ammonium bicarbonate, pH 7.8 and then reduced with DTT to a final concentration of 5mM. $CaCl_2$ was added to a final

concentration of 1 mM. Samples were digested and analyzed utilizing the LC/MS process as described for AMT peptide identification above.

The peak matching process gives a list of peptide matches and observed abundance estimates for each of the samples. Since the samples were run in replicate (2-3 per sample), an average peptide abundance and corresponding standard deviation was computed for each peptide across the replicates. An abundance estimate for each of the identified open reading frames (ORFs) was computed by averaging the peptide abundance estimates for the ORF, using only those peptides whose intensities were ≥33% of the most abundant peptide for the given ORF. Over 200 top hits for peptides found in each of the PSII preparations were scanned for fold changes across the samples.

Statistical Analysis of Peptide Identification Data

A threshold of 0.18 units was applied to the peptide abundance data to discard all measurements below the chosen noise threshold. Replicate data for each peptide were averaged, and the average abundances used to calculate $\log_2$ (mutant / wild type) ratios for each peptide. Peptides that were not present in at least two replicates for both wild type and mutant were discarded. The remaining peptides were then used to calculate average $\log_2$ ratios for their respective proteins. Standard errors were calculated for the replicates. The results of this proteomics study have been deposited with NCBI under the accession number GSE9577.

Protein Visualization

SDS-PAGE was performed as described previously (Kashino Y, 2007), using a gel with 18-24% acrylamide gradient and 6 M urea. After transfer to 0.22 μm nitrocellulose, PsbO and PsbQ were detected by using specific antiserum against each protein, and both were reacted with goat-anti-rabbit horseradish peroxidase conjugated antiserum (Pierce Biotech, Rockford, IL) developed in West Pico (Pierce Biotech, Rockford, IL) for 5 min. PsbV was visualized by reacting its cofactor with SuperSignal West Pico Substrate (Pierce Biotech, Rockford, IL). Blots were visualized in a

Fujifilm LAS-1000plus imager (Fujifilm, Stamford, CT) for 1 to 5 min. Digital images were quantified using ImageJ software (Abramoff et al., 2004). Determinations of antibody linearity across proteins concentrations were done as previously described (Thornton et al., 2004).

RT-PCR

Total RNA was isolated from *Synechocystis* 6803 using Triazol reagent (GIBCO-BRL, Grand Island, NY) and purified using RNA Clean-Up Kit (Zymo Research, Orange, CA). Single cDNA strands were synthesized (Ogawa et al., 2002) using SuperscriptII (Invitrogen, Carlsbad, CA). Four primers were used in separate reactions to create cDNA to different overlapping sections of the operon (5'GGCATGCCAGTGTTGATGAE-3', 5'-AACAGGGGTTTTAATTTCCCG-3', 5'-GGTAA CACCATGGCCACCT-3', 5'-TCCTAGGGTCAT CATTTCTGC-3'). A primer for RNAseP (5'-ACCAAATTCCTCAAAGCG-3') provided a positive control. The cDNA was then treated with RNaseH (Invitrogen, Orange, CA) for 30 mins at 37°C and amplified by PCR to create four overlapping products. PCR primers used were 5'GGCATGCCAGTGTTGATGAT-3', 5'-TGAGC AAACAGTAACTTCCCC-3', 5'-AACAGGGGTT TTAATTTCCCG-3', 5'-GTTGGGAAGCCCAAA AGC, 5'-GGTAACACCATGGCCACCT-3', 5'-TGCACTGATTAGCGTTTTG-3', 5'-TCCTAGG GTCATCATTTCTGC-3', and 5'-CTGCCAAGCC AAACTGATTT-3' to amplify *slr0144 – slr0152* operon and 5'-ACCAAATTCCTCAAAGCG-3' and 5'-CAAACTTGCTGGGTAAC-3' to amplify RNaseP.

slr0144 – slr0152 Deletion Construction

The predicted ORFs of *slr0144*, *slr0145*, *slr0146, slr0147*, *slr0148*, *slr0149*, *slr0150*, *slr0151*, and *slr0152* were replaced by a Cm resistance gene. The 430 bps upstream of the *slr0144* ORF (PCR amplified using primers 5'-ACGTACGAGCTCACAAAGTTG GCCGGTCACTCC-3' and 5'-CATGGTCATAGCTGTTTCAACGGGCAAATGCTCTGAAA-3') and 460 bps downstream of the *slr0152* ORF (PCR amplified using primers 5'-ACGTACGCATGCAT TTCTGGCTAGTCATGGTGG-3' and 5'- GGCATGCCAGTGTTGATGAT-3') were cloned into

flanking positions of the Cm resistance gene in a pUC18 derivative. The construct was transformed into *Synechocystis* 6803 and segregation of the mutation confirmed by PCR. Knockout construction and segregation of mutant shown in Fig 7. To generate the *Δslr0144-slr0152* HT47GM mutant, the *Δslr0144-slr0152* mutation was introduced into the HT47GM strain, which contains a hexahistidine tag on the CP47 protein (Roose, 2008).

Fluorescence Measurements

Kautsky fluorescence induction and Q_A- reoxidation were measured at room temperature using a FL100 flash kinetic fluorometer (Photon Systems, Instruments, Brno, Czech Republic) with FluorWin software (version 3.6.3.3). The Chl concentration for each sample was adjusted to 5 µg of Chl/ml as measured on a DW2000 spectrophotometer (SLM-Aminco, Urbana, IL). The samples were dark-adapted for 3 min prior to measuring.

Steady State Oxygen Evolution

A Clarke-type electrode was used to determine the rate of photosynthetic oxygen evolution (Mannan and Pakrasi, 1993). Oxygen evolution was measured for whole cells at a concentration of 5 µg Chl/mL in the presence of 0.5 mM 2.6-dichloro-*p*-benzoquinone (Eastman-Kodak, Rochester, NY) and 1 mM K_3FeCN_6. Light intensity was adjusted by use of neutral density filters. Oxygen evolution for isolated PSII complexes was measured at 3 µg Chl/mL in 50 mM MES-NaOH (pH 6.0)/20 mM $CaCl_2$/0.5 M sucrose (Roose et al., 2007).

Flash Yield Oxygen Evolution and Calculation of S-state distribution

Flash yield oxygen evolution was measured on a bare platinum electrode (Artisan Scientific Co., Urbana, IL). Cells were incubated in the dark for 2 mins prior to electrode polarization at 0.65V for 10 s and a series of 16 flashes were applied. Data points were collected at intervals of 10 µs during the flash train. This data was then analyzed utilizing the in-house software program

Oxygen Revolution and peak data for each sample were fit to a four-step homogenous model of Mn cluster S-state cycling (Meunier, 1993). Model-fitting calculations were done using MathCad software (MathSoft Engineering and Education, Inc., Cambridge, MA).

Mixed Culture Experiments

The mixed culture experiments were performed essentially as described (Ivleva et al., 2000). WT and Δ*slr0144 – slr0152* were grown in a 50 ml liquid culture of BG11 until mid-exponential phase. Mixed cultures containing an equal number of WT and Δ*slr0144 – slr0152* cells were started at OD_{730nm} of 0.05 and grown under low (10 μmol photons m^{-2} s^{-1}), medium (30 μmol photons m^{-2} s^{-1}) or high (100 μmol photons m^{-2} s^{-1}) light. A sample was taken for DNA extraction every 72 h and the culture was diluted back to OD_{730nm} of 0.05. Each mixed culture was sub-cultured five times. PCR was used to analyze the *slr0144 – slr0152* locus in each isolated DNA sample. PCR products were separated on 1% agarose gels, visualised using the Kodak 1D Image Analysis software (Rochester, NY), and quantified using ImageJ software (Abramoff et al., 2004).

Mn Measurements

Concentrations of Mn were measured on an AA600 atomic absorption spectrophotometer (PerkinElmer Life Sciences, Wellesley, MA). PSII samples were diluted to 5 μg Chl/mL in deionized water before analysis. The Mn:PSII ratio was calculated based on 41 molecules of Chl/PSII (Kashino et al., 2002).

RESULTS

Identification of over 200 PSII associated proteins with differential abundance in lumenal protein mutants.

To look for assembly intermediates, we compared the protein composition of HT3 PSII and PSII isolated from the lumenal protein mutants Δ*psbV* HT3, Δ*psbQ* HT3, and Δ*psbP* HT3 (Bricker et al., 1998; Kashino et al., 2002; Thornton et al., 2004; Roose et al., 2007). The complexes were analyzed using LC/MS and the component peptides identified using the AMT library described in Chapter 2. This more sensitive global proteomic technique revealed over 200 proteins differentially expressed in the lumenal protein mutants as compared to the wild type HT3 (Sup Table 1). These additional proteins may represent factors that are not part of stable, mature complexes, but are associated transiently at some point during the PSII lifecycle, such as assembly, repair, and degradation partners.

Of those identified, 15 were proteins previously identified as PSII associated proteins (D1, D2, CP43, CP47, PsbE, PsbF, PsbH, PsbL, PsbO, PsbV, PsbU, PsbQ, Psb27, Psb28, and Psb29). To confirm the validity of this proteomic analysis, we compared levels of PSII stoichiometric components as determined by this proteomics analysis and by established immunological methods. Previous studies have shown that loss of any of the lumenal proteins results in a destabilization of the entire lumenal face of PSII and correlates with reduced levels of the other lumenal proteins (Roose and Pakrasi, 2004; Inoue-Kashino et al., 2005; Kashino et al., 2006; Roose et al., 2007). Levels of PsbO, PsbQ, and PsbV in the strains HT3, Δ*psbV* HT3, Δ*psbQ* HT3, and Δ*psbP* HT3 were analyzed by comparative immunoblotting experiments. These experiments demonstrated the decrease of additional lumenal proteins in the mutants as compared to the HT3 strain. The band intensities were calculated using ImageJ (Abramoff et al., 2004).

Comparison of the ratios of PsbO, PsbQ, and PsbV levels in the strains HT3, Δ*psbV* HT3, Δ*psbQ* HT3, and Δ*psbP* HT3 observed from the AMT analysis to ratios determined using immunological assays showed that the data from both detection methods closely corresponded, confirming the AMT methodology for quantification of protein abundances (Fig. 2). The linearity of band intensities across protein concentrations was confirmed using known amounts of these proteins expressed in *E. coli* (Fig. 3).

Previously, the interactions of the extrinsic proteins have been analyzed by the genetic deletion or affinity tagging of individual PSII subunit and analyzing the corresponding changes in the polypeptide profiles of the complex. In contrast, this high throughput approach provides a comprehensive data set to analyze PSII interactions. For instance, analysis of PsbQ using affinity tagging has shown that PsbQ is found solely in fully assembled complexes (Roose et al., 2007). Correspondingly, levels of PsbQ in complexes from Δ*psbV* HT3, and Δ*psbP* HT3 mutants are decreased (Fig. 4). Similarly, mutant analysis of Psb27 has shown that this protein associates with PSII pre-complexes which do not contain the lumenal proteins PsbO, PsbU, PsbV, and PsbQ and are not capable of oxygen evolution activity (Roose and Pakrasi, 2004; Nowaczyk et al., 2006; Mamedov et al., 2007; Roose and Pakrasi, 2008) and that functional complexes containing PsbQ do not contain Psb27 (Roose et al., 2007). Thus it is not surprising that levels of Psb27 increase in the Δ*psbV* HT3, Δ*psbQ* HT3, and Δ*psbP* HT3 PSII complexes (Fig. 4). Additionally, levels of PsbV have been shown to decrease in the absence of *psbQ* (Kashino et al., 2006), which corresponds to decreased levels of PsbV seen in all mutants in this study (Fig. 4). Psb28 and Psb29 are conserved among a variety of photosynthetic organisms and although they have been shown to display PSII association and function (Keren et al., 2005; Thornton et al., 2005; Kashino et al., 2007), their functions have not been elucidated. Thus it is intriguing that Psb28 increases significantly in abundance in all three mutants and Psb29 increases markedly in Δ*psbQ* HT3 and Δ*psbP* HT3 and decreases in Δ*psbV* HT3.

Of the 200 proteins initially identified, 50 were proteins of unknown function whose levels were altered significantly in the mutants as compared to HT3 (Sup Table 1). While a concomitant loss of additional proteins with the deletion of PsbP, PsbQ, and PsbV is well documented (Ifuku et al., 2005; Inoue-Kashino et al., 2005; Kashino et al., 2006; Roose et al., 2007), the large group of proteins that increased in abundance as a result of these deletions is intriguing. This group of proteins may represent assembly and degradation factors associated with the lifecycle-arrested complexes.

Proteins in a single genic cluster have increased abundance in ΔpsbV HT3, ΔpsbQ HT3, and ΔpsbP HT3 PSII complexes.

Analysis of the proteins that increased the most in the mutant PSII complexes revealed 4 proteins, Slr0146, Slr0147, Slr0149, and Slr0151, which were up to 12.5 times more abundant in the mutant PSII complexes. A closer look at the context of these proteins revealed that their ORFs are located within the same genic context in the *Synechocystis* genome (Fig. 5A).

Previously published microarray experiments describe this gene cluster, *slr0144 - slr0152*, as one of the most highly coordinated in *Synechocystis* and reveal that transcripts are downregulated in cells experiencing oxidative stress due to low iron or treatment with hydrogen peroxide (Singh et al., 2004). Additionally, expression of these genes is downregulated in mutants lacking photosystem I (PSI) or PSI and phycobilisome proteins (Singh et al., 2004). This suggests that the coordinated increase in protein levels observed in this study is not a general stress response and is specific to PSII function. RT-PCR experiments confirmed that the ORFs *slr0144 – slr0152* are located on a single transcript and thus are in an operon (data not shown).

It is important to note that Slr0144 and Slr0145 were also observed in the isolated PSII samples in several replicates, but because different peptides were observed in the HT3 and *ΔpsbV HT3, ΔpsbQ HT3,* and *ΔpsbP HT3 PSII* samples, we were not able to quantify those peptides in subsequent replicates. Thus, out of the nine ORF operon, only the products of 3

genes, *slr0148*, *slr0150*, and *slr0152*, were not observed to be associated with PSII. Slr0148, Slr0150, and Slr0152 are not included in the AMT database and thus nothing can be noted from their absence in this study. The Slr0144, Slr0145, Slr0146, Slr0147, Slr0149, and Slr0151 proteins are present at low levels in the HT3 complexes, as indicated by the low ion counts for the corresponding peptides (Sup Table 1). This agrees with the findings of Singh et al (2004) that the genes of the *slr0144* – *slr0152* cluster are transcribed at low levels. Intriguingly, these proteins are found only in a small set of cyanobacteria. However, in the species in which they are found, the genes of the *slr0144* – *slr0152* operon exhibit synteny, suggesting that the operon organization is important for its function (Fig. 5B).

The operon contains binding domains for cofactors important in photosynthesis.

Although the function of these proteins is unknown, their sequences provide interesting insights into possible roles in photosynthesis. All 9 proteins are predicted to be located in the cytoplasm (Juncker et al., 2003; Bendtsen et al., 2004). Many of these proteins contain binding motifs for cofactors involved in photosynthesis, as well as regulatory elements (Fig. 6). Slr0144 and Slr0147 both contain a 4-vinyl reductase (V4R) domain (Singh et al., 2004; Quevillon et al., 2005). This domain is predicted to be a small-molecule-binding domain (SMBD) and a protein containing this domain has been shown to be involved in Chl biosynthesis in *Rhodobacter capsulatus* (Anantharaman et al., 2001). These two proteins contain the only 2 V4R domains found in *Synechocystis* 6803. Slr0148 and Slr0150 are putative ferredoxins and contain motifs for 2Fe-2S iron-sulfur clusters, cofactors that mediate electron transfer and are found in the cytochrome b_6f complex and the PSI associated terminal ferredoxin (Singh et al., 2004; Quevillon et al., 2005). Additionally Slr0146 and Slr0149 have domains for the binding of bilins, a cofactor of the phycobilisome, the light harvesting system of cyanobacteria (Quevillon et al., 2005). Slr0151 contains a TPR (tetratricopeptide repeats) domain, hypothesized to be involved in protein-protein interactions, suggesting that these proteins may complex with each other or with as yet unidentified partners (Singh et al., 2004; Quevillon et al., 2005). Slr0152, also named PknD,

encodes a Ser/Thr kinase, which may function as a regulatory element for the operon (Singh et al., 2004; Quevillon et al., 2005).

Deletion of slr0144 - slr0152 does not alter photoautotrophic growth.

To investigate the role of the *slr0144 - slr0152* operon in PSII function, the entire coding region of the operon was deleted and replaced with a Cm resistance gene (Fig. 7). Deletion of the operon did not alter photosynthetic growth (Fig. 8A). Depletion of $CaCl_2$ from the culture media did not affect the rate of photoautotrophic growth, as seen in other PSII extrinsic mutants (Table 1). Growth of the mutant in high (100 µmol photons m^{-2} s^{-1}) or low (20 µmol photons m^{-2} s^{-1}) light conditions also showed no difference from wild type (Table 1).

The ∆slr0144 - slr0152 mutant displays normal fluorescence kinetics.

Fluorescence measurements with the deletion mutant did not exhibit any defects in PSII electron transfer. Measurements of fluorescence induction (Kautsky effect) show no differences among values for F_o, F_m, and F_v (data not shown). Similarly, measurements of Q_{A^-} reoxidation using the herbicide DCMU also showed no differences in these fluorescence parameters. This indicates that electron flow through the core of PSII is largely unaffected by the deletion of *slr0144 – slr0152*.

The ∆slr0144 – slr0152 mutant displays altered water oxidation.

Careful analysis revealed that the ∆*slr0144 – slr0152* mutant has impaired oxygen evolution activity (Fig. 8B). The mutant produces only ~80% as much oxygen as wild type, indicating an impairment of PSII complexes upon deletion of the *slr0144 – slr0152* operon. Further analysis of oxygen evolution by measuring flash oxygen yield showed a four period oscillation similar to wild type but with decreased yield in the ∆*slr0144 – slr0152* mutant (Fig. 8C). Quantification of this data revealed that prior to illumination, ∆*slr0144 – slr0152* shows no significant change in the percentage of centers at the S_0 state, but has a decreased percentage

of reaction centers in the S_1 state and increased percentages of centers in the S_2 and S_3 states. A similar increase in S2 stabilization is seen in the *ΔpsbV* mutants (Shen et al., 1998) (Fig 8D). Based on this data, we have named the products of the *slr0144 – slr0152* operon Photosystem II assembly proteins (Pap).

Slr0144 – Slr0152 confers fitness to Synechocystis

To further analyze and understand the cellular role of *slr0144 – slr0152*, we investigated its role in organismal fitness. We conducted a mixed culture experiment in which equal numbers of WT and Δ*slr0144 – slr0152* cells were incubated together in a single flask, forcing the two strains to compete for available nutrients. The flasks were subcultured every 3 d and samples were collected for PCR analysis to detect the amount of each strain present. This experimental setup has previously been described in detail (Ivleva et al., 2000).

While both strains showed similar ratios under low (10 μmol photons m^{-2} s^{-1}) or moderate (30 μmol photons m^{-2} s^{-1}) light intensities, there was an increase of the ratio of WT to Δ*slr0144 – slr0152* under high light (100 μmol photons m^{-2} s^{-1}) intensities. After the fifth subculture timepoint (5), the PCR band corresponding to Δ*slr0144 – slr0152* is no longer detectable (Fig. 9). Thus Δ*slr0144 – slr0152* confers a fitness advantage under high light.

Isolated Δslr0144 – slr0152 PSII complexes have reduced activity and altered composition

To determine the role of *slr0144 – slr0152 in PSII assembly and function,* PSII complexes were isolated and analyzed from the mutant using the strain Δ*slr0144 – slr0152* HT47GM via a histidine tag on the core PSII protein CP47. Analysis of protein profiles by SDS-PAGE normalized by Chl concentrations showed that there were significant changes in protein levels in Δ*slr0144 – slr0152* HT47GM*,* particularly an increase in the low molecular weight proteins Sll1390, Psb27, PsbE, PsbV, and PsbQ (Fig 10A). However, if the isolated complexes were loaded by equal protein concentrations, most of the protein levels appeared unaltered in Δ*slr0144 – slr0152*

HT47GM as compared to HT47GM, with the exception of an increase in Sll1390 and PsbV (Fig 10A). Analysis of Chl concentrations per amount of protein present (determined by BCA assays) in the isolated complexes revealed that Δ*slr0144 – slr0152* HT47GM complexes contain 70% of the Chl of WT complexes (Table 2). Western blots for the CP47 and D1 proteins confirmed that the levels of these proteins are unchanged when isolated PSII complexes are loaded on the basis of protein, but when complexes are loaded on an equal Chl basis, there is a significant decrease in the amount in the multi-Chl containing protein CP47 as compared to the D1 protein, which only contains 2 Chl molecules (Fig. 10B). However there is no significant difference of the Chl concentration per cell between WT and Δ*slr0144 – slr0152* (Table 2), suggesting that Chl biosynthesis itself is largely unaffected by the removal of these genes. This indicates that the loss of the *slr0144 – slr0152* proteins has a dramatic affect on Chl integration in PSII. It is also possible that there is a decrease in Chl integration in PSI complexes.

Analysis of Mn content of the isolated complexes using atomic absorption spectroscopy showed that there was no difference in Mn content when compared on a per mg protein basis (Table 3). This indicates that the catalytic Mn clusters are assembled in the mutant complex. However, isolated Δ *slr0144 – slr0152* HT47GM PSII complexes have only 30% activity compared to HT47GM complexes, regardless of how the samples are loaded (Table 4). Thus Slr0144 – Slr0152 function to stabilize oxygen evolution independent of manganese cluster formation.

DISCUSSION

Identification of novel PSII-associated proteins.

Using a sensitive proteomic approach to investigate the composition of PSII, we identified over 200 proteins associated with the complex, 169 more proteins than had been identified using more conventional methods. Additionally, the small number of PSI and PSI-associated proteins that were identified in the proteomics study (5% of the total identified proteins) suggest that the PSII samples were relatively pure and that the majority of the proteins identified are indeed PSII associated. These additional proteins may represent factors that are transiently associated with PSII and play roles in complex assembly, repair, or degradation. In the past, it has proven difficult to identify these proteins due to the relatively short periods of association in comparison to stable mature, active PSII complexes. This type of proteomics analysis is a valuable tool in investigating proteins involved in the complex assembly of PSII.

Identification of a novel operon involved in PSII activity.

Using established histochemical methods, we were able to confirm that this proteomic approach is an accurate method to establish quantitative protein profiles in isolated PSII complexes. Of the 50 PSII associated proteins identified with unknown functions, four of the proteins that were increased in abundance in the PSII mutants were located in a single genic region. These proteins are encoded in a 9-gene operon known to be highly coordinated transcriptionally and at least six operon products co-purify with PSII complexes. Additionally, the *slr0144* – *slr0152* operon contains domains for binding the cofactors Chl, 2Fe-2S iron sulfur centers, and bilin, which are all components of the electron transport chain.

The conservation of synteny of the operon, along with the diversity of the cyanobacterial species (mesophiles, thermophiles, and nitrogen fixers) in which the genes of the *slr0144* – *slr0152* operon has been observed suggests that these genes play an important role in cellular processes. Thus it is intriguing that only two of the genes, *slr0150* and *slr0152*, are conserved in

higher photosynthetic organisms (Altschul et al., 1997), suggesting that the mode of this action is specific to cyanobacteria.

It has long been known that genes in bacterial operons undergo coordinated transcriptional regulation. However, it is unclear whether those transcripts then undergo coordinated translation and assembly into a complex, though there are examples such as the ribosomal operons. Because the Slr0144, Slr0145, Slr0146, Slr0147, Slr0149, and Slr0151 proteins co-purified with PSII complexes under stringent conditions, it appears that not only is transcription of this operon tightly regulated, as shown by Singh *et al*. (2004), but also that the transcripts undergo coordinated translation and bind to the same complex.

Role of Paps in PSII assembly and function.

Because there is no change in photoautotrophic growth of the ∆*slr0144 – slr0152* mutant in any of the conditions tested, this suggests that the role of *slr0144 – slr0152* is non-essential and primarily involved in increasing photosynthetic efficiency. Additionally, the lack of altered fluorescence kinetics suggests that the core complex of PSII is fully assembled in ∆*slr0144 – slr0152.* Thus it is intriguing that in high light, Sll0144 – Slr0152 provide a competitive fitness advantage. However, the decrease in PSII activity suggests that with the loss of the Paps there are a decreased number of fully assembled PSII complexes. Alternatively this decreased PSII activity could also be due to complexes, which are fully assembled but are somehow impaired for photochemistry.

The ∆*slr0144 – slr0152* mutation demonstrates a case of cross talk between the lumenal and cytosolic proteins of PSII. It is intriguing that deletion of the lumenal proteins PsbP, PsbQ, and PsbV lead to an increase in abundance in the cytosolic Pap proteins (Supplemental Table 1) and conversely, the deletion of the Pap proteins results in increased levels in PsbV, Sll1390, and Psb27 (Fig. 10A), which all contain targeting sequences for the lumen. The increase of these proteins in non-fully assembled PSII complexes suggest that the Pap proteins function in assembly of complexes and are aggregating on these sub-assembled complexes or are

functioning in degrading the non-fully functional complexes. Additionally, the decrease in oxygen evolution activity and the altered S state distribution in the Δ*slr0144 – slr0152* mutant are phenotypes traditionally associated with mutation in the lumenal PsbO, PsbU, PsbV, PsbQ, and PsbP proteins (Shen et al., 1998; Thornton et al., 2004; Kashino et al., 2006), suggesting that the lumenal side of the complex is unstable in the absence of the Pap proteins. This suggests that there is feedback across the membrane plane of PSII that increases Pap protein levels when the lumenal surface is non-fully assembled and that the Pap proteins are necessary to fully assemble the lumenal side of PSII.

PSII has an intricate lifecycle and the rudimentary steps of assembly have been elucidated. However the assembly of the proteins and cofactors are not yet fully understood. The discovery of Paps may aid our understanding how the non-protein cofactors are inserted or recycled into new and repaired complexes. It is possible that the PSII defects seen in this study indicate that Slr0144 and Slr0147 function to sequester Chl molecules to prevent damage to the cell prior to initial complex assembly and during repair, similar to the SCP proteins (Vavilin and Vermaas, 2007). Future work demonstrating that the cofactor binding sites of the Pap proteins are functional and that they are able to transfer cofactors could provide exciting insight into how these cofactors are assembled into the complex. Additionally, Pap proteins shed new light on the crosstalk that must occur between the cytosolic and lumenal compartments of the cyanobacterial cell. A model of Pap-containing PSII complexes is shown in Figure 11.

In addition, future work will need to focus on whether Paps are key to PSII assembly or if they aid in assembly of other complexes in the electron transport chain. Because the operon contains binding domains for 2Fe-2S clusters and bilin, cofactors of cytochrome b_6f complex, ferredoxins, and the phycobilisome, in addition to domains for Chl binding which is integral to both PSI and PSII function, Pap must serve as a cofactor repository for the entire photosynthetic chain. Preliminary data suggests that the deletion of *slr0144 – slr0152* does not affect the abundance or connectivity of PSI or the phycobilisome, perhaps because these systems are less

sensitive to the affects of the removal of *pap* on than PSII. However, it is clear from this study that these proteins play an important role in PSII.

REFERENCES

Abramoff MD, Magelhaes PJ, Ram SJ (2004) Image processing with ImageJ. Biophotonics International **11:** 36-42

Allen MM (1968) Simple conditions for growth of unicellular blue-green algae on plates. J Phycol **4:** 1-4

Altschul SF, Madden TL, Schäffer AA, Zhang J, Zhang Z, Miller W, Lipman DJ (1997) Gapped BLAST and PSI-BLAST: a new generation of protein database search programs. Nucleic Acids Res **25:** 3389-3402

Anantharaman V, Koonin EV, Aravind L (2001) Regulatory potential, phyletic distribution and evolution of ancient, intracellular small-molecule-binding domains. J Mol Biol **307:** 1271-1292

Andersson B, Aro EM (2001) Photodamage and D1 Protein Turnover. *In* EM Aro, B Andersson, eds, Regulation of Photosynthesis, Vol 11. Kluwer, Dordrecht, pp 377-394

Bendtsen JD, Nielsen H, von Heijne G, Brunak S (2004) Improved prediction of signal peptides: SignalP 3.0. J Mol Biol **340:** 783-795

Bricker TM, Morvant J, Masri N, Sutton HM, Frankel LK (1998) Isolation of a highly active photosystem II preparation from *Synechocystis* 6803 using a histidine-tagged mutant of CP47. Biochim Biophys Acta **1409:** 50-57

Eng J, McCormack AL, Yates JR (1994) An approach to correlate tandem mass spectral data of peptides with amino acid sequences in a protein database. J Am Soc Mass Spectrom **5:** 976-989

Ferreira KN, Iverson TM, Maghlaoui K, Barber J, Iwata S (2004) Architecture of the photosynthetic oxygen-evolving center. Science **303:** 1831-1838

Harkewicz R, Belov ME, Anderson GA, Pasa-Tolic L, Masselon CD, Prior DC, Udseth HR, Smith RD (2002) ESI-FTICR mass spectrometry employing data-dependent external ion selection and accumulation. J Am Soc Mass Spectrom **13:** 144-154

Ifuku K, Yamamoto Y, Ono TA, Ishihara S, Sato F (2005) PsbP protein, but not PsbQ protein, is essential for the regulation and stabilization of photosystem II in higher plants. Plant Physiol **139:** 1175-1184

Inoue-Kashino N, Kashino Y, Satoh K, Terashima I, Pakrasi HB (2005) PsbU provides a stable architecture for the oxygen-evolving system in cyanobacterial photosystem II. Biochemistry **44:** 12214-12228

Ivleva NB, Shestakov SV, Pakrasi HB (2000) The carboxyl-terminal extension of the precursor D1 protein of photosystem II Is required for optimal photosynthetic performance of the cyanobacterium *Synechocystis* sp. PCC 6803. Plant Physiol **124:** 1403-1412

Juncker AS, Willenbrock H, Von Heijne G, Brunak S, Nielsen H, Krogh A (2003) Prediction of lipoprotein signal peptides in Gram-negative bacteria. Protein Sci **12:** 1652-1662

Kashino Y HT, Pakrasi HB, Satoh K (2007) Preparation of membrane proteins for analysis by two-dimensional gel electrophoresis. J Chromatogr B Analyt Technol Biomed Life Sci **849:** 282-292

Kashino Y, Inoue-Kashino N, Roose JL, Pakrasi HB (2006) Absence of the PsbQ protein results in destabilization of the PsbV protein and decreased oxygen evolution activity in cyanobacterial photosystem II. J Biol Chem **281:** 20834-20841

Kashino Y, Lauber WM, Carroll JA, Wang Q, Whitmarsh J, Satoh K, Pakrasi HB (2002) Proteomic analysis of a highly active photosystem II preparation from the cyanobacterium *Synechocystis* sp. PCC 6803 reveals the presence of novel polypeptides. Biochemistry **41:** 8004-8012

Kashino Y, Takahashi T, Inoue-Kashino N, Ban A, Ikeda Y, Satoh K, Sugiura M (2007) Ycf12 is a core subunit in the photosystem II complex. Biochim Biophys Acta **1767:** 1269-1275

Keren N, Liberton M, Pakrasi HB (2005) Photochemical competence of assembled photosystem II core complex in cyanobacterial plasma membrane. J Biol Chem **280:** 6548-6553

Loll B, Kern J, Saenger W, Zouni A, Biesiadka J (2005) Towards complete cofactor arrangement in the 3.0 A resolution structure of photosystem II. Nature **438:** 1040-1044

Mamedov F, Nowaczyk MM, Thapper A, Rogner M, Styring S (2007) Functional characterization of monomeric photosystem II core preparations from *Thermosynechococcus elongatus* with or without the Psb27 protein. Biochemistry **46:** 5542-5551

Mannan RM, Pakrasi HB (1993) Dark heterotrophic growth conditions result in an increase in the content of photosystem II units in the filamentous cyanobacterium *Anabaena variabilis* ATCC 29413. Plant Physiol **103:** 971-977

Meunier P (1993) Oxygen evolution by Photosystem II: the contribution of backward transitions to the anomalous behavior of double-hits revealed by a new analysis method. Photosyn Res **36:** 111-118

Muller B, Eichacker LA (1999) Assembly of the D1 precursor in monomeric photosystem II reaction center precomplexes precedes chlorophyll a-triggered accumulation of reaction center II in barley etioplasts. Plant Cell **11:** 2365-2377

Nakamura Y, Kaneko T, Hirosawa M, Miyajima N, Tabata S (1998) CyanoBase, a www database containing the complete nucleotide sequence of the genome of *Synechocystis* sp. strain PCC6803. Nuc Acids Res **26:** 63-67

Nowaczyk MM, Hebeler R, Schlodder E, Meyer HE, Warscheid B, Rogner M (2006) Psb27, a cyanobacterial lipoprotein, is involved in the repair cycle of photosystem II. Plant Cell **18:** 3121-3131

Ogawa T, Bao DH, Katoh H, Shibata M, Pakrasi HB, Bhattacharyya-Pakrasi M (2002) A two-component signal transduction pathway regulates manganese homeostasis in *Synechocystis* 6803, a photosynthetic organism. J Biol Chem **277:** 28981-28986

Porra RJ, Thompson WA, Kriedemann PE (1989) Determination of accurate extinction coefficients and simulatneous equations for assaying chlorophylls a and b extracted with

four different solvents: verification of the concentration of chlorophyll standards by atomic absorption spectroscopy. Biochim Biophys Acta **975:** 384–339

Quevillon E, Silventoinen V, Pillai S, Harte N, Mulder N, Apweiler R, Lopez R (2005) InterProScan: protein domains identifier. Nucleic Acids Res **33:** W116-120

Rokka A, Suorsa M, Saleem A, Battchikova N, Aro EM (2005) Synthesis and assembly of thylakoid protein complexes: multiple assembly steps of photosystem II. Biochem J **388:** 159-168

Roose JL (2008) Assembly and function of cyanobacterial photosystem II. Washington University in St. Louis, St. Louis

Roose JL, Kashino Y, Pakrasi HB (2007) The PsbQ protein defines cyanobacterial Photosystem II complexes with highest activity and stability. Proc Natl Acad Sci U S A **104:** 2548–2553

Roose JL, Pakrasi HB (2004) Evidence that D1 processing is required for manganese binding and extrinsic protein assembly into photosystem II. J Biol Chem **279:** 45417-45422

Roose JL, Pakrasi HB (2008) The Psb27 protein facilitates manganese cluster assembly in Photosystem II. J Biol Chem **283:** 4044-4050

Seidler A (1996) The extrinsic polypeptides of Photosystem II. Biochim Biophys Acta **1277:** 35-60

Shen JR, Qian M, Inoue Y, Burnap RL (1998) Functional characterization of *Synechocystis* sp. PCC 6803 delta psbU and delta psbV mutants reveals important roles of cytochrome c-550 in cyanobacterial oxygen evolution. Biochemistry **37:** 1551-1558

Singh AK, Li H, Sherman LA (2004) Microarray analysis and redox control of gene expression in the cyanobacterium *Synechocystis* sp. PCC 6803. Physiol Plant **120:** 27-35

Thornton LE, Ohkawa H, Roose JL, Kashino Y, Keren N, Pakrasi HB (2004) Homologs of plant PsbP and PsbQ proteins are necessary for regulation of photosystem II activity in the cyanobacterium *Synechocystis* 6803. Plant Cell **16:** 2164-2175

Thornton LE, Roose JL, Ikeuchi M, B. PH (2005) The Low Molecular Weight Components: New Insights from Proteomics, Genomics, and Structural Studies. *In* T Wydrzynski, Satoh, K., ed, Photosystem II: The Light-Driven Water:Plastoquinone Oxioreductase. Springer, Dordrecht

Vavilin D, Vermaas W (2007) Continuous chlorophyll degradation accompanied by chlorophyllide and phytol reutilization for chlorophyll synthesis in *Synechocystis* sp. PCC 6803. Biochim Biophys Acta **1767:** 920-929

Zhang L, Aro EM (2002) Synthesis, membrane insertion and assembly of the chloroplast-encoded D1 protein into photosystem II. FEBS Lett **512:** 13-18

Table 1. Rates of Photoautotrophic Growth for Δ*slr0144 - slr0152* and WT. Relative rates are based on ΔOD_{730nm}/24 hours for WT at med light. Standard deviation is given for n=3.

Strain	Condition	ΔOD_{730nm}/ 24 h	Relative Rate
WT	Med Light	0.163±0.015	100%
Δ*slr014–slr0152*	Med Light	0.176±0.050	107%
WT	High light	0.192±0.090	118%
Δ*slr014–slr0152*	High light	0.166±0.028	102%
WT	Low light	0.122±0.055	75%
Δ*slr014–slr0152*	Low light	0.117±0.008	72%
WT	-$CaCl^2$	0.014±0.003	9%
Δ*slr014–slr0152*	-$CaCl^2$	0.024±0.009	15%

Table 2. Analysis of isolated PSII complexes. Protein measurements determined by BCA assay of 25uL purified PSII. Measurements for chlorophyll and cell number (OD_{730nm}) were determined spectrophotometrically. Standard deviation is given for n=3.

Sample	**Type**	**Chl (ug/mL)/ OD_{730nm}**	**[protein] (ug/mL)**	**[chl] (ug/mL)**	**[chl] / [protein]**
HT47GM	Whole Cells	20.95 ± 0.21	-	-	-
HT47GM	PSII	-	3511	14	0.0039
Δ*slr0144 – slr0152* HT47GM	Whole Cells	20.81 ± 0.18	-	-	-
Δ*slr0144 – slr0152* HT47GM	PSII	-	3223	9	0.0028

Table 3. Manganese levels/chlorophyll and proteins levels. Mn content per PSII sample, measured by atomic absorption spectra

Sample	Mn (ug/L)	Mol Mn per g chl	Mol Mn per g protein
HT47GM	29.7	3.14E-6	1.57E-5
Δ*slr0144 – slr0152* HT47GM	42.7	1.55E-4	1.71E-5

Table 4. Oxygen evolution rates of isolated complexes. Oxygen evolution was measured on a Clark-type electrode in the presence of 1 mM potassium ferricyanide and 0.5 mM DCBQ at 8250 μmol photons m^{-2} s^{-1} white light. Standard deviation is given for n=3.

Sample	O_2 evolution (umol O_2/mg chl/hr)	O_2 evolution (umol O_2/mg protein/hr)
HT47GM	862.3 ± 35	216
Δ*slr0144-slr0152* HT47GM	254.3 ± 39	90

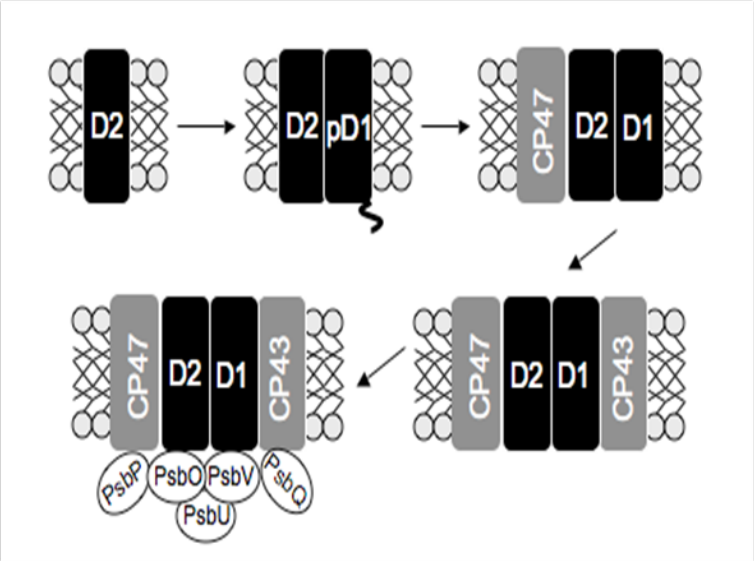

Fig. 1. Schematic of PSII assembly. The pre-D1 protein (pD1) is inserted into the pre-complex containing D2. CtpA processes pD1 and CP47 joins the complex. The last core protein CP43 is then assembled. The lumenal proteins PsbP, PsbQ, PsbO, PsbV, and PsbU then bind, forming the functional PSII complex.

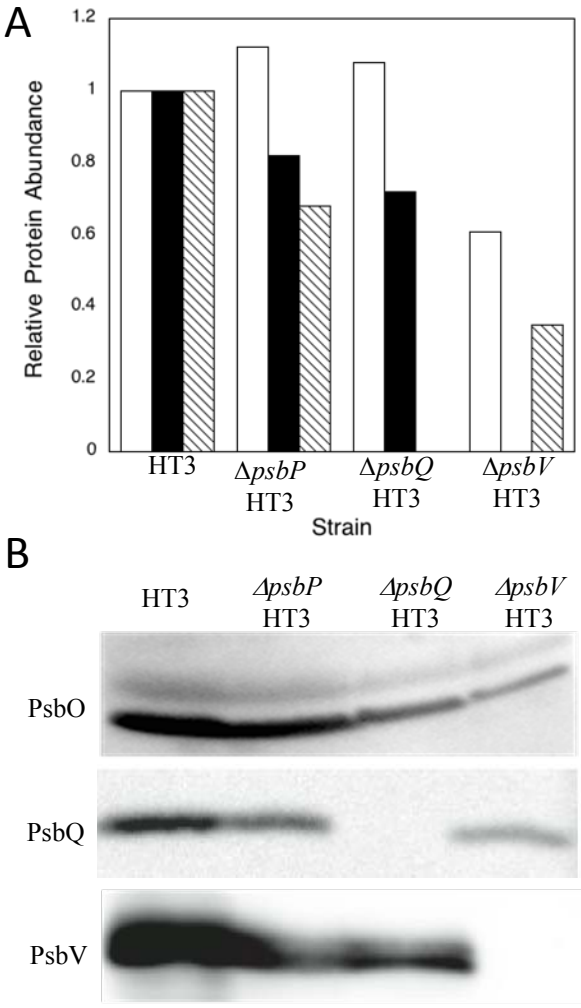

Fig. 2. Comparison of protein quantification determined by proteomic and immunoblot analysis. (**A**) Levels of PsbO (white bars), PsbV (black bars), and PsbQ (hashed bars) as determined by proteomics analysis. (**B**) Western blot analysis of PsbO, PsbQ, and PsbV. (**C**) Comparison of PsbO, PsbQ, and PsbV levels as determined from proteomic and from immunoblot analysis, as quantified by ImageJ software. n.d – not detected.

C

Protein	Mutant	Relative Amounts (Mutant/HT3)	
		Proteomics	Immunoblot
PsbO	*ΔpsbP* HT3	1.12	0.91
	ΔpsbQ HT3	1.00	0.69
	ΔpsbV HT3	0.61	0.61
PsbQ	*ΔpsbP* HT3	0.68	0.71
	ΔpsbQ HT3	n.d.	n.d.
	ΔpsbV HT3	0.35	0.43
PsbV	*ΔpsbP* HT3	0.82	0.68
	ΔpsbQ HT3	0.72	0.56
	ΔpsbV HT3	n.d.	n.d.

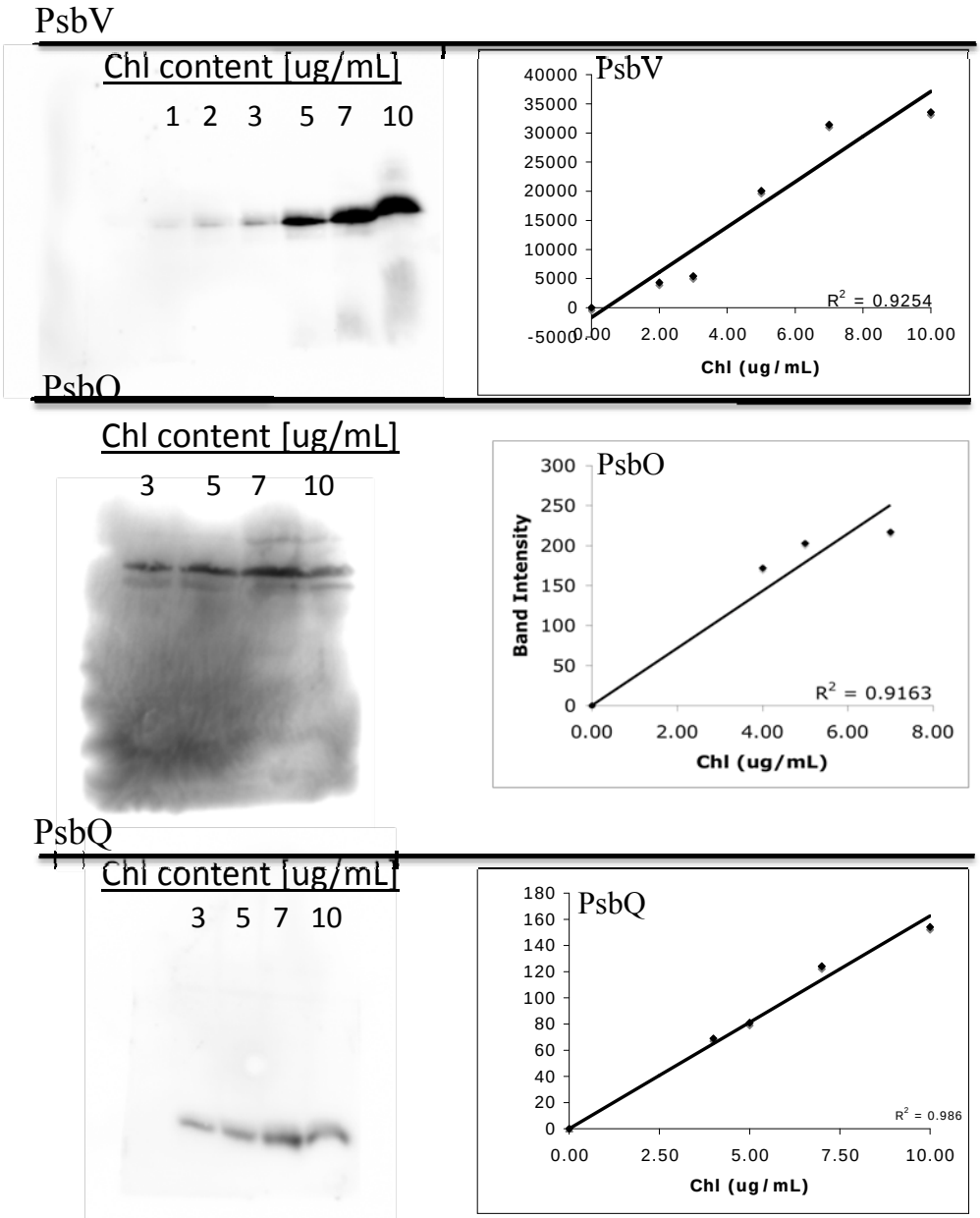

Fig 3. Linearity of PsbO, PsbQ, and PsbV over a range of concentrations. The linear range of PsbO, PsbQ, and PsbV detection in isolated PSII complexes was determined by comparative immunoblotting. The signal intensity for each antigen band (determined using ImageJ) was plotted against the chlorophyll concentration of HT3 PSII loaded. Each line was generated as a standard linear curve fit.

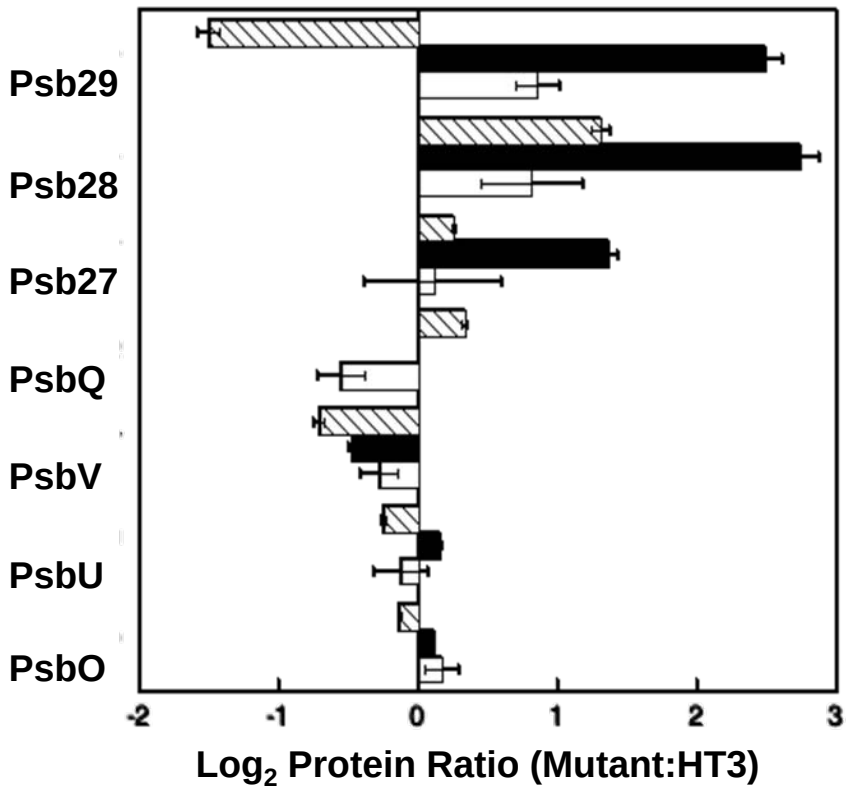

Fig. 4. Levels of PSII extrinsic proteins in Δ*psbP* HT3, Δ*psbQ* HT3, and Δ*psbV* HT3. Levels are determined as the $\log_2$ ratio of ion counts for the corresponding protein in Δ*psbP* HT3 (white bars), Δ*psbQ* HT3 (black bars), and Δ*psbV* HT3 (hashed bars) PSII as compared to HT3 PSII. Error bars indicated standard error.

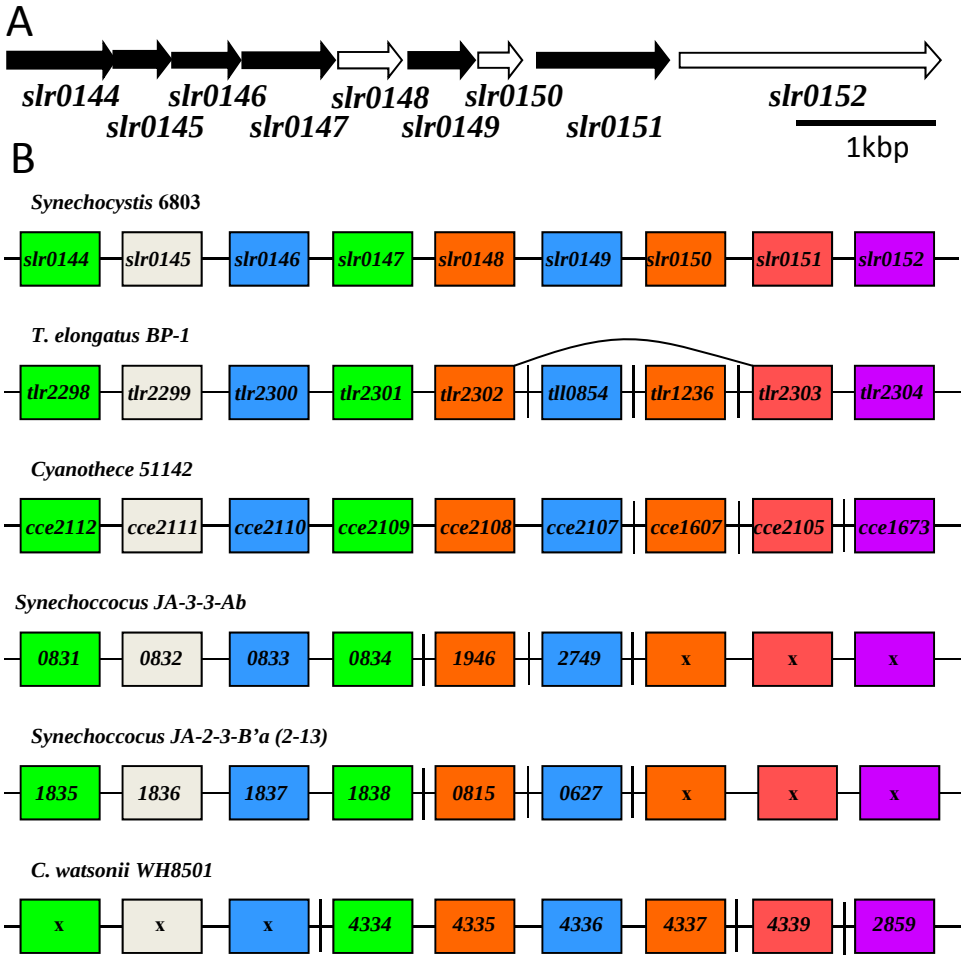

Fig. 5. The *slr0144 – slr0152* operon in *Synechocystis* 6803 and other cyanobacteria. (A) Organization of the *slr0144 – slr0152* operon in Synechocystis 6803. Arrows in black indicate ORFs whose products were observed to be differentially expressed in PSII complexes isolated from various mutant strains. **(B)** Synteny of the *slr0144 – slr0152* operon in various cyanobacteria. / indicates genes are not clustered together. X indicates that there is no ortholog in the genome. The numbers correspond to the gene designation or contig number in various cyanobacteria. Data used for this analysis are from the EMBL/GenBank data libraries with accession numbers: *Synechocystis* 6803 [BA000022, AP004310, AP004311, AP004312, AP006585]; *T. elongatus BP-1* [BA000039]; *Cyanothece* sp. ATCC 51142 [NC010547].

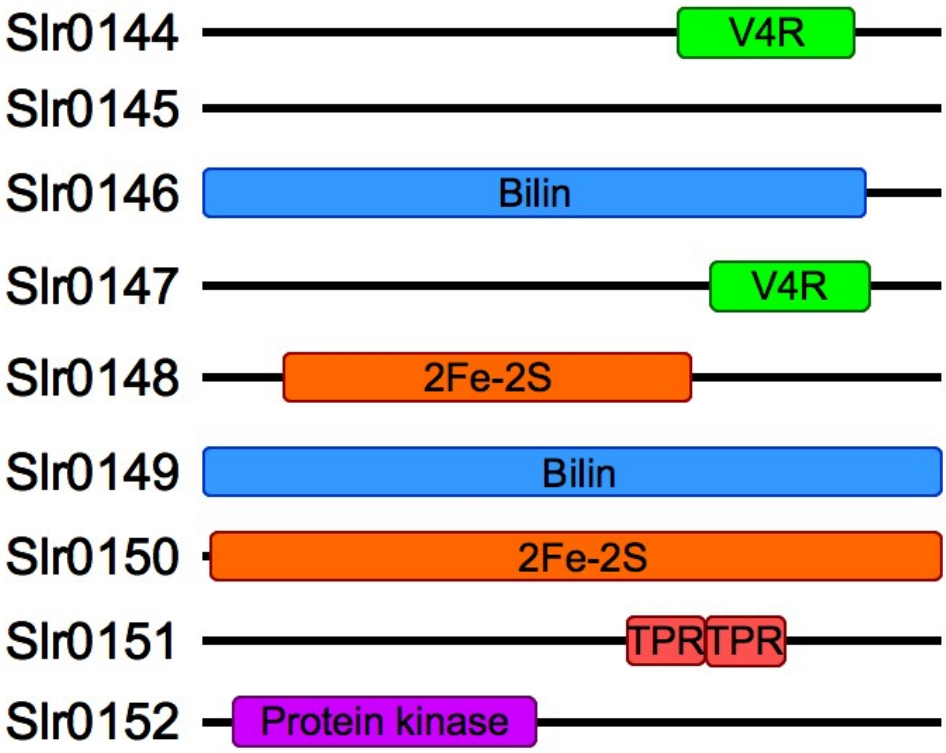

Fig. 6. The predicted domains of Slr0144 – Slr0152 proteins.
slr0144 and *slr0147* contain V4R domains that are predicted to bind chlorophyll. *slr0146* and *slr0149* contain putative bilin binding domains. *slr0148* and *slr0150* contain putative 2Fe-2S cluster binding domains. Additionally, *slr0151* contains two TPR domains and *slr0152* contains a putative protein kinase domain.

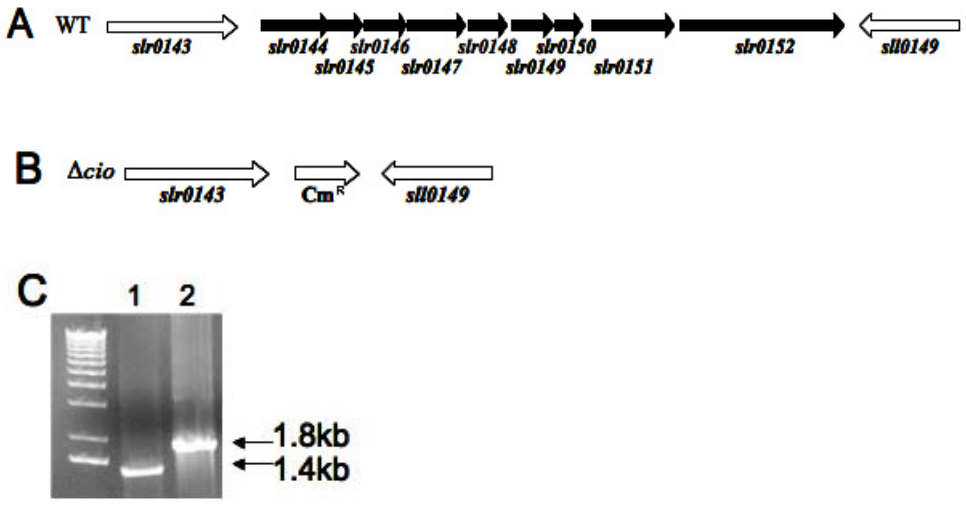

Fig. 7. Construction of Δ*slr0144 – slr0152* mutant. The *slr0144 – slr0152* locus in (**A**) WT and in (**B**) Δ*slr0144 – slr0152* mutant in which the operon is replaced by a chloramphenicol resistance gene. Genes of the *slr0144 – slr0152* operon are indicated in black. (**C**) PCR of the *slr0144 – slr0152* locus in WT (1) and Δ*slr0144 – slr0152* (2) cells.

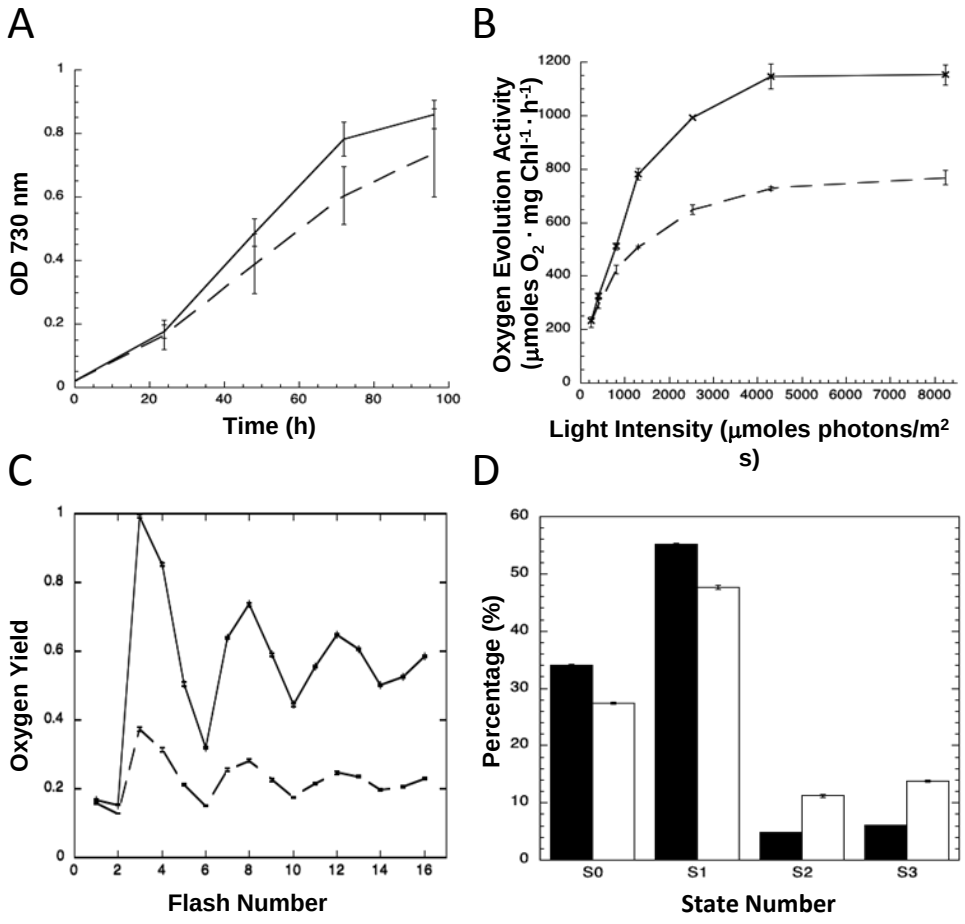

Fig. 8. Growth and activity of Δ*slr0144 – slr0152* mutant strain.
(**A**) Photoautotrophic growth of Δ*slr0144 – slr0152* (dashed line) and WT (solid line) in BG11 medium. Error bars represent the standard deviation of the mean (n=3). (**B**) Oxygen evolution of Δ*slr0144 – slr0152* (dashed line) and WT (solid line) in BG11 medium. Error bars represent the standard deviation of the mean (n=3) (**C**) Flash induced oxygen evolution of Δ*slr0144 – slr0152* (dashed line) and WT (solid line). Error bars represent the standard deviation of the mean (n=4). (**D**) Quantification of S-state distribution from flash oxygen evolution of the *slr0144 – slr0152* mutant (indicated by white bars) and WT (black bars). Error bars represent the standard deviation of the mean (n=4).

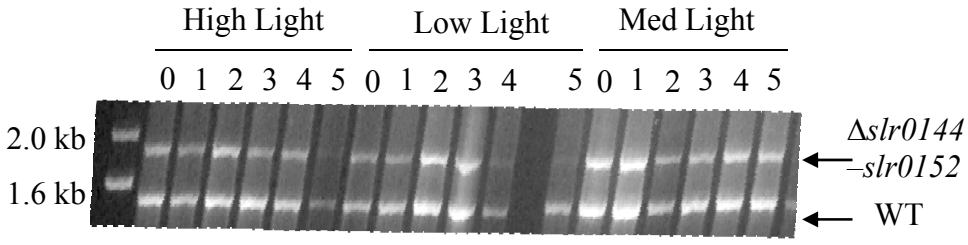

Fig. 9. Competition of WT and Δ*slr0144–slr0152* grown under low (10 μmol photons m^{-2} s^{-1}), medium (30 μmol photons m^{-2} s^{-1}) or high (100 μmol photons m^{-2} s^{-1}) light. At each time point, genomic DNA was isolated and PCR conducted to determine the relative abundance of each strain. A representative gel is shown.

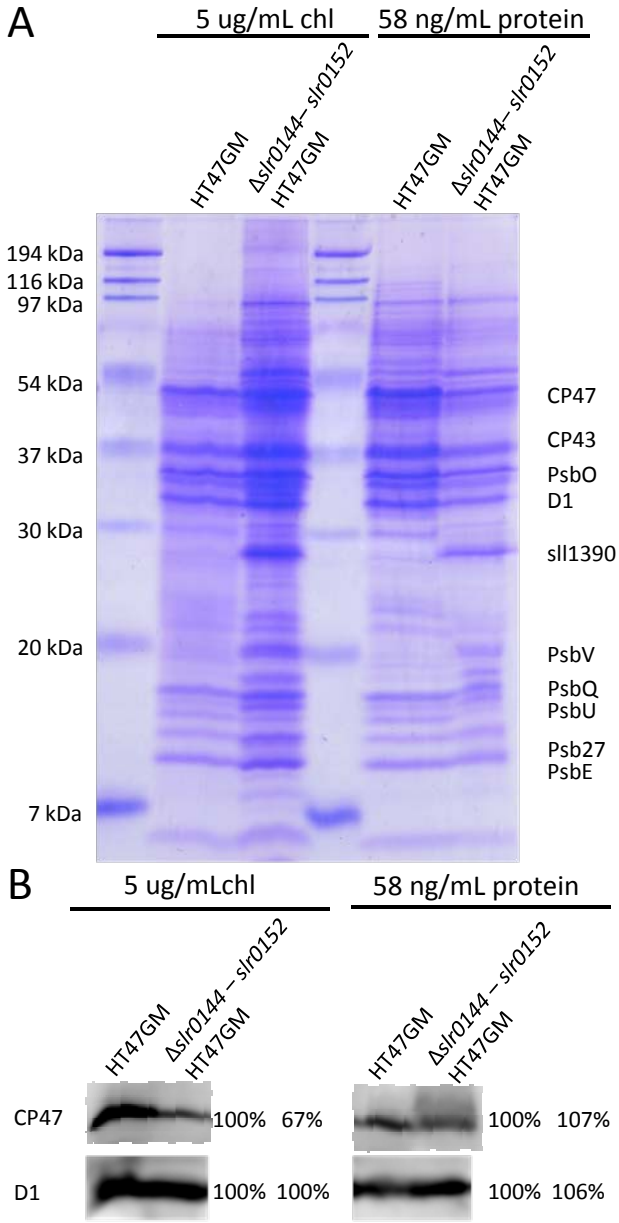

Fig. 10. Protein composition of isolated HT47GM and Δ*slr0144–slr0152* HT47GM PSII complexes. (A) SDS-PAGE protein profiles of PSII complexes loaded on an equal chlorophyll or protein basis. **(B)** Immunoblots of CP47 and D1 proteins in isolated complexes loaded by equal chlorophyll or protein levels. ImageJ used for quantification.

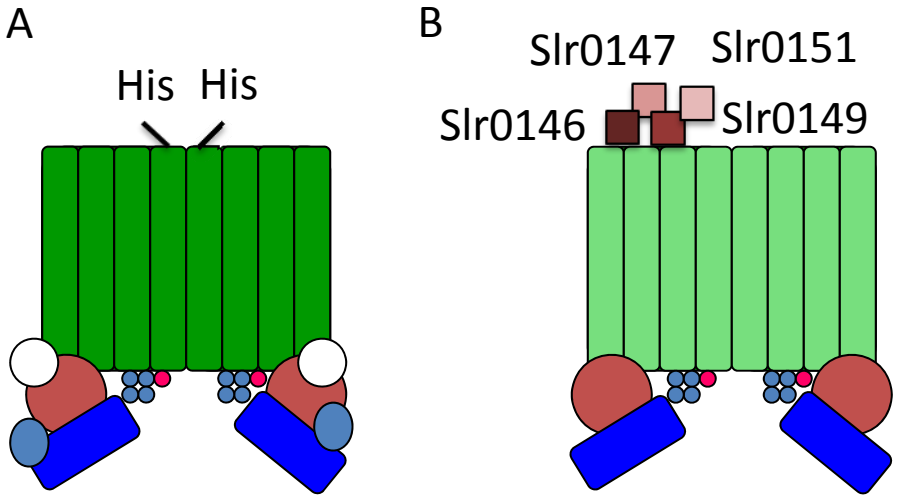

Fig. 11. Model of Pap-containing PSII. (A) Diagram of PSII complexes isolated using a histidine tag on CP47 **(B)** Diagram of Pap-containing PSII complexes.

Chapter 4

THE Psb32 PROTEIN AIDS IN REPAIRING PHOTODAMAGED PHOTOSYSTEM II

SUMMARY

Photosystem II (PSII), a membrane protein, catalyzes photochemical oxidation of water to molecular oxygen. This enzyme complex consists of approximately 20 stoichiometric protein components. However, due to the highly energetic reactions it catalyzes as part of its normal activity, PSII is continuously damaged and repaired. With advances in protein detection technologies, an increasing number of sub-stoichiometric PSII proteins have been identified, many of which aid in the biogenesis and assembly of this protein complex. Psb32 (Sll1390) has previously been identified as a protein associated with highly active purified PSII preparations from the cyanobacterium *Synechocystis* sp. PCC 6803. To investigate its function, we analyzed subcellular localization of Psb32 and the impact of genetic deletion of the *psb32* gene on PSII. Here we show that Psb32 is an integral membrane protein, primarily located in the thylakoid membranes. Although not required for cell viability, Psb32 protects cells from oxidative stress and additionally confers a selective fitness advantage in mixed culture experiments. Specifically, Psb32 protects PSII from photodamage and accelerates its repair. Thus, we propose that Psb32 plays an important role in minimizing the effect of photoinhibition on PSII.

INTRODUCTION

Oxygenic photosynthesis is a series of enzymatic reactions in which photons are converted to chemical energy in cyanobacteria and chloroplasts. Photosystem II (PSII) is the first enzyme complex of the pathway, oxidizing water into molecular oxygen, generating protons that are used for ATP generation, and electrons which move down the electron transport chain to ultimately reduce NADP. This reaction and many of the core proteins of PSII evolved in cyanobacteria and thus are conserved in the chloroplasts of higher photosynthetic organisms.

Crystallographic studies of cyanobacterial PSII show that the complex contains at least 20 proteins and 70 cofactors, including chlorophylls, carotenoids, and manganese (Loll et al., 2005). However, *in vivo*, at any one time, organisms contain a mixed population of PSII complexes. Traditionally, studies have relied on isolation of PSII using a histidine tag on the large core protein CP47. Because insertion of CP47 is an early step in biogenesis, these isolations actually contain a complex mixture of fully assembled active PSII complexes, damaged complexes with reduced activity, and partially assembled complexes containing accessory proteins. SDS-PAGE separation of traditional purifications of active PSII, followed by mass spectrometry and N-terminal sequencing revealed that even highly active purified PSII may have as many as 31 polypeptides associated (Kashino et al., 2002). Recently, high throughput liquid chromatography tandem mass spectrometry analysis of active PSII complexes from *Synechocystis* sp. PCC 6803 (hereafter *Synechocystis*) without initial PAGE separation identified over 200 proteins (Wegener et al., 2008). Closer analysis of some of these non-stoichiometric proteins shows that they are indeed associated with sub populations of complexes and are not contaminants. In particular, cyanobacterial PsbP is associated with 5% of all PSII complexes (Thornton et al., 2004).

Study of these partially assembled complexes has revealed that PSII biogenesis and repair requires a host of accessory proteins. Some well studied examples of these assembly proteins include CtpA, a protease which must process the D1 protein before PSII can be

assembled (Roose and Pakrasi, 2004). Other accessory proteins identified through proteomic study of PSII (Kashino et al., 2002; Wegener et al., 2008) include Psb27, which was subsequently shown to aid in assembly of the catalytic manganese cluster (Nowaczyk et al., 2006; Roose and Pakrasi, 2008) and Psb29, which provides PSII tolerance to high light intensities (Wang, 2004; Keren et al., 2005).

This assembly process is crucial to photosynthesis, because although light is required for photosynthetic reactions, it is also damaging to the photosynthetic reaction centers. In particular PSII is highly susceptible to light damage, termed photodamage (Powles, 1984; Prásil et al., 1992; Aro et al., 1993; Andersson and Aro, 2001). Photodamage is repaired by *de novo* protein synthesis, allowing PSII function returns to normal (Prásil et al., 1992; Aro et al., 1993; Andersson and Aro, 2001). This damage and repair cycle allows photosynthesis to function at certain light intensities. While photodamage occurs constantly, it increases proportionally with light intensity (Park et al., 1995; Tyystjärvi and Aro, 1996; Anderson and Chow, 2002; Nishiyama et al., 2004). When the rates of damage exceed the rates of repair, PSII is no longer functional, a process termed photoinhibition.

In addition to light, reactive oxygen species (ROS) can also cause damage to PSII. ROS can be produced as a byproduct of the light reactions of photosynthesis. Reduction of oxygen by photosystem I, the acceptor side of photosynthesis, can lead to the generation of superoxide radicals (O_2^-), which can convert to hydrogen peroxide (H_2O_2) and hydroxyl radicals ($^{\cdot}OH$) (Asada, 2003). On the donor side, transfer of excitation energy from chlorophyll to oxygen can result in the production of singlet oxygen ($^1O_2$) (Knox and Dodge, 1985; Asada, 2003). Cells have many strategies for dealing with ROS, including antioxidants, like α-tocopherol and β-carotene, and ROS scavenging enzymes, such as superoxide dismutase (Asada, 2003; Havaux et al., 2005). However, like photodamage and repair, this cycle of ROS damage and repair can also be stressed by increased light intensity so that damage accumulates (Asada, 2003).

To maintain photosynthesis, the PSII enzyme undergoes frequent turnover, due mainly to irreversible damage of the D1 protein (Andersson and Aro, 2001; Aro et al., 2005). The damaged

D1 protein must be detected, proteolytically removed and replaced with a newly synthesized copy, a process that requires at least partial disassembly of the complex. The removal of the D1 protein is suspected to require partial disassembly of the complex by requiring the dissociation of the lumenal proteins and the catalytic manganese cluster. Specifically, the manganese atoms of the oxygen evolving center and the extrinsic proteins must be released from the damaged complex, and then re-bound to newly assembled PSII centers to restore activity (Roose and Pakrasi, 2004).

Another sub-stoichiometric protein, Sll1390, which we have named Psb32, was also identified through PSII proteomic studies (Kashino et al., 2002; Wegener et al., 2008). In isolated PSII complexes lacking either of the lumenal proteins PsbQ or PsbP, levels of Psb32 were increased 1.24 and 1.19 fold respectively as compared to WT PSII complexes (Wegener et al., 2008). However in isolated complexes lacking the lumenal protein PsbV, Psb32 levels were decreased to 0.57 of the levels found in WT complexes (Wegener et al., 2008). Recent large-scale proteomics studies of *Synechocystis* under various nutrient stresses showed that Psb32 was present under all conditions tested (14 peptides identified, 53.8% coverage), with the exception of the early stages of recovery with ammonia after nitrogen starvation (Wegener, KM, Singh, AK, Jacobs, JM, Elvitigala, T, Welsh, EA, Keren, N, Gritsenko, MA, Ghosh, BK, Camp II, DG, Smith, RD, and Pakrasi, HB, Mol Cel Proteomics, under review). Indeed the quantitative subset of these experiments showed that Psb32 levels were severely decreased in sulfur and nitrogen starvation, as were all other PSII proteins observed (Wegener et al., 2010, under review).

To date, only one homolog of Psb32, TLP18.3 (At1g54780) in *Arabidopsis thaliana* has been investigated (Sirpio et al., 2007). TLP18.3 was identified by proteomic study of 2D SDS/PADE of thylakoid-associated polysome nascent chain complexes, the site of translation in the chloroplast for many of the nuclear encoded photosynthetic proteins. While plants lacking TLP18.3 showed no significant phenotypes under normal growth conditions, these mutants did

display increased susceptibility to photoinhibition and altered growth under fluctuating light. The authors found that this was due to decreased efficiency of repair of PSII due to decreased D1 turnover and decreased complex dimerization (Sirpio et al., 2007).

In this work, we show that Psb32 is located in the primarily thylakoid membranes and is an integral membrane protein. While not necessary for cell viability, Psb32 provides protection from oxidative stress. The presence of Psb32 confers fitness in mixed culture experiments. Additionally Psb32 protects cells from photodamage and accelerates PSII repair. Taken together, these data suggest that Psb32 associates with PSII during the assembly process and facilitates repair of damaged complexes.

MATERIALS AND METHODS

Bioinformatics Analyses

Signal peptides, TMHs, and domains were predicted using LipoP, SignalP, TMHMM, and InterPro Scan (Krogh et al., 2001; Juncker et al., 2003; Bendtsen et al., 2004; Quevillon et al., 2005). The phylogenic tree was generated by blasting the Psb32 (Sll1390) amino acid sequence from CyanoBase (Nakamura et al., 1998) against all non redundant genomes in NCBI GenBank (Benson et al., 2008). All free-living organisms above the cutoff of 1e-4 were used. Sequences were aligned and generated into a tree in MAFTT v6.0 (Katoh et al., 2002). The tree was refined using Fig Tree v1.3.1 (available at http://tree.bio.ed.ac.uk/software).

Bacterial Strains and Culture Conditions

Synechocystis sp. PCC 6803 was grown at 30 °C with 30 μmol photons m^{-2} s^{-1} of white light in BG11 media (Allen, 1984). The mutant Δ*psb32* was supplemented with 10ug/mL Cm. Growth was monitored using OD_{730nm} on a μQuant Biotek plate reader (Bio-Tek Instruments, Winooski, VT). For H_2O_2 growth experiments, cells were incubated with 0, 0.5, 1, or 1.5 mM H_2O_2 under 30 μmol photons m^{-2} s^{-1} of white light. For rose bengal growth experiments, cells were incubated with 7.5 μM rose bengal and 200 μmol photons m^{-2} s^{-1} white light. For methyl viologen growth experiments, cells were incubated with 0, 0.5, 1, or 1.5 μM methyl viologen under 30 μmol photons m^{-2} s^{-1} white light.

Antibody Generation and Immunological Detections

To generate the polyclonal Psb32 antibody, the *psb32* gene was cloned, without the signal and C-terminal transmembrane sequences, into the pET41b expression system (Novagen, San Diego, CA) using primers anti 1390F and anti 1390R (Table I). Antibodies against the purified protein were raised in rabbits (Cocalico Biologicals, Reamstown, CA). The polyclonal PsbV

antibody was raised in rabbits against the internal surface exposed peptide N-CGLADLAGAEPRRDN-C (Sigma Genosys, The Woodlands, TX). All other antibodies used in this work have been previously described (Zak et al., 2001). Membrane fractions were separated using SDS-PAGE (20% acrylamide, 6M urea), blotted to nitrocellulose, and incubated with antisera. Chemiluminescent signals were developed with Immobilon HRP reagent (Millipore, Billerica, MA) and visualized with a Fujifilm LAS-1000 plus imager (Fujifilm, Stamford, CT).

Psb32 Localization

Membranes were isolated as previously described (Norling et al., 1998). Plasma membranes and thylakoid membranes were separated with a two-phase dextran PEG polymer system (Keren et al., 2005). Total membranes (100 µg chlorophyll/ml) were treated with Triton X-114 to disrupt weak protein membrane associations (Bricker and Sherman, 1984).

Mutant Strain Generation

The Δ*psb32* mutant was generated by PCR amplification of a 5' section of *psb32* using primers 1390F upstream and 1390R upstream and of a 3' section of psb32 using primers 1390F downstream and 1390R downstream (see Table I for primer sequences). The fragments were cloned into puc118 where they flanked a chloramphenicol resistance cassette.

RT-PCR

To assay expression of *psb32* and the downstream gene *sll1866* in the Δ*psb32* mutant, we preformed RT-PCR as described previously (Wegener et al., 2008) with the following modifications. Random hexamer primers (Invitrogen, Carlsbad, CA) were used to generate cDNA with Superscript II reverse transcriptase (Invitrogen). Primers used for PCR of cDNA can be found in Table I.

Mixed Culture Experiments

The mixed culture experiments were performed essentially as described (Ivleva et al., 2000). WT and Δ*psb32* were grown in a 50 ml liquid culture of BG11 until mid-exponential phase. Mixed cultures containing an equal number of WT and Δ*psb32* cells were started at OD_{730nm} of 0.05 and grown under 5 (LL), 45 (GL) or 150 (HL) μmol photons m^{-2} s^{-1}. A sample was taken for DNA extraction every 72 h and the culture was diluted back to OD_{730nm} of 0.05. Each mixed culture was sub-cultured five times. PCR was used to analyze the *psb32* locus in each isolated DNA sample. PCR products were separated on 1% agarose gels, visualized using the Kodak 1D Image Analysis software (Rochester, NY), and quantified using ImageJ software (Abramoff et al., 2004).

Photoinhibition and recovery

Three d old cultures of WT and Δ*psb32* (3 μg/mL chlorophyll) were incubated at 30°C for 1 h at 20 μmol μmol photons m^{-2} s^{-1} red and blue LED light (Photon System Incorporated, Czech Republic) and bubbled with air. To induce photoinhibition, 20 μg/ml of the protein synthesis inhibitor lincomycin (Sigma; St. Louis, MO) was added to prevent *de novo* synthesis of proteins and the light intensity was subsequently increased to 200 μmol photons m^{-2} s^{-1} red and blue LED light (equivalent to ~1000 μmol photons m^{-2} s^{-1} white incandescent light). Variable fluorescence yield (Fv/Fm) was measured every 30 min (FL200; Photon System Incorporated, Czech Republic). After 1 h incubation with lincomycin, the cultures were spun at 6,000 rpm 3 min and washed twice with BG11. Subsequently cultures were re-suspended in a prewash volume of warmed BG11 and incubated at 20 μmol photons m^{-2} s^{-1} red and blue LED light for the rest of the experiment.

RESULTS

Gene Structure and Conservation of Psb32

Bioinformatics predictions suggest that Psb32 contains an N-terminal signal peptide for thylakoid membrane localization (Juncker et al., 2003; Bendtsen et al., 2004). This signal peptide is predicted to be cleaved between residues 46-47 by Signal Peptidase I (Juncker et al., 2003), suggesting that Psb32 is transported by the Sec pathway, crossing the membrane unfolded (reviewed in Natale et al., 2008). There is also a predicted C-terminal transmembrane helix (TMH), indicating that Psb32 is an integral membrane protein (Krogh et al., 2001). Lastly, Psb32 also contains a domain of unknown function (DUF477), which though uncharacterized, is found in both prokaryotes and eukaryotes (Quevillon et al., 2005). The basic structure of *psb32* is shown in Fig. 1A.

Ancestral relatives of modern cyanobacteria were the progenitors of the chloroplast found in plants and algae (Goksoyr, 1967) and many PSII subunits are conserved throughout cyanobacteria, algae, and plants (Hankamer et al., 2001). As previously published, similarity of the amino acid sequences showed that Psb32 is conserved in all classes of oxygenic photosynthetic organisms (Roose et al., 2007). Taking advantage of the increased number of photosynthetic genomes available, we analyzed similarity among Psb32 homologs (Fig. 1B). Psb32 is restricted oxygenic photosynthetic organism with thylakoid membranes, with the exception of several of the cyanobacterial *Prochlorococcus* species that have undergone severe genome reduction. We found that the majority of cyanobacterial homologs clustered together, with the exception of the chlorophyll-d containing *Acaryochloris marina.* Similarly, plant and green algal homologs also clustered.

Psb32 is localized in the thylakoid membrane

To determine the subcellular localization of Psb32, we isolated total cellular membranes from wild type (WT) *Synechocystis* and separated thylakoid membranes (TM) and plasma

membranes (PM) by polyethylene glycol (PEG) dextran two-phase partitioning (Fig. 2A). Psb32 localized to both membrane systems but was enriched in the TM. The core PSII protein CP47 localized to the TM (Keren et al., 2005) and the sodium dependent bicarbonate transporter protein SbtA localized to the PM as expected, demonstrating that there was no contamination between the fractions.

To further pinpoint the nature of Psb32's membrane association, total cellular membranes were treated with Triton X-114 to allow for separation of soluble and aqueous proteins. After Triton X-114 treatment, Psb32 remained associated with the membrane, suggesting its predicted single transmembrane helix is anchoring it. The intrinsic PSII protein D2 also remains associated with membrane, while the peripheral membrane PSII protein PsbV is released into the soluble fraction, as previously reported (Bricker and Sherman, 1984) (Fig 2B).

Genetic deletion of psb32 results in increased sensitivity to oxidative stress

To further investigate the role of *psb32*, we created a deletion mutant by replacing the middle portion of the gene with a chloramphenicol (Cm) resistance gene (Fig. 3A). We confirmed that this mutation was integrated into all copies of the *Synechocystis* genome by PCR of the locus (Fig. 3B). Additionally we established via RT-PCR that there is no *psb32* transcript made but that expression of the closest locus *sll1866* is unaffected by the insertion in *psb32* (Fig 3C).

Deletion of *psb32* did not significantly affect pigment levels, fluorescence, photosynthetic parameters or growth rates (data not shown). However, in the presence of hydrogen peroxide, the loss of *psb32* greatly impaired growth (Fig. 4A). Additionally, in the presence of the photo oxidizer rose bengal under 200 μmol photons m^{-2} s^{-1}, growth was impaired in the Δ*psb32* mutant (Fig. 4B). Interestingly, Δ*psb32* did not exhibit decreased growth in the presence of methyl viologen (data not shown). Taken together, these data suggest that *psb32* protects cells from oxidative stress.

Psb32 confers fitness to Synechocystis

To further analyze and understand the cellular role of *psb32*, we investigated its role in organismal fitness. We conducted a mixed culture experiment in which equal numbers of WT and Δ*psb32* cells were incubated together in a single flask, forcing the two strains to compete for available nutrients. The flasks were subcultured every 3 d and samples were collected for PCR analysis to detect the amount of each strain present. This experimental setup has previously been described in detail (Ivleva et al., 2000).

While both strains showed similar ratios under low (5 μmol photons m^{-2} s^{-1}) or moderate (45 μmol photons m^{-2} s^{-1}) light intensities, there was an increase of the ratio of WT to Δ*psb32* under high light (150 μmol photons m^{-2} s^{-1}) intensities. After the fifth subculture timepoint (t5), the PCR band corresponding to Δ*psb32* is no longer detectable (Fig 5A). Quantization of multiple biological replicates showed that this increase in WT signal and decrease in Δ*psb32* signal is quantifiable and repeatable (Fig 5B).

Psb32 protects against photoinhibition

To narrow the range of possible functions for Psb32, we investigated the extent of D1 damage under high light and subsequent recovery. To do this, we incubated WT and Δ*psb32* under high light (~200 μmol photons m^{-2} s^{-1} red and blue light) to damage the D1 protein in the presence of the protein synthesis inhibitor lincomycin to halt *de novo* protein synthesis. After a period of 1 h, the cells were washed to remove the lincomycin and returned to low light to facilitate PSII recovery. Measurements of variable fluorescence (Fv/Fm) showed that in the presence of lincomycin (0 to 60 min), both WT and Δ*psb32* strains exhibit decreased fluorescence as D1 is degraded (Fig. 6A). However, Δ*psb32* exhibits accelerated photoinhibition, suggesting that *psb32* protects the D1 protein, as has been previously shown for the Psb27 protein (Roose and Pakrasi, 2008). After removal of the lincomycin, WT cells recover to 94% of their initial variable fluorescence levels after 2 h. However, Δ*psb32* displays slowed recovery,

only achieving 86% of its initial variable fluorescence levels (Fig. 6B). This suggests that in the absence of Psb32, as in the absence of Psb27, PSII is not repaired as efficiently (Roose and Pakrasi, 2008).

DISCUSSION

Psb32 protects PSII from ROS and photodamage

Growth in photosynthetic organisms is a balancing act between the processes of photodamage and repair. When the rate of damage exceeds the rate of repair, organisms experience photoinhibition. Our data shows that the presence of H_2O_2 and rose bengal greatly reduces or abolishes growth in the Δ*psb32* mutant (Fig 4A and B). Interestingly, previous studies have shown that ROS have dramatic effects on the ability of PSII to repair itself after photodamage. Hydroxyl radicals from H_2O_2 added to culture media promote photoinhibition by slowing PSII repair (Nishiyama et al., 2001). Additionally, singlet oxygen produced by the combination of rose bengal and high light has also been shown to slow repair of PSII without affecting the rate of photodamage (Nishiyama et al., 2004). In both singlet oxygen and hydroxyl radical damage, it was found that the reason for the impeded repair was the arrest of translation elongation of the *psbA* gene, which encodes the D1 protein (Nishiyama et al., 2001; Nishiyama et al., 2004). Thus it could be that the effects we see of ROS on the growth rates of Δ*psb32* are actually a reflection of the decreased rate of PSII repair of the damage caused by the ROS. That is further supported by our photoinhibition experiments in which Δ*psb32* exhibits a decreased rate of recovery after damage (Fig 6B). This slowed recovery is further exacerbated by the increased rate of photodamage that the Δ*psb32* mutant displays (Fig. 6A).

However, Δ*psb32* does not exhibit any defect in the presence of methyl viologen (data not shown). While the superoxide radical produced by the addition of methyl viologen can by converted to H_2O_2 and thus produce hydroxyl radicals, the primary mode of action of superoxide radicals is distinctly different from singlet oxygen and hydroxyl radicals. While damage to PSII occurs on the donor side in the presence of singlet oxygen and hydroxyl radicals, damage due to superoxide occurs on the acceptor side (Knox and Dodge, 1985; Asada, 2003). The reaction of Δ*psb32* to damage on the donor side but not the acceptor side is further evidence that Psb32 functions to aid in assembly of PSII, which coincides with the lumenal localization of the protein

(Fig 2A and B). This slowed repair, in addition to the observed accelerated rate of photodamage, could explain why the presence of Psb32 confers a selective advantage to fitness during competition under high light (Fig 5), when ROS damage and light induced photoinhibition are at their highest.

Conserved role of Psb32 among phototrophs

Because *psb32* is conserved among the majority of thylakoid containing photosynthetic organisms, it is interesting to consider its role among this class of organisms. To date, the only other study of a Psb32 homolog was conducted in Arabidopsis (Sirpio et al., 2007). In both Arabidopsis and *Synechocystis*, neither protein affects viability or pigment accumulation. In *Synechocystis*, we found that Psb32 protects PSII from photodamage and aids in the efficient repair. This is in agreement with data observed for the Arabidopsis homolog, TPL18.3 (Sirpio et al., 2007). The possible role of Psb32 as a PSII assembly nicely explains the decreased efficiency of PSII repair in both *Synechocystis* and Arabidopsis. Nevertheless there are differences in the subcellular localizations of the two proteins. While location of the TLP18.3 was only investigated in isolated thylakoid membranes, it was observed in both grana and stroma thylakoids (Sirpio et al., 2007). However, we found that Psb32 localizes to both the thylakoid and periplasmic membranes, suggesting that Psb32 might be associated with pre-PSII complexes which are assembled at the periplasmic membrane before they are translocated to the thylakoid membrane for completion (Keren et al., 2005).

CONCLUSIONS

It had previously been shown that the Psb32 co-purified with cyanobacterial PSII complexes. In this work, we generated a genetic mutant and a specific antibody to fully elucidate the function of this gene. We found that Psb32 is predominantly present in the thylakoid membranes, where it is an integral membrane protein. Additionally we found that while Psb32 is not required for survival in complete media, it does provide an advantage under PSII-specific oxidative stressors hydrogen peroxide and rose bengal and under competition. This is possibly due to the increased tendency of cells without *psb32* to be both more quickly photodamaged and slower to repair damage. Taken together, this data suggests that Psb32 aids in repair or assembly of PSII.

REFERENCES

Abramoff MD, Magelhaes, P.J., Ram, S.J. (2004) Image Processing with ImageJ. Biophotonics International **11:** 36-42

Allen MM (1984) Cyanobacterial Cell Inclusions. Annu Rev Microbiol **38:** 1-25

Anderson JM, Chow WS (2002) Structural and functional dynamics of plant photosystem II. Philos Trans R Soc Lond B **357:** 1421-1430

Andersson B, Aro EM (2001) Photodamage and D1 Protein Turnover. *In* EM Aro, B Andersson, eds, Regulation of Photosynthesis, Vol 11. Kluwer, Dordrecht, pp 377-394

Aro EM, Suorsa M, Rokka A, Allahverdiyeva Y, Paakkarinen V, Saleem A, Battchikova N, Rintamaki E (2005) Dynamics of photosystem II: a proteomic approach to thylakoid protein complexes. J Exp Bot **56:** 347-356

Aro EM, Virgin I, Andersson B (1993) Photoinhibition of Photosystem II. Inactivation, protein damage and turnover. Biochim Biophys Acta **1143:** 113-134

Asada K (2003) The water-water cycle in chloroplasts: Scavenging of active Oxygens and dissipation of excess photons. Annu Rev Plant Phys **50:** 601-639

Bendtsen JD, Nielsen H, von Heijne G, Brunak S (2004) Improved prediction of signal peptides: SignalP 3.0. J Mol Biol **340:** 783-795

Benson DA, Karsch-Mizrachi I, Lipman DJ, Ostell J, Wheeler DL (2008) GenBank. Nucleic Acids Res. **36:** D25-30

Bricker TM, Sherman LA (1984) Triton X-114 phase fractionation of membrane proteins of the cyanobacterium *Anacystis nidulans* R2. Arch Biochem Biophys **235:** 204-211

Dyrlov Bendtsen J, Nielsen H, von Heijne G, Brunak S (2004) Improved prediction of signal peptides: SignalP 3.0. J Mol Biol **340:** 783-795

Goksoyr J (1967) Evolution of eucaryotic cells. Nature **214:** 1161

Hankamer B, Morris E, Nield J, Carne A, Barber J (2001) Subunit positioning and transmembrane helix organisation in the core dimer of photosystem II. FEBS Letters **504:** 142-151

Havaux M, Eymery F, Porfirova S, Rey P, Dormann P (2005) Vitamin E protects against photoinhibition and photooxidative stress in *Arabidopsis thaliana*. Plant Cell **17:** 3451-3469

Ivleva NB, Shestakov SV, Pakrasi HB (2000) The carboxyl-terminal extension of the precursor D1 protein of Photosystem II Is required for optimal photosynthetic performance of the cyanobacterium *Synechocystis* sp. PCC 6803. Plant Physiol **124:** 1403-1412

Juncker AS, Willenbrock H, Heijne Gv, Brunak Sr, Nielsen H, Krogh A (2003) Prediction of lipoprotein signal peptides in Gram-negative bacteria. Protein Science **12:** 1652-1662

Kashino Y, Lauber WM, Carroll JA, Wang Q, Whitmarsh J, Satoh K, Pakrasi HB (2002) Proteomic analysis of a highly active photosystem II preparation from the cyanobacterium *Synechocystis* sp. PCC 6803 reveals the presence of novel polypeptides. Biochemistry **41:** 8004-8012

Katoh K, Misawa K, Kuma KI, Miyata T (2002) MAFFT: a novel method for rapid multiple sequence alignment based on fast Fourier transform. Nucleic Acids Res **30:** 3059-3066

Keren N, Liberton M, Pakrasi HB (2005) Photochemical competence of assembled photosystem II core complex in cyanobacterial plasma membrane. J Biol Chem **280:** 6548-6553

Keren N, Ohkawa H, Welsh EA, Liberton M, Pakrasi HB (2005) Psb29, a conserved 22-kD protein, functions in the biogenesis of Photosystem II complexes in *Synechocystis* and *Arabidopsis*. Plant Cell**:** tpc.105.035048

Knox JP, Dodge AD (1985) Singlet oxygen and plants. Phytochemistry **24:** 889-896

Krogh A, Larsson B, von Heijne G, Sonnhammer EL (2001) Predicting transmembrane protein topology with a hidden Markov model: application to complete genomes. J Mol Biol **305:** 567-580

Loll B, Kern J, Saenger W, Zouni A, Biesiadka J (2005) Towards complete cofactor arrangement in the 3.0 A resolution structure of photosystem II. Nature **438:** 1040-1044

Nakamura Y, Kaneko T, Hirosawa M, Miyajima N, Tabata S (1998) CyanoBase, a www database containing the complete nucleotide sequence of the genome of *Synechocystis* sp. strain PCC6803. Nucleic Acids Res **26:** 63-67

Natale P, Bruser T, Driessen AJM (2008) Sec- and Tat-mediated protein secretion across the bacterial cytoplasmic membrane-Distinct translocases and mechanisms. Biochim Biophys Acta **1778:** 1735-1756

Nishiyama Y, Allakhverdiev SI, Yamamoto H, Hayashi H, Murata N (2004) Singlet oxygen inhibits the repair of Photosystem II by suppressing the translation elongation of the D1 protein in *Synechocystis* sp. PCC 6803. Biochemistry **43:** 11321-11330

Nishiyama Y, Yamamoto H, Allakhverdiev SI, Inaba M, Yokota A, Murata N (2001) Oxidative stress inhibits the repair of photodamage to the photosynthetic machinery. EMBO J **20:** 5587-5594

Norling B, Zak E, Andersson B, Pakrasi H (1998) 2D-isolation of pure plasma and thylakoid membranes from the cyanobacterium *Synechocystis* sp. PCC 6803. FEBS Letters **436:** 189-192

Nowaczyk MM, Hebeler R, Schlodder E, Meyer HE, Warscheid B, Rogner M (2006) Psb27, a cyanobacterial lipoprotein, is involved in the repair cycle of photosystem II. Plant Cell **18:** 3121-3131

Park YI, Chow WS, Anderson JM (1995) Light inactivation of functional photosystem II in leaves of peas grown in moderate light depends on photon exposure. Planta **196:** 401-411

Powles SB (1984) Photoinhibition of photosynthesis induced by visible light. Annu Rev Plant Physiol **35:** 15-44

Prásil O, Adir N, Ohad I (1992) Dynamics of photosystem II: mechanism of photoinhibition and recovery processes. *In* J Barber, ed, Topics in Photosynthesis: The Photosystems:

Structure, Function and Molecular Biology, Vol 11. Elsevier Science Publishers, Amsterdam, pp 295-348

Quevillon E, Silventoinen V, Pillai S, Harte N, Mulder N, Apweiler R, Lopez R (2005) InterProScan: protein domains identifier. Nucleic Acids Res **33:** W116-120

Quevillon E, Silventoinen V, Pillai S, Harte N, Mulder N, Apweiler R, Lopez R (2005) InterProScan: protein domains identifier. Nucleic Acids Res **33:** W116-120

Roose JL, Pakrasi HB (2004) Evidence that D1 processing is required for manganese binding and extrinsic protein assembly into photosystem II. J Biol Chem **279:** 45417-45422

Roose JL, Pakrasi HB (2008) The Psb27 protein facilitates manganese cluster assembly in photosystem II. J Biol Chem **283:** 4044-4050

Roose JL, Wegener KM, Pakrasi HB (2007) The extrinsic proteins of Photosystem II. Photosynth Res **92:** 369-387

Sirpio S, Allahverdiyeva Y, Suorsa M, Paakkarinen V, Vainonen J, Battchikova N, Aro EM (2007) TLP18.3, a novel thylakoid lumen protein regulating photosystem II repair cycle. Biochem J **406:** 415-425

Thornton LE, Ohkawa H, Roose JL, Kashino Y, Keren N, Pakrasi HB (2004) Homologs of plant PsbP and PsbQ proteins are necessary for regulation of photosystem ii activity in the cyanobacterium *Synechocystis* 6803. Plant Cell **16:** 2164-2175

Tyystjärvi E, Aro EM (1996) The rate constant of photoinhibition, measured in lincomycin-treated leaves, is directly proportional to light intensity. Proc Natl Acad Sci U S A **93:** 2213-2218

Wang HL, Postier BL, Burnap RL. (2004) Alterations in global patterns of gene expression in *Synechocystis* sp. PCC 6803 in response to inorganic carbon limitation and the inactivation of ndhR, a LysR family regulator. J Biol Chem **279:** 5739-5751

Wegener KM, Welsh EA, Thornton LE, Keren N, Jacobs JM, Hixson KK, Monroe ME, Camp DG, 2nd, Smith RD, Pakrasi HB (2008) High sensitivity proteomics assisted discovery of a novel operon involved in the assembly of photosystem II, a membrane protein complex. J Biol Chem **283:** 27829-27837

Zak E, Norling B, Maitra R, Huang F, Andersson B, Pakrasi HB (2001) The initial steps of biogenesis of cyanobacterial photosystems occur in plasma membranes. Proc Natl Acad Sci U S A **98:** 13443-13448

Table I. Primers used for the cloning of the *Δpsb32* mutant, antibody generation and RT-PCR.

Name	Sequence
1390F upstream	5’-ACGAAGCTTAATAGCCGTTGTTCCGCTCA-3’
1390R upstream	5-TCATGGATCCTTGATTGCTCTGGCTGGCTT-3’
1390F downstream	5’-TCATGGATCCGCGGAA GAAACCGACGATA-3’
1390R downstream	5’-GCAGGAATTCTGCACGG CAGTACCAAAGTT-3’
Anti 1390F	5’-GCTCGAGCATATGTCCCCTTATG ACCTGCCAATTTTGTC-3'
Anti 1390R	5’-ATGATTAGTATTCTCGAGGGTGG CACTGGTATCGTCGG-3´
RT-PCR 1390F	5’-TGGTGCTAGATACCCTCACCAAGCA-3’
RT-PCR 1390R	5’-GGGTTTCCCGCAGTAAACTATCCA-3’
RT PCR 1866F	5’-ATATTGCCGAAACTTTCCCTGCCG-3’
RT PCR 1866R	5’-CCCTTGGCGCAGAATTTGGAAGAT-3’
RT PCR RNAseP F	5’-CAAACTTGCTGGGTAAC-3’
RT PCR RNAseP R	5’-ACCAAATTCCTCAAGCG-3’

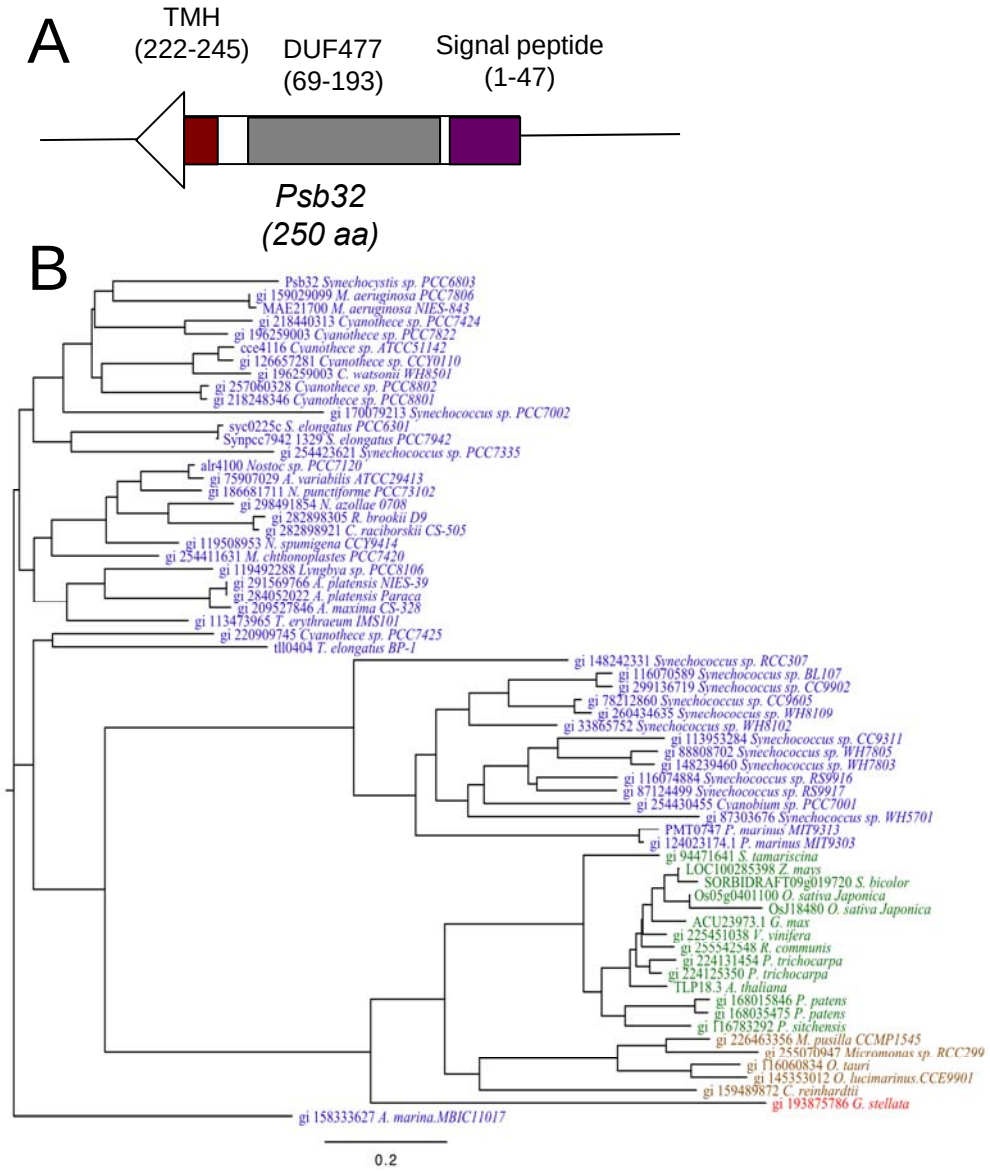

Figure 1. Organization and conservation of Psb32. A, *psb32* contains an N-terminal signal peptide for transit, an internal DUF477 domain, and a C-terminal TMH. B, Phylogenic tree of Psb32 homologs. Star indicates Psb32 in *Synechocystis* 6803. Colors indicate taxonomy: blue - cyanobacteria; green - eukaryotic plants; brown - green algae; red - red algae

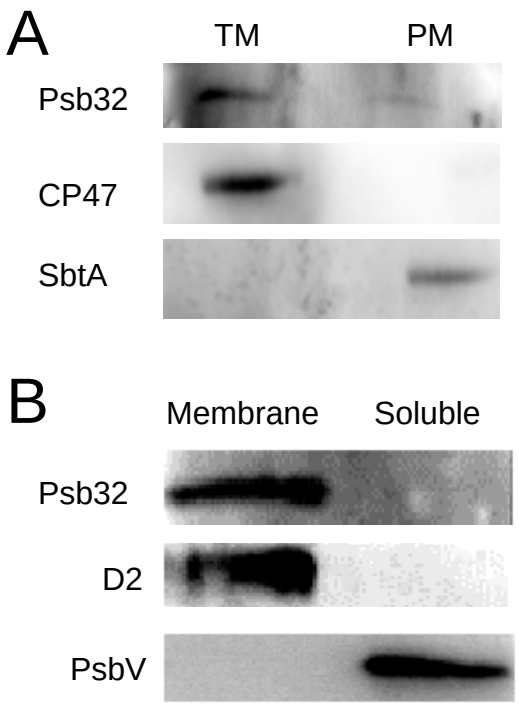

Figure 2. Subcellular localization of Psb32. A, Total cellular membranes were isolated and then separated by PEG/dextran two phase partitioning to isolate TM and PM. B, Total cellular membranes were treated with to 1% Triton X-114 to release loosely associated proteins from the membrane.

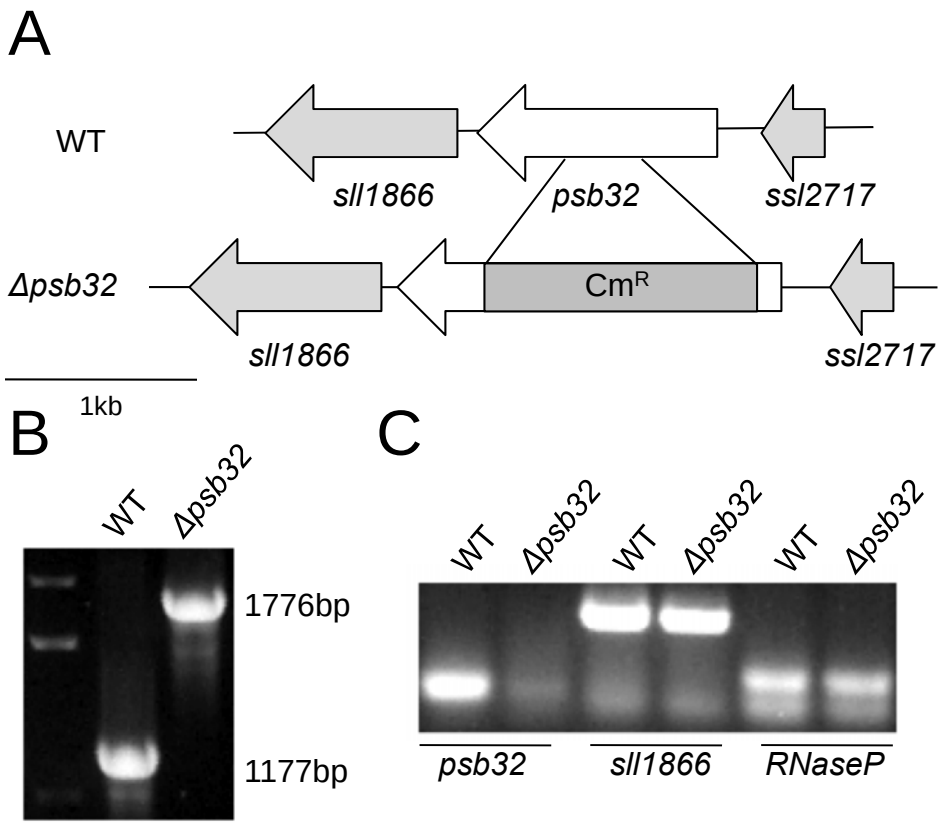

Figure 3. Genetic deletion of *psb32*. A, Deletion scheme in which *psb32* is disrupted by a Cm resistance cassette. B, PCR confirming segregation of *Δpsb32* mutation. C, RT-PCR to evaluate expression of *psb32*, the downstream gene *sll1866*, and the control *RNaseP* in *Δpsb32*.

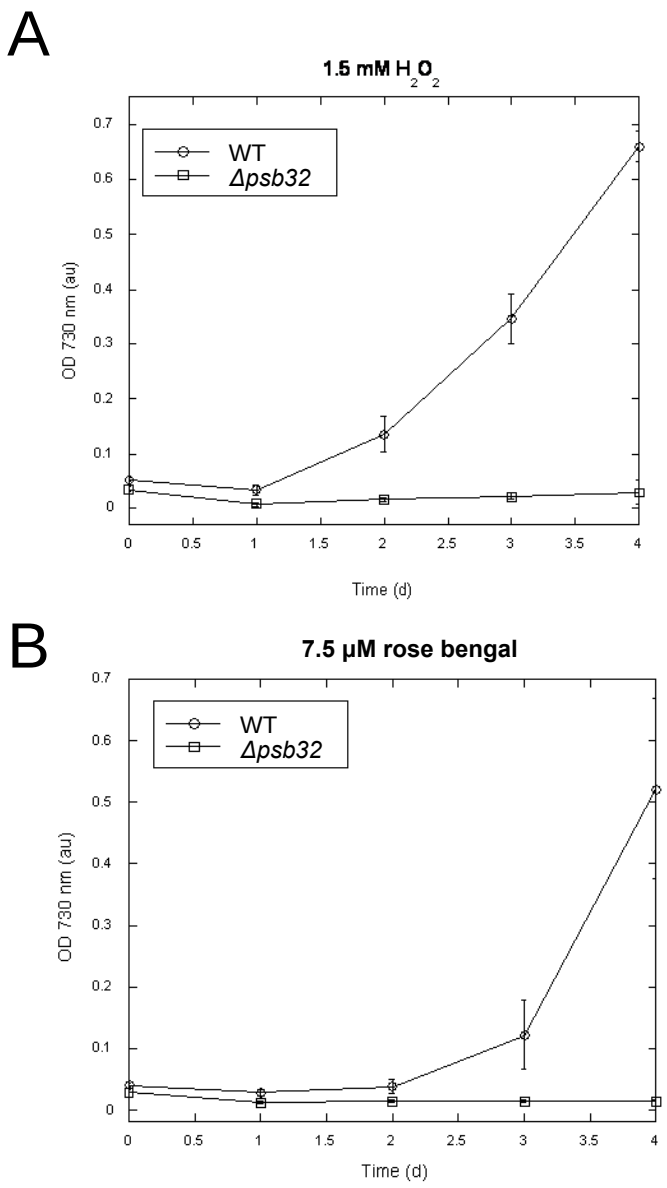

Figure 4. Growth under various oxidative stresses. Open shapes indicate WT, black shapes indicate *Δpsb32*. A, Growth of WT and *Δpsb32* in the presence of 1.5mM H_2O_2. B, Growth of WT and *Δpsb32* in the presence of 7.5 µM rose bengal and 200 µmol photons m^{-2} s^{-1} white light. Error bars indicate standard deviation, n=3.

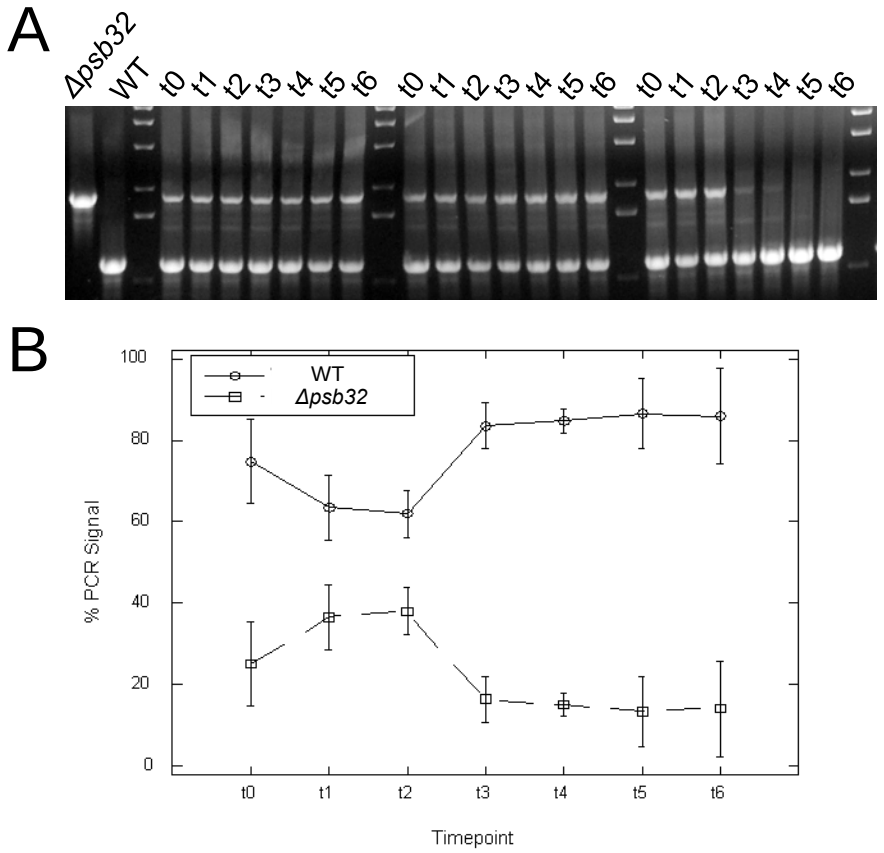

Figure 5 Competition of WT and Δ*psb32* under low light (LL), growth light (GL) and high light (HL). A, At each time point, genomic DNA was isolated and PCR conducted to determine the relative abundance of each strain. A representative gel is shown. B, Quantitation of the PCR band intensity of the HL grown samples. Error bars indicate standard deviation, n=3.

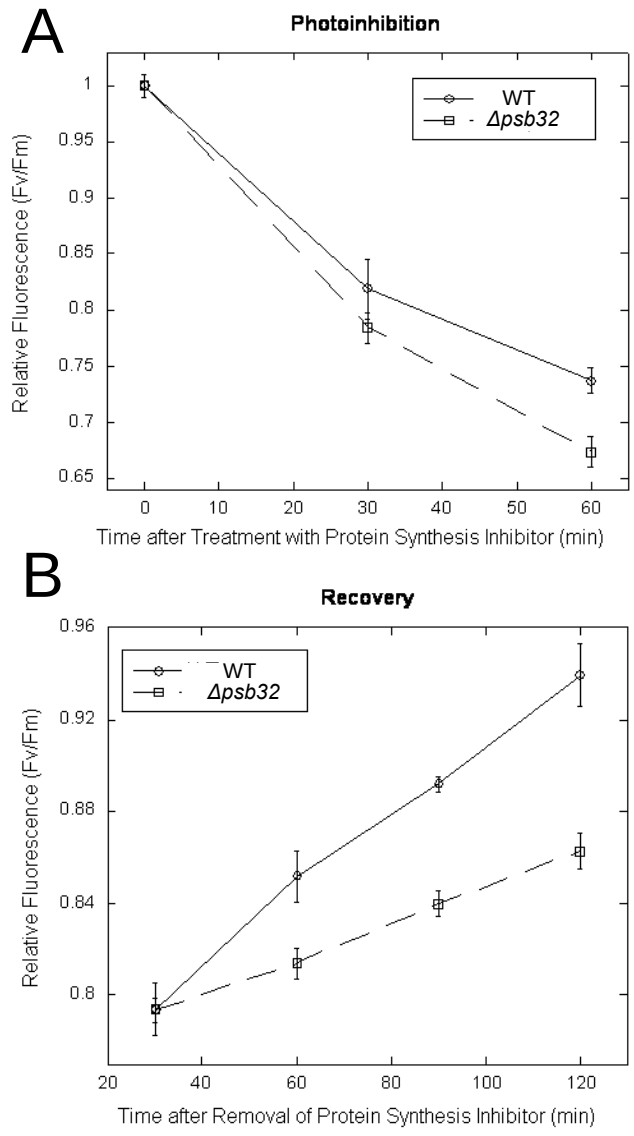

Figure 6. *Δpsb32* displays increased photoinhibition and decreased recovery. Open shapes indicate WT, black shapes indicate *Δpsb32*. A, Cells were incubated in the presence of lincomycin and high light for 60 min. Fv/Fm was measured every 30 min. B, Cells were washed and allowed to recover in BG11 under low light. Fv/Fm was measured every 30 min. Error bars indicate standard deviation, n=3.

Chapter 5

Psb32 is Associated with Inactive PSII Complexes

SUMMARY

PSII catalyzes the conversion of light energy into molecular oxygen and produces the reducing power for carbon fixation, one of Earth's most important biochemical reactions. Psb32 (Sll1390) has been previously identified as co-purifying with PSII complexes that have been isolated using a histidine tag on the core PSII protein CP47. In this study, we characterized complexes containing Psb32 after purification via a C-terminal His tag. These HisPsb32 complexes have altered PSII fluorescence properties, reduced oxygen evolution activity, and decreased manganese content, suggesting that they are not fully functional complexes. To further clarify its function, we over expressed Psb32 to determine the effect of excess protein on cellular physiology and PSII composition and function. Excess Psb32 severely retarded growth in the absence of $CaCl_2$ and also significantly reduced oxygen evolution activity in isolated PSII complexes. Taken together, these data suggest that Psb32 is a true component of PSII and associates with partially assembled complexes to aid in their completion.

INTRODUCTION

PSII is a multi-component enzyme complex in cyanobacteria, algae and plants that catalyzes the light-driven oxidation of water to molecular oxygen. The active complex is a dimer consisting of 2 identical monomers with more than 20 proteins, identified through genetic, biochemical, and structural studies. In addition to its protein components, PSII also has a large number of cofactors including chlorophylls, pheophytins, plastoquinones, Mn atoms, calcium, chloride, non-heme iron, and heme groups (Ferreira et al., 2004; Loll et al., 2005). Removal of these subunits or cofactors can slow or even completely halt water oxidation. Recent proteomic studies have identified a significantly larger number of proteins that purify with the active PSII complex and may aid in the assembly or function (Kashino et al., 2002; Wegener et al., 2008).

Due to the high energetics of the reactions it catalyzes, PSII is frequently damaged and repaired as part of its normal function (Powles, 1984; Prásil et al., 1992; Aro et al., 1993; Andersson and Aro, 2001). Thus at any one time, an organism contains a mixed population of complexes in various states of assembly which may include multiple accessory proteins not found in the final active complex. Traditionally, studies have relied on isolation of PSII using a histidine tag on the large core protein CP47. This protein is inserted into pre-PSII complexes very early in assembly, and thus these preparations, while highly active, are also heterogeneous.

Psb32 (Sll1390) has been previously identified as co-purifying with PSII complexes that have been isolated using a histidine tag on the core PSII protein CP47 (Kashino et al., 2002; Wegener et al., 2008). This protein is conserved throughout most oxygenic photosynthetic organisms containing thylakoid membranes. It has also been shown to affect D1 turnover in both *Synechocystis* (Chapter 4) and *Arabidopsis thaliana* (Sirpio et al., 2007). However there has been little direct evidence that Psb32 is a bona fide PSII protein. To answer this question, we isolated and characterized Psb32 containing complexes from *Synechocystis* utilizing a C-terminal His tag on Psb32. Additionally, we over expressed Psb32 under the control of the strong *psbA2* promoter

to investigate the effects over accumulation of this protein has on cellular physiology as well as function and composition of isolated PSII complexes. We found that over expressed Psb32 greatly reduced growth in the absence of $CaCl_2$ and also reduced oxygen evolution activity in isolated PSII complexes. Isolated HisPsb32 complexes displayed altered PSII fluorescence properties, diminished oxygen evolution activity, and reduced manganese content, suggesting that they are not fully functional complexes. Taken together, these data suggest that Psb32 is a true component of PSII and associates with partially assembled complexes to aid in their completion.

MATERIALS AND METHODS

Bacterial Strains and Culture Conditions

Synechocystis sp. PCC 6803 was grown at 30 °C with 30 μmol photons m^{-2} s^{-1} of white light in BG11 media (Allen, 1984). Stock cultures were maintained on solid medium (BG11 supplemented with 1.5% (w/v) agar), and used to inoculate liquid cultures for each experiment. The mutants HisPsb32 and Psb32OE were supplemented with 10 ug/mL chloramphenicol. HT47GM strains were maintained with 5 ug/mL gentamicin. Experiments utilizing low and high light were conducted at 10 and 100 μmol photons m^{-2} s^{-1}, respectively. For H_2O_2 growth experiments, cells were incubated with 0, 0.5, 1, or 1.5 mM H_2O_2 under 30 μmol photons m^{-2} s^{-1} of white light.

Mutant Strain Generation

To create a histidine tagged version of the Psb32 protein, the C-terminus of the *psb32* gene was modified by adding a leucine, glycine and histidine before a stop codon. Nucleotides 1821491-1820892 of the *Synechocystis* genome (http://bacteria.kazusa.or.jp) (Kaneko T et al., 1996) were amplified via PCR and cloning into the pET41b vector in front of the His-tag. From there the fragment was amplified including the HIS tag and cloned into pUC118. The *E.coli* construct comprising of the modified *psb32* sequence, a chloramphenicol resistance marker directly behind the stop codon and a 600 bp long downstream sequence (nucleotides 1820888-1820138) was transformed into WT *Synechocystis* 6803 via double homologues recombination.

To create the Psb32OE strain, the full length Psb32 protein was cloned into the pCTP2031v vector, which contains a chloramphenicol resistance gene, the *psbA2* promoter, and targeting sequences for homologous recombination into the *slr2031-2032* locus in *Synechocystis*

(Satoh et al., 2001; Muramatsu et al., 2009). To create the Psb32OE HT47GM strain, the Psb32OE construct was introduced into the HT47GM background (Roose, 2008).

PSII Preparation

PSII was isolated from HT47GM, HisPsb32, and Psb32OE Ht47GM strains as described previously (Kashino et al., 2002). HT47GM indicates the 6-His tagged CP47 used to affinity purify the complex (Roose, 2008). The final eluate from a Ni-NTA Agarose (Qiagen, Inc., Valencia, CA) column was suspended in 50 mM MES-NaOH pH 6.0, 10 mM $CaCl_2$, 25% glycerol with 0.04% dodecyl maltoside. In isolations from the HT47GM and Psb32OE HT47GM strains, flow through and eluate were evaluated at 436nm to detect chlorophyll absorbance and for HisPsb32 flow through and eluate were evaluated at 280nm to monitor protein absorbance.

Spectrophotometric Assays

Cell growth was monitored by measuring light scattering at 730nm on a μQuant microplate spectrophotometer (Bio-Tek Instruments, Inc., Toronto, Canada). Chlorophyll concentrations were determined by methanol extraction and absorbance at 652 and 665 nm in a DW2000 spectrophotometer (SLM-Aminco, Urbana, IL) (Porra et al., 1989). Protein concentrations were measured by absorbance at 280 nm using a NanoDrop1000 (NanoDrop, Wilmington, DE) (Desjardins et al., 2009).

Protein Visualization

SDS-PAGE was performed as described previously (Kashino et al., 2002), using a gel with 18-24% acrylamide gradient and 6 M urea. After transfer to 0.22 μm nitrocellulose, Psb32

and D1 were detected by using specific antiserum (described in Chapters 3 and 4), and reacted with goat-anti-rabbit horseradish peroxidase conjugated antiserum (Pierce Biotech, Rockford, IL) developed in West Pico (Pierce Biotech, Rockford, IL) for 5 min. Blots were visualized in a Fujifilm LAS-1000plus imager (Fujifilm, Stamford, CT) for 1 to 5 min. Digital images were quantified using ImageJ software (Abramoff et al., 2004).

Steady State Oxygen Evolution

A Clarke-type electrode was used to determine the rate of photosynthetic oxygen evolution (Mannan and Pakrasi, 1993). Oxygen evolution was measured for whole cells at a concentration of 5 μg Chl/mL in the presence of 0.5 mM 2.6-dichloro-*p*-benzoquinone (Eastman-Kodak, Rochester, NY) and 1 mM K_3FeCN_6. Light intensity was adjusted by use of neutral density filters. Oxygen evolution for isolated PSII complexes was measured at 3 μg chlorophyll/mL in 50 mM MES-NaOH (pH 6.0), 20 mM $CaCl_2$, 0.5 M sucrose (Roose et al., 2007).

Fluorescence Measurements

PSII samples were diluted in buffer containing 50 mM MES (2- (N-Morpholino) ethanesulfonic acid, monohydrate)-NaOH, pH 6.0, 5 mM $CaCl_2$, 10 mM $MgCl_2$, 25% glycerol, 0.04% dodecylmaltoside and fluorescence emission spectra at 77 K were measured on a Fluoromax-2 fluorometer with excitation at 440 nm (Jobin Yvon, Cedex, France) (Kashino et al., 2002). Fluorescence emission spectra were normalized by $(F-F_{660})/(F_{683}-F_{660})$.

Mn Measurements

Concentrations of Mn were measured on an AA600 atomic absorption spectrophotometer (PerkinElmer Life Sciences, Wellesley, MA). PSII samples were diluted to 5 μg Chl/mL in

deionized water before analysis. The Mn:PSII ratio was calculated based on 41 molecules of Chl/PSII (Kashino et al., 2002).

RESULTS

Generation of HisPsb32 and Psb32OE strains

To better understand the function of Psb32, we generated new Psb32 mutant lines. The HisPsb32 strain contains a C-terminal hexahistidine tag followed by a chloramphenicol resistance gene in the native *psb32* locus. The Psb32OE strain contains the wild type copy of *psb32* under the control of the strong *psbA2* promoter followed by a chloramphenicol resistance gene, inserted into the *slr2031-slr2032* locus. These strains are diagrammed in Figure 1. Immunological assay utilizing the antibody against Psb32 shows that the HisPsb32 line has a slightly larger version of the Psb32 as compared to WT and that the Psb32OE strain has significantly more Psb32 expressed than WT (Figure 2).

Effects of HisPsb32 and Psb32OE on photoautotrophic growth

In complete BG11 under low, moderate or high light intensities, neither HisPsb32 nor Psb32OE displays altered growth (Figure 3A-C). Similarly, growth under moderate light in the presence of the hydrogen peroxide is not affected in either HisPsb32 or Psb32OE (Figure 3E). However, when Psb32OE was grown in the absence of $CaCl_2$, its growth was severely inhibited as compared to WT, ΔPsb32, and HisPsb32 (Figure 3D). This suggests that the over accumulation of Psb32 is impeding photosynthesis in the absence of $CaCl_2$.

Measurements of absorbance showed that neither HisPsb32 nor Psb32OE have altered pigment distribution (Figure 4). Additionally, measurements of whole cell oxygen evolution showed that HisPsb32 and Psb32OE display rates similar to that of WT and ΔPsb32 across various light intensities (Table 1).

Isolated Complexes from HisPsb32 and Psb32OE HT47GM

To better define the role of Psb32 in PSII function, we isolated complexes from utilizing the his tag on Psb32 in the HisPsb32 strain and the his tag on the core protein CP47 in the Psb32OE HT47GM mutant. Solubilized membranes from the Psb32 mutant strains, as well as the control HT47GM, were applied to a Ni^{2+} affinity column and eluted with excess histidine. Chlorophyll absorbance at 436 nm was monitored during the Psb32OE HT47GM and HT47GM isolations, while protein absorbance at 280 nm was monitored during HisPsb32 isolations. All three strains exhibited a single eluate peak. Representative chromatograms for isolations from HT47GM, Psb32OE HT47GM, and HisPsb32 are shown in Figure 5. The concentrated elution peaks were analyzed for characteristic PSII 77K fluorescence properties. HT47GM PSII complexes display the characteristic PSII fluorescence signature of peaks at 683 and 691 nm PSII, as do the Psb32OE HT47GM complexes (Figure 6). However, while the HisPsb32 isolations are clearly enriched for PSII (although residual PSI remains in all isolations, as evidenced by fluorescence at 720 nm), it contains 1 large peak that is shifted to 685 nm and a very small peak at 695nm (Figure 6).

The polypeptide profiles of HT47GM, HisPsb32, and Psb32OE HT47GM were surprisingly similar (Figure 7). HisPsb32 contains comparable levels of CP47, PsbV, and PsbQ as HT47GM and Psb32OE HT47GM, but contains less CP43 and PsbO. Interestingly, HisPsb32 contains remarkably less D1 protein (Figure 8). Interestingly, when maximal oxygen evolution activity was measured, complexes from HisPsb32 and Psb32OE HT47GM displayed significantly reduced rates as compared to HT47GM (9% and 27%, respectively) (Table 2). Thus it is not surprising that the ratios of protein to chlorophyll in isolated complexes from HisPsb32 are significantly higher than those found in complexes from HT47GM (66 vs 0.9, respectively), suggesting that the HisPsb32 complexes either have notably less chlorophyll or additional non-

chlorophyll containing proteins not present in HT47GM PSII complexes (Table 3). In addition, measurements of the amount of manganese in the HisPsb32 complexes show that the HisPsb32 complexes contain only 2.57 manganese per PSII complex, as opposed to the theoretical 4 manganese per PSII and the 3.86 measured for HT47GM PSII complexes (Table 4).

DISCUSSION

Previous studies have shown that Psb32 co-purifies with PSII (Kashino et al., 2002; Wegener et al., 2008) and that the absence of PSb32 affects D1 turnover (Sirpio et al., 2007) (Chapter 4). The reciprocal purification of PSII complexes utilizing the HisPsb32 protein conducted in this work demonstrates that Psb32 is indeed a component of the complex. Although many high resolution structures exist for cyanobacterial PSII (Zouni et al., 2001; Ferreira et al., 2004; Loll et al., 2005), due to the nature of X-crystallography, they cannot fully capture the dynamic changes that occur in the complex as part of the assembly, damage, and repair process.

Complexes containing Psb32 contain a similar polypeptide composition to those isolated via his tag on CP47. However the abundances of specific proteins, notably D1, PsbO and CP43, appear decreased in the HisPsb32 complexes (Figures 7 and 8). Moreover, the Psb32 containing complexes have increased protein to chlorophyll ratios (Table 3) and a decreased number of Mn per PSII (Table 4). Thus it is not surprising that these impaired complexes display such severely reduced rates of oxygen evolution (Table 2). Taken together, these data suggest that Psb32 associates with non-fully assembled and thus non-fully functional, complexes. While Psb32 has been identified at low abundance in isolations from HT47GM, this is likely a reflection of the heterogeneity of complexes isolated using the CP47 tag, as has been previously shown (Lakshmi et al., 2002; Kashino et al., 2006). A model of Psb32 containing complexes is shown in Figure 9.

Interestingly the overexpression Psb32 under the psbA2 promoter resulted in very few effects on whole cell physiology. For the majority of conditions, growth was unaffected by the increased amount of Psb32, with the notable exception of in the absence of $CaCl_2$ (Figure 3). Calcium and chloride are crucial ions for photosynthesis. Mutants of the lumenal PSII proteins, PsbV, PsbO, PsbP, and PsbQ, have been shown to exhibit severe growth limitations in the absence of $CaCl_2$ (Philbrick et al., 1991; Shen et al., 1998; Thornton et al., 2004). It is possible that the over accumulation of Psb32 is hindering photoautotrophic growth in the absence of $CaCl_2$

by impeding access of the other lumenal proteins to their binding sites, reducing growth rates. While whole cell rates of oxygen evolution are unaffected by excess Psb32, the isolated complexes from Psb32OE HT47GM exhibit only 30% of the oxygen evolution activity of PSII complexes from HT47GM (Tables 1-2). This may be due to the decreased levels of the PsbO protein found in the Psb32OE HT47GM complexes (Figure 7). Further quantitative analysis of both the HisPsb32 and Psb32OE HT47GM complexes will allow final definitive statements about the role of Psb32 in PSII assembly and repair.

CONCLUSIONS

The work presented in this Chapter shows that Psb32 not only co-purifies with PSII, but is indeed associated with the complex. Reciprocal purification utilizing a his tag on Psb32 demonstrated that this protein is associated with complexes that exhibit significantly reduced oxygen evolution and decreased levels of manganese. This suggests that Psb32 is associated with a small percentage of intermediary PSII complexes *in vivo*. Overexpression of Psb32 led to growth sensitivity under $CaCl_2$ depletion, perhaps because excess amounts of the Psb32 limited access of the other lumenal PSII proteins, which are crucial to growth in the absence of $CaCl_2$. Furthermore overexpression of Psb32 resulted in decreased rates of oxygen evolution activity in isolated complexes.

REFERENCES

Abramoff MD, Magelhaes PJ, Ram SJ (2004) Image processing with ImageJ. Biophotonics International **11:** 36-42

Allen MM (1984) Cyanobacterial Cell Inclusions. Annu Rev Microbiol **38:** 1-25

Andersson B, Aro EM (2001) Photodamage and D1 Protein Turnover. *In* EM Aro, B Andersson, eds, Regulation of Photosynthesis, Vol 11. Kluwer, Dordrecht, pp 377-394

Aro EM, Virgin I, Andersson B (1993) Photoinhibition of Photosystem II. Inactivation, protein damage and turnover. Biochim Biophys Acta **1143:** 113-134

Desjardins P, Hansen J, Allen M (2009) Microvolume spectrophotometric and fluorometric determination of protein concentration. Curr Protocols Protein Sci **3.10:** S55-56

Ferreira KN, Iverson TM, Maghlaoui K, Barber J, Iwata S (2004) Architecture of the photosynthetic oxygen-evolving center. Science **303:** 1831-1838

Kaneko T, Sato S, Kotani H, Tanaka A, Asamizu E, Nakamura Y, Miyajima N, Hirosawa M, Sugiura M, Sasamoto S, Kimura T, Hosouchi T, Matsuno A, Muraki A, Nakazaki N, Naruo K, Okumura S, Shimpo S, Takeuchi C, Wada T, Watanabe A, Yamada M, Yasuda M, Tabata S (1996) Sequence analysis of the genome of the unicellular cyanobacterium *Synechocystis* sp. strain PCC 6803. II. Sequence determination of the entire genome and assignment of potential protein-coding regions. DNA Res **3:** 109-136

Kashino Y, Inoue-Kashino N, Roose JL, Pakrasi HB (2006) Absence of the PsbQ protein results in destabilization of the PsbV protein and decreased oxygen evolution activity in cyanobacterial photosystem II. J Biol Chem **281:** 20834-20841

Kashino Y, Lauber WM, Carroll JA, Wang Q, Whitmarsh J, Satoh K, Pakrasi HB (2002) Proteomic analysis of a highly active photosystem II preparation from the cyanobacterium *Synechocystis* sp. PCC 6803 reveals the presence of novel polypeptides. Biochemistry **41:** 8004-8012

Lakshmi K, Reifler M, Chisholm D, Wang J, Diner B, Brudvig G (2002) Correlation of the cytochrome c 2 content of cyanobacterial Photosystem II with the EPR properties of the oxygen-evolving complex. Photosynth Res **72:** 175-189

Loll B, Kern J, Saenger W, Zouni A, Biesiadka J (2005) Towards complete cofactor arrangement in the 3.0 A resolution structure of photosystem II. Nature **438:** 1040-1044

Mannan RM, Pakrasi HB (1993) Dark heterotrophic growth conditions result in an increase in the content of photosystem II units in the filamentous cyanobacterium *Anabaena variabilis* ATCC 29413. Plant Physiol **103:** 971-977

Muramatsu M, Sonoike K, Hihara Y (2009) Mechanism of downregulation of photosystem I content under high-light conditions in the cyanobacterium *Synechocystis* sp. PCC 6803 Microbiol **155:** 989-996

Philbrick JB, Diner BA, Zilinskas BA (1991) Construction and characterization of cyanobacterial mutants lacking the manganese-stabilizing polypeptide of photosystem II. J Biol Chem **266:** 13370 -13376

Porra RJ, Thompson WA, Kriedemann PE (1989) Determination of accurate extinction coefficients and simulatneous equations for assaying chlorophylls a and b extracted with four different solvents: verification of the concentration of chlorophyll standards by atomic absorption spectroscopy. Biochim Biophys Acta **975:** 384–339

Powles SB (1984) Photoinhibition of photosynthesis induced by visible light. Annu Rev Plant Physiol **35:** 15-44

Prásil O, Adir N, Ohad I (1992) Dynamics of photosystem II: mechanism of photoinhibition and recovery processes. *In* J Barber, ed, Topics in Photosynthesis: The Photosystems: Structure, Function and Molecular Biology, Vol 11. Elsevier Science Publishers, Amsterdam, pp 295-348

Roose JL (2008) Assembly and function of cyanobacterial photosystem II. Washington University in St. Louis, St. Louis

Roose JL, Kashino Y, Pakrasi HB (2007) The PsbQ protein defines cyanobacterial Photosystem II complexes with highest activity and stability. Proc Natl Acad Sci U S A **104:** 2548–2553

Satoh S, Ikeuchi M, Mimuro M, Tanaka A (2001) Chlorophyll b expressed in cyanobacteria functions as a light-harvesting antenna in Photosystem I through flexibility of the proteins. J Biol Chem **276:** 4293-4297

Shen JR, Qian M, Inoue Y, Burnap RL (1998) Functional characterization of *Synechocystis* sp. PCC 6803 delta psbU and delta psbV mutants reveals important roles of cytochrome c-550 in cyanobacterial oxygen evolution. Biochemistry **37:** 1551-1558

Sirpio S, Allahverdiyeva Y, Suorsa M, Paakkarinen V, Vainonen J, Battchikova N, Aro EM (2007) TLP18.3, a novel thylakoid lumen protein regulating photosystem II repair cycle. Biochem J **406:** 415-425

Thornton LE, Ohkawa H, Roose JL, Kashino Y, Keren N, Pakrasi HB (2004) Homologs of plant PsbP and PsbQ proteins are necessary for regulation of photosystem II activity in the cyanobacterium *Synechocystis* 6803. Plant Cell **16:** 2164-2175

Wegener KM, Welsh EA, Thornton LE, Keren N, Jacobs JM, Hixson KK, Monroe ME, Camp DG, 2nd, Smith RD, Pakrasi HB (2008) High sensitivity proteomics assisted discovery of a novel operon involved in the assembly of photosystem II, a membrane protein complex. J Biol Chem **283:** 27829-27837

Zouni A, Witt HT, Kern J, Fromme P, Krauss N, Saenger W, Orth P (2001) Crystal structure of photosystem II from *Synechococcus elongatus* at 3.8 A resolution. Nature **409:** 739-743

Table 1. Whole cell rates of oxygen evolution for Psb32 mutants. Measurements were conducted in the presence of presence of the electron acceptors 0.5 mM DCBQ and 1 mM potassium ferricyanide on a Clark-type electrode. Standard deviation is given for n=3.

Irradiance (μmol photon m^{-2} s^{-1})	Rate of Oxygen Evolution (μmol O_2 mg chl^{-1} hr^{-1})			
	WT	**ΔPsb32**	**HisPsb32**	**Psb32OE**
8250	622 ± 31	632 ± 22	599 ± 59	712 ± 53
4300	561 ±30	620 ± 4	578 ± 82	691 ± 11
2525	563 ± 54	534 ± 66	628 ± 60	672 ± 1
1310	448 ± 25	479 ± 57	473 ± 40	528 ± 23
800	406 ± 4	423 ± 20	452 ± 77	423 ± 10

Table 2. Rates of oxygen evolution for isolated complexes from Psb32 mutants. Measurements were conducted at 8250 µml photons m^{-2} s^{-1} in the presence of presence of the electron acceptors 0.5 mM DCBQ and 1 mM potassium ferricyanide on a Clark-type electrode. Standard deviation is given for n=3.

Sample	Rate of Oxygen Evolution (µmol O_2 mg chl^{-1} hr^{-1})	Relative Rate to HT47GM
HT47GM	493 ± 26	-
HisPsb32	45 ± 20	9%
Psb32OE HT47GM	134 ± 26	27%

Table 3. Ratios of protein and chlorophyll of isolated complexes.

	HT47GM	HisPsb32
Chlorophyll (μg/mL)	1441	64
Protein (mg/mL)	1.3	4.25
Ratio (μg protein/μg chlorophyll)	0.9	66

Table 4. Ratio of Mn per PSII as measured by atomic absorption spectrometry.

Sample	Mn:PSII
HT47GM	3.86
HisPsb32	2.57

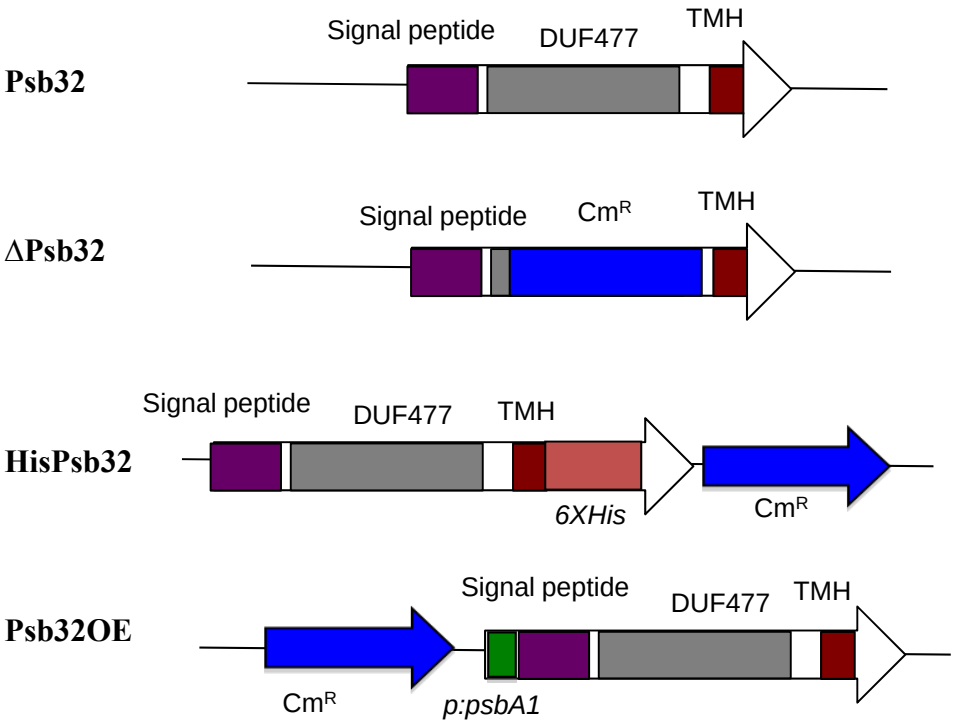

Figure 1. Schematic of HisPsb32 and Psb32OE lines.

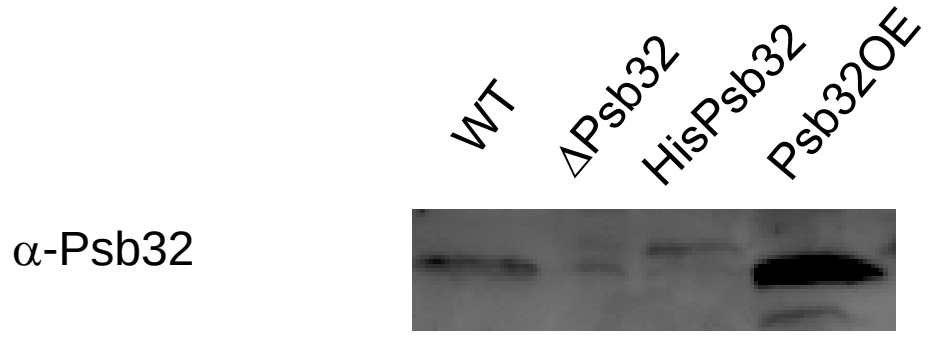

Figure 2. Levels of Psb32 in HisPsb32 and Psb32OE.

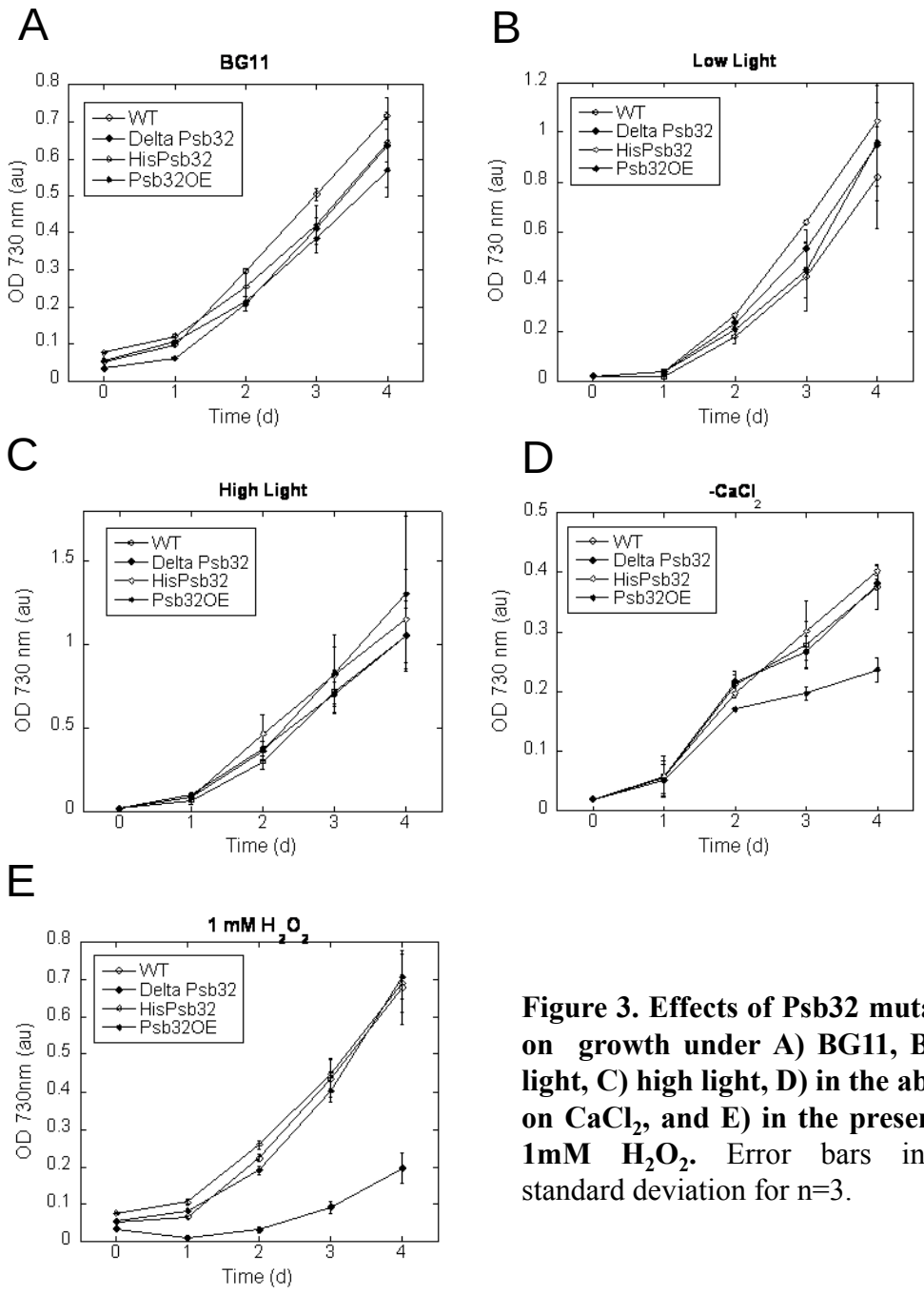

Figure 3. Effects of Psb32 mutations on growth under A) BG11, B) low light, C) high light, D) in the absence on $CaCl_2$, and E) in the presence of 1mM H_2O_2. Error bars indicate standard deviation for n=3.

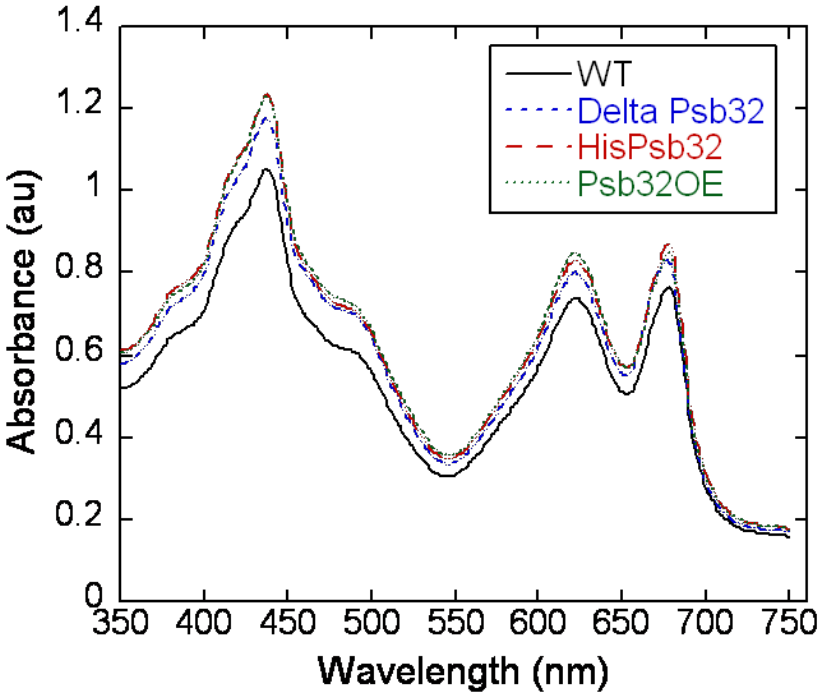

Figure 4. Whole cell absorbance spectra of WT, ΔPsb32, HisPsb32, and Psb32OE.

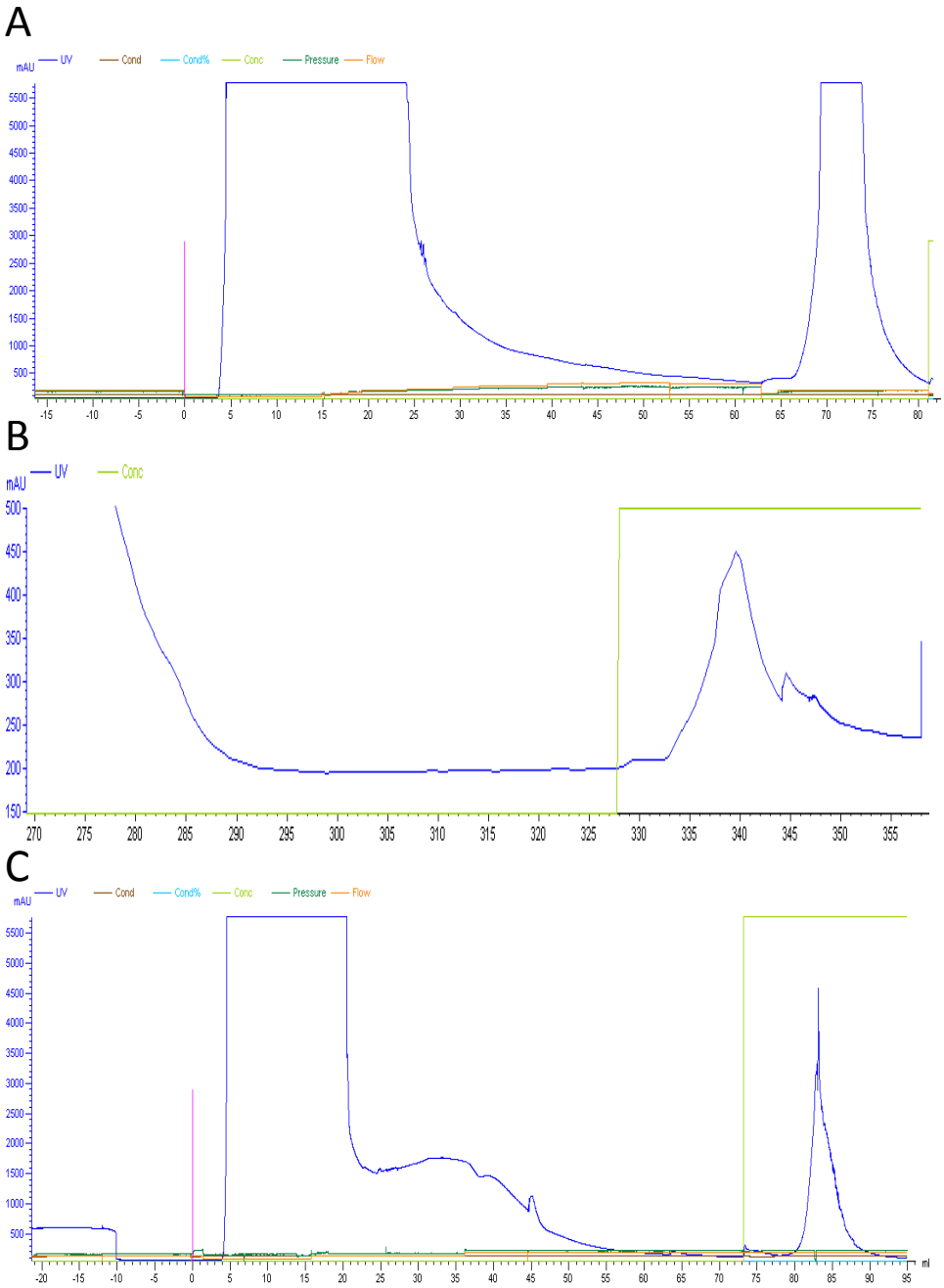

Figure 5. Representative chromatograms for isolations of His tagged complexes from A) HT47GM B) His32 and C) HT47GM Psb32OE. Blue lines represent readings at 436 nm for A and C and 280nm for B.

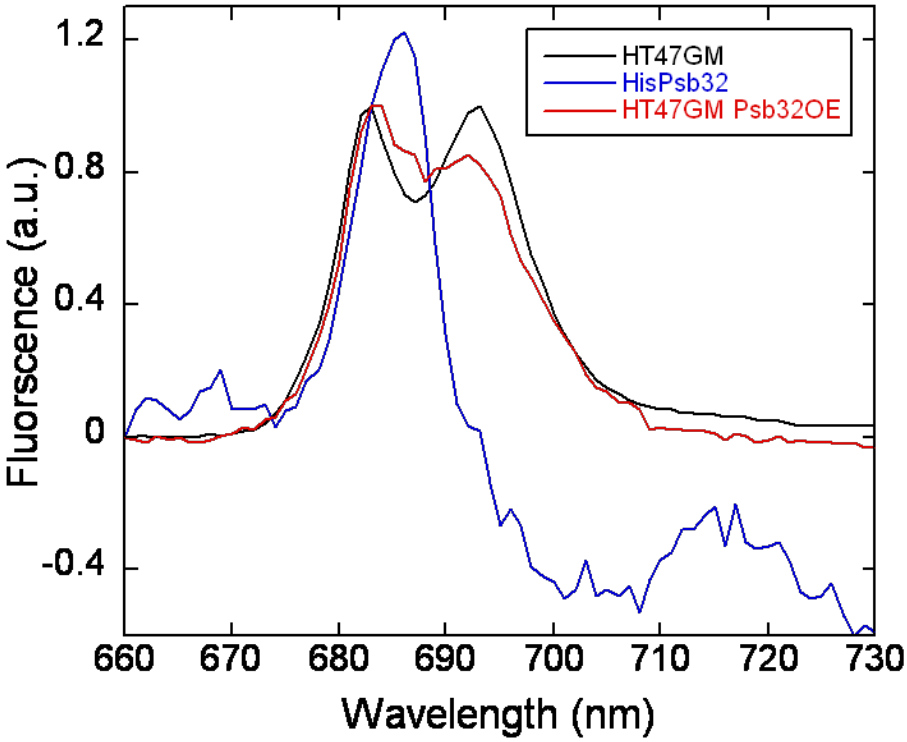

Figure 6. 77K fluorescence of isolated his tagged complexes from HT47GM, HisPsb32, and HT47GM Psb32OE. Samples were excited at 440nm and fluorescence emission spectra were normalized by $(F-F_{660})/(F_{683}-F_{660})$.

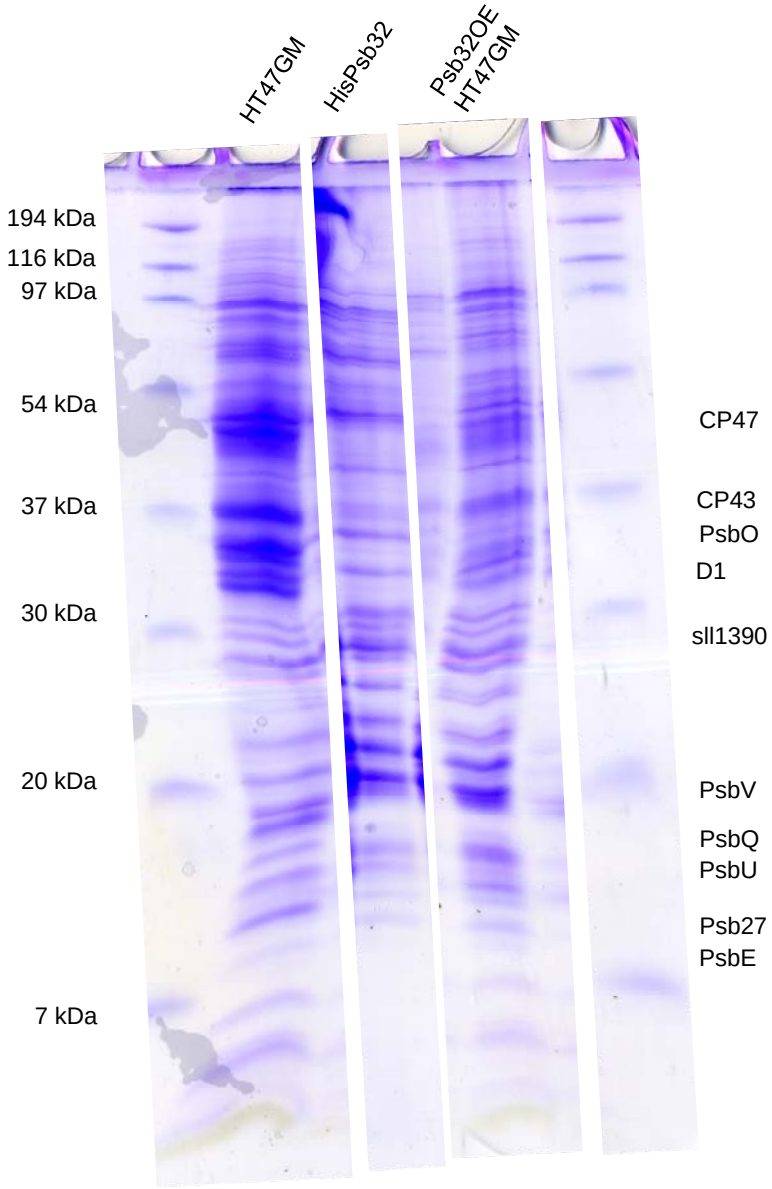

Figure 7. Polypeptide profile of isolated complexes from HT47GM, HisPsb32, and HT47GM Psb32OE. Samples were loaded at 3 µg/mL chlorophyll per lane.

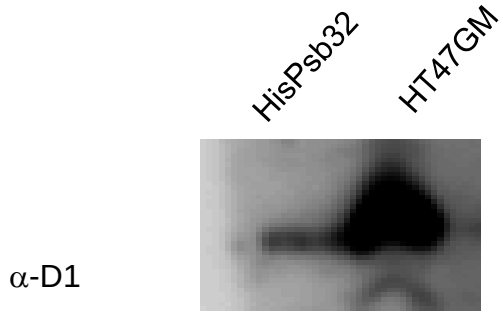

Figure 8. Levels of D1 in Psb32 containing PSII. Immunoblots of D1 protein in isolated complexes loaded by equal protein.

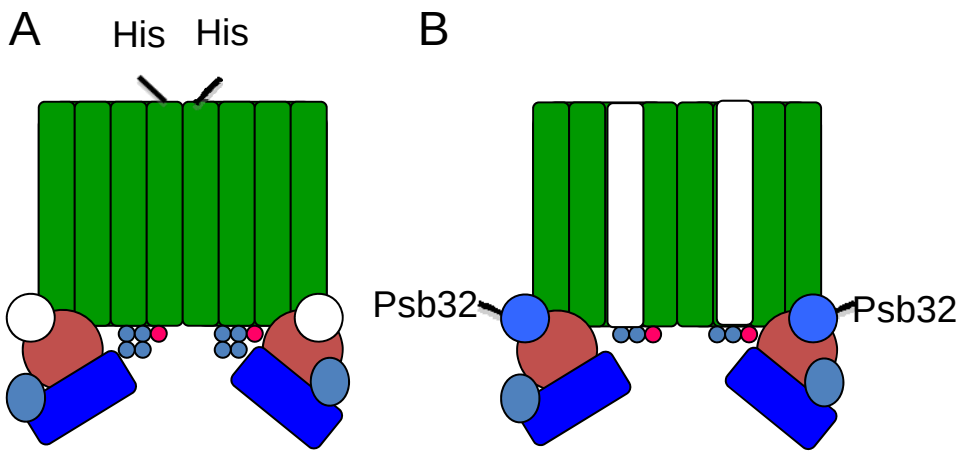

Figure 9. Model of Psb32 containing PSII. (A) Diagram of PSII complexes isolated using a histidine tag on CP47 **(B)** Diagram of Psb32 containing PSII complexes.

Chapter 6

Conclusions

SUMMARY AND CONCLUSIONS OF THIS WORK

This work has contributed significant new findings as to the quantity and importance of accessory proteins involved in PSII assembly and repair. Utilizing high through put proteomics, we were able to define the *Synechocystis* proteome during various environmental stresses, when many of the cell's protein complexes are being turned over to scavenge elements for survival. Use of the resulting proteomic library allowed for detailed study of the composition of PSII. We found over 200 proteins associated with the complex and were able to compare the protein abundance changes in complexes lacking the lumenal proteins PsbQ, PsbP, and PsbV. Of those novel PSII associated proteins identified, the proteins of Slr0144-Slr0152 (Pap) were required for optimal function and assembly of PSII. Additionally another novel Psb32 was also found to be required for proper PSII assembly.

Environmental Effects of the Proteome

While we traditionally study *Synechocystis* under controlled light, temperature, and nutritional conditions, to subsist outside the laboratory, these organisms must continually adjust their physiology to environmental changes. During their evolution, cyanobacteria have survived large changes in environmental conditions (Kasting, 2004). They can readily adapt their cellular metabolism to daily changes in light quality and quantity. Integration of nutrient specific pathways with photosynthetic processes is a key survival mechanism employed by cyanobacteria under changing environmental conditions (Tsinoremas et al., 1991; Lindahl and Florencio, 2003; Singh et al., 2008). Such adaptation strategies allow cyanobacteria to balance the supply of electrons from photosynthetic processes with the demands of cellular metabolism, and prevent the generation of damaging reactive oxygen species by excess reducing power.

Nitrogen and carbon metabolism are sinks for ATP and reducing power produced during photosynthesis. Protein complexes involved in the photosynthetic processes are in themselves a major metabolic store for iron, sulfur, nitrogen, and carbon. Thus, adjusting the proteins of PSII, the first enzyme of electron transport, is crucial to organismal survival. Of the canonical PSII proteins (Kashino et al., 2002), we identified 23 proteins in our study, which were distributed between the 33 environmental conditions (Chapter 2, Supplemental Table 4). Thus it is interesting that the identifications of PSII proteins from a particular nutrient starved condition do not drastically differ from those in the replete condition, even though the accompanying replete conditions display dramatically increased photosynthetic rates (Table 1). This indicates that fine-tuning photosynthesis due to environmental conditions is not as simple as the presence or absence of particular proteins. Analysis of changes in protein abundances after stress as compared to level found in BG11 grown cells provides more insight. As a whole, all detected PSII proteins were differentially less abundant under nitrate and sulfur depletion conditions (Chapter 2, Supplemental Tables 6 and 7). This agrees with previous data showing that these two conditions have detrimental effects on photosynthetic capacity. However, in all conditions where it was possible to determine differential ratios, the manganese stabilizing protein, PsbO (Sll0427), was increased in abundance as compared to levels found in BG11.

PSII Assembly

In the last ten years a small number of accessory proteins, including CtpA, (Roose and Pakrasi, 2004), PratA, (Klinkert B, 2004), Psb27, (Nowaczyk et al., 2006; Roose and Pakrasi, 2008) and Psb29, (Wang, 2004; Keren et al., 2005) have been identified and characterized. The proteomic study of isolated complexes described in Chapter 3 identified 217 proteins that copurify with PSII (Chapter 3, Supplemental 1). Although a fraction of these may represent contamination or non-specific associations, this sheer number of proteins of the complex suggest that PSII

assembly requires many more additional players than is currently thought (see Chapter 1 and Chapter 1 Figure 2B for more details on current model of PSII assembly). These additional proteins may represent factors that are transiently associated with PSII and play roles in complex assembly, repair, or degradation. In the past, it has proven difficult to identify these proteins due to the relatively short periods of association in comparison to stable mature, active PSII complexes.

Pap proteins

Analysis of the proteins of the *slr0144 – slr0152* operon showed that they aid in PSII-mediated oxygen evolution and maintaining a normal distribution of the S states of the catalytic Mn cluster. PSII complexes isolated from *⊿sllr0144 – slr0152* also show decreased photosynthetic capacity and altered polypeptide composition. These data demonstrate that the proteins encoded by the genes in this operon are necessary for optimal function of PSII and function as accessory proteins during assembly of the PSII complex in *Synechocystis*.

The discovery of Paps may aid our understanding how non-protein cofactors are inserted or recycled into new and repaired complexes. It is possible that the PSII defects seen in *⊿sllr0144 – slr0152* HT47GM indicate that Slr0144 and Slr0147 function to sequester chlorophyll molecules to prevent damage to the cell prior to initial complex assembly and during repair, similar to the SCP proteins (Vavilin and Vermaas, 2007). Future work demonstrating that the cofactor binding sites of the Pap proteins are functional and that they are able to transfer cofactors could provide exciting insight into how these cofactors are assembled into the complex.

The ∆*slr0144 – slr0152* mutation demonstrates a case of cross talk between the lumenal and cytosolic proteins of PSII. It is intriguing that deletion of the lumenal proteins PsbP, PsbQ, and PsbV lead to an increase in abundance in the cytosolic Pap proteins (Chapter 3,

Supplemental Table 1) and conversely, the deletion of the Pap proteins results in increased levels in PsbV, Sll1390, and Psb27 (Chapter 2, Fig. 10A), which all contain targeting sequences for the lumen. The increase of these proteins in non-fully assembled PSII complexes suggest that the Pap proteins function in assembly of complexes and are aggregating on these sub-assembled complexes or are functioning in degrading the non-fully functional complexes. Additionally, the decrease in oxygen evolution activity and the altered S state distribution in the ∆*slr0144 – slr0152* mutant are phenotypes traditionally associated with mutation in the lumenal PsbO, PsbU, PsbV, PsbQ, and PsbP proteins (Shen et al., 1998; Thornton et al., 2004; Kashino et al., 2006), suggesting that the lumenal side of the complex is unstable in the absence of the Pap proteins. This suggests that there is feedback across the membrane plane of PSII that increases Pap protein levels when the lumenal surface is non-fully assembled and that the Pap proteins are necessary to fully assemble the lumenal side of PSII.

Psb32

Psb32 was identified has previously been identified as a protein associated with highly active purified PSII preparations from the cyanobacterium *Synechocystis* (Kashino et al., 2002) (Chapter 3). Psb32 plays a role in protecting cells from photodamage and ROS damage. This protective effect is perhaps due by facilitating the ability of PSII to repair itself after photodamage. ROS damage has been shown to slow PSII repair arresting of translation elongation of the *psbA* gene, which encodes the D1 protein (Nishiyama et al., 2001; Nishiyama et al., 2004). Thus it could be that the effects we see of ROS on the growth rates of Δ*psb32* are actually a reflection of the decreased rate of PSII repair of the damage caused by the ROS. That is further supported by our photoinhibition experiments; in which Δ*psb32* exhibits a decreased rate of recovery after damage and an increased rate of photodamage that the Δ*psb32* mutant displays (Chapter 4, Figure 6).

However, Psb32 only protects cells from damage on the donor side, not on the acceptor side. The reaction of Δ*psb32* to damage on the donor side but not the acceptor side is further evidence that Psb32 functions to aid in assembly of PSII, which coincides with the lumenal localization of the protein (Chapter 4, Figure 2A and B). This slowed repair, in addition to the observed accelerated rate of photodamage, could explain why the presence of Psb32 confers a selective advantage to fitness during competition under high light (Chapter 4, Figure 5), when ROS damage and light induced photoinhibition are at their highest. The role of Psb32 in protecting PSII from photodamage and aiding in the efficient repair is conserved in its *Arabidopsis* homolog, TPL18.3 (Sirpio et al., 2007). The possible role of Psb32 as a PSII assembly nicely explains the decreased efficiency of PSII repair in both *Synechocystis* and *Arabidopsis*, suggesting that this role is conserved among oxygenic phototrophs.

The experiments described in Chapter 5 demonstrate that Psb32 is a true component of PSII and associates with partially assembled complexes to aid in their completion. Characterization of HisPsb32 complexes revealed that Psb32 is associated with a subpopulation of PSII that have altered PSII fluorescence properties, reduced oxygen evolution activity, and decreased manganese content, suggesting that they are not fully functional complexes. Overexpression of Psb32 severely retarded growth in the absence of $CaCl_2$ and also significantly reduced oxygen evolution activity in isolated PSII complexes. This growth defect is particularly interesting in that, mutants of other lumenal PSII proteins, PsbV, PsbO, PsbP, and PsbQ, exhibit severe growth limitations in the absence of $CaCl_2$ (Philbrick et al., 1991; Shen et al., 1998; Thornton et al., 2004). The effect of excess Psb32 on growth in the absence of $CaCl_2$ may be due to impeding access of the other lumenal proteins to their binding sites, reducing growth rates. In the absence of PsbP and PsbQ, levels of Psb32 increase respectively to 1.19 and 1.24 fold of levels in HT3 PSII complexes (Chapter 2, Supplemental Table 1), suggesting that in the absence of these lumenal proteins, Psb32 has a higher binding affinity to PSII.

Implications of this work

PSII populations

Taken together, this work highlights the plasticity of PSII. Due to the constantly changing cellular conditions that accompany photosynthesis, PSII is continually being assembled, damaged, degraded, and repaired. While the majority of complexes are fully assembled and fully functional, at any given time a heterogeneous population of complexes exist *in vivo*, producing the average rates of PSII activity for a cell. Many of these populations are short lived and so difficult to identify using traditional biochemical purification of PSII via his tagged CP47 followed by SDS-PAGE separations. However, new approaches, such as reciprocal purification of alternately tagged proteins and highly sensitive proteomic analysis of complexes provide the tools necessary to isolate and characterize the alternate PSII complexes. These new techniques have enabled the identification of new PSII subassemblies in this work and can be further applied to gain a full understanding of the PSII assembly and repair cycle.

PSII composition under alternate environmental conditions

Oxygenic photosynthetic organisms in general, and cyanobacteria in particular, inhabit almost every ecological niche on the planet, surviving in temperatures from 4°C to 75°C, under widely varying nutritional environs. In addition to the dynamics of PSII within cyanobacterial cells, the advent of the genomics era has revealed that there are significant differences in PSII protein composition between different types of cyanobacteria (Thornton et al., 2005; Roose et al., 2007). While this work has focused on the proteome changes that occur both globally, and specifically for PSII, in *Synechocystis* 6803, many other cyanobacteria face and adapt to other environmental challenges. This is not surprising given the wide range of environments these organisms inhabit:

surviving in both fresh and salt water, temperatures from 4°C to 75°C, with widely diverse nutritional availability. Some classes must also balance diverse and opposing metabolic processes, such as N_2 fixation and oxygenic photosynthesis in the same cell. A phylogenetic tree of the cyanobacteria for which genome sequence data are available is shown in Figure 1.

The recently finished genomes of multiple species of *Prochlorococcus* have shed new light on the minimal set of genes needed for a free living oxygenic photosynthetic organism (Dufresne et al., 2005). Genome sequence for several species of *Prochlorococcus,* including MED4, show that the *psbU, psbV* and *psbQ* genes have been lost from these organisms. Absence of any of these genes in *Synechocystis* results in significantly reduced PSII activity and combinatorial mutants are unable to survive photoautotrophically (Summerfield et al., 2005). MED4 grows in deep ocean environments where the concentration of bioavailable iron is low (nM). Thus, dispensing with the gene product of *psbV*, an iron-containing monoheme *c*-type cytochrome, may confer a reasonable advantage for these organisms. Additionally, x-ray structure of PSII shows that PsbU is bound to PSII via PsbV (Fig. 1A). PsbQ genetically interacts with PsbV (Summerfield et al., 2005; Kashino et al., 2006). Apparently, the PsbV/PsbU/PsbQ triad serves a function that is not essential for PSII function in the seawater environment.

However, our preliminary studies in *Synechocystis* on the effect of low iron on photoautotrophic growth have shown that PsbV, and to a lesser extent PsbU and PsbQ, are critical to growth in iron deplete conditions (Figure 2). Another obvious difference between seawater and fresh water environments is the high concentration of salt in the former. Indeed, seawater contains as high as 2% (w/w) Cl- and 1.1% Na+ (http://www.seafriends.org.nz/oceano/seawater.htm-salinity). BG11, the fresh water medium widely used to culture *Synechocystis*, in contrast, has nearly 1000-fold lower concentrations of Cl- (Rippka, 1988). The Δ*psbV* mutant cannot grow in Cl- depleted BG11 medium (Shen et al., 1998; Kobayashi et al., 2006). Also, we have shown the genetic deletion of *psbU* results in severely reduced growth in Cl- depleted

medium (Inoue-Kashino et al., 2005). It seems that a crucial function of the PsbV/PsbU/ PsbQ triad is as a Cl- concentrator.

Diurnal D1 regulation

While this work has examined the alternate PSII forms in *Synechocystis 6803, the* unicellular N_2-fixing cyanobacterium *Cyanothece ATCC* 51142 faces a unique set of physiological challenges that affect its PSII composition. This organism exhibits striking diurnal rhythms in its metabolism required because the enzyme that fixes atmospheric N_2, nitrogenase, is highly sensitive to O_2, an obligatory product of the PSII reaction. Because this is a unicellular organism, it uses time as a way of separating the peaks of photosynthesis from peaks of nitrogenase activity. As such, it tightly regulates PSII activity throughout its diurnal cycle, ensuring peak PSII activity during the day and minimal activity at night. This interesting lifestyle makes *Cyanothece* an apt model system for studying PSII dynamics. Recently genomic, transcriptomic, and proteomic tools have been developed for the study of this organism (Stöckel J et al., 2008; Welsh EA et al., 2008). As shown in Figure 1, *Synechocystis* and *Cyanothece* are close relatives on an evolutionary time scale.

In *Cyanothece* cells grown under a 12h light/12h dark cycle in a medium lacking any N_2 source, PSII activity peaks later in the light period (L6-L9), while nitrogenase activity exhibits a sharp peak of activity early in the dark phase (D3-D5) (Figure 3A). Concomitant with nitrogenase activity, cells lose their capacity for O_2 evolution (Sherman et al., 1998; Meunier et al., 19998) (Meunier et al., 1998; Sherman et al., 1998). In contrast, in other cyanobacteria, such as *Synechocystis*, PSII complexes are quite stable in the dark and retain 90% of their activity after 6 hours of dark incubation (Burnap et al., 1996). This indicates that *Cyanothece* cells actively shut down PSII O_2-evolving activity in the dark and regenerate active PSII complexes in the ensuing light period. It is clear from recent structural studies (Ferreira et al., 2004; Loll et al., 2005) that

PSII complexes must disassemble to some extent to eliminate O_2-evolving activity, and then reassemble into active complexes.

All cyanobacterial strains have multiple copies of the *psbA* gene (encoding the D1 protein), and *Cyanothece* has four such genes (*psbA1-4*). In diurnal microarray experiments, the majority of *psbA* gene copies (*psbA1-3)* peak at L9 (Stöckel J et al., 2008), correlating well with the peak in PSII-mediated O_2 evolution activity (Colon-Lopez and Sherman, 1998; Sherman et al., 1998). However, the expression profile of *psbA4* is shifted, peaking at time points D1 and again at D9 (Figure 3B). The protein D1 provides ligands to many critical cofactors such as manganese, chlorophyll, pheophytin and quinone in PSII. Interestingly, the translation product of *psbA4* contains amino acid changes that have been shown by mutational analyses in other cyanobacteria to abolish O_2-evolving activity (Debus, 2001). An alignment of the C-terminal residues of D1 proteins from *Cyanothece* and one copy from *Synechocystis* is shown in Figure 4A. The residues shown in red indicate amino acid changes that eliminate O_2-evolving activity and also affect the processing of the C-terminal extension of the precursor form of D1 (pD1) to its mature form (Taguchi et al., 1993; Debus, 2001). The residues shown in blue indicate additional amino acid changes observed in PsbA4 relative to the other PsbA proteins shown.

Initial global proteomics analysis of *Cyanothece* identified a unique peptide corresponding to this alternate D1*,* which confirms that *psbA4* is indeed translated into a protein, which we have designated D1† (Stöckel *et al*., submitted to Molecular and Cellular Proteomics, Manuscript number MO:00173-MCP). Based on the amino acid differences, the D1† protein is predicted to result in a loss of the catalytic Mn cluster (Figure 4A and B) and also likely retains its C-terminal extension (Taguchi et al., 1993; Debus, 2001). It is noteworthy that without the C-terminal processing of pD1, PSII cannot catalyze O_2 evolution (Anbudurai et al., 1994; Roose and Pakrasi, 2004). Insertion of D1† in PSII during the dark period is consistent with previously published observations that O_2-evolution capacity decreases and Mn clusters can not be

assembled into *Cyanothece* PSII complexes in the dark period (Meunier et al., 1998; Sherman et al., 1998).

Genomic information available for a number of other unicellular, N_2-fixing cyanobacteria (*Crocosphaera watsonii, Synechococcus* OS-A and *Synechococcus* OS-B') (Kulikova et al., 2004) supports this hypothesis as a general way of suppressing PSII O_2-evolving capacity in the dark period (Figure 1). Each of these organisms contains a number of *psbA* genes encoding the normal D1 protein, but also has one copy analogous to the *psbA4* gene in *Cyanothece*. Figure 4C shows protein alignments of representative D1 and $D1^{\dagger}$ proteins from each strain. This suggests that inclusion of a non-functional $D1^{\dagger}$ protein into PSII complexes may be a conserved mode of action among unicellular nitrogen fixers to prevent photosynthesis.

Future Directions

A hallmark of PSII is the plasticity of its form and functions. Genomic analysis of cyanobacterial species from diverse ecological niches has suggested that the composition of PSII undergoes significant changes in response to variations in nutritional and other environmental conditions. In view of the dynamic nature of this membrane protein complex, the current challenge is to elucidate the intricate pathway for the biogenesis and assembly of PSII that is responsible for one of the most thermodynamically unfavorable reactions in biology, the evolution of dioxygen from water.

The amount of data generated through the high throughput studies described in Chapters 2 and 3 certainly provide many avenues for further research. Of the 212 co-purifying PSII proteins, only Psb27, Psb29, Psb32, Sll1414, Slr0146, Slr0147, Slr0149, and Slr0151 have been investigated and confirmed to have PSII function. Many of the other co-purifying proteins have greater differential abundances in the *ΔpsbV*, *ΔpsbP*, and *ΔpsbQ* mutants than those currently characterized and so could provide great insight into PSII assembly. Recent studies have shown that the presence of the PsbQ protein is a marker for fully assembled complexes (Roose et al., 2007). Thus it would be interesting to investigate proteins that show reduced abundance in the *ΔpsbQ* complexes, but not in the *ΔpsbV* and *ΔpsbP* PSII complexes, which represent an earlier stage of assembly.

Though the isolated complexes from *Δslr0144-slr0152* HT47GM and HisPsb32 have been analyzed for the presence and absence of major PSII protein after SDS-PAGE separation, it would be intriguing to subject these complexes to the same proteomic analysis conducted on complexes isolated from *ΔpsbV*, *ΔpsbP*, and *ΔpsbQ* described in Chapter 2. This would allow for through identification of all co-purifying proteins and efficient estimates of protein abundances of those proteins.

While reciprocal purification strategies will provide a great deal of information as to PSII sub-assemblies, these studies still provide static snapshots of PSII. Future work should focus on better understanding the dynamics of the changes occurring in PSII composition. While

radiolabelling studies of PSII have been conducted in plant chloroplasts (Aro et al., 2005), no such studies have been conducted in cyanobacteria. The simpler cyanobacterial system will allow for a clearer picture of PSI assembly. This could be done with simple pulse chase experiments in which *Synechocystis* cells are given a short pulse of ^{35}S-methionine, and then quenched with unlabeled methionine (chase). At various time points following the pulse, membranes would be isolated. Thus, the PSII-associated proteins synthesized during the short pulse, like the frequently turned-over D1 protein, can then be followed through the biogenesis pathway. In order to determine the nature of the labeled PSII complexes during the chase period, *Synechocystis* membranes will be solubilized and fractionated by native gel electrophoresis. Those complexes that are labeled earlier in the chase period will represent early PSII assembly intermediates, and those labeled in subsequent time points will represent PSII complexes progressing through the assembly pathway. Once the labeling information is used to place various protein complexes in a temporal order, the protein components of each intermediate complex will be identified. To provide information on all of the protein components of each assembly intermediate, 2-dimensional BN/SDS-PAGE will be used. Mass spectrometry can be used to identify proteins for which antibodies are not available.

REFERENCES

Anbudurai PR, Mor TS, Ohad I, Shestakov SV, Pakrasi HB (1994) The ctpA gene encodes the C-terminal processing protease for the D1 protein of the photosystem II reaction center complex. Proc Natl Acad Sci U S A **91:** 8082-8086

Aro EM, Suorsa M, Rokka A, Allahverdiyeva Y, Paakkarinen V, Saleem A, Battchikova N, Rintamaki E (2005) Dynamics of photosystem II: a proteomic approach to thylakoid protein complexes. J Exp Bot **56:** 347-356

Burnap RL, Qian M, Pierce C (1996) The manganese stabilizing protein of photosystem II modifies the i*n vivo* deactivation and photoactivation kinetics of the H2O oxidation complex in *Synechocystis* sp. PCC6803. Biochemistry **35:** 874-882

Colon-Lopez MS, Sherman LA (1998) Transcriptional and translational regulation of photosystem I and II genes in light-dark- and continuous-light-grown cultures of the unicellular cyanobacterium *Cyanothece* sp. strain ATCC 51142. J Bacteriol **180:** 519-526

Debus RJ (2001) Amino acid residues that modulate the properties of tyrosine Y(Z) and the manganese cluster in the water oxidizing complex of photosystem II. Biochim Biophys Acta **1503:** 164-186

Dufresne A, Garczarek L, Partensky F (2005) Accelerated evolution associated with genome reduction in a free-living prokaryote. Genome Biol **6:** R14

Ferreira KN, Iverson TM, Maghlaoui K, Barber J, Iwata S (2004) Architecture of the photosynthetic oxygen-evolving center. Science **303:** 1831-1838

Inoue-Kashino N, Kashino Y, Satoh K, Terashima I, Pakrasi HB (2005) PsbU provides a stable architecture for the oxygen-evolving system in cyanobacterial photosystem II. Biochemistry **44:** 12214-12228

Kashino Y, Inoue-Kashino N, Roose JL, Pakrasi HB (2006) Absence of the PsbQ protein results in destabilization of the PsbV protein and decreased oxygen evolution activity in cyanobacterial photosystem II. J Biol Chem **281:** 20834-20841

Kashino Y, Lauber WM, Carroll JA, Wang Q, Whitmarsh J, Satoh K, Pakrasi HB (2002) Proteomic analysis of a highly active photosystem II preparation from the cyanobacterium *Synechocystis* sp. PCC 6803 reveals the presence of novel polypeptides. Biochemistry **41:** 8004-8012

Kasting JF (2004) When methane made climate. Sci Am **291:** 78-85

Keren N, Ohkawa H, Welsh EA, Liberton M, Pakrasi HB (2005) Psb29, a conserved 22-kD protein, functions in the biogenesis of Photosystem II complexes in *Synechocystis* and *Arabidopsis*. Plant Cell **17:** 2768-2781

Klinkert B OF, Sikorski M, Berry S, Eichacker L, Nickelsen J (2004) PratA, a periplasmic tetratricopeptide repeat protein involved in biogenesis of photosystem II in *Synechocystis* sp. PCC 6803. J Biol Chem **279:** 44639-44644

Kobayashi M, Katoh H, Ikeuchi M (2006) Mutations in a putative chloride efflux transporter gene suppress the chloride requirement of the Photosystem II in the cytochrome c550 deficient mutant. Plant Cell Physiol **47:** 700-804

Kulikova T, Aldebert P, Althorpe N, Baker W, Bates K, Browne P, van den Broek A, Cochrane G, Duggan K, Eberhardt R, Faruque N, Garcia-Pastor M, Harte N, Kanz C, Leinonen R, Lin Q, Lombard V, Lopez R, Mancuso R, McHale M, Nardone F, Silventoinen V, Stoehr P, Stoesser G, Tuli MA, Tzouvara K, Vaughan R, Wu D, Zhu W, Apweiler R (2004) The EMBL Nucleotide Sequence Database. Nucleic Acids Res **32:** D27-30

Lindahl M, Florencio FJ (2003) Thioredoxin-linked processes in cyanobacteria are as numerous as in chloroplasts, but targets are different. Proc Natl Acad Sci U S A **100:** 16107-16112

Loll B, Kern J, Saenger W, Zouni A, Biesiadka J (2005) Towards complete cofactor arrangement in the 3.0 A resolution structure of photosystem II. Nature **438:** 1040-1044

Meunier PC, Colon-Lopez MS, Sherman LA (1998) Photosystem II cyclic heterogeneity and photoactivation in the diazotrophic, unicellular cyanobacterium cyanothece species ATCC 51142. Plant Physiol **116:** 1551-1562

Meunier PC, Colon-Lopez MS, Sherman LA (19998) Photosystem II cyclic heterogeneity and photoactivation in the diazotrophic, unicellular cyanobacterium cyanothece species ATCC 51142. Plant Physiol **116:** 1551-1562

Nishiyama Y, Allakhverdiev SI, Yamamoto H, Hayashi H, Murata N (2004) Singlet oxygen inhibits the repair of Photosystem II by suppressing the translation elongation of the D1 protein in *Synechocystis* sp. PCC 6803. Biochemistry **43:** 11321-11330

Nishiyama Y, Yamamoto H, Allakhverdiev SI, Inaba M, Yokota A, Murata N (2001) Oxidative stress inhibits the repair of photodamage to the photosynthetic machinery. EMBO J **20:** 5587-5594

Nowaczyk MM, Hebeler R, Schlodder E, Meyer HE, Warscheid B, Rogner M (2006) Psb27, a cyanobacterial lipoprotein, is involved in the repair cycle of photosystem II. Plant Cell **18:** 3121-3131

Philbrick JB, Diner BA, Zilinskas BA (1991) Construction and characterization of cyanobacterial mutants lacking the manganese-stabilizing polypeptide of photosystem II. J Biol Chem **266**

Rippka R (1988) Isolation and purification of cyanobacteria. Methods Enzymol **167:** 3-27

Roose JL, Kashino Y, Pakrasi HB (2007) The PsbQ protein defines cyanobacterial Photosystem II complexes with highest activity and stability. Proc Natl Acad Sci U S A **104:** 2548–2553

Roose JL, Pakrasi HB (2004) Evidence that D1 processing is required for manganese binding and extrinsic protein assembly into photosystem II. J Biol Chem **279:** 45417-45422

Roose JL, Pakrasi HB (2008) The Psb27 protein facilitates manganese cluster assembly in photosystem II. J Biol Chem **283:** 4044-4050

Roose JL, Wegener KM, Pakrasi HB (2007) The extrinsic proteins of Photosystem II. Photosynth Res

Shen JR, Qian M, Inoue Y, Burnap RL (1998) Functional characterization of *Synechocystis* sp. PCC 6803 delta psbU and delta psbV mutants reveals important roles of cytochrome c-550 in cyanobacterial oxygen evolution. Biochemistry **37:** 1551-1558

Sherman LA, Meunier P, ColÃ³n-LÃ³pez MS (1998) Diurnal rhythms in metabolism: A day in the life of a unicellular, diazotrophic cyanobacterium. Photosynth Res **58:** 25-42

Sherman LA, Meunier P, Colon-Lopez MS (1998) Diurnal rhythms in metabolism: A day in the life of a unicellular, diazotrophic cyanobacterium. Photosynth Res **58:** 25-42

Singh AK, Elvitigala T, Bhattacharyya-Pakrasi M, Aurora R, Ghosh B, Pakrasi HB (2008) Integration of carbon and nitrogen metabolism with energy production is crucial to light acclimation in the cyanobacterium *Synechocystis*. Plant Physiol **148:** 467-478

Sirpio S, Allahverdiyeva Y, Suorsa M, Paakkarinen V, Vainonen J, Battchikova N, Aro EM (2007) TLP18.3, a novel thylakoid lumen protein regulating photosystem II repair cycle. Biochem J **406:** 415-425

Stöckel J, Welsh EA, Liberton M, Kunnvakkam R, Aurora R, HB P (2008) Global transcriptomic analysis of *Cyanothece* 51142 reveals robust diurnal oscillation of central metabolic processes. Proc Natl Acad Sci U S A **105:** 6156-6161

Summerfield TC, Shand JA, Bentley FK, Eaton-Rye JJ (2005) PsbQ (Sll1638) in *Synechocystis* sp. PCC 6803 is required for photosystem II activity in specific mutants and in nutrient-limiting conditions. Biochemistry **44:** 805-815

Taguchi F, Yamamoto Y, Inagaki N, Satoh K (1993) Recognition signal for the C-terminal processing protease of D1 precursor protein in the photosystem II reaction center. An analysis using synthetic oligopeptides. FEBS Lett **326:** 227-231

Thornton LE, Ohkawa H, Roose JL, Kashino Y, Keren N, Pakrasi HB (2004) Homologs of plant PsbP and PsbQ proteins are necessary for regulation of photosystem II activity in the cyanobacterium *Synechocystis* 6803. Plant Cell **16:** 2164-2175

Thornton LE, Roose JL, Ikeuchi M, Pakrasi HB (2005) The Low Molecular Components: New Insights from Proteomics, Genomics, and Structural Studies. *In* T Wydrzynski, K Satoh,

eds, Photosystem II: The Light-Driven Water:Plastoquinone Oxidoreductase, Vol 22. Springer, Dordrecht, pp 121-137

Tsinoremas NF, Castets AM, Harrison MA, Allen JF, Tandeau de Marsac N (1991) Photosynthetic electron transport controls nitrogen assimilation in cyanobacteria by means of posttranslational modification of the glnB gene product. Proc Natl Acad Sci U S A **88:** 4565-4569

Vavilin D, Vermaas W (2007) Continuous chlorophyll degradation accompanied by chlorophyllide and phytol reutilization for chlorophyll synthesis in *Synechocystis* sp. PCC 6803. Biochim Biophys Acta **1767:** 920-929

Wang HL, Postier BL., Burnap RL (2004) Alterations in global patterns of gene expression in *Synechocystis* sp. PCC 6803 in response to inorganic carbon limitation and the inactivation of ndhR, a LysR family regulator J Biol Chem **279:** 5739-5751

Welsh EA, Liberton M, Stöckel J, Loh T, Elvitigala T, Wang C, Wollam A, Fulton RS, Clifton SW, Jacobs JM, Aurora R, Ghosh BK, Sherman LA, Smith RD, Wilson RK, HB P (2008) The genome of *Cyanothece* 51142, a unicellular diazotrophic cyanobacterium important in the marine nitrogen cycle. Proc Natl Acad Sci U S A **105:** 15094-15099

Table 1. Presence or absence of PSII proteins under nutrient deplete (dep) or replete (rep) conditions.

Protein	Annotation	BG11	Fe Dep 24h	Fe Rep 4h	Fe Rep 24h	N Dep 24h	N Rep 4h	N Rep 24h	NH_3 Rep 4h	NH_3 Rep 24h	P Dep 24h	P Rep 4h	P Rep 24h	S Dep 24h	S Rep 4h	S Rep 24h
Sll0247	IsiA	+	+	+	+	-	-	+	-	+	+	-	+	-	-	-
Sll0258	PsbV	+	+	+	+	+	+	+	+	+	+	+	+	+	+	+
Sll0427	PsbO	+	+	+	+	+	+	+	+	+	+	+	+	+	+	+
Sll0849	PsbD (D2)	+	+	+	+	+	+	+	+	+	+	+	+	+	+	+
Sll0851	PsbC (CP43)	+	+	+	+	+	+	+	+	+	+	+	+	+	+	+
Sll1194	PsbU	+	+	+	+	+	+	+	+	+	+	+	+	+	+	+
Sll1252	hypothetical	-	+	-	+	-	+	+	-	+	-	-	+	+	-	+
Sll1390	Psb32	+	+	+	+	+	+	+	-	+	+	+	+	+	+	+
Sll1398	Psb28	+	+	+	+	+	-	+	+	+	+	+	+	+	-	+
Sll1414	hypothetical	+	+	-	+	+	+	+	-	+	+	-	+	+	-	+
Sll1418	PsbP2	-	+	-	+	-	+	+	-	+	+	-	+	+	-	+
Sll1638	PsbQ	+	+	+	+	+	+	+	+	+	+	+	+	+	+	+
Sll1867	PsbA3 (D1)	+	+	+	+	+	+	+	+	+	+	-	+	+	-	+
Slr0172	hypothetical	+	+	+	+	+	+	+	+	+	+	+	+	+	+	+
Slr0906	PsbB (CP47)	+	+	+	+	+	+	+	+	+	+	+	+	+	+	+
Slr0927	PsbD2 (D2)	+	+	+	+	+	+	+	+	+	+	+	+	+	+	+
Slr1181	PsbA1 (D1)	-	+	-	+	+	+	+	+	+	+	-	+	+	-	+
Slr1311	PsbA2 (D1)	+	+	+	+	+	+	+	+	+	+	-	+	+	-	+
Slr1645	Psb27	+	+	+	+	+	+	+	-	+	+	-	+	+	+	+
Slr1739	PsbW	-	+	-	-	-	-	-	-	-	+	-	+	-	-	+
Slr2034	ycf48	+	+	+	+	-	+	+	+	+	+	-	+	+	+	+
Slr2048	PratA	-	-	-	+	-	-	+	-	+	-	-	-	-	-	-
Sml0007	PsbY	-	+	-	-	-	-	-	-	-	-	-	+	-	-	+
Smr0006	PsbF	+	+	-	+	+	-	+	-	+	+	-	+	+	-	+
Smr0007	PsbL	+	-	-	-	-	-	-	-	-	-	-	-	-	-	-
Ssl2598	PsbH	+	+	-	+	+	+	+	-	+	+	+	+	+	+	+
Ssr3451	PsbE	+	+	+	+	+	+	+	-	+	+	+	+	+	+	+

Table 2. Log_2 ratios of PSII protein abundance changes under environmental stress conditions. Dep – Depletion, 6d. Rep – repletion 24h.

Protein	Annotation	CO_2	Cold	Heat	Fe Dep	Fe Rep	N Dep	N Rep	NH_3 Rep	P Dep	P Rep	S Dep	S Rep
Sll0247	IsiA			2.322	3.700	1.585			1.585	1.585	4.459		
Sll0427	PsbO	1.259	1.215	1.974	1.237	1.259		0.893		0.865	0.893		0.893
Sll0849	PsbD (D2)						-1.536					-0.951	
Sll0851	PsbC (CP43)						-1.213					-0.672	
Sll1194	PsbU						-1.858					-0.951	
Sll1252	hypothetical protein								1.585			2.585	1.585
Sll1390	Psb32						-4.459						
Sll1414	hypothetical protein	1.322							2.807			1.322	1.322
Sll1418	PsbP2				-1.459		-3.459						
Sll1638	PsbQ			0.585	0.807								
Slr0172	hypothetical protein	1.848	1.848										
Slr0906	PsbB (CP47)						-1.483					-0.639	
Slr0927	PsbD2 (D2)						-1.536					-0.951	
Slr1181	PsbA1 (D1)		-1.700			-2.115	-1.700						
Slr1645	Psb27		1.678	2.000	1.263	1.585		1.926					1.263
Slr1739	PsbW									2.000	2.322		
Slr2034	ycf48			1.248	1.087		-3.000	2.129	1.807				
Ssl2598	PsbH											-0.807	
Ssr3451	PsbE											-1.585	

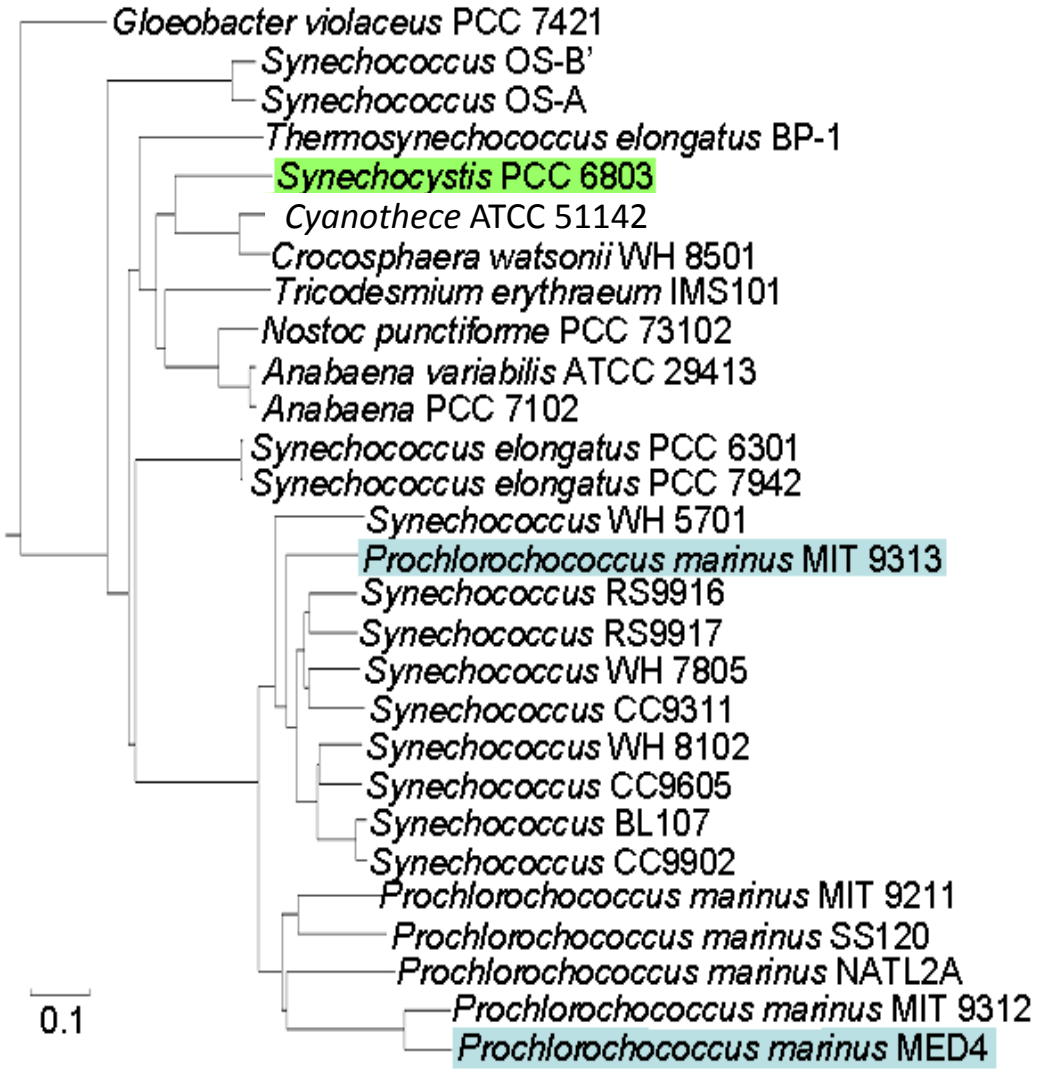

Figure 1. Phylogenetic Tree of 28 Sequenced Cyanobacteria. The tree was generated from the analysis of 435 sets of proteins, co-orthologous in all 28 of the strains (E. A. Welsh, unpublished). *Synechosystis* 6803 is shown in green and the relevant *Prochlorocci* are shown in blue.

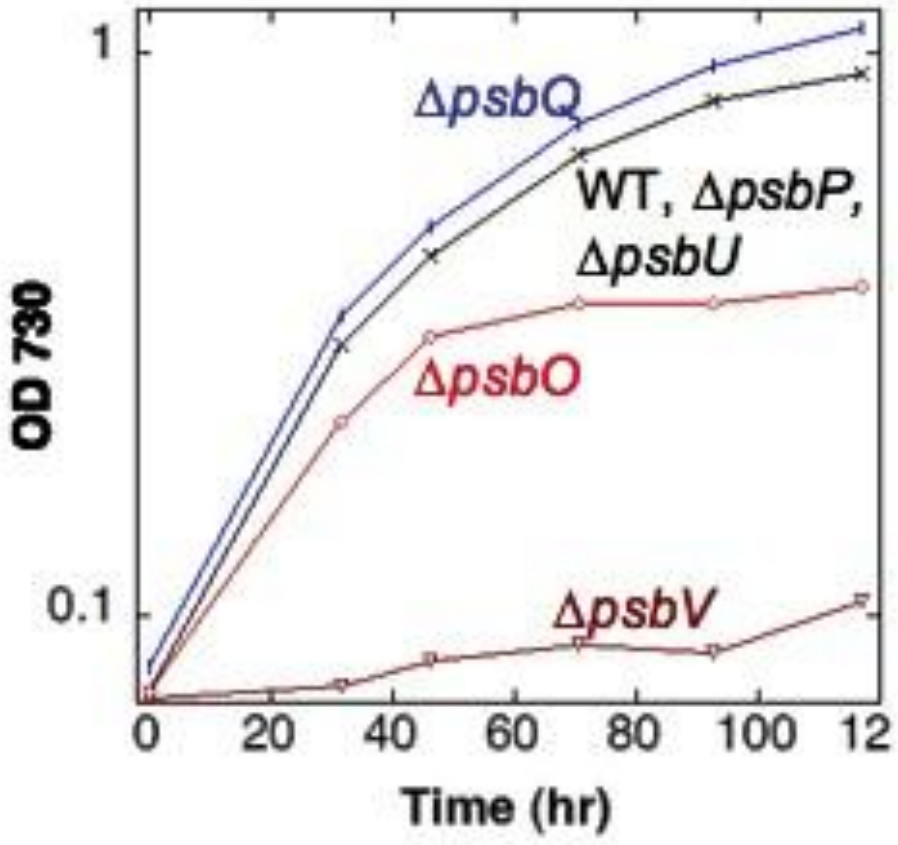

Figure 2. Growth of mutants missing genes for extrinsic PSII proteins in iron deplete medium in *Synechosystis* 6803.

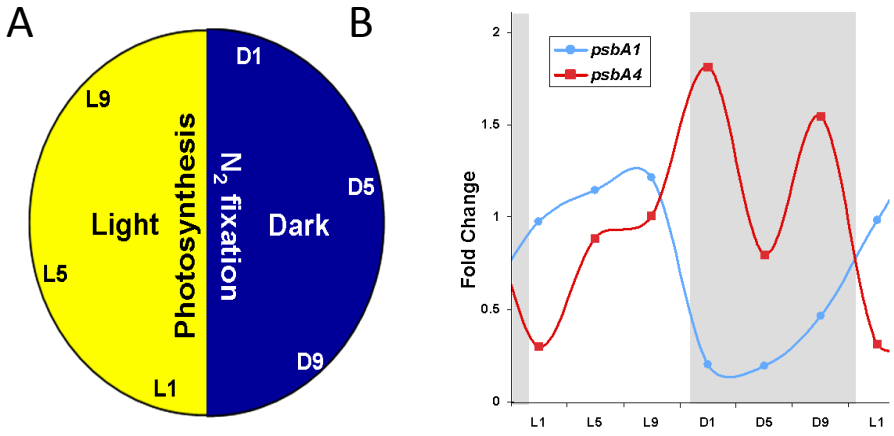

Figure 3. *Cyanothece* Diurnal Cycle. A) Diurnal timing of cellular processes. separation of The numbers denote hours in the light (L) or the dark (D) phase. **B)** Diurnal regulation of *psbA* transcripts in *Cyanothece*.

A

```
Synechocystis PsbA2 301 NFNQSILDSQGRVIGTWADVLNRANIGFEVMHERNAHNFPLDLASGEQAPVALTAPAVNG 360
Cyanothece    PsbA1 301 NFNQSILDSQGRVIGTWADVLNRAGIGMEVMHERNAHNFPLDLASAEP----VSAPVING 356
Cyanothece    PsbA3 300 NFNQSVLDSQGRVIGTWADVLNRAGIGMEVMHERNAHNFPLDLASGEQ-----TLIALK- 353
Cyanothece    PsbA2 302 NFNGSVLDSQGRVINTWADVINRANIGIEVMHERNAHNFPLDLALGDS---QPIAMAVNS 358
Cyanothece    PsbA4 305 NFNQSILDSQGRTIPTEADLLNRANLGIRSMHAPNTHHFPLTLASGKA-------TVIS- 356
                        *** *:******.* * **::***.:*:. **  *:*:*** ** ..       .:.
```

B

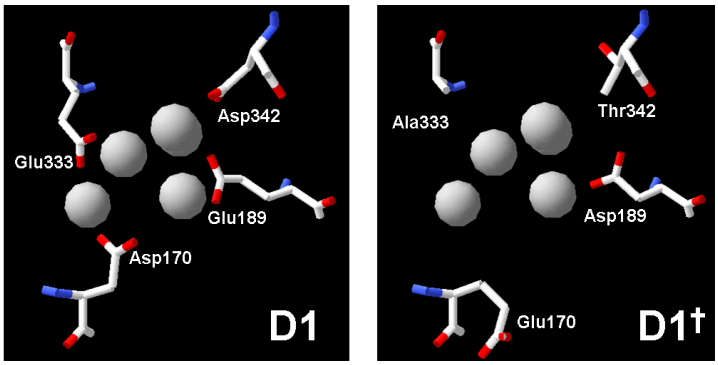

C

```
Synechocystis PCC 6803 PsbA2    301 NFNQSILDSQGRVIGTWADVLNRANIGFEVMHERNAHNFPLDLASGEQAPVALTAPAVNG 360
Cyanothece ATCC 51142 PsbA1    301 NFNQSILDSQGRVIGTWADVLNRAGIGMEVMHERNAHNFPLDLASAEP----VSAPVING 356
Crocospheara watsonii  PsbA1423 301 NFNQSILDSQGRVIGTWADVLNRAGIGMEVMHERNAHNFPLDLASAEP----VSAPAING 356
Synechococcus OS-B'    PsbA0371 301 NFNQSIVDSNGRVVGTWADVLNRANLGMEVMHERNAHNFPLDLAAVEV------APAVRG 354
Synechococcus OS-A     PsbA1274 301 NFNQSIVDSNGRVVGTWADVLNRANLGMEVMHERNAHNFPLDLAAVEV------APAIRG 354
Cyanothece ATCC 51142 PsbA4    305 NFNQSILDSQGRTIPTEADLLNRANLGIRSMHAPNTHHFPLTLASGKAT-------VIS- 356
Crocospheara watsonii  PsbA4668 305 NFNQSILDSQGRAIPTEADLLNRANLGIRSMHAPNTHHFPLTLA---------------- 348
Synechococcus OS-B'    PsbA0216 305 NFNQSILDSQGRFIPTYADLLNRANLGIQVMHAPNAHHFPLLLAAQP------------- 351
Synechococcus OS-A     PsbA1748 305 NFNQSILDSQGRFIPTYADLLNRANLGIQAMHAPNAHHFPLLLAAKAD------------ 352
                                    ******:**:** : * **:****.:*:. **  *:*:*** **
```

Figure 4. D1 variants in cyanobacteria. A) Alignments of the C-terminal parts of D1 proteins in *Cyanothece* and *Synechocystis*. B) Mn cluster ligands in the D1 and D1† proteins. C) Alignments of the C-terminal parts of D1 and D1† (shaded) in *Synechocystis* and 4 unicellular N_2-fixing cyanobacteria. The naturally occurring 'mutations' in the D1† proteins are shown in red

Appendix I

The Extrinsic Proteins of Photosystem II

This chapter was adapted from:

Adapted from: Roose JL, **Wegener KM**, and Pakrasi, HB. (2007) The extrinsic proteins of Photosystem II. Photosynth Res., 92: 369-387.

SUMMARY

Years of genetic, biochemical, and structural work have provided a number of insights into the oxygen evolving complex (OEC) of Photosystem II (PSII) for a number of photosynthetic organisms. However questions still remain about the function and interactions among the various subunits that make up the OEC. After a brief introduction to the individual subunits Psb27, PsbP, PsbQ, PsbR, PsbU, and PsbV, a current picture of the OEC as a whole in cyanobacteria, red algae, green algae, and higher plants will be presented. Additionally the role that these proteins play in the dynamic life cycle of PSII will also be presented.

INTRODUCTION

Photosystem II (PSII) is the multi-component enzyme of cyanobacteria, algae and plants that catalyzes the light-driven oxidation of water to molecular oxygen. This protein complex consists of more than 20 subunits including both integral membrane and extrinsically associated proteins. In addition to its protein components, PSII also has a large number of associated cofactors including chlorophylls, pheophytins, plastoquinones, manganese atoms, a non-heme iron, calcium, chloride, and two heme groups. Despite the large number of components, PSII can be divided into two functional domains (1) the electron transfer domain, comprised of the integral membrane helices and cofactors and (2) the oxygen evolving complex (OEC), located on the lumenal face of the complex including the loop regions of several membrane proteins and the extrinsic proteins.

The catalytic center of the OEC is a tetranuclear manganese cluster that together with calcium and chloride ions sequentially removes four electrons from two water molecules to form molecular oxygen. All of the crystal structures of cyanobacterial PSII show that the ligands to this catalytic center are provided by the intrinsic protein components (Kamiya and Shen, 2003; Ferreira et al., 2004; Loll et al., 2005). This is in agreement with previous biochemical and genetic studies in a number of different organisms that have shown the extrinsic proteins are not necessary for oxygen evolution activity. However, the extrinsic proteins are required to enhance oxygen evolution activity and serve important roles *in vivo* including forming a protective barrier around the manganese cluster and concentrating the essential Ca^{2+} and Cl^- ions within the OEC (Seidler, 1996).

While the core membrane protein components of PSII are generally conserved in sequence and spatial arrangement among different organisms, there is considerable heterogeneity regarding the extrinsic proteins of the OEC. In most organisms, three to four extrinsic proteins are associated with the lumenal side of PSII, but only one protein, PsbO (the 33 kDa or Manganese Stabilizing Protein), is present in all oxygenic photosynthetic organisms. The

other extrinsic proteins are PsbP (23, 24 kDa protein), PsbQ (16-18 kDa protein in plants, 20 kDa protein in red algae), PsbR (10 kDa protein), PsbU (12 kDa protein), PsbV (cytochrome c_{550}) and Psb27 (11 kDa protein), which associate with PSII in various combinations depending on the organism. Note that for clarity the nomenclature used in this manuscript refers to the proteins by their four letter name and not by their apparent molecular weight. Table 1 shows the distribution of the different extrinsic proteins among the different types of photosynthetic organisms (cyanobacteria, red algae, green algae, and plants). Recent reviews have addressed the evolutionary implications of sequence divergences and extrinsic protein distributions among the different organisms (Seidler, 1996; De Las Rivas et al., 2004; De Las Rivas and Roman, 2005; Enami et al., 2005).

This review focuses on the functions of the variable protein components of the OEC (PsbP, PsbQ, PsbR, PsbU, PsbV, and Psb27) and how they interact in the different types of OECs. Each protein will be discussed individually followed by sections describing them collectively in the context of the different types of PSII OECs- cyanobacterial, red algal, green algal and plant. Because the PsbO protein will be addressed in a separate article in this issue, it will only be mentioned briefly in the context of the structures of the different types of OECs. Finally, the dynamic nature of PSII will be discussed as a number of these extrinsic proteins have been implicated in facilitating the assembly of this large membrane protein complex.

Individual Extrinsic Lumenal Subunits

PsbP

The PsbP protein is also known as the 23 or 24 kDa extrinsic protein in plants. While it was first determined to be a component of PSII in plants (reviewed in Seidler, 1996). homologs have been identified in the genomes across the entire spectrum of photosynthetic organisms from cyanobacteria to plants (Table 1). In fact, *psbP* can even be found in the primitive cyanobacterium *Gloeobacter violaceus* (referred to hereafter as *Gloeobacter*), which lacks thylakoids, suggesting an ancient role for this protein in PSII. Genome analysis of *Arabidopsis thaliana* (referred to hereafter as *Arabidopsis*) yielded ten copies of the *psbP* gene, and remarkably, eight of these were found to be expressed proteins in the thylakoid lumen (Peltier et al., 2002). Thus, plants must require a variety of PsbP isoforms to fine tune photosynthetic activity. Although *psbP* genes can be identified in all of the different classes of oxyphototrophs, little is known about the function of the PsbP protein in cyanobacteria or red algae.

The majority of functional studies regarding PsbP have been performed in plants. PsbP was first identified during release-reconstitution experiments in higher plants (Seidler, 1996). The PsbP and PsbQ proteins are removed by treatment with 1 M NaCl with a concomitant decrease in oxygen evolution activity due to the loss of Ca^{2+} and Cl^- ions (Akerlund et al., 1982; Kuwabara and Murata, 1983). Addition of $Ca^{2+}$and Cl^- to the assay medium restores PSII activity without the addition of these proteins (Ghanotakis et al., 1984; Miyao and Murata, 1985). Specifically, PsbP was found to modulate the Ca^{2+} requirement for PSII activity (Miyao and Murata, 1984). Therefore, PsbP has been hypothesized to act as a Ca^{2+} concentrator and prevent the release of Ca^{2+} during turnover of PSII. Another study has shown that the kinetics of Ca^{2+} binding are altered in the absence of the PsbP and PsbQ proteins (Adelroth et al., 1995). However, PsbP has also been implicated along with PsbQ to modulate the Cl^- requirement as well. Structurally, the presence of PsbP protects the manganese cluster from attack by exogenous reductants (Ghanotakis et al., 1984).

The first genetic studies on the *in vivo* role of PsbP was conducted in the green alga *Chlamydomonas reinhardtii* (referred to hereafter as *Chlamydomonas*) in which the FUD39 mutant lacks the PsbP protein (de Vitry et al., 1989; Rova et al., 1994; Rova et al., 1996). While these cells accumulate wild type levels of PSII centers, high concentrations of Cl^- were necessary to promote oxygen evolution activity. Subsequently, it was shown that there were significant defects in the light-driven assembly of the manganese cluster (termed photoactivation) in this mutant. This inefficient photoactivation process and decreased Cl^- affinity resulted in a substantial amount of competing donor side damage. Together, these data highlight the role of PsbP and the Cl^- ion in the functional assembly of the manganese cluster.

Advances in RNAi technology have greatly facilitated genetic analysis in plants, especially in cases where the gene of interest is present in multiple copies. RNAi allowed for the *in vivo* characterization of PsbP in *Nicotiana tabacum* (referred to hereafter as *Nicotiana*) which contains four *psbP* genes (Ifuku et al., 2005; Ishihara et al., 2005). The PsbP knock-down plants exhibited a lower variable fluorescence yield and oxygen evolution activity. Most PSII subunits did accumulate in these plants except for PsbQ, which has been shown to require PsbP for binding to PSII in plants. While the stability of the manganese cluster was also affected, it was rapidly reassembled in the light in contrast to the results seen in the *Chlamydomonas* mutant. Differential RNAi technology was used to dissect the importance of each of the different PsbP isoforms in *Nicotiana* (Ishihara et al., 2005). This study showed that all of the isoforms are required for optimal activity, but generally PSII activity was correlated with the total amount of PsbP protein.

Recently, the PsbP protein was identified in PSII preparations from the cyanobacterium *Synechocystis* (Thornton et al., 2004). Sequence comparison revealed a key difference between transport of the plant and cyanobacterial PsbP proteins. The plant PsbP protein is translocated to the thylakoid lumen via the twin arginine translocation (TAT) pathway (Mould and Robinson, 1991; Robinson and Bolhuis, 2004) while cyanobacterial PsbP is predicted to be cleaved by signal peptidase II to yield an N-terminal lipid-modified cysteine (predicted by SignalP, (Bendtsen et al., 2004) and LipoP, (Juncker et al., 2003)). Currently, there is disagreement about the

abundance of the PsbP protein in the thylakoid membranes of cyanobacteria. Thornton et al (2004) determined the amount of PsbP to be approximately 3% of that of CP47 in the thylakoid membranes. Ishikawa et al (2005) determined the amount of PsbP in the thylakoid membranes to be equal to that of PsbO.

Mutational studies in cyanobacteria have yielded somewhat conflicting results as to the function of PsbP (Thornton et al., 2004; Ishikawa et al., 2005; Summerfield et al., 2005). Ishikawa et al (2005) confirmed cyanobacterial PsbP is indeed associated with PSII and that its translation is highly dependent on the presence of PSII intrinsic components, but they observed no detectable photosynthetic phenotype in a mutant lacking PsbP. In contrast, other groups did observe photoautotrophic growth defects and decreased oxygen evolution activity in medium lacking either Ca^{2+} or Cl^- for *ΔpsbP* cells (Thornton et al., 2004; Summerfield et al., 2005). The *ΔpsbP* phenotype was not as severe as the phenotype of other cyanobacterial extrinsic protein mutants and differences in sample preparation or assay conditions could explain this phenotypic discrepancy. Summerfield et al (2005a) also examined double deletion mutants of *psbP* in combination with each of the other cyanobacterial extrinsic proteins. In most cases, additional inactivation of *psbP* did not result in any exacerbated phenotype. However, an increase in doubling time was observed for the *ΔpsbO:ΔpsbP* mutant under Cl^--limiting conditions. These results are consistent with the hypothesis that PsbP is only associated with a small population of PSII complexes.

The PsbP protein is not present in the current crystallographic models of cyanobacterial PSII (Kamiya and Shen, 2003; Ferreira et al., 2004; Loll et al., 2005). Structural studies of plant PSII complexes do not have the resolution to provide detailed information on the structure of PsbP within the complex, but most likely the position of PsbP is not analogous to any of the other extrinsic subunits observed in the current cyanobacterial models (Nield and Barber, 2006). Many studies indicate that the mode of association of PsbP with PSII varies among different organisms. As described above for cyanobacteria, PsbP is predicted to contain an N-terminal lipid anchor, which confers some hydrophobic characteristics (Thornton et al., 2004). In plants, binding of the

PsbP protein requires PsbO and is hypothesized to be a largely electrostatic interaction (Seidler, 1996). In contrast, PsbP from green algae has been shown to bind independently of the other extrinsic proteins (Suzuki et al., 2003). Refer to the sections for the organism-specific OECs for further discussion.

Currently, a high resolution (1.6 Å) crystal structure of PsbP from *Nicotiana* is available (Ifuku et al., 2004). The core of PsbP is an anti-parallel β-sheet with α-helices on either side; however, electron densities of the N-terminal 15 residues and two loop regions were not resolved. This result may indicate possible stabilizing conformational changes in PsbP upon binding. Because the N-terminus of PsbP is critical for ion retention in PSII, no mechanism for its function could be proposed. The asymmetric surface charge distribution did give some clues about its association with the PSII complex; in that the basic surface is proposed to interact with PSII (Ifuku et al., 2004; De Las Rivas and Roman, 2005).

Surprisingly, the structure of PsbP hints at a more exotic role for PsbP in plant PSII. PsbP is very similar to that of Mog1p, a regulatory protein for a Ran GTPase suggesting it may be a possible GTP/GDP-sensitive regulator (Ifuku et al., 2004; De Las Rivas and Roman, 2005). While biochemical studies have not previously demonstrated such a role for the PsbP protein, recent studies have shown that GTP/GDP metabolism in the chloroplast thylakoid lumen regulates the turnover of PSII components (Spetea et al., 1999; Spetea et al., 2000; Spetea et al., 2004). Another study has also implicated the PsbP protein in the assembly of PSII, suggesting it plays a direct role in the light-induced assembly of the manganese cluster (Bondarava et al., 2005). Refer to the section on “PSII Biogenesis and Turnover” for a discussion on possible roles for the extrinsic proteins in this process.

PsbP clearly plays a structural role in the plant OEC to sequester the Ca^{2+} and Cl^{-} ions and protect the manganese cluster from exogenous reductants, but the exact position of PsbP within the complex and mechanism for this function remains unknown. The studies described above demonstrate that PsbP is essential for normal *in vivo* PSII activity. The presence of *psbP* genes in a number of photosynthetic organisms emphasizes the need for more functional

analyses of this protein in cyanobacteria and algae. Additionally, further analysis of PsbP in cyanobacteria is necessary to determine whether its function is conserved from cyanobacteria to plants or whether it has specialized functions in different organisms. More studies are necessary to elucidate the function of PsbP as a possible regulatory protein in PSII assembly and disassembly.

PsbQ

Genes for *psbQ* have been identified in a number of different photosynthetic organisms (Table 1). However, there are some notable exceptions- *Gloeobacter* as well as the *Prochlorococci* strains. *Arabidopsis* contains multiple copies of *psbQ* genes, four of which have been identified as expressed proteins in the thylakoid lumen (Peltier et al., 2002; Schubert et al., 2002). Because of the apparently random distribution of *psbQ* genes, it has been hypothesized that PsbQ is the protein most recently incorporated into the OEC (De Las Rivas and Barber, 2004).

The first analyses of PsbQ were release-reconstitution studies in spinach, which indicate that PsbQ plays a role in modulating the ionic requirements for optimal oxygen evolution activity (Seidler, 1996). PsbQ is released along with PsbP upon treatment with 1 M NaCl resulting in a decrease in oxygen evolution activity, which can be restored by the addition of Ca^{2+} and Cl^- ions (Akerlund et al., 1982; Kuwabara and Murata, 1983; Ghanotakis et al., 1984; Miyao and Murata, 1985). While PsbP was shown to contribute mainly to the Ca^{2+} requirement, recent results implicate PsbQ in Ca^{2+} retention as well (Ifuku and Sato, 2002; Barra et al., 2005). PsbQ in concert with PsbP functions to lower the Cl^- requirement for optimal activity (Akabori et al., 1984; Ghanotakis et al., 1984; Miyao and Murata, 1985). Along with the PsbO and PsbP proteins, PsbQ plays a structural role within the plant OEC to protect the manganese cluster from inactivation by reductants in the thylakoid lumen (Ghanotakis et al., 1984).

Recently, genetic studies in plants have investigated the role of the PsbQ protein *in vivo*. RNAi was used to knock-down PsbQ in *Nicotiana* (Ifuku et al., 2005). Although transgenic plants

exhibited strong, stable gene silencing, they did not display any observable phenotype under the conditions assayed. In another study, RNAi was used to examine PsbQ in *Arabidopsis* (Yi et al., 2006). Under normal growth conditions the mutant plants were similar to wild type, akin to the results in *Nicotiana*, but detailed analysis of their photosynthetic machinery indicated the OEC was quite unstable. The mutant plants died after 3-4 weeks under low light conditions, indicating that PsbQ is essential for growth under these conditions. It is possible that in the absence of PsbQ the manganese cluster more readily dissociates from PSII, but cannot be reassembled into the complex efficiently enough to maintain the PSII activity required for survival in low light.

The 20 kDa PSII extrinsic protein in red algae has recently been renamed PsbQ' because it has low but significant homology to PsbQ from green algae (Ohta et al., 2003). This protein was originally identified in PSII preparations from *Cyanidium caldarium* and it is released from these complexes along with PsbO, PsbU and PsbV upon treatment with 1 M $CaCl_2$ (Enami et al., 1995; Enami et al., 1998). While PsbQ' can bind PSII independently, it alone does not enhance oxygen evolution activity. These results suggest that PsbQ' is not directly involved in water oxidation in red algae, but it is important for the association of the PsbV and PsbU proteins (Enami et al., 1998). Despite differences in red algal and plant OECs, in both cases PsbQ stabilizes the protein components of the OEC for optimal activity.

PsbQ in cyanobacteria was first identified during a proteomic analysis of PSII isolated purified using a histidine-tagged mutant of the CP47 protein (Kashino et al., 2002). It was not previously identified as an extrinsic component of cyanobacterial PSII because it was not removed by treatment with 1 M $CaCl_2$ or 1 M Tris-HCl, pH 8.0 (Shen et al., 1992; Kashino et al., 2002). Sequence analysis provided an explanation for the hydrophobic nature of cyanobacterial PsbQ; it is predicted to be cleaved by signal peptidase II to yield an N-terminal lipid-modified cysteine (predicted by SignalP, (Bendtsen et al., 2004) and LipoP, (Juncker et al., 2003)). Indeed, a recent study has confirmed the hydrophobic nature of PsbQ and showed that it is lumenally exposed (Kashino et al., 2006). This is in contrast to the plant PsbQ protein that was easily

removed by treatments with high salt. Therefore, PsbQ exhibits a highly variable mode of association with PSII complexes from the different classes of photosynthetic organisms.

Data suggests that PsbQ is a stoichiometric component of PSII in cyanobacteria (Thornton et al., 2004). Inactivation of the *psbQ* gene in cyanobacteria resulted in a mutant with photosynthetic defects under Ca^{2+}- and Cl^{-} -limiting conditions, which is consistent with the biochemical studies of plant PsbQ (Thornton et al., 2004; Summerfield et al., 2005). However, the phenotype observed for the *ΔpsbQ* mutant was less severe relative to that of other cyanobacterial extrinsic protein mutants like *ΔpsbV* or *ΔpsbO* (Thornton et al., 2004; Summerfield et al., 2005). Double mutants where *psbQ* was inactivated in combination with each of the other cyanobacterial extrinsic proteins showed exacerbated photosynthetic defects. In fact, the *ΔpsbQ:ΔpsbV* mutant could not grow photoautotrophically in nutrient replete medium and assembled low amounts of PSII centers (30% relative to wild type). Interestingly, photoautotrophic growth could be restored when cells were grown at pH 10.0 (vs. pH 7.5), but the mechanism behind this pH-sensitivity remains unknown (Summerfield et al., 2005).

A more detailed analysis of the PSII complexes in the *ΔpsbQ* mutant showed a partial loss of the PsbV protein and destabilization of the OEC (Kashino et al., 2006). This finding is consistent with previous results of the PsbQ' protein from red algae described above. While much of the cyanobacterial *ΔpsbQ* phenotype could be explained by the loss of the PsbV protein, the results from the *ΔpsbQ:ΔpsbV* double mutant suggest a synergistic relationship between the cyanobacterial PsbQ and PsbV proteins or perhaps an additional role for PsbQ.

Currently, there is little structural information on the PsbQ protein within the PSII OEC. While it has been found in the genomes of the cyanobacterial strains used for PSII crystallization, it is not present in the current structural models and there is no unassigned electron density that could be attributed to PsbQ (Kamiya and Shen, 2003; Ferreira et al., 2004; Loll et al., 2005). Analysis of low resolution plant PSII structural reconstructions in comparison to the cyanobacterial models indicate that the position of the PsbQ protein does not correspond to that of any currently resolved cyanobacterial extrinsic proteins (Nield and Barber, 2006). Evidence for

an independent binding site for PsbQ supports the hypothesis that PSII complexes in some organisms contain PsbQ in addition to PsbO, PsbU, PsbV and even PsbP.

High resolution crystal structures of isolated spinach PsbQ are available and have shed new light on its association with PSII (Calderone et al., 2003; Balsera et al., 2005). PsbQ can be divided into two structural domains; a C-terminal four helix bundle with an asymmetric charge distribution and a more flexible N-terminus. Structural features of the PsbQ N-terminal region include two short β-strands surrounding a large flexible loop region (residues 14-33) and a polyproline type II motif (Balsera et al., 2005), which may obtain a more rigid conformation upon binding PSII. Sequence comparison of the N-terminal region may explain the differences in binding characteristics of PsbQ among the different organisms (Balsera et al., 2005). For example, only plant PsbQ proteins contain the polyproline motif as well as a hydrophilic motif bordered by two conserved hydrophobic domains. While all PsbQ sequences analyzed contained the flexible loop region, the cyanobacterial PsbQ proteins lack the two short β-strands. In contrast, the C-terminus region is more conserved including a number of conserved positively charged residues which have been implicated as binding determinants for PsbQ in plants (Gao et al., 2005; Meades et al., 2005). Interestingly, the crystal structures of PsbQ show two bound Zn^{2+} atoms, where the coordinating residues of one atom are entirely conserved in the plant PsbQ proteins (Calderone et al., 2003; Balsera et al., 2005). While Zn^{2+} was specifically required for crystal growth, the biological significance of this result has yet to be determined.

The cumulative data on PsbQ indicate it is a key structural component of OECs from a number of different organisms, but many questions remain regarding its function and its mode of association with PSII. High resolution structures of PSII complexes containing PsbQ are necessary to provide insights into its role in the ionic requirement for oxygen evolution activity and its location relative to the other protein components of the OEC. Targeted mutagenesis of the N-terminal structural elements of PsbQ together with reconstitution analysis will unravel the differences in binding requirements among various photosynthetic organisms.

PsbR

PsbR, also referred to the 10 kDa PSII polypeptide, still remains something of a mystery. Though it does contain a lumenal targeting sequence like the other OEC components, it is quite unusual in its gene structure. The other OEC proteins have a N-terminal chloroplast transit sequence that contains a hydrophobic loop, the cleavage of which is thought to be necessary for entry of the mature protein into the lumen. In contrast, PsbR contains much shorter precursor sequence and does not contain the N-terminal hydrophobic loop thought to be necessary for cleavage (Lautner et al., 1988; Webber et al., 1989). It does have a similar motif at the C-terminus and it has been suggested that the shortened N-terminal sequence acts to target PsbR into the chloroplast and could be cleaved off in the stroma and that the C terminal region then acts as a noncleavable signal for lumen import (Webber et al., 1989). The final protein product is predicted to contain a C-terminal transmembrane span and a lumenally exposed 70 amino acid N-terminus.

Because PsbR is not present in cyanobacteria, the current structures available for PSII are not helpful in approximating a location for PsbR. Based on the presence of the leader sequence and experimental Tris washes, PsbR is predicted to be in the lumen (Ljungberg, 1984; Ljungberg et al., 1986). Moreover, shown associations of PsbR with CP47, PsbO, and PsbP support this localization (Ljungberg et al., 1984; Harper, 1998).

The function of PsbR remains unclear. Certainly PsbR is necessary for the optimization of electron transfer and water oxidation. PSII activity is impaired with the loss of PsbR function, as shown by multiple lines of evidence (Ljungberg et al., 1986; Stockhaus et al., 1990; Suorsa et al., 2006). Additionally loss of PsbR results in diminished electron transfer from the plastoquinone pool, an increased PSII excitation pressure and a higher PSI:PSII ratio (Suorsa et al., 2006).

Interestingly, the lack of PsbR results in a post transcriptional reduction in PsbQ and PsbP, with nearly undetectable levels under low light conditions, perhaps suggesting the PsbR is important for PsbP docking (Suorsa et al., 2006). Also, the absence of PsbR and PsbP in *ΔpsbJ* mutant further suggests that these three low molecular weight proteins are interdependent for the

proper assembly of the PSII complex (Suorsa et al., 2006). See the sections “Plant OEC” and “Green Algal OEC” for further information on interactions between PsbR and the PsbQ and PsbP.

PsbU

PsbU, originally identified in the cyanobacterium *Phormidium laminosumis*, is found in most cyanobacteria and red algae (Table 1) and was formerly referred to as the 12kDa and 9 kDa polypeptide in these organisms, respectively (Stewart, 1985). Cyanobacterial PsbU has a single N-terminal loop that forms a cleavable transit sequence while algal PsbU has a two-part transit sequence to allow transport across the chloroplast envelope and into the lumen (Shen et al., 1997; Ohta et al., 1999).

The function of PsbU is generally assigned as enhancing the structural stability of PSII and shielding the manganese cluster. Indeed the removal of PsbU affects the lumenal side, the core, and the stromal side of PSII. The donor side of PSII is impaired in the absence of PsbU as has been shown by a variety of measures of photosynthetic efficiency. (Shen et al., 1997; Inoue-Kashino et al., 2005; Balint et al., 2006). Additionally, the stability of the PSII core is affected; in the *ΔpsbU* mutant the core is more susceptible to photodamage, resulting in rapid degradation of D1 (Inoue-Kashino et al., 2005; Balint et al., 2006). Even the stromal surface of the PSII complex is affected by the loss of PsbU, as evidenced by the increased uncoupling of the light harvesting machinery, the phycobilisome, and PSII (Veerman et al., 2005).

Several specific ways that PsbU may be enhancing stability for PSII have been proposed. One of these is that PsbU specifically stabilizes the ion environment for oxygen evolution. This is supported by evidence of decreased growth of PsbU mutants in medium that lacks Ca^{2+} or Cl^{-} (Shen et al., 1997) and a further decrease PSII activity without supplied Ca^{2+} and a further dramatic decrease without supplied Cl^{-} (Ohta et al., 1999; Inoue-Kashino et al., 2005). It is also suspected that PsbU may contribute to the thermal stability of the OEC, as PsbU mutants in both thermophilic and mesophilic cyanobacteria do not have the ability to acclimate to higher temperatures and exogenously applied PsbU enhances thermostability (Nishiyama et al., 1997;

Nishiyama et al., 1999). Another possible role for PsbU is protection from reactive oxygen species, as PsbU mutants have enhanced mechanisms to detoxify exogenously applied H_2O_2 (Balint et al., 2006). The interactions of PsbU with the rest of the PSII complex will be addressed further in the sections “Cyanobacterial OEC” and “Red Algal OEC”.

PsbV

PsbV, also referred to as cytochrome c_{550}, is found in cyanobacteria and red algae (Table 1). Additionally, its homology to other c-type cytochromes makes it the only extrinsic protein with similarity to anoxygenic and non-photosynthetic bacteria proteins (Raymond and Blankenship, 2004). Like the other lumenal proteins, it contains a lumenal localization signal that is similar to that of the transit sequence of PsbO and PsbU in cyanobacteria (Shen et al., 1995). Genome sequence of the red algae *Cyanidioschyzon merolae* shows that *psbV* (as well as *psbO*) are both nuclear-encoded but have rather different targeting signals with only 15% identity (Matsuzaki et al., 2004). In both systems, the PsbV protein could be removed by treatment with high salt buffers resulting in a decrease of oxygen evolution activity (Enami et al., 1998; Shen et al., 1993).

The function of PsbV, like that of PsbU, is regarded as stabilizing PSII structure and electron transfer. The PsbV mutant has a severe growth phenotype. Under normal conditions growth of the PsbV mutant is severely retarded and the absence of Ca^{2+} or Cl^- in the growth media eliminates the capacity for growth, suggesting that PsbV aids in maintaining the proper ion environment within the OEC (Shen and Inoue, 1993; Shen et al., 1995; Shen et al., 1998). The PsbV mutant specifically has defects in the catalytic cycle of water oxidation (Shen et al., 1998; Kimura et al., 2002). Additionally, the overall stability of the PSII is reduced in the PsbV mutant. Dark treatment as well as heat reduces photosynthetic capacity more dramatically in the PsbV mutant (Kimura et al., 2002). Like PsbU, PsbV has also been shown to enhance thermostability, as PsbV mutants have a decreased 50% inactivation temperature, slowed growth with increasing temperature, and the inability to acclimate to higher temperatures (Nishiyama et al., 1994). Thus PsbV functions in several capacities to protect and stabilize the OEC and the manganese cluster.

The discovery of a second expressed copy of PsbV (~44% identity) in *Thermosynechococcus elongatus* (referred to hereafter as *Thermosynechococcu*s) also raises questions as to the function of PsbV. PsbV2 exhibits similar spectral properties of a six-coordinated, low-spin c-type cytochrome (Kerfeld et al., 2003). PsbV2 can functionally rescue a *ΔpsbV* mutant in *Synechocystis* with the exception of reduced growth in the absence of Ca^{2+} or Cl^- (Katoh et al., 2001). The role of this second PsbV, found only in a small subset of cyanobacteria remains unclear.

In addition to its typical role as a protein component of the OEC, PsbV is a particularly interesting cytochrome. It is a water-soluble c-type monoheme cytochrome, but has a much lower reduction potential (-240 mV vs +0 mV) (Pettigrew and Moore, 1987; Krogmann and Smith, 1990). The general structure of the heme environment does not account for this difference, as electric paramagnetic resonance (EPR) and resonance Raman spectroscopy showed that the heme has a bishistidine ligation that is similar to other c cytochromes (Vrettos et al., 2001).

Three factors have been identified that partially explain the low potential. One of these is solvent exposure of the heme which generally reduces the potential of cytochromes (Tezcan et al., 1998). Roncel et al (2003) have shown that PsbV bound to PSII has a higher potential (-80 mV), in agreement with studies by Vrettos et al (2001). Additionally, the presence of ionizable residues may effect the reduction potential. It has been shown that the potential of bound PsbV is pH independent, while the unbound form shows an increase of 58 mV per pH unit when the pH is under 9.0 (Roncel et al., 2003). This ionizable group must be in the vicinity of the heme and has been proposed to be either a tyrosine or asparigine residue (Roncel et al., 2003; Ishikita and Knapp, 2005). Lastly, the bishistidine heme ligation typically has a lower potential than the other two possible ligands, lysine or methionine. Alteration of PsbV the histidine ligands resulted in a small increase in potential without affecting PSII activity (Kirilovsky et al., 2004; Andrews et al., 2005). Taken together these factors begin to explain, but cannot fully account for, the low reduction potential of PsbV. These studies highlight the important role of the unusual c-type cytochrome PsbV in cyanobacterial PSII, but its exact function is unclear. Mutations that increase

the reduction potential of PsbV do not exhibit PSII defects (Kirilovsky et al., 2004; Andrews et al., 2005).

In light of the fact that the role of a cytochrome has not been shown to play a role in PSII in redox and given that plant and green algal OECs do not contain any cytochrome equivalents, it has been hypothesized that PsbV plays another, as-yet uncharacterized, role in cyanobacteria and red algae. It has been proposed that PsbV may be involved in anaerobic removal of electrons from carbohydrate reserves or fermentation for increased survival during long dark and anaerobic conditions (Krogmann and Smith, 1990; Krogmann, 1991). This is supported by experimental evidence form Shen and Inoue that PsbV, in the presence of dithionite, can accept electrons from ferredoxin II (Shen and Inoue, 1993). It has also been proposed that PsbV may accept electrons from ferredoxin during NADPH oxidation and in cyclic phosphorylation.

The structural models of cyanobacterial PSII have provided new information on the interactions of PsbV with the other proteins of the OEC. See the "Cyanobacterial OEC" section for further discussion. The PsbV protein is also associated with PSII complexes in red algae, where it also plays a role in the ionic requirement for oxygen evolution activity (Enami et al., 1998). Less is known about the protein architecture of the red algal OEC, but studies suggest the binding properties of algal PsbV differs from that of cyanobacteria (Enami et al., 1998; Enami et al., 2003). Refer to the "Red Algal OEC" section for further details.

Psb27

The Psb27 subunit was first identified as part of a purified PSII preparation from *Synechocystis* 6803 using N-terminal sequencing (Ikeuchi et al., 1995). This 11 kDa protein was first named PsbZ; however, according to a new nomenclature was changed to Psb27 (Kashino et al., 2002). A distinctly different smaller protein is now referred to as PsbZ (Swiatek et al., 2001; Shi et al., 2004).

This small basic (pI= 9) protein is predicted by to be targeted to the thylakoid lumen in *Synechocystis* 6803 and cleaved by signal peptidase II to yield an N-terminal lipid modification

(predicted by SignalP, (Bendtsen et al., 2004) and LipoP, (Juncker et al., 2003)). Indeed, Psb27 was not removed by washes (1 M $CaCl_2$ or 1 M Tris-HCl, pH 8.0), which typically deplete cyanobacterial PSII of its extrinsic subunits (Kashino et al., 2002). One of the two Arabidopsis Psb27 homologs (At1g03600) was found in a proteomic analysis of the thylakoid lumen (Peltier et., 2002; Schubert et al., 2002). In those studies, Psb27 was predicted to be targeted to the thylakoid lumen via the TAT pathway suggesting a possible difference in its interaction with PSII in higher plants.

Homologs of *psb27* are present in all oxygenic photosynthetic organisms except *Gloeobacter*, a primitive cyanobacterium that lacks a separate thylakoid membrane system (Table 1). However, Psb27 is not present in the recent cyanobacterial PSII crystal structures (Kamiya et al., 2003; Ferreira et al., 2004; Loll et al., 2005). While no mutants of this protein have been described, Psb27 is hypothesized to function in the PSII biogenesis because it was found to accumulate on mutant PSII complexes arrested early in the PSII assembly pathway (Roose and Pakrasi, 2004). Refer to the “PSII Biogenesis and Turnover” section for further discussion on Psb27.

OEC Systems in Different Organisms

Cyanobacterial OEC

The cyanobacterial OEC (modeled off that of *Synechocystis* and *Thermosynechococcus*) contains 5 lumenal proteins: PsbO, PsbU, PsbV, PsbP, and PsbQ. In regards to PsbO, PsbV, and PsbU, it represents the best understood OEC, thanks to numerous release reconstitution experiments and crystal structures (Zouni et al., 2001; Kamiya and Shen, 2003; Ferreira et al., 2004; Loll et al., 2005) . PsbP and PsbQ remain more ambiguous as they are not present in the crystal structures and their relatively recent discovery in cyanobacteria means there are fewer reconstitution experiments. Figure 1a represents a cartoon model of the current known structure of the cyanobacterial OEC.

The binding order of PsbO, PsbU, and PsbV has been well established. It has long been known that PsbO can rebind $CaCl_2$ washed PSII in the absence of any other proteins. PsbV can bind to approximately 80% of levels before washing without PsbO or PsbU, but an increase of 10% is seen with the addition of PsbO and another 10% in the presence of both PsbO and PsbU (Shen and Inoue, 1993). PsbU can not rebind at all without PsbO or PsbV. Binding of PsbU increases to 25% with the addition of PsbO, to 40% with the addition of PsbV, and to over 100% in the presence of both (Shen and Inoue, 1993). These results suggest that PsbO can bind the core monomer independently, PsbV can bind the core monomer independently but PsbO enhances binding, and PsbU cannot bind the core monomer independently and must interact with PsbO and PsbV to bind.

Recent crystal structures have provided specifics as to the binding of PsbU, PsbV, and PsbO. PsbO is a β-barrel consisting of 8 anti-parallel β-strands with a loop between strands 5 and 6 that is involved with binding PsbO to PSII (De Las Rivas and Barber, 2004; Ferreira et al., 2004). PsbO is positioned over the D1/CP47 side of the reaction center (Zouni et al., 2001). PsbO stabilizes the AB loop and C terminus of D1, the location of many of the ligands to the manganese cluster, and interacts with the large E loop of CP47 (Ferreira et al., 2004; Nield and

Barber, 2006). This is in agreement with experiments showing that deletions in the E loops of CP47 in concert with the deletion of PsbO that abolished photoautotrophic growth (Morgan et al., 1998; Clarke and Eaton-Rye, 1999) and site directed mutagenesis studies which show a binding domain for PsbO at CP47 Arg384 and Arg385 (Putnam-Evans and Bricker, 1992; Putnam-Evans et al., 1996; Qian et al., 1997).

PsbV is mainly alpha helical with a two-stranded beta sheet near the N-terminus (Kerfeld et al., 2003). PsbV is located over the D1/CP43 side of the reaction center (Zouni et al., 2001). Deletions in the E loop of CP43 result in a loss of photoautrophic growth and PSII activity, suggesting that CP43 stabilizes the OEC (Kuhn and Vermaas, 1993). The specific mutation R305S in CP43 prevents strong association of PsbV with PSII, although the amount of PsbV is unaffected on a cellular basis (Bricker et al., 2002).

PsbU is composed of five or more short α-helices, with no homologous structure in the database (Kamiya and Shen, 2003). The crystal structures places PsbU between PsbO and PsbV with a majority of its contacts to these two proteins (Kamiya and Shen, 2003; Ferreira et al., 2004; Loll et al., 2005). This supports release reconstitution studies showing that PsbO is not required for PsbU binding but that PsbV is (Shen and Inoue, 1993; Shen et al., 1997; Eaton-Rye et al., 2003). While there is a significant amount of distance between PsbU and the membrane, it interacts with PsbV, PsbO, CP47 and CP43 (Eaton-Rye, 2005). Combinatorial mutants of the CP47 E loop and *ΔPsbU* affect PSII stability, not growth, whereas the combination of the E loop and CP47 and *ΔPsbV* abolish photoautotrophic growth. In light of crystal structure data, the latter OEC mutant must be severely destabilized due to reduced binding of PsbU and loss of PsbV (Morgan et al., 1998; Clarke and Eaton-Rye, 1999).

PsbP and PsbQ proteins have recently been identified as cyanobacterial PSII components (Kashino et al., 2002; Thornton et al., 2004). Their binding properties are significantly different from that of PsbP and PsbQ in other systems, in that, they are not easily removed by salt-washing treatments (Kashino et al., 2002). Cyanobacterial PsbP and PsbQ are

predicted to an N-terminal lipid-modified cysteine (see above discussion of PsbP and PsbQ). While the precise lipid moiety has not been identified, a recent study demonstrated that cyanobacterial PsbQ has hydrophobic characteristics, but is still highly exposed on the lumenal face of the thylakoid membrane (Kashino et al., 2002).

The PsbQ protein is hypothesized to be a stoichiometric component of PSII complexes in cyanobacteria, but there is some debate over the stoichiometry of PsbP (Thornton et al., 2004; Ishikawa et al., 2005). One recent study indicates that the absence of PsbQ destabilizes PsbV similar to observations in red algae, suggesting a location near PsbV (Enami et al., 1998; Kashino et al., 2006). Less is known about the possible location of PsbP. Thornton et al (2004) have proposed that it is present in only 3% of cyanobacterial PSII centers, while Ishikawa et al (2005) argue that it is a stoichiometric subunit. With the prediction of the N-terminal lipid anchor and no other constraints from reconstitution or genetic studies, the cyanobacterial PsbP protein could bind anywhere on the lumenal side of the complex in cyanobacteria.

Despite the wealth of experimental information available for the cyanobacterial OEC, there are still many unanswered questions. It remains unclear what the role of the PsbV cytochrome is, especially in light that none of the extrinsic proteins in the plant OEC are cytochromes. Additionally the low redox potential of PsbV also is intriguing. The crystal structures show that PsbV is bound to PSII in such a way that the heme edge is facing PsbO and periplasmic surface of PSII, making it likely that the heme edge has much lower solvent accessibility and thus that the reduction potential is even higher than has been reported for bound PsbV (-80 mV) (Roncel et al., 2003). Knowing the actual redox potential for PsbV would perhaps show that the low potential reported is an artifact of removal from the complex. Resolving the locations and stoichiometries of PsbP and PsbQ in cyanobacterial PSII will be a topic of intense future research. And although this portrayal of the cyanobacterial OEC was based on that of *Synechocystis* and *Thermosyechococcus*, there are other cyanobacterial species that contain variations on this theme. Most interesting are *Gleobacter* and certain *Prochlorococci* strains such

as MED4 and SS120. The genome sequences of these species do not contain PsbU or PsbV. This raises interesting questions as to the structures and efficacy of these unusual PSIIs.

Red Algal OECs

Red algae have an OEC comprised of PsbO, PsbU, PsbV, and PsbQ'. Currently there are only low resolution electron microscopy models and a handful of release reconstitution and cross release reconstitution studies to illustrate the OEC structure in red algae. Figure 1b illustrates the current model of red algal OEC.

Electron microscopy and single particle analysis of the *Porphyridium cruentun* revealed that the PSII structure and location of PsbO, PsbV and PsbU in red algae is similar to the published crystal structures of cyanobacteria (Kimura et al., 2002; Kamiya and Shen, 2003; Bumba et al., 2004; Ferreira et al., 2004; Loll et al., 2005). PsbQ' was not seen in this structure. However, there are likely differences in red algae OEC in comparison to the cyanobacterial OEC, as seen by differences in their binding patterns. As in cyanobacteria, PsbO can bind $CaCl_2$ washed PSII independently (Enami et al., 1998). PsbQ can also partially rebind independently, but the binding of PsbQ does not affect oxygen evolution activity (Enami et al., 1998). However, while PsbV can bind independently in cyanobacteria, in red algae PsbV, as well as PsbU, require the presence of all four of the extrinsic proteins (Enami et al., 1998). When cross release reconstitution experiments were done between red algae and cyanobacteria, red algal PsbV could independently bind to cyanobacterial PSII indicating that the binding of the extrinsic proteins is determined by the intrinsic proteins (Enami et al., 2003). These experiments also showed that all four extrinsic proteins are needed for full binding and recovery of activity (Enami et al., 1998).

Red algae are considered to represent a transitional state between cyanobacterial and photosynthetic eukaryotes. They have thylakoids more similar to those of cyanobacteria, rather than to the stacked thylakoids of green algae and higher plants. Thus it's intriguing that red algae lack PsbP, as opposed to PsbU or PsbV that are not present in higher photosynthetic organisms.

A higher resolution structure of the red algal OEC would aid in understanding the similarities of the red algal OEC to that of cyanobacteria and higher plants.

Green Algal OEC

The protein content of the green algal OEC is analogous to that of plants (PsbO, PsbP, PsbQ, and PsbR), but there are significant differences in the way these proteins interact with the PSII complex and each other. Currently there is only one low resolution structural study of the OEC from green algae, but clear differences between cyanobacterial and algal OECs can be seen (Nield et al., 2000). Many biochemical and genetic studies in *Chlamydomonas* have been useful in characterizing the interactions among the OEC proteins. Based on these studies, Figure 1C shows a cartoon structure of the OEC in green algae.

Release-reconstitution studies of *Chlamydomonas* PSII complexes isolated using a histidine-tagged CP47 protein have shown a release of extrinsic proteins analogous to that of plants (Suzuki et al., 2003). Surprisingly, all three algal proteins can bind to PSII independently of each other (Suzuki et al., 2003) . Upon addition of PsbO, activity was only partially restored and activity was highly dependent on the addition of Ca^{2+} and Cl^{-} ions similar to observations in spinach. However, the addition of PsbP alone or in combination with PsbQ also restored activity in contrast to previous observations for plant PSII. While the PsbQ protein was able to bind independently, it alone does not restore any level of oxygen evolution activity.

These findings are consistent with previous genetic studies of a *Chlamydomonas* mutant lacking the PsbO protein, which was shown to still bind the PsbP and PsbQ proteins (de Vitry et al., 1989). However, PsbQ could not associate with PSII complexes in a mutant lacking the PsbP protein (de Vitry et al., 1989). Therefore, while *in vitro* conditions indicate that it is possible for PsbQ to associate independently of the other extrinsic proteins, it is not significant *in vivo*.

Cross-reconstitution studies using plant and green algal components have provided new insights into the functional exchangeability of the extrinsic proteins (Suzuki et al., 2005). It was found that algal PsbP and PsbQ proteins could not bind independently to spinach PSII, and

spinach PsbP and PsbQ only bound to non-specifically sites on algal PSII. These results suggest that the determinants for independent binding reside on the intrinsic PSII components. They also highlight that the majority of the PsbQ binding sites reside on the corresponding organisms PsbO and PsbP proteins.

The green algal OEC is quite similar to that of plants, but further structural studies will be useful in defining the details within the algal OEC that confer altered binding properties to its extrinsic proteins.

Plant OEC

The protein components of the plant OEC include PsbO, PsbP, PsbQ and PsbR. Currently only low resolution electron microscopy structural models are available for plant PSII (Bumba and Vacha, 2003). Yet, together with detailed reconstitution studies and high resolution crystal structures of some of the individual subunits, a clearer picture of the OEC is emerging. Figure 1D is a cartoon version, which represents the current structural model of the plant OEC.

In contrast to many of the other systems, the plant extrinsic proteins appear to have a strict binding order. While the PsbO protein can bind to PSII independently, PsbP requires the presence of the PsbO protein and PsbQ requires the presence of both PsbO and PsbP (Miyao and Murata, 1983, 1983). One recent study challenges this model, as treatment with $HgCl_2$ could effectively remove the PsbO protein leaving the PsbP and PsbQ proteins intact (Yu et al., 2006). Higher resolution structures are necessary to determine the extent of the interactions of the PsbP and PsbQ proteins with the intrinsic components that could provide for independent binding of these subunits.

The PsbP and PsbQ proteins can be removed by washing with 1 M NaCl suggesting a strong electrostatic component for their association with the complex. A number of studies have investigated the roles of certain types of residues using chemically modified proteins in reconstitution experiments. Negatively charged carboxylate groups on the PsbO have been shown to be necessary for the binding of PsbP (Bricker and Frankel, 2003). In agreement with

these results, it was found that positively charged groups on PsbP were essential for its association with PsbO, but negatively charged groups were not (Tohri et al., 2004). Positively charged groups on the PsbQ protein have also been shown to be critical for its association with PsbP (Gao et al., 2005; Meades et al., 2005). The structure of PsbP revealed an asymmetric surface charge distribution on the protein which can explain the chemical modification data (Ifuku et al., 2004). The positive face of the protein is predicted to interact with the acidic PsbO surface, while the negative side of PsbP interacts with the PsbQ protein. Additionally, the N-termini are critical for binding.

Comparisons of the plant PSII data to the higher resolution models from cyanobacteria indicate that the location of the PsbO protein is similar between the two systems. On the other hand, the locations of the PsbU and PsbV proteins do not correspond to that of PsbP and PsbQ (Nield and Barber, 2006). The individual x-ray structures for PsbP and PsbQ were fit into the electron density observed for the plant PSII complex. According to this fit, the PsbP protein interacts with the PsbO subunit as well as the lumenal face of the CP43 protein, and PsbQ spans between the PsbO and PsbP proteins. While this type of analysis can stimulate new hypotheses regarding the structure of the OEC in plants, higher resolution structures with assignments for all of the extrinsic proteins are necessary to determine how each of these proteins contributes to the water oxidation reaction.

A number of studies have indicated significant conformational changes occur upon the binding of the extrinsic proteins. Investigations of the extrinsic proteins individually have demonstrated they have highly flexible domains in solution, which are likely to be stabilized upon binding to the complex (Calderone et al., 2003; Ifuku et al., 2004; Balsera et al., 2005). The intrinsic core components of PSII also shift upon binding and release of the extrinsic proteins (Boekema et al., 2000). Specifically, removal of PsbP and PsbQ affect the peripheral antenna proteins and further removal of the PsbO protein also destabilizes the dimeric structure of PSII. These linked conformational changes may be significant for the assembly and disassembly of the PSII complex.

Currently, little is known about the structure of the PsbR protein, as it is unaccounted for in the PSII complexes used for structural studies and there is no structure of the purified protein. The PsbR protein is considered an extrinsic subunit, but there is also evidence that the C-terminus of the protein is hydrophobic. Biochemical analysis has indicated the PsbR protein is in close proximity to the PsbO, PsbP and CP47 proteins. Genetic analyses also implicated a role for PsbR in the stable association of the PsbP and PsbQ proteins (Suorsa et al., 2006). Mutational studies have, in turn, shown that the intrinsic PsbJ subunit is necessary for the association of PsbR (Suorsa et al., 2006). Analysis of PSII assembly intermediates suggest that PsbR can bind independently of the other extrinsic subunits as it is found in CP43-less monomers which lack these proteins (Rokka et al., 2005). Additional mutational and biochemical studies should further elucidate the position of PsbR relative to the other plant OEC components.

A number of different techniques have contributed to our understanding of the structure of the plant OEC, and advances in plant genetic analysis and structural methods will be key tools for resolving certain details. Obviously, the interactions among the different extrinsic subunits and the PSII core need to be more explicitly defined. Also, plants have a number of different isoforms for each extrinsic protein and it is not clear why so many are necessary.

Photosystem II Biogenesis and Turnover

The complex architecture of PSII requires precise and regulated assembly to ensure the proper positioning of all the essential redox active cofactors. Studies have shown that the assembly pathway is clearly an ordered step-wise association of the PSII subunits. Furthermore, as a consequence of normal PSII activity, the core D1 protein is irreversibly damaged and must be replaced with a newly synthesized copy (Baena-Gonzalez and Aro, 2002; Aro et al., 2005). PSII biogenesis and turnover is a complex and frequent process, and the details of this cycle are the focus of intense PSII research. In this section, the roles of some of the extrinsic proteins in the dynamic life cycle will be discussed.

In addition to its role as a structural component of the plant OEC, PsbP may play a more direct role in the light-driven assembly of the manganese cluster (Bondarava et al., 2005). Upon release of the three extrinsic proteins components PsbP sequesters manganese ions (Bondarava et al., 2005). Furthermore, photoactivation assays showed that the manganese-containing PsbP protein specifically facilitated manganese cluster assembly and restoration of oxygen evolution activity. Note that these experiments were also conducted in the presence of PsbO as it is required for PsbP association with PSII. While these results agree with previous characterization of the PsbP-deficient mutant in *Chlamydomonas* (Rova et al., 1996), no defects in photoactivation were observed in the *Nicotiana* PsbP-RNAi plants (Ifuku et al., 2005). However, photoactivation in the PsbP-RNAi plants was not extensively characterized and it is possible that the plants may show exacerbated defects under different growth conditions.

Little is known about the function of the Psb27 protein, but data suggest it may play a role in PSII assembly. While it is a component of cyanobacterial PSII complexes isolated using a histidine-tagged CP47 protein (Kashino et al., 2002), it was shown to be more abundant on PSII complexes in which the precursor D1 protein did not undergo the necessary C-terminal cleavage to yield the mature functional D1 protein (Roose and Pakrasi, 2004). This population of PSII complexes lacks the manganese cluster and the PsbO, PsbQ, PsbU, and PsbV extrinsic proteins (Roose and Pakrasi, 2004). These findings suggest that Psb27 associates with PSII complexes at

an early step in assembly and may exclude the binding of the other extrinsic proteins. It is not clear whether the Psb27 protein plays a role in the pD1-processing event or serves another function in the biogenesis pathway. It is likely that Psb27 only transiently associates with PSII during assembly, but is not part of the functional complex. Additional experiments are necessary to elucidate the function of this protein *in vivo.*

In addition to addressing the forward pathway of assembly, it is also necessary to consider the disassembly steps required for the removal of the damaged D1 protein. The current PSII structural models position the D1 protein in the center of the PSII core with numerous interactions with the manganese cluster and extrinsic proteins (Kamiya and Shen, 2003; Ferreira et al., 2004; Loll et al., 2005). Thus, the OEC must be disassembled to remove the damaged D1 protein. Notably, the interaction of the extrinsic proteins with PSII is affected by the presence of the assembled manganese cluster (Kavelaki and Ghanotakis, 1991). Furthermore, the release of the extrinsic proteins results in significant changes in the intrinsic components and destabilizes the dimeric form of PSII (Boekema et al., 2000). Consequently, release of the manganese cluster would ensure an efficient disassembly of the entire OEC with additional effects on the core components. Interestingly, under normal conditions free extrinsic proteins in the thylakoid lumen are not targeted for degradation, which could facilitate reassembly.

Experiments have identified a GTP requirement for the primary proteolytic cleavage of the damaged D1 protein (Spetea et al., 1999; Spetea et al., 2000). It has been reported that the primary cleavage event occurs in isolated PSII complexes, suggesting that perhaps a PSII subunit or co-purified protein is responsible (Salter et al., 1992; De Las Rivas et al., 1993). Subsequent reports have shown that the PsbO protein can bind GTP indicating this ubiquitous extrinsic protein may be involved in regulating D1 degradation (Spetea et al., 2004). The current models of PSII do not provide any additional evidence for this hypothesis. Interestingly, recent analysis of the PsbP protein indicates it is structurally similar to Mog1p, a regulator of Ran-GTPase in yeast (Ifuku et al., 2004). This result presents yet another possible role of the PsbP

protein in the PSII life cycle. More experiments are necessary to determine whether the PSII extrinsic proteins play a more active role in the turnover of the D1 protein.

CONCLUSION

The unique reaction of water oxidation is similar among all photosynthetic organisms. Yet the protein complement of the OEC varies significantly. Future studies should focus on assigning function to the individual extrinsic proteins. Higher resolution structural work will allow us a complete picture of the various OECs as a whole. It's important to keep in mind that a static structure cannot tell the entire story of PSII, as it is a dynamic complex undergoing constant assembly and degradation. Future studies should also be directed to gain an understanding of PSII as a dynamic structure.

REFERENCES

Adelroth P, Lindberg K, Andreasson LE (1995) Studies of Ca2+ binding in spinach photosystem II using 45Ca2+. Biochemistry **34:** 9021-9027

Akabori K, Imaoka A, Y. T (1984) The role of lipids and 17-kDa protein in enhancing the recovery of O2 evolution in cholate-treated thylakoid membranes. FEBS Lett **173:** 36-40

Akerlund HE, Jansson C, Andersson B (1982) Reconstitution of photosynthetic water splitting in inside-out thylakoid vesicles and identification of a participating polypeptide. Biochim Biophys Acta **681:** 1-10

Andrews H, Li Z, Altuve-Blanco A, Rivera M, Burnap RL (2005) Expression, mutagenesis, and characterization of recombinant low-potential cytochrome c_{550} of Photosystem II. Biochemistry **44:** 6092-6100

Aro EM, Suorsa M, Rokka A, Allahverdiyeva Y, Paakkarinen V, Saleem A, Battchikova N, Rintamaki E (2005) Dynamics of photosystem II: a proteomic approach to thylakoid protein complexes. J Exp Bot **56:** 347-356

Baena-Gonzalez E, Aro EM (2002) Biogenesis, assembly and turnover of photosystem II units. Philos Trans R Soc Lond B Biol Sci **357:** 1451-1459; discussion 1459-1460

Balint I, Bhattacharya J, Perelman A, Schatz D, Moskovitz Y, Keren N, Schwarz R (2006) Inactivation of the extrinsic subunit of photosystem II, PsbU, in *Synechococcus* PCC 7942 results in elevated resistance to oxidative stress. FEBS Lett **580:** 2117-2122

Balsera M, Arellano JB, Revuelta JL, de las Rivas J, Hermoso JA (2005) The 1.49 A resolution crystal structure of PsbQ from photosystem II of *Spinacia oleracea* reveals a PPII structure in the N-terminal region. J Mol Biol **350:** 1051-1060

Barra M, Haumann M, Dau H (2005) Specific loss of the extrinsic 18 KDa protein from photosystem II upon heating to 47 degrees C causes inactivation of oxygen evolution likely due to Ca release from the Mn-complex. Photosynth Res **84:** 231-237

Bendtsen JD, Nielsen H, von Heijne G, Brunak S (2004) Improved prediction of signal peptides: SignalP 3.0. J Mol Biol **340:** 783-795

Boekema EJ, van Breemen JF, van Roon H, Dekker JP (2000) Conformational changes in photosystem II supercomplexes upon removal of extrinsic subunits. Biochemistry **39:** 12907-12915

Bondarava N, Beyer P, Krieger-Liszkay A (2005) Function of the 23 kDa extrinsic protein of Photosystem II as a manganese binding protein and its role in photoactivation. Biochim Biophys Acta **1708:** 63-70

Bricker TM, Frankel LK (2003) Carboxylate groups on the manganese-stabilizing protein are required for efficient binding of the 24 kDa extrinsic protein to photosystem II. Biochemistry **42:** 2056-2061

Bricker TM, Young A, Frankel LK, Putnam-Evans C (2002) Introduction of the 305Arg-->305Ser mutation in the large extrinsic loop E of the CP43 protein of *Synechocystis* sp. PCC 6803 leads to the loss of cytochrome c(550) binding to Photosystem II. Biochim Biophys Acta **1556:** 92-96

Bumba L, Havelkova-Dousova H, Husak M, Vacha F (2004) Structural characterization of photosystem II complex from red alga *Porphyridium cruentum* retaining extrinsic subunits of the oxygen-evolving complex. Eur J Biochem **271:** 2967-2975

Bumba L, Vacha FE (2003) Electron microscopy in structural studies of Photosystem II. Photosynth Res **77:** 1-19

Calderone V, Trabucco M, Vujicic A, Battistutta R, Giacometti GM, Andreucci F, Barbato R, Zanotti G (2003) Crystal structure of the PsbQ protein of photosystem II from higher plants. EMBO Rep **4:** 900-905

Clarke SM, Eaton-Rye JJ (1999) Mutation of Phe-363 in the photosystem II protein CP47 impairs photoautotrophic growth, alters the chloride requirement, and prevents photosynthesis in the absence of either PSII-O or PSII-V in *Synechocystis* sp. PCC 6803. Biochemistry **38:** 2707-2715

De Las Rivas J, Balsera M, Barber J (2004) Evolution of oxygenic photosynthesis: genome-wide analysis of the OEC extrinsic proteins. Trends Plant Sci **9:** 18-25

De Las Rivas J, Barber J (2004) Analysis of the Structure of the PsbO Protein and its Implications. Photosynth Res **81:** 329-343

De Las Rivas J, Roman A (2005) Structure and evolution of the extrinsic proteins that stabilize the oxygen-evolving engine. Photochem Photobiol Sci **4:** 1003-1010

De Las Rivas J, Shipton CA, Ponticos M, Barber J (1993) Acceptor side mechanism of photoinduced proteolysis of the D1 protein in photosystem II reaction centers. Biochemistry **32:** 6944-6950

de Vitry C, Olive J, Drapier D, Recouvreur M, Wollman F (1989) Posttranslational events leading to the assembly of photosystem II protein complex: a study using photosynthesis mutants from *Chlamydomonas reinhardtii*. J Cell Biol **109:** 991-1006

Eaton-Rye JJ (2005) Requirements for different combinations of the extrinsic proteins in specific cyanobacterial photosystem II mutants. Photosynth Res **84:** 275-281

Eaton-Rye JJ, Shand JA, Nicoll WS (2003) pH-dependent photoautotrophic growth of specific photosystem II mutants lacking lumenal extrinsic polypeptides in *Synechocystis* PCC 6803. FEBS Lett **543:** 148-153

Enami I, Iwai M, Akiyama A, Suzuki T, Okumura A, Katoh T, Tada O, Ohta H, Shen J-R (2003) Comparison of binding and functional properties of two extrinsic components, Cyt c550 and a 12 kDa protein, in cyanobacterial PSII with those in red algal PSII. Plant Cell Physiol **44:** 820-827

Enami I, Kikuchi S, Fukuda T, Ohta H, Shen JR (1998) Binding and functional properties of four extrinsic proteins of photosystem II from a red alga, *Cyanidium caldarium*, as studied by release-reconstitution experiments. Biochemistry **37:** 2787-2793

Enami I, Murayama H, Ohta H, Kamo M, Nakazato K, Shen JR (1995) Isolation and characterization of a Photosystem II complex from the red alga *Cyanidium caldarium:* association of cytochrome c-550 and a 12 kDa protein with the complex. Biochim Biophys Acta **1232:** 208-216

Enami I, Suzuki T, Tada O, Nakada Y, Nakamura K, Tohri A, Ohta H, Inoue I, Shen JR (2005) Distribution of the extrinsic proteins as a potential marker for the evolution of photosynthetic oxygen-evolving photosystem II. FEBS J **272:** 5020-5030

Ferreira KN, Iverson TM, Maghlaoui K, Barber J, Iwata S (2004) Architecture of the photosynthetic oxygen-evolving center. Science **303:** 1831-1838

Gao JP, Yong ZH, Zhang F, Ruan KC, Xu CH, Chen GY (2005) Positive charges on lysine residues of the extrinsic 18 kDa protein are important to its electrostatic interaction with spinach photosystem II membranes. Acta Biochim Biophys Sin (Shanghai) **37:** 737-742

Ghanotakis DF, Babcock GT, Yocum CF (1984) Calcium reconstitutes high rates of oxygen evolution in polypeptide depleted Photosystem II preparations. FEBS Lett **167:** 127-130

Ghanotakis DF, Topper JN, Yocum CF (1984) Structural organization of the oxidizing side of photosystem II. Exogenous reductants reduce and destroy the Mn-complex in photosystems II membranes depleted of the 17 and 23 kDa polypeptides. Biochim Biophys Acta **767:** 524-531

Harper R, Bassi, R., Testi, M.G., and Schafer, C. (1998) Nearest-neighbor analysis of a Photosystem II complex from *Marchantia polymorpha* L. (liverwort), which contains reaction center and antenna proteins. FEBS Lett **255:** 196-205

Ifuku K, Nakatsu T, Kato H, Sato F (2004) Crystal structure of the PsbP protein of photosystem II from *Nicotiana tabacum*. EMBO Rep **5:** 362-367

Ifuku K, Sato F (2002) A truncated mutant of the extrinsic 23-kDa protein that absolutely requires the extrinsic 17-kDa protein for Ca2+ retention in photosystem II. Plant Cell Physiol **43:** 1244-1249

Ifuku K, Yamamoto Y, Ono TA, Ishihara S, Sato F (2005) PsbP protein, but not PsbQ protein, is essential for the regulation and stabilization of photosystem II in higher plants. Plant Physiol **139:** 1175-1184

Ikeuchi M, Inoue Y, Vermaas W (1995) Characterization of photosystem II subunits from the cyanobacterium *Synechocystis* sp. PCC 6803. In Photosynthesis: From Light to Biosphere, P Mathis, ed (Dordrecht: Kluwer Academic Publishers), pp 297-300

Inoue-Kashino N, Kashino Y, Satoh K, Terashima I, Pakrasi HB (2005) PsbU provides a stable architecture for the oxygen-evolving system in cyanobacterial photosystem II. Biochemistry **44:** 12214-12228

Ishihara S, Yamamoto Y, Ifuku K, Sato F (2005) Functional analysis of four members of the PsbP family in photosystem II in *Nicotiana tabacum* using differential RNA interference. Plant Cell Physiol **46:** 1885-1893

Ishikawa Y, Schroder WP, Funk C (2005) Functional analysis of the PsbP-like protein (sll1418) in *Synechocystis* sp. PCC 6803. Photosynth Res **84:** 257-262

Ishikita H, Knapp EW (2005) Redox potential of cytochrome c550 in the cyanobacterium *Thermosynechococcus elongates*. FEBS Lett **579:** 3190-3194

Juncker AS, Willenbrock H, Von Heijne G, Brunak S, Nielsen H, Krogh A (2003) Prediction of lipoprotein signal peptides in Gram-negative bacteria. Protein Sci **12:** 1652-1662

Kamiya N, Shen JR (2003) Crystal structure of oxygen-evolving photosystem II from *Thermosynechococcus vulcanus* at 3.7-A resolution. Proc Natl Acad Sci U S A **100:** 98-103

Kashino Y, Inoue-Kashino N, Roose JL, Pakrasi HB (2006) Absence of the PsbQ Protein results in destabilization of the PsbV protein and decreased oxygen evolution activity in cyanobacterial Photosystem II. J Biol Chem **281:** 20834-20841

Kashino Y, Lauber WM, Carroll JA, Wang Q, Whitmarsh J, Satoh K, Pakrasi HB (2002) Proteomic analysis of a highly active photosystem II preparation from the cyanobacterium *Synechocystis* sp. PCC 6803 reveals the presence of novel polypeptides. Biochemistry **41:** 8004-8012

Katoh H, Itoh S, Shen JR, Ikeuchi M (2001) Functional analysis of psbV and a novel c-type cytochrome gene psbV2 of the thermophilic cyanobacterium *Thermosynechococcus elongatus* strain BP-1. Plant Cell Physiol **42:** 599-607

Kavelaki K, Ghanotakis DF (1991) Effect of the manganese complex on the binding of the extrinsic proteins (17, 23 and 33 kDa) of Photosystem II. Photosynth Res **29:** 149-155

Kerfeld CA, Sawaya MR, Bottin H, Tran KT, Sugiura M, Cascio D, Desbois A, Yeates TO, Kirilovsky D, Boussac A (2003) Structural and EPR characterization of the soluble form of cytochrome c-550 and of the psbV2 gene product from the cyanobacterium *Thermosynechococcus elongatus*. Plant Cell Physiol **44:** 697-706

Kimura A, Eaton-Rye JJ, Morita EH, Nishiyama Y, Hayashi H (2002) Protection of the oxygen-evolving machinery by the extrinsic proteins of photosystem II is essential for development of cellular thermotolerance in *Synechocystis* sp. PCC 6803. Plant Cell Physiol **43:** 932-938

Kirilovsky D, Roncel M, Boussac A, Wilson A, Zurita JL, Ducruet JM, Bottin H, Sugiura M, Ortega JM, Rutherford A (2004) Cytochrome c_{550} in the cyanobacterium *Thermosynechococcus elongatus*. J Biol Chem **279:** 52869-52880

Krogmann DW (1991) The low-potential cytochrome c of cyanobacteria and algae. Biochim Biophys Acta **1058:** 35-37

Krogmann DW, Smith S (1990) Low potential cytochrome *c550* function in cyanobacteria and algae. *In* M Baltscheffsky, ed, Current Research in Photosynthesis, Vol **2.** Kluwer Academic, Dordrecht, The Netherlands, pp 687-690

Kuhn MG, Vermaas WF (1993) Deletion mutations in a long hydrophilic loop in the photosystem II chlorophyll-binding protein CP43 in the cyanobacterium *Synechocystis* sp. PCC 6803. Plant Mol Biol **23:** 123-133

Kuwabara T, Murata N (1983) Quantitative analysis of the inactivation of photosynthetic oxygen evolution and the release of polypeptides and manganese in the Photosystem II particles of Spinach chloroplasts. Plant Cell Physiol **24:** 741-747

Lautner A, Klein R, Ljungberg U, Reilander H, Bartling D, Andersson B, Reinke H, Beyreuther K, Herrmann RG (1988) Nucleotide sequence of cDNA clones encoding the complete precursor for the "10-kDa" polypeptide of photosystem II from spinach. J Biol Chem **263:** 10077-10081

Ljungberg U, Akerlund HE, Andersson B (1986) Isolation and characterization of the 10-kDa and 22-kDa polypeptides of higher plant photosystem 2. Eur J Biochem **158:** 477-482

Ljungberg U, Akerlund HE, Larsson C, Andersson B (1984) Identification of polypeptides associated with the 23 and 33 kDa proteins of photosynthetic oxygen evolution. Biochim Biophys Acta **767**

Ljungberg U, Akerlund, H.E., & Andersson, B. (1984) The release of a 10-kDa polypeptide from everted photosystem II thylakoid membranes by alkaline Tris. FEBS Lett **175:** 255-258

Loll B, Kern J, Saenger W, Zouni A, Biesiadka J (2005) Towards complete cofactor arrangement in the 3.0 A resolution structure of photosystem II. Nature **438:** 1040-1044

Matsuzaki M, Misumi O, Shin IT, Maruyama S, Takahara M, Miyagishima SY, Mori T, Nishida K, Yagisawa F, Nishida K, Yoshida Y, Nishimura Y, Nakao S, Kobayashi T, Momoyama Y, Higashiyama T, Minoda A, Sano M, Nomoto H, Oishi K, Hayashi H, Ohta F, Nishizaka S, Haga S, Miura S, Morishita T, Kabeya Y, Terasawa K, Suzuki Y, Ishii Y, Asakawa S, Takano H, Ohta N, Kuroiwa H, Tanaka K, Shimizu N, Sugano S, Sato N, Nozaki H, Ogasawara N, Kohara Y, Kuroiwa T (2004) Genome sequence of the ultrasmall unicellular red alga *Cyanidioschyzon merolae* 10D. Nature **428:** 653-657

Meades GD, Jr., McLachlan A, Sallans L, Limbach PA, Frankel LK, Bricker TM (2005) Association of the 17-kDa extrinsic protein with photosystem II in higher plants. Biochemistry **44:** 15216-15221

Miyao M, Murata N (1983) Partial disintegration and reconstitution of the photosynthetic oxygen evolution system. Binding of 24 kilodalton and 18 kilodalton polypeptide. Biochim Biophys Acta **725:** 87-93

Miyao M, Murata N (1983) Partial reconstitution of the photosynthetic oxygen evolution system by rebinding of the 33-kDa polypeptide. FEBS Lett **164:** 375-378

Miyao M, Murata N (1984) Calcium ions can be substituted for the 24-kDa polypeptide in photosynthetic oxygen evolution. FEBS Lett **168:** 118-120

Miyao M, Murata N (1985) The Cl- effect on photosynthetic oxygen evolution: interaction of Cl- with 18-kDa, 24-kDa and 33-kDa proteins. FEBS Lett. **180:** 303-308

Morgan TR, Shand JA, Clarke SM, Eaton-Rye JJ (1998) Specific requirements for cytochrome c-550 and the manganese-stabilizing protein in photoautotrophic strains of *Synechocystis* sp. PCC 6803 with mutations in the domain Gly-351 to Thr-436 of the chlorophyll-binding protein CP47. Biochemistry **37:** 14437-14449

Mould R, Robinson C (1991) A proton gradient is required for the transport of two lumenal oxygen- evolving proteins across the thylakoid membrane. J. Biol. Chem. **266:** 12189-12193

Nield J, Barber J (2006) Refinement of the structural model for the Photosystem II supercomplex of higher plants. Biochim Biophys Acta **1757:** 353-361

Nield J, Kruse O, Ruprecht J, da Fonseca P, Buchel C, Barber J (2000) Three-dimensional structure of *Chlamydomonas reinhardtii* and *Synechococcus elongatus* photosystem II complexes allows for comparison of their oxygen-evolving complex organization. J Biol Chem **275:** 27940-27946

Nishiyama Y, Hayashi H, Watanbe T, Murata N (1994) Photosynthetic Oxygen Evolution is Stabilized by Cytochrome c_{550} against Heat Inactivation in *Synechococcus* sp PCC 7002. Plant Physiol **105:** 1313-1319

Nishiyama Y, Los DA, Hayashi H, Murata N (1997) Thermal protection of the oxygen-evolving machinery by PsbU, an extrinsic protein of photosystem II, in *Synechococcus* species PCC 7002. Plant Physiol **115:** 1473-1480

Nishiyama Y, Los DA, Murata N (1999) PsbU, a protein associated with photosystem II, is required for the acquisition of cellular thermotolerance in *Synechococcus* species PCC 7002. Plant Physiol **120:** 301-308

Ohta H, Okumura A, Okuyama S, Akiyama A, Iwai M, Yoshihara S, Shen JR, Kamo M, Enami I (1999) Cloning, expression of the psbU gene, and functional studies of the recombinant 12-kDa protein of photosystem II from a red alga *Cyanidium caldarium.* Biochem Biophys Res Commun **260:** 245-250

Ohta H, Suzuki T, Ueno M, Okumura A, Yoshihara S, Shen JR, Enami I (2003) Extrinsic proteins of photosystem II: an intermediate member of PsbQ protein family in red algal PS II. Eur J Biochem **270:** 4156-4163

Peltier JB, Emanuelsson O, Kalume DE, Ytterberg J, Friso G, Rudella A, Liberles DA, Soderberg L, Roepstorff P, von Heijne G, van Wijk KJ (2002) Central functions of the lumenal and peripheral thylakoid proteome of Arabidopsis determined by experimentation and genome-wide prediction. Plant Cell **14:** 211-236

Pettigrew GW, Moore GR (1987) Cytochromes c: biological aspects. Springer, Berlin Heidelberg New York

Putnam-Evans C, Bricker TM (1992) Site-directed mutagenesis of the CPa-1 protein of photosystem II: alteration of the basic residue pair 384,385R to 384,385G leads to a defect associated with the oxygen-evolving complex. Biochemistry **31:** 11482-11488

Putnam-Evans C, Burnap R, Wu J, Whitmarsh J, Bricker TM (1996) Site-directed mutagenesis of the CP 47 protein of photosystem II: alteration of conserved charged residues in the domain 364E-444R. Biochemistry **35:** 4046-4053

Qian M, Al-Khaldi SF, Putnam-Evans C, Bricker TM, Burnap RL (1997) Photoassembly of the photosystem II (Mn)4 cluster in site-directed mutants impaired in the binding of the manganese-stabilizing protein. Biochemistry **36:** 15244-15252

Raymond J, Blankenship RE (2004) The evolutionary development of the protein complement of photosystem 2. Biochim Biophys Acta **1655:** 133-139

Robinson C, Bolhuis A (2004) Tat-dependent protein targeting in prokaryotes and chloroplasts. Biochim Biophys Acta **1694:** 135-147

Rokka A, Suorsa M, Saleem A, Battchikova N, Aro EM (2005) Synthesis and assembly of thylakoid protein complexes: multiple assembly steps of photosystem II. Biochem J **388:** 159-168

Roncel M, Boussac A, Zurita JL, Bottin H, Sugiura M, Kirilovsky D, Ortega JM (2003) Redox properties of photosystem II cytochromes *b*559 and *c*550 in the cyanobacterium *Thermosynechococcus elogatus*. J Biol Inorg Chem **8:** 206-216

Roose JL, Pakrasi HB (2004) Evidence that D1 processing is required for manganese binding and extrinsic protein assembly into photosystem II. J Biol Chem **279:** 45417-45422

Rova EM, Mc Ewen B, Fredriksson PO, Styring S (1996) Photoactivation and photoinhibition are competing in a mutant of *Chlamydomonas reinhardtii* lacking the 23-kDa extrinsic subunit of photosystem II. J Biol Chem **271:** 28918-28924

Rova M, Franzacn L-G, Fredriksson P-O, Styring S (1994) Photosystem II in a mutant of *Chlamydomonas reinhardtii* lacking the 23 kDa psbP protein shows increased sensitivity to photoinhibition in the absence of chloride. Photosynth Res **39:** 75-83

Salter AH, Virgin I, Hagman A, Andersson B (1992) On the molecular mechanism of light-induced D1 protein degradation in photosystem II core particles. Biochemistry **31:** 3990-3998

Schubert M, Petersson UA, Haas BJ, Funk C, Schroder WP, Kieselbach T (2002) Proteome map of the chloroplast lumen of *Arabidopsis thaliana*. J Biol Chem **277:** 8354-8365

Seidler A (1996) The extrinsic polypeptides of Photosystem II. Biochim Biophys Acta **1277:** 35-60

Shen JR, Ikeuchi M, Inoue Y (1992) Stoichiometric association of extrinsic cytochrome c550 and 12 kDa protein with a highly purified oxygen-evolving photosystem II core complex from *Synechococcus vulcanus*. FEBS Lett **301:** 145-149

Shen JR, Ikeuchi M, Inoue Y (1997) Analysis of the psbU gene encoding the 12-kDa extrinsic protein of photosystem II and studies on its role by deletion mutagenesis in *Synechocystis* sp. PCC 6803. J Biol Chem **272:** 17821-17826

Shen JR, Inoue Y (1993) Binding and functional properties of two new extrinsic components, cytochrome c-550 and a 12-kDa protein, in cyanobacterial photosystem II. Biochemistry **32:** 1825-1832

Shen JR, Qian M, Inoue Y, Burnap RL (1998) Functional characterization of *Synechocystis* sp. PCC 6803 delta psbU and delta psbV mutants reveals important roles of cytochrome c-550 in cyanobacterial oxygen evolution. Biochemistry **37:** 1551-1558

Shen JR, Vermaas W, Inoue Y (1995) The role of cytochrome c-550 as studied through reverse genetics and mutant characterization in *Synechocystis* sp. PCC 6803. J Biol Chem **270:** 6901-6907

Shi LX, Schroder WP (2004) The low molecular mass subunits of the photosynthetic supracomplex, photosystem II. Biochim Biophys Acta **1608**:75–96

Spetea C, Hundal T, Lohmann F, Andersson B (1999) GTP bound to chloroplast thylakoid membranes is required for light-induced, multienzyme degradation of the photosystem II D1 protein. Proc Natl Acad Sci U S A **96:** 6547-6552

Spetea C, Hundal T, Lundin B, Heddad M, Adamska I, Andersson B (2004) Multiple evidence for nucleotide metabolism in the chloroplast thylakoid lumen. Proc Natl Acad Sci U S A **101:** 1409-1414

Spetea C, Keren N, Hundal T, Doan JM, Ohad I, Andersson B (2000) GTP enhances the degradation of the photosystem II D1 protein irrespective of its conformational heterogeneity at the Q(B) site. J Biol Chem **275:** 7205-7211

Stewart AC, Ljungberg, U., Akerlund, H.E., and Andersson, B. (1985) Studies on the polypeptide composition of the cyanobacterial oxygen-evolving complex. Biochim Biophys Acta **808:** 353-362

Stockhaus J, Hofer M, Renger G, Westhoff P, Wydrzynski T, Willmitzer L (1990) Anti-sense RNA efficiently inhibits formation of the 10 kd polypeptide of photosystem II in transgenic potato plants: analysis of the role of the 10 kd protein. EMBO J **9:** 3013-3021

Summerfield TC, Shand JA, Bentley FK, Eaton-Rye JJ (2005) PsbQ (Sll1638) in *Synechocystis* sp. PCC 6803 is required for photosystem II activity in specific mutants and in nutrient-limiting conditions. Biochemistry **44:** 805-815

Summerfield TC, Winter RT, Eaton-Rye JJ (2005) Investigation of a requirement for the PsbP-like protein in *Synechocystis* sp. PCC 6803. Photosynth Res **84:** 263-268

Suorsa M, Sirpio S, Allahverdiyeva Y, Paakkarinen V, Mamedov F, Styring S, Aro EM (2006) PsbR, a missing link in the assembly of the oxygen-evolving complex of plant photosystem II. J Biol Chem **281:** 145-150

Suzuki T, Minagawa J, Tomo T, Sonoike K, Ohta H, Enami I (2003) Binding and functional properties of the extrinsic proteins in oxygen-evolving photosystem II particle from a green alga, *Chlamydomonas reinhardtii* having his-tagged CP47. Plant Cell Physiol **44:** 76-84

Suzuki T, Ohta H, Enami I (2005) Cross-reconstitution of the extrinsic proteins and photosystem II complexes from *Chlamydomonas reinhardtii* and *Spinacia oleracea*. Photosynth Res **84:** 239-244

Swiatek M, Kuras R, Sokolenko A, Higgs D, Olive J, Cinque G, Muller B, Eichacker LA, Stern DB, Bassi R, Herrmann RG, Wollman FA (2001) The chloroplast gene ycf9 encodes a photosystem II (PSII) core subunit, PsbZ, that participates in PSII supramolecular architecture. Plant Cell **13**: 1347-1367

Tezcan FA, Winkler JR, Gray HB (1998) Effects of Ligation and Folding on Reduction Potentials of Heme Proteins. J Am Chem Soc **120:** 13383-13388

Thornton LE, Ohkawa H, Roose JL, Kashino Y, Keren N, Pakrasi HB (2004) Homologs of plant PsbP and PsbQ proteins are necessary for regulation of photosystem ii activity in the cyanobacterium *Synechocystis* 6803. Plant Cell **16:** 2164-2175

Tohri A, Dohmae N, Suzuki T, Ohta H, Inoue Y, Enami I (2004) Identification of domains on the extrinsic 23 kDa protein possibly involved in electrostatic interaction with the extrinsic 33 kDa protein in spinach photosystem II. Eur J Biochem **271:** 962-971

Veerman J, Bentley FK, Eaton-Rye JJ, Mullineaux CW, Vasil'ev S, Bruce D (2005) The PsbU subunit of photosystem II stabilizes energy transfer and primary photochemistry in the phycobilisome-photosystem II assembly of *Synechocystis* sp. PCC 6803. Biochemistry **44:** 16939-16948

Vrettos JS, Reifler MJ, Kievet O, Lakshmi KV, de Paula JC, Brudvig GW (2001) Factors that determine the unusually low reduction potential of cytochrome c_{550} in cyanobacterial photosystem II. J Biol Inorg Chem **6:** 708-716

Webber AN, Packman LC, Gray JC (1989) A 10 kDa polypeptide associated with the oxygen-evolving complex of photosystem II has a putative C-terminal non-cleavable thylakoid transfer domain. FEBS Lett **242:** 435-438

Yi X, Hargett SR, Frankel LK, Bricker TM (2006) The PsbQ protein is required in arabidopsis for photosystem II assembly/stability and photoautotrophy under low light conditions. J Biol Chem **281**: 26260-26267

Yu H, Xu X, Britt RD (2006) The 33 kDa protein can be removed without affecting the association of the 23 and 17 kDa proteins with the lumenal side of PS II of spinach. Biochemistry **45:** 3404-3411

Zouni A, Witt HT, Kern J, Fromme P, Krauss N, Saenger W, Orth P (2001) Crystal structure of photosystem II from *Synechococcus elongatus* at 3.8 A resolution. Nature **409:** 739-743

Table 1 Photosystem II extrinsic proteins in different organisms

Photosystem II gene	*G. violaceus* PCC 7421	*Synechocystis* sp. PCC 6803	*T. elongatus* BP-1	*Synechococcus* sp. WH 8102	*Anabaena* sp. PCC 7120	*Trichodesmium erythraeum*	*P. marinus* MED4	*P. marinus* SS120	*P. marinus* MIT9313	*Cyanidioschyzon merolae*	*Chlamydomonas reinhardtii*	*Arabidopsis thaliana*
psbO: manganese-stabilizing protein	*glr3691*	*sll0427*	*tll0444*	*SYNW0303*	*all3854*	*yes*	*PMM0228*	*Pro0257*	*PMT1800*	*CMI296C*	*yes*	*At5g66570* At3g50820**
psbP: 23 kDa extrinsic protein	*gll1440*	*sll1418*	*tlr2075*	*SYNW0927*	*all3076*	*yes*	*PMM1098*	*Pro1097*	*PMT1078*	*CMN296C CMT368C*	*yes*	*At1g06680* At1g76450* At1g77090* At2g28605 At2g30790* At2g39470* At3g55330* At3g56650* At4g15510* At5g11450*
psbQ: 16 kDa extrinsic protein	*no*	*sll1638*	*tll2057*	*SYNW2505*	*all1355*	*yes*	*no*	*no*	*no*	*CMC133C*	*yes*	*At1g14150* At2g01918 At4g21280* At4g05180* At3g01440**
psbR: 10 kDa extrinsic protein	*no*	*No*	*no*	*no*	*no*	*no*	*no*	*no*	*no*	*no*	*yes*	*At1g79040*
psbU: 12 kDa extrinsic protein	*gll2873*	*sll1194*	*tll2409*	*SYNW2191*	*alr1216*	*yes*	*no*	*no*	*PMT0178*	*CMI248C*	*no*	*no*
psbV: cytochrome c_{550}	*gll2337 gll2338*	*sll0258*	*tll1285 tll1284*	*SYNW0537*	*all0259*	*2 genes*	*no*	*no*	*PMT1427*	*CMV208C*	*no*	*no*
psb27: 11 kDa extrinsic protein	*no*	*slr1645*	*tll2464*	*SYNW1772*	*all1258*	*yes*	*PMM0507*	*Pro0507*	*PMT1260*	*CMK176C*	*yes*	*At1 g03660* At1g05385*
psb28: 13 kDa extrinsic protein	*glr1041 gsl0928*	*sll1398 slr1739*	*tlr0493*	*SYNW1065*	*all0801, all1082*	*yes*	*PMM0926*	*Pro0771*	*PMT0604*	*CMV089C*	*yes*	*At4g28660*
sll1390	*no*	*sll1390*	*tll0404*	*SYNW1218*	*alr4100*	*yes*	*no*	*no*	*PMT0747*	*CMK075C*	*yes*	*At1g54780**

Table 1. Photosystem II Extrinsic Proteins in Different Organisms

Complete names for the organisms included in the table are: *Gloeobacter violaceus, Synechocystis* sp. PCC 6803, *Thermosynechococcus elongatus* BP-1, *Synechococcus* sp. WH8102, *Anabaena* sp. PCC 7120, *Prochlorococcus marinus* MED4, *Prochlorococcus marinus* SS120, *Prochlorococcus marinus* MIT9313, *Cyanidioschyzon merolae, Trichodesmium erythaeum, Chlamydomonas reinhardtii,* and *Arabidopsis thaliana*. Gene name and/or BLAST search analysis was used to identify the genes listed in the table in the different organisms (performed July 2006). Yes, indicates the presence of the gene confirmed by BLAST search, but the annotation is incomplete. Asterisks indicate expressed isoforms in the thylakoid lumen of *Arabidopsis thaliana* (Peltier et al., 2002; Schubert et al., 2002). Locations for the databases used for this analysis are as follows: Cyanobase (http://www.kazusa.or.jp/cyano/), DOE Joint Genome Institute (http://genome.jgi-psf.org/draft_microbes/trier/trier.home.html and http://genome.jgi-psf.org/Chlre3/Chlre3.home.html), *Cyanidioschyzon merolae* Genome Project (http://merolae.biol.s.u-tokyo.ac.jp/) and The *Arabidopsis* Information Resource (http://www.arabidopsis.org/).

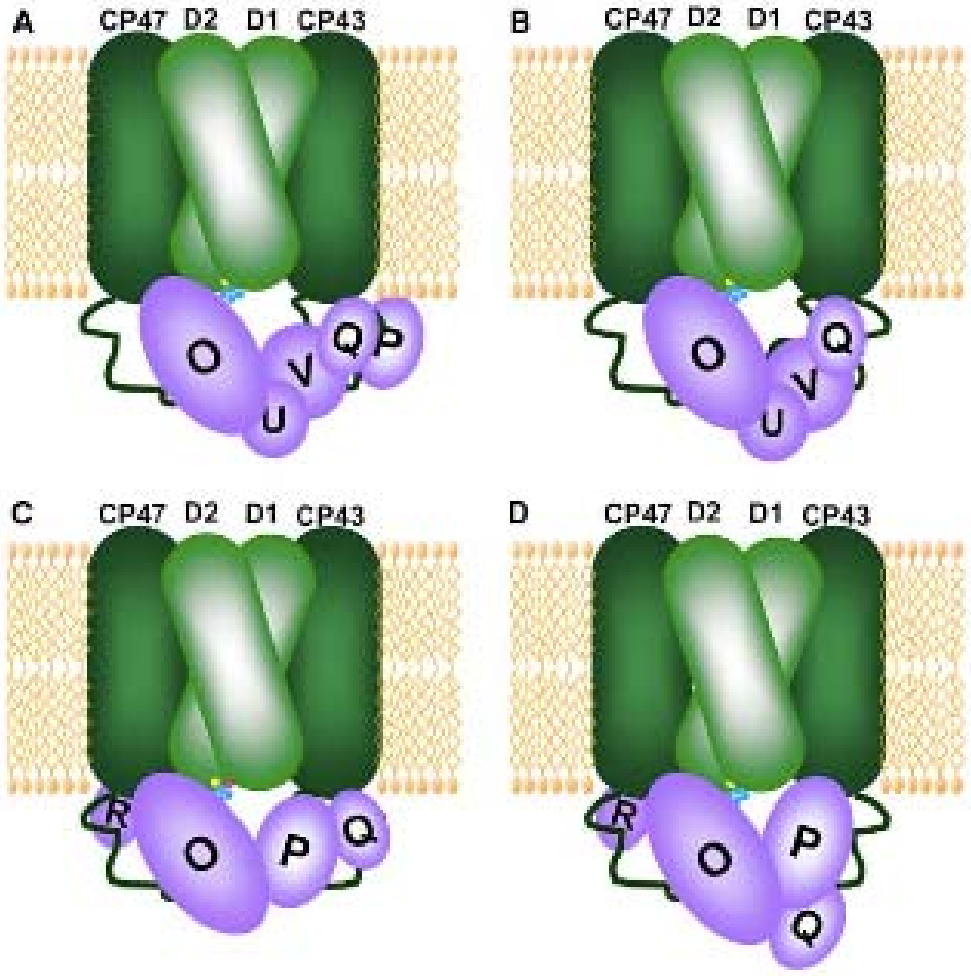
A
CP47
D2
D1
CP43
O
V
Q
P
U
B
CP47
D2
D1
CP43
O
Q
V
U
C
CP47
D2
D1
CP43
R
O
P
Q
D
CP47
D2
D1
CP43
R
O
P
Q

Figure 1. Models for the OECs in Different Organisms

Based on the current structural, biochemical and genetic data discussed in the manuscript, the structures of the OECs in cyanobacteria (A), red algae (B), green algae (C), and plants (D) are modeled in cartoon form. The intrinsic components D1, D2, CP43 and CP47 are labeled and the large lumenal portions of CP43 and CP47 are shown as solid loops. The manganese cluster is also represented by small dots on the lumenal side of the D1 protein. The extrinsic proteins are labeled as O (PsbO), P (PsbP), Q (PsbQ), R (PsbR), U, (PsbU) and V (PsbV). The cyanobacterial OEC (A) shows the presence of five extrinsic proteins, but PsbP may not be a stoichiometric component of these complexes. In the green algal (C) and plant (D) OEC models, the PsbR protein is positioned behind the PsbP and PsbQ proteins such that it is closer to the intrinsic PsbJ protein beyond the CP43 and D2 proteins. These models are designed to aid the reader in conceptualizing the relative locations of the indicated subunits among the different organisms, but by no means replace the more detailed structural analyses discussed in the manuscript. Refer to the text for more detailed discussions about the individual proteins or organismal OECs.